IMPERIAL COLLEGE LONDON

Distributed Control in the Smart Grid

Antonio De Paola

A thesis submitted in fulfilment of the requirements
for the degree of Doctor of Philosophy

in the

Control and Power Research Group
Electrical & Electronic Engineering Department
Imperial College London

June 2015

Declaration of Originality

I hereby declare that the material contained in this thesis is the result of my own work and that any ideas or quotations from the work of other people, published or otherwise, are appropriately referenced.

Antonio De Paola

Imperial College London

London, United Kingdom

June 29th, 2015

Copyright Declaration

Abstract

This thesis addresses some of the challenges that arise when the new smart grid paradigm is applied to power systems. In particular, novel control strategies are designed to deal in a decentralized matter with the increasing complexity of the network. Two main areas are investigated: participation to frequency control of variable-speed wind turbines and management of large populations of competing agents (e.g. micro-storage devices and "smart appliances") that exchange energy with the system.

The first part of this work presents two different techniques that allow wind turbines to provide frequency response: following the trip of a large power plant, the turbines population increases its aggregate generated power, reducing the resulting drop in frequency. A first method models the wind turbines as stochastic hybrid systems: the generators switch randomly between two operative modes characterized by different efficiency and generated power at equilibrium. Transitions are driven by frequency-dependent switching functions: single generators behave randomly while large populations perform deterministically, changing the total power in response to frequency variations. The second proposed control strategy allows a prescribed increase in generation, distributing the control effort among the individual turbines in order to maximize the duration of frequency support or minimize the resulting kinetic energy losses.

The second part of the thesis deals with large populations of agents which determine their operation strategy in response to a broadcast price signal. Micro-storage devices performing energy arbitrage are initially considered: each agent charges/discharges during the day in order to maximize its profit. By approximating the number of devices as infinite, modelling the population as a continuum and describing the problem through a differential game with infinite players (mean field game), it is possible to avoid synchronicity phenomena and determine an equilibrium for the market. Finally, the similar case of flexible demand is analyzed, with price-responsive appliances that schedule their power consumption in order to minimize their energy cost. Necessary and sufficient conditions for the existence of a Nash equilibrium are provided, extending the results by introducing time-varying constraints on the power rate and considering partial flexibility of the devices.

Acknowledgements

First, I would like to thank my supervisor Dr David Angeli for his constant guidance and advice during my PhD. I am happy I had the opportunity to learn from his knowledge and experience. I would also like to express my sincere gratitude to my second supervisor Prof Goran Strbac who has been a source of inspiration and motivation.

A special mention to all the people of the CAP group, the ones still at Imperial and the ones who have found their place somewhere else: these have been great years and I will always have fond memories of the time spent together.

I want to thank my parents for their unconditional love and support, for the encouragement in following my aspirations and the help to pursue them. My biggest thank goes to Inma with whom I shared the ups and downs of research and so much more.

Antonio

Contents

List of Figures

Abbreviations

DFIM	**D**oubly-**F**ed **I**nduction **M**achine
FP	**F**okker-**P**lanck equation
HJB	**H**amilton-**J**acobi-**B**ellman equation
MFG	**M**ean **F**ield **G**ame
ODE	**O**rdinary **D**ifferential **E**quation
OPPT	**O**ptimum **P**ower **P**oint **T**racking
PDE	**P**artial **D**ifferential **E**quation
PMP	**P**ontryagin's **M**inimum **P**rinciple
PMSM	**P**ermanent **M**agnet **S**ynchronous **M**achine
SOS	**S**um **O**f **S**quares
WT	**W**ind **T**urbine

To my parents

Chapter 1

Introduction

1.1 Background and Motivation

The rapid changes in the way energy is produced and consumed are creating new and stimulating challenges that involve the structure and the organization of the future electric power network. In particular, following environmental concerns on global warming and future scarcity of traditional energy sources, there is a clear trend of increasing penetration of renewable energy in power systems. The United Kingdom has set an ambitious target of delivering 15% of its energy consumption from renewables by 2020 [3], reducing by 80% its carbon emissions by 2050 [4]. Similar objectives on decarbonisation of the electric sector have also been proposed at a European level [5], [6].

In order to achieve these goals, power systems will undergo the most significant transformation of the last 50 years. If one considers, for example, the increasing penetration of wind generation in the system that will occur in the next decades to satisfy the expected renewable quotas, a whole new set of challenges arise. In fact, wind turbines present significant technological differences with respect to traditional synchronous generators. As their presence becomes more significant, they will be required to participate in the control and management of the power system, providing ancillary services (such as frequency and voltage control) which nowadays are mainly offered by traditional power plants.

The evolution of the electric network is also driven by the considerable technological advancements in fields such as information technology, power electronics and transportation. It is envisioned that in the next years there will be an electrification of important sectors such as transportation [7] and heating [8]. This will cause a positive reduction of carbon emissions, but it will also alter the traditional energy consumption patterns and

require a more efficient utilization of the current system assets. With the development of smart meters and cheap storage devices, customers will have a more active role in the operation of the network. The introduction of an underlying communication infrastructure within the power system will also allow to improve its security, flexibility and quality of supply.

The new emerging paradigm which integrates all these elements in the electric network of the future is the so called smart grid [9], [10]. One of its defining elements is the conceptual shift in network operation. The centralized management which is currently performed at most levels of the power system will be replaced by distributed and decentralized mechanisms. The most significant example is probably the matching between demand and supply. Currently demand is (mostly) considered as an external factor which the system follows by a centralized scheduling of the generators provided by the system operator. As a result of the increased level of uncertainty deriving from the presence of renewable generators and the considerable shift in power consumption patterns introduced by new technologies (e.g. electric vehicles, "smart" appliances and domestic micro-storage devices), this approach may not be viable or economically sustainable in the future. This means that customers should play an active role and dynamically adapt their consumption to the state of the network. Novel distributed control techniques will be required, regulating the global behaviour of the population while taking into account the decisions of the single agent. Similar problems arise if one considers the increasing penetration of renewable generators (especially wind turbines and photovoltaic panels). Proper coordination amongst large number of these machines must be achieved in order to provide reliable ancillary services for the network.

When approaching these difficult tasks, one must consider that the future power system will be also characterized by an increased controllability and a much larger amount of recorded data. The control strategies proposed in this work for frequency response from wind turbines, energy arbitrage with micro-storage devices and management of flexible demand take into account these aspects and, at the same time, are designed for a decentralized implementation. In this way scalability of the proposed techniques is guaranteed, preserving their validity for a fast growing power system.

1.2   Thesis Objectives

Among the different aspects and issues that have been mentioned in the previous section, the work described in this thesis has addressed two broad research questions:

- Given a considerable number of renewable generators (in particular wind turbines) what are the best control strategies that allow a global participation of these machines to the frequency regulation of the network? Is it possible to design decentralized or stochastic control techniques that are robust, preserve a good efficiency of the turbines and do not require additional communication infrastructure?

- For price-responsive agents that will operate in the future energy market, such as privately owned micro-storage devices and flexible appliances, there exist distributed control mechanisms which are able to coordinate their operation strategies in order to achieve an equilibrium in the market?

1.3   Thesis Outline

The rest of this thesis is structured as follows: **Chapter 2** presents an overview of the new control challenges that arise from the increasing penetration of wind generation in power systems, presenting the main approaches proposed in the literature for frequency response with wind turbines. It also describes a novel distributed control strategy for wind farms, considering large populations of generators and modelling the single element as a stochastic hybrid system with two discrete states, to which correspond different operation modes. An alternative approach is presented in **Chapter 3** where the frequency response of the turbines is provided through temporary overproduction, slowing down the generators and releasing part of their kinetic energy stored in the rotating shafts. The control strategy is formulated through the minimization of the resulting efficiency losses. Two different cases are considered, assuming respectively that the electric torque of the turbines is defined by two different expressions or can be arbitrarily set.

The second part of the thesis deals with the control of a large number of competing agents in the power system. The problem of energy arbitrage with micro-storage is analysed in **Chapter 4**, presenting the state of the art in the management of large populations of price-responsive devices in the energy market. The proposed approach considers a competitive game framework, approximating the number of appliances as infinite and describing the whole population as a continuum. The energy arbitrage can then be modelled as a mean field game and solved through numerical integration of coupled partial differential equations. The similar problem of determining Nash equilibria in energy markets with a large number of flexible appliances is considered in **Chapter 5**. Necessary and sufficient conditions for equilibrium are provided by comparing two functions which describe respectively the valley capacity of the system and the global properties of the appliances population. These results are extended by introducing proportional constraints on the maximum power and the case of partial flexibility is also

analyzed. Finally, **Chapter 6** contains some concluding remarks, presenting the more promising research directions that can be followed to extend the results presented in this thesis.

1.4 Contributions

The main elements of novelty and original contributions of this work can be summarized as follows:

- A distributed control strategy is designed for frequency regulation through variable speed wind turbines. While the single generator performs randomly according to frequency-dependent switching functions, the whole population exhibits a deterministic behaviour. Stability and robustness of the chosen approach (which does not require additional communication infrastructure) are proved theoretically and then shown in simulations.

- A similar problem is tackled with a deterministic strategy, determining the power profiles of the wind turbines in order to provide frequency response and, at the same time, minimize the resulting efficiency losses.

- A new approach to the problem of energy arbitrage with micro-storage devices is introduced, adopting a game theory framework to model the competing interactions between the single agents and achieve an equilibrium in the market.

- In a similar setting, the coordination of price-responsive flexible appliances is analyzed, providing necessary and sufficient conditions for equilibrium. The results are then extended by introducing power constraints and considering partial flexibility of the devices.

1.4.1 List of publications

Journal Publications

- **A. De Paola**, D. Angeli and G. Strbac, "Distributed Control of Micro-storage Devices with Mean Field Games," in IEEE Transactions on Smart Grid, [Accepted for publication]. Online DOI: 10.1109/TSG.2015.2405338.

- **A. De Paola**, D. Angeli and G. Strbac, "Scheduling of Wind Farms for Optimal Frequency Response and Energy Recovery," in IEEE Transactions on Control Systems Technology, [Submitted].

Conference Publications

- D. Angeli, **A. De Paola** and G. Strbac, "Distributed Frequency Control by means of Responsive Wind Generation," in IEEE 51st Annual Conference on Decision and Control, pp. 5834-5839, Dec. 2012. Online DOI: 10.1109/CDC.2012.6427061

- **A. De Paola**, D. Angeli and G. Strbac, "Frequency Support by Scheduling of Variable-Speed Wind Turbines," in 19th IFAC World Congress, vol. 19, pp. 7904-7910, Aug. 2014. Online DOI: 10.3182/20140824-6-ZA-1003.01014

- **A. De Paola**, D. Angeli and G. Strbac, "Analysis of Nash Equilibria in Energy Markets with Large Populations of Price-Responsive Flexible Appliances," submitted to 54th Annual Conference on Decision and Control.

Chapter 2

Stochastic Distributed Control of Wind Farms for Frequency Response

The main features of variable-speed wind generators and the state of the art on frequency support from wind farms are initially outlined. A novel control strategy is then proposed for the provision of frequency response from large number of wind turbines. In particular, the single generator is modelled as a stochastic hybrid system with two discrete states, characterized by different efficiency and generated power. Transitions between these states are driven by frequency-dependent switching functions: the individual turbine behaves randomly while large populations perform deterministically, varying the aggregate power in response to frequency variations. Stability and disturbance rejection of the control strategy are assessed, presenting also simulative results.

2.1 Introduction

Following the increasing contribution of wind turbines to total generation, new problems arise in the control and management of the power system. This section discusses the role of wind farms in providing ancillary services, focusing in particular on frequency control. A general overview of the problem and the main approaches proposed in the literature to tackle it are presented, highlighting the main differences with respect to the stochastic control law described in the next sections of this chapter.

2.1.1 Power System Stability and Frequency Regulation

Frequency stability is the *ability of a power system to maintain steady frequency follow-ing a severe system upset resulting in a significant imbalance between generation and load* [11]. In a power grid the system frequency is an indicator of the balance that must be preserved at all times between supply (generation) and demand (load). The frequency will drop from its nominal value of $50Hz$ if demand levels exceed the available supply, as represented in Fig. 2.1. Such imbalances are usually caused by trips of large generating plants or sudden load increases and are corrected through three main elements, with different characteristic time-scales: synchronous generators slowing down and releasing kinetic energy (inertial response), increased generation from other plants (governor/primary response) and AGC response [12].
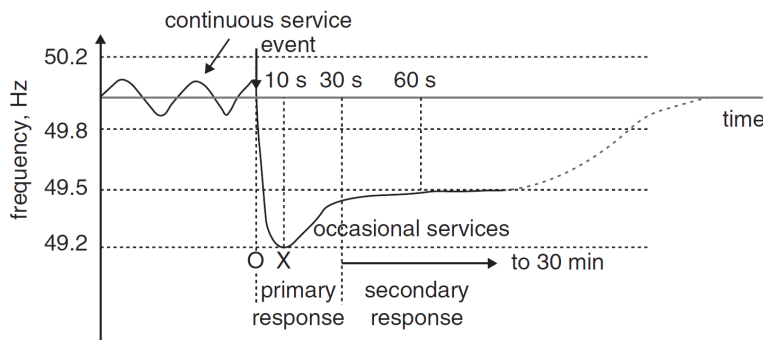
FIGURE 2.1: Representation of a typical frequency event and subsequent frequency response in the power system. Source: [1].

2.1.2 Variable-speed Wind Turbines

The growing environmental concerns about traditional power sources and the constant advances in technology have caused an increasing penetration of wind energy in power systems: in 2007 wind energy overtook hydropower to become the largest renewable generation source in the UK and, in the same country, the 2009 Renewable Energy Directive set a target to achieve 15% of energy consumption from renewable sources by 2020 [13]. Therefore, in the near future, wind turbines will represent a significant component of the total supply and will be required to provide the same services that nowadays are performed by conventional synchronous generators [14]. An element of particular importance and interest is the provision of frequency control [15], as requested for example in [16], [17], [18], [19]. In particular, the UK grid code requires that all wind plants supply a primary frequency response of up to 10% of their ratings, depending on the actual loading at the instant of frequency events [19]. To understand the main

challenges related to this task, it is useful to provide a basic description of these renewable generators.

The most common typologies of wind turbines that are currently being installed are Doubly-Fed Induction Machines (DFIM) and Permanent Magnet Synchronous Machines (PMSM) [20], [21]. One important feature of these generators is the possibility to control their power output: their steady-state active power depends in general on the mechanical energy extracted from the wind but it is possible to obtain a different transient behaviour by resorting to the system kinetic energy (rotating blades of the turbine). Furthermore, the presence of power electronic converters between the electrical machine and the power system allows to operate at an asynchronous rotor speed which can be set in order to maximize power extraction over a wide range of wind conditions. This is usually achieved by a speed controller which adapts the steady state generated power (or torque) to a reference value, obtained by predefined power-speed curves or through algebraic expressions [22]. A different control strategy is adopted at low wind speeds (generator is kept at a constant low speed) and at high wind speeds (the pitch angle of the turbine blades is increased so as to not exceed technical limitations of the generator).

A significant drawback of the decoupling introduced by power electronics between the wind turbine and the network is the loss of inertial response. Differently from traditional synchronous generators, the speed reduction and the resulting release of kinetic energy following a frequency fall in the network are absent [23] or consistently reduced [24] for the considered typologies of turbines. This means that alternative methods must be devised for the provision of a satisfactory frequency response.

2.1.3   Frequency Control and Wind Turbines

Consistent research work has investigated how variable-speed wind turbines can provide inertial response and frequency support for the grid. One possibility is to keep a power reserve by operating the turbines at a deloaded maximum power curve, as proposed in [25] and [26]. This means that, when a frequency fall is detected, the turbines can respond by following the optimal power curve and increase their generated power. The main problem with this approach is the economic loss which results from the turbines operating, in normal conditions, with an energy efficiency that is not optimal. An alternative solution to the problem is temporary overproduction: when a frequency drop occurs the turbines slow down, releasing part of the kinetic energy stored in their rotating shafts. This can be obtained, for example, emulating the inertial response of synchronous generators by adding an extra term, proportional to the frequency variation, to the torque reference of the speed controller [27]. The frequency derivative can represent

an extra input of such controller [28] or, modified by a filter and a shaping function, can be used by an additional control loop to regulate the slip of the generator [1] or improve system damping [29]. Two substantially different approaches are presented in [30], which indicates how to achieve the de-loading of the turbine operating on the pitch angle of the blades, and [31] which adopts model predictive control to explicitly account for the safety constraints of the generators.

2.1.4 Proposed Stochastic Control Strategy

The different approaches to frequency regulation described in Section 2.1.3 implicitly assume that individual turbines are all controlled in the same way in case of frequency drops. In the next sections and in Chapter 3 this assumption is removed and alternative solutions are investigated. We initially consider a stochastic control technique that has been previously applied to dynamic-demand management. In [32] decentralized random controllers are used to modify the duty-cycle (and consequently the absorbed power) of electric appliances when a frequency fall is detected. A dual approach is now adopted: the wind turbines are considered as active elements that are able to reduce generation-side fluctuations and contribute to the frequency control of the network. This can be achieved by assuming that each renewable generator can operate at different levels of efficiency (to which correspond different quantities of generated power) and the switching between these operating points is driven by frequency-dependent functions. The designed control technique is fully decentralized and each turbine acts in an autonomous setting. This choice avoids the huge costs and the potential safety issues related to an additional communication infrastructure but, on the other hand, is a severe constraint and complicates the problem. The difficulties introduced by the decentralized approach can be overcome by adopting a stochastic control strategy: the individual generator randomly switches between its operating points and, at the same time, large populations of turbines perform deterministically.

The preliminary modelling of the single generator dynamics and the wind turbine population has been carried out by Dr David Angeli and is presented in Section 2.2. The stability of the system is assessed in Section 2.3 and the proposed control strategy is described in Section 2.4 where its disturbance-rejection properties are also discussed. Simulation results are finally presented in Section 2.5.

2.2   Modelling: Wind Farm and Network Frequency

The single wind turbine has been modelled as a simple device that extracts mechanical power from the wind, stores it as rotational kinetic energy and releases part of it to the network in the form of electric power. To make the problem amenable for analysis, a first-order model has been chosen. Given the positive parameters α and β, we have:

$$\dot{\omega}(t) = -\beta\omega(t) + w(t) - \alpha\omega(t) \qquad\qquad P = K\alpha\omega^2(t) \qquad\qquad (2.1)$$

where ω is the rotor angular speed of the turbine, $\beta\omega$ is the mechanical friction of the generator while the terms w and $\alpha\omega$ are proportional to wind torque and electrical torque applied by the turbine, respectively. The corresponding generated power P will be given by the product of $\omega \times \alpha\omega = \alpha\omega^2$ for some positive constant K. The model, despite its simplicity, captures the main power flows involved in a realistic scenario and makes for a challenging control problem that constitutes a meaningful starting point if more accurate representations of the turbine need to be considered. If the term w is assumed to be constant, it is straightforward to calculate the angular speed at equilibrium ω^e and the corresponding generated power P^e:

$$\omega^e = \frac{w}{\alpha + \beta} \qquad P^e = K\alpha\frac{w^2}{(\alpha + \beta)^2} \qquad\qquad (2.2)$$

If one considers P^e as a function of α it can be noted that, independently from wind torque, it has a maximum for $\alpha = \beta$. Suppose now that each turbine can set α to two distinct values and switch between the point of optimal efficiency ($\alpha_1 = \beta$) and another operating point achieved with $\alpha_2 = \gamma\beta$ for some $\gamma \neq 1$. For this purpose a stochastic algorithm is adopted and transitions occur according to frequency-dependent switching functions $\lambda_1(f)$ and $\lambda_2(f)$ which will be designed later on. The probability that the switching from α_1 to α_2 will take place in the interval $(t, t + dt]$ is given by $\lambda_1(f(t))dt$ (for the transition in the opposite sense one must consider $\lambda_2(f(t))$). The switching function can therefore be interpreted as the instantaneous rate at which the corresponding transition occurs. With this approach, the population of turbines can generate different quantities of power with respect to the same wind torque and therefore provide frequency response. From the mathematical point of view, each turbine can be described as a stochastic hybrid system with two discrete states [33], as summarized in Fig. 2.2. We remark that in our idealized model transitions between these states are instantaneous but in real applications a delay would be involved.

In a practical implementation of this model, the individual turbine will monitor the network frequency $f(t)$ and update its operating mode according to the following algorithm
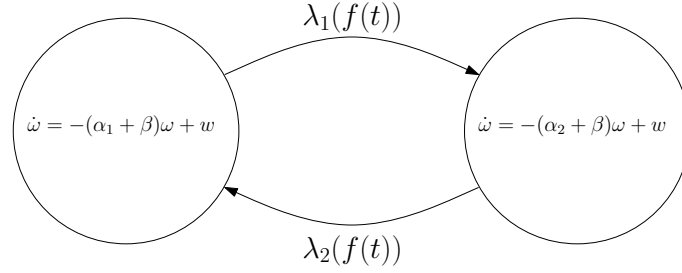
FIGURE 2.2: Turbine model as a stochastic hybrid system.

[34], where RND denotes a random number uniformly distributed in the interval $[0, 1]$:

- When the turbine enters the optimal mode $(\alpha = \alpha_1 = \beta)$ at time t:

  1. Set $t_0 = t$ and $r = $ RND.

  2. Start evaluating the integral $I(t) = \int_{t_0}^{t} \lambda_1(f(\tau))d\tau$.

  3. Switch to suboptimal operating mode at time t'
     for which $I(t') \geq -\ln(r)$.

- When the turbine enters suboptimal mode $(\alpha = \alpha_2 = \gamma\beta)$ at time t:

  1. Set $t_0 = t$ and $r = $ RND.

  2. Start evaluating the integral $I(t) = \int_{t_0}^{t} \lambda_2(f(\tau))d\tau$.

  3. Switch to optimal operating mode at time t'
     for which $I(t') \geq -\ln(r)$.

The unnormalized pdf of the generator speed in the optimal $(\alpha_1 = \beta)$ and suboptimal $(\alpha_2 = \gamma\beta)$ regimes of operation, denoted respectively by $\rho_+(t, \omega)$ and $\rho_-(t, \omega)$, are now introduced. Their evolution can be described by the following set of Kolmogorov forward equations [35]:

$$
\begin{aligned}
\frac{\partial \rho_+}{\partial t} &= -\frac{\partial}{\partial \omega}\left[\rho_+ \cdot (-(\alpha_1 + \beta)\omega + w)\right] - \lambda_1(f)\rho_+ + \lambda_2(f)\rho_- \\
\frac{\partial \rho_-}{\partial t} &= -\frac{\partial}{\partial \omega}\left[\rho_- \cdot (-(\alpha_2 + \beta)\omega + w)\right] - \lambda_2(f)\rho_- + \lambda_1(f)\rho_+
\end{aligned}
\tag{2.3}
$$

Even if, in general, equations (2.3) do not admit a closed-form solution, it is possible to obtain a set of ODEs which describe the time evolution of the associated (uncentered) low-order moments, defined as follows:

$$
\pi_+(t) = \int_{-\infty}^{+\infty} \rho_+(t, \omega)\, d\omega \quad \omega_+(t) = \int_{-\infty}^{+\infty} \omega\rho_+(t, \omega)\, d\omega \quad W_+(t) = \int_{-\infty}^{+\infty} \omega^2\rho_+(t, \omega)\, d\omega
$$

$$
\pi_-(t) = \int_{-\infty}^{+\infty} \rho_-(t, \omega)\, d\omega \quad \omega_-(t) = \int_{-\infty}^{+\infty} \omega\rho_-(t, \omega)\, d\omega \quad W_-(t) = \int_{-\infty}^{+\infty} \omega^2\rho_-(t, \omega)\, d\omega
$$

$$
\tag{2.4}
$$

Assuming sufficiently smooth density functions of bounded support, taking derivatives with respect to time in (2.4) and integrating by parts where needed yields:

$$
\begin{aligned}
\dot{\pi}_+(t) &= -\lambda_1(f)\pi_+(t) + \lambda_2(f)\pi_-(t) \\
\dot{\pi}_-(t) &= -\lambda_2(f)\pi_-(t) + \lambda_1(f)\pi_+(t) \\
\dot{\omega}_+(t) &= -(\alpha_1 + \beta + \lambda_1(f))\omega_+(t) + \lambda_2(f)\omega_-(t) + w\pi_+(t) \\
\dot{\omega}_-(t) &= -(\alpha_2 + \beta + \lambda_2(f))\omega_-(t) + \lambda_1(f)\omega_+(t) + w\pi_-(t) \\
\dot{W}_+(t) &= -(2\alpha_1 + 2\beta + \lambda_1(f))W_+(t) + 2w\omega_+(t) + \lambda_2(f)W_-(t) \\
\dot{W}_-(t) &= -(2\alpha_2 + 2\beta + \lambda_2(f))W_-(t) + 2w\omega_-(t) + \lambda_1(f)W_+(t)
\end{aligned}
\tag{2.5}
$$

where $\alpha_1 = \beta$ and $\alpha_2 = \gamma\beta$ for some $\gamma \neq 1$. In addition, the following conservation law is fulfilled:

$$
\pi_+(t) + \pi_-(t) = 1 \quad \forall t \in \mathbb{R}
\tag{2.6}
$$

Remark 2.1. A deterministic interpretation can be provided for the moments of ρ_+ and ρ_- if one considers large populations of identical turbines. In particular, π_+ and π_- represent the fraction of generators in the two regimes of operation. Moreover, W_+ and W_- denote the average value of the squared rotor speed ω in the two cases. Considering (2.1) and introducing N as a rescaling factor, it is possible to define the total power P_{TOT} generated by the wind farm population:

$$
P_{TOT}(t) = N \cdot K \left(\alpha_1 W_+(t) + \alpha_2 W_-(t)\right)
\tag{2.7}
$$

Analysis of system (2.5) is straightforward given its cascaded structure and its linearity with respect to state-variables. In fact, for each constant input f, there exists a unique globally asymptotically stable equilibrium $x^e(f)$ which we define as:

$$
x^e(f) = \left[\pi_+^e(f) \ \pi_-^e(f) \ \omega_+^e(f) \ \omega_-^e(f) \ W_+^e(f) \ W_-^e(f)\right]'.
\tag{2.8}
$$

Similarly, the aggregate power at equilibrium corresponds to:

$$
P_{TOT}^e(f) = N \cdot K \left(\alpha_1 W_+^e(f) + \alpha_2 W_-^e(f)\right)
$$

To provide some additional properties for system (2.5) and its equilibrium state x^e, it is useful to introduce the following assumption:

Assumption 2.1. *The transition rates $\lambda_1(f)$ and $\lambda_2(f)$ are nonnegative and, respectively, monotonic increasing and decreasing functions of the network frequency f. This is coherent with the balancing task to be performed by the turbines: when frequency decreases a higher number of turbines will switch to the operation mode of maximum efficiency, generating an higher amount of power, and vice versa.*

It is now possible to state the following for the total power at equilibrium:

Proposition 2.1. *Consider system (2.5) with a constant input f. If $\alpha_1 = \beta \neq \alpha_2$, the quantity $P_{TOT}^e(f)$ is monotonic decreasing with respect to f.*

Proof. The states at equilibrium W_+^e and W_-^e are denoted with a hat subscript when computed as functions of the switching rates $\hat{\lambda}_1 = \lambda_1(f)$ and $\hat{\lambda}_2 = \lambda_2(f)$. Explicit calculations show that, when $\alpha_1 = \beta \neq \alpha_2$, it holds:

$$\frac{\partial}{\partial\hat{\lambda}_1}\left(\alpha_1\hat{W}_+^e(\hat{\lambda}_1,\hat{\lambda}_2) + \alpha_2\hat{W}_-^e(\hat{\lambda}_1,\hat{\lambda}_2)\right) < 0 \quad \frac{\partial}{\partial\hat{\lambda}_2}\left(\alpha_1\hat{W}_+^e(\hat{\lambda}_1,\hat{\lambda}_2) + \alpha_2\hat{W}_-^e(\hat{\lambda}_1,\hat{\lambda}_2)\right) > 0$$

Hence, given the monotonicity properties of $\lambda_1(f)$ and $\lambda_2(f)$ presented in Assumption 2.1, from the application of the chain rule it follows that:

$$\frac{dP_{TOT}^e(f)}{df} = N \cdot K \cdot \frac{d}{df}\left(\alpha_1\hat{W}_+^e(\lambda_1(f),\lambda_2(f)) + \alpha_2\hat{W}_-^e(\lambda_1(f),\lambda_2(f))\right) \leq 0$$

<div align="right">□</div>

2.2.1 Frequency Representation and Analysis of Equilibria

In order to design the switching functions $\lambda_1(\cdot)$ and $\lambda_2(\cdot)$, which constitute the core of the proposed distributed control, it is necessary to determine the relationship between load variations and the frequency of the network. To this end, we denote as d the power balance in the system between other kinds of generation and demand, introduce the positive constants k and k_1 and model the network frequency with a first order linear system:

$$\begin{aligned}\dot{f}(t) &= -kf(t) + k_1[P_{TOT}(t) + d(t)]\\&= -kf(t) + k_1[NK(\alpha_1 W_+(t) + \alpha_2 W_-(t)) + d(t)]\end{aligned} \tag{2.9}$$

Coherently with the qualitative description of the power system provided in Section 2.1.1, when the difference between generation and demand (represented in the present case by $P_{TOT} + d$) is negative the frequency will decrease and the opposite will occur when $P_{TOT} + d$ is positive. The choice of a simple model for the network frequency has been made in order to simplify the analysis and it does not introduce loss of generality as long as the network can be modelled by a passive linear transfer function. In this case, one can introduce a pre-filter in each frequency sensor device in order to perform a suitable pole-zero cancellation so that the network is seen as a first order system with respect to this filtered signal. Hence, the set of equations (2.5) and (2.9) represent a full description of the closed-loop system constituted by the wind farm and the electric network, as shown in Fig. 2.3.
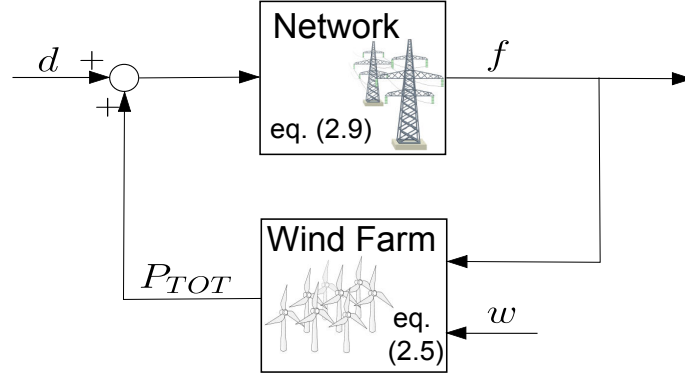
FIGURE 2.3: Block representation of the closed-loop system.

To study the equilibria of this system consider that (2.9), for the frequency f^e at equilibrium, becomes:

$$0 = -kf^e + k_1(P^e_{TOT}(f^e) + d^e)$$

where $P^e_{TOT}(f)$ is the map $f \to NK(\alpha_1 W^e_+(f) + \alpha_2 W^e_-(f))$.

Proposition 2.2. *For constant values of d^e and w, the system described by (2.5) and (2.9) admits a unique equilibrium when $\alpha_1 = \beta \neq \alpha_2$.*

Proof. Taking into account that the open-loop system (2.5) has an equilibrium for any positive value of f, the equilibria of the closed-loop system will be given by the intersection of the curves $kf - k_1 d^e$ and the positive quantity $k_1 P^e_{TOT}(f)$. Since $\alpha_1 = \beta \neq \alpha_2$, it follows from Proposition 2.1 that $k_1 P^e_{TOT}(f)$ is monotonically decreasing with respect to the frequency f. Given that $kf - k_1 d^e$ is linear with positive slope, we can conclude that a single equilibrium exists in the positive orthant for all feasible values of parameters and it is denoted by X^e:

$$X^e = \begin{bmatrix} \pi^e_+(f^e) & \pi^e_-(f^e) & \omega^e_+(f^e) & \omega^e_-(f^e) & W^e_+(f^e) & W^e_-(f^e) & f^e \end{bmatrix}'. \qquad (2.10)$$

$\square$

2.3 Stability Analysis

2.3.1 Local Stability Properties

The analysis on the properties of the equilibrium point (2.10) has been carried out performing a linearization of the closed-loop system equations. The second equation in (2.5) has been replaced with (2.6), denoting the state variable by $\bar{X} = X - X^e$. Considering implicitly the dependency of the equilibrium values from f^e for a more compact notation

and assuming differentiability of the switching functions at the equilibrium frequency, the linearized system about the equilibrium point X^e can be described by the following equations:

$$\dot{\bar{\pi}}_+ = -(\lambda_1(f^e) + \lambda_2(f^e))\bar{\pi}_+ - \left(\dot{\lambda}_1(f^e)\pi_+^e - \dot{\lambda}_2(f^e)(1 - \pi_+^e)\right)\bar{f}$$

$$\dot{\bar{\omega}}_+ = -(\alpha_1 + \beta + \lambda_1(f^e))\bar{\omega}_+ + \lambda_2(f^e)\bar{\omega}_- + w\bar{\pi}_+ - \left(\dot{\lambda}_1(f^e)\omega_+^e - \dot{\lambda}_2(f^e)\omega_-^e\right)\bar{f}$$

$$\dot{\bar{\omega}}_- = -(\alpha_2 + \beta + \lambda_2(f^e))\bar{\omega}_- + \lambda_1(f^e)\bar{\omega}_+ - w\bar{\pi}_+ + \left(\dot{\lambda}_1(f^e)\omega_+^e - \dot{\lambda}_2(f^e)\omega_-^e\right)\bar{f}$$

$$\dot{\bar{W}}_+ = -(2\alpha_1 + 2\beta + \lambda_1(f^e))\bar{W}_+ + \lambda_2(f^e)\bar{W}_- + 2w\bar{\omega}_+ - \left(\dot{\lambda}_1(f^e)W_+^e - \dot{\lambda}_2(f^e)W_-^e\right)\bar{f}$$

$$\dot{\bar{W}}_- = -(2\alpha_2 + 2\beta + \lambda_2(f^e))\bar{W}_- + \lambda_1(f^e)\bar{W}_+ + 2w\bar{\omega}_- + \left(\dot{\lambda}_1(f^e)W_+^e - \dot{\lambda}_2(f^e)W_-^e\right)\bar{f}$$

$$\dot{\bar{f}} = -k\bar{f} + k_1(NK(\alpha_1\bar{W}_+ + \alpha_2\bar{W}_-) + \bar{d})$$

$$(2.11)$$

which can be rewritten as:

$$\dot{\bar{X}} = A_l\bar{X} + B_l\bar{d} \qquad (2.12)$$

Furthermore, the equilibrium values for the state components in (2.5) have been analytically calculated with respect to the parameters of the system and the value of the switching functions at equilibrium. Replacing their expressions in (2.11), the matrices A_l and B_l will only be dependent on the parameters α, β, w, the switching functions at equilibrium $\lambda_1(f_e)$ and $\lambda_2(f_e)$ and their derivatives $\dot{\lambda}_1(f_e)$, $\dot{\lambda}_2(f_e)$.

Theorem 2.1. *Assuming differentiable switching functions $\lambda_1(\cdot)$ and $\lambda_2(\cdot)$, the linear system (2.12) is globally exponentially stable for any positive value of w, $\lambda_1(f_e)$ and $\lambda_2(f_e)$ if:*

$$\alpha_1 = \beta \qquad 0 < \alpha_2 \leq \alpha_1 \qquad \dot{\lambda}_1(f^e) > 0 \qquad \dot{\lambda}_2(f^e) < 0$$

Proof. The stability of the system can be proved using the Hurwitz Criterion [36], which allows to verify the sign of the roots for the characteristic polynomial $P_A(s)$ of the matrix A_l. We denote by C_i, with $i = 1\ldots 6$, the leading principal minors of the Hurwitz matrix for $P_A(s)$, reminding that the roots of $P_A(s)$ will all have negative real part if and only if $C_i > 0$ for $i = 1\ldots 6$. We also carry out the substitution $\alpha_1 = \alpha_2 + y$ where y, under the current assumptions, is always greater than or equal to zero. An explicit calculation shows that the Hurwitz determinants C_i are polynomials of positive coefficients in the variables y, α_2, w, $\lambda_1(f_e)$, $\lambda_2(f_e)$, $\dot{\lambda}_1(f^e)$ and $-\dot{\lambda}_2(f^e)$. Since these are all positive or nonnegative quantities, we can conclude that the determinants C_i are greater than zero, all the roots of $P_A(s)$ have negative real parts and therefore the theorem claim is verified. □

It is worth remarking that Theorem 2.1 implies that the closed-loop system described by (2.5) and (2.9) is locally asymptotically stable. Different approaches have been considered to prove global stability: considering quadratic and 1-norm Lyapunov functions, exploiting the positivity of the system parameters to use a Sum of Square (SOS) optimization toolbox [37], [38] and determining local monotonicity properties on certain subsets of the state space. Unfortunately, none of these approaches has provided conclusive results.

2.3.2 Instability Phenomena

Since the local stability of the system has been proved only for $\alpha_2 \leq \alpha_1$, it is worth investigating if any limit cycle or unstable behaviour arises for different values of α_2. In this respect, the following result provides interesting clues:

Theorem 2.2. *If $\alpha_1 = \beta$, $\alpha_2 > \alpha_1$, $\lambda_1(f), \lambda_2(f) \in C^1$, $\Gamma = \dot{\lambda}_1(f^e) = -\dot{\lambda}_2(f^e) \geq 0$, the following holds: for all positive values of w there exists $\Gamma_p > 0$ such that, for $\Gamma < \Gamma_p$, all eigenvalues of the linearized system (2.12) have negative real part while, for $\Gamma = \Gamma_p$, the system has a couple of imaginary eigenvalues.*

Proof. In order to study the eigenvalues of the system, we consider the Hurwitz determinants C_i $(i = 1 \ldots 6)$ for the characteristic polynomial $P_A(s)$ of the matrix A_l in (2.12). Denoting by y the positive term $\alpha_2 - \alpha_1$, explicit calculations provide the following expression for the Hurwitz coefficients:

$$C_i = \sum_{j=0}^{i-1} (-1)^j m_{ij} \Gamma^j \quad i = 1..5$$

(2.13)

$$C_6 = (m_{61} + m_{62}\Gamma)C_5$$

where the polynomials m_{ij} are constituted by monomials with positive coefficients in the nonnegative variables α_1, w, $\lambda_1(f_e)$, $\lambda_2(f_e)$ and y. Notice that the coefficient of the degree 0 term in $P_A(s)$ equals $m_{61} + m_{62}\Gamma$ and it is therefore always positive, ruling out the possibility of eigenvalues in 0. From (2.13) it is possible to verify that all C_i coefficients are positive if $\Gamma = 0$. Furthermore, there exists $\bar{\Gamma}$ such that, for $\Gamma = \bar{\Gamma}$, C_2 is equal to zero while, for $\Gamma > \bar{\Gamma}$, C_2 is negative. Hence, for $\Gamma > \bar{\Gamma}$, the linearized system admits eigenvalues with strictly positive real part. By continuity of eigenvalues with respect to matrix entries, it follows that Γ_p exists as in the claim. $\square$

Theorem 2.2 shows that, for certain values of Γ, a couple of complex eigenvalues of the linearized system crosses the imaginary axis. If we consider the Andronov-Hopf

Bifurcation Theorem [39] we can notice how this condition strongly hints to the presence of a Hopf Bifurcation in the system for $\alpha_2 > \alpha_1$. However, a rigorous proof of this fact is not provided since the additional technical conditions required in [39] are difficult to check in general. We can then conclude that, in order to avoid any periodic solution of the system and, at the same time, arbitrarily choose the slope of the switching functions with respect to frequency, it is necessary to impose $\alpha_2 < \alpha_1$. If one considers (2.2), this corresponds to choose a suboptimal working point with higher angular speed at equilibrium than the optimal one.

2.4 Proposed Control Law

The expressions of the switching functions $\lambda_1(f)$ and $\lambda_2(f)$ which are hereby considered are the following:

$$\lambda_1(f) = \begin{cases} 0 & \text{if } f \leq f_n \\ \Lambda_1 & \text{if } f \geq f_n \end{cases} \qquad \lambda_2(f) = \begin{cases} 0 & \text{if } f \geq f_n \\ \Lambda_2 & \text{if } f \leq f_n \end{cases} \tag{2.14}$$

where Λ_1 and Λ_2 are some positive constants and f_n is the nominal frequency of the power system. Notice that, due to discontinuity of λ_1 and λ_2, the solution of equation (2.5) in feedback to (2.9) needs to be considered in a generalized sense, according to Filippov definition [40]. Existence of such solution is guaranteed if the state derivates are bounded while uniqueness, albeit not theoretically proved, should follow from the structure of the problem and the assumptions on λ_1 and λ_2. Moreover, the last component of the resulting equilibrium point X^e will be exactly at frequency f_n (provided d ranges in a suitable interval) and constitutes a sliding-mode solution. If the switching functions are chosen according to (2.14), the turbines working at the optimal point will possibly switch to the suboptimal mode (with $\alpha = \alpha_2 \neq \beta$) only if the frequency rises over its nominal value while the switching of the other turbines will possibly occur only when the frequency drops below its nominal value.

2.4.1 Rejection of Demand Variations

This choice of the switching functions is seen to achieve a good disturbance rejection at steady-state since the power curve $P^e_{TOT}(f)$, in this case, is vertical around the nominal frequency f_n. If we consider that the steady-state value of the frequency is determined by the intersection of the curve $k_1 P^e_{TOT}(f)$ with the curve $kf - k_1 d^e$, it is evident that considerable variations of d^e will not introduce changes to the value of frequency at equilibrium. In order to quantify the rejection of time-varying load variations the transfer

function $W_{df}(s)$ between the power balance variation $\bar{d}$ and the network frequency variation $\bar{f}$ (considered as output) has been calculated for the linearized system (2.12). In doing so, it is assumed that the derivatives of the switching functions at the equilibrium frequency, for some positive constant Γ, are equal to:

$$\dot{\lambda}_1(f^e) = \Gamma \qquad \dot{\lambda}_2(f^e) = -\Gamma \qquad (2.15)$$

Letting Γ tend to infinity is considered a good local approximation of the nonlinear system when the switching functions are defined according to (2.14). The magnitude of the frequency response for W_{df} has been numerically calculated for increasing values of Γ and the results are shown in Fig. 2.4. The parameters have been chosen in order to achieve a nominal generated power of $2MW$ for the individual turbine, with a reduction of 7% in the suboptimal state:

$$\alpha_1 = \beta = 562.9s^{-1} \qquad \gamma = 0.6 \qquad \alpha_2 = 333.7s^{-1}$$

$$(2.16)$$

$$k = 0.149s^{-1} \qquad f_e = 50Hz \qquad k_1 = 1s^{-2}W^{-1} \qquad N = 1000$$
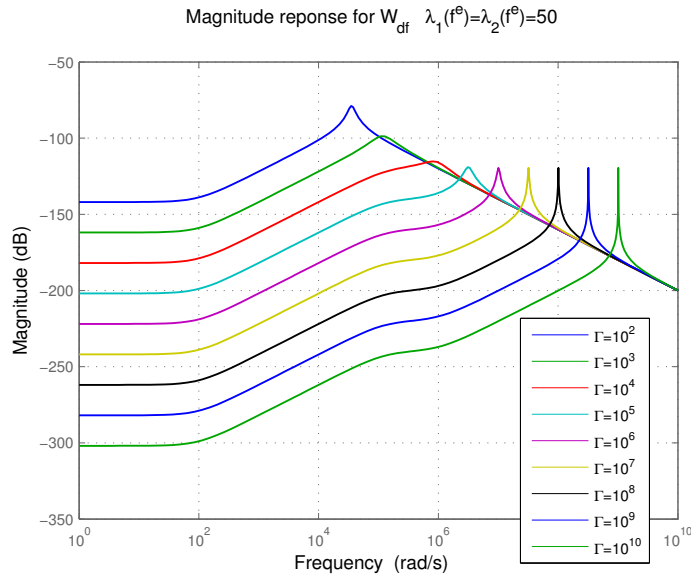
FIGURE 2.4: Magnitude Bode plot of W_{df} for increasing values of Γ.

It can be seen from Fig. 2.4 that higher values of Γ reduce in general the sensitivity of frequency to variations of the signal d which represents the net balance between other sources of generation and total demand. On the other hand, the figure shows a resonance peak that, albeit acceptable, appears not to be reduced to zero by higher values of Γ.

We define $M_d(\Gamma)$ as follows:

$$M_d(\Gamma) = \max_{\omega} |W_{df}(j\omega, \Gamma)| \qquad (2.17)$$

It is possible to analytically calculate the limit of $M_d(\Gamma)$ for Γ that goes to infinity, quantifying the upper bound of the frequency sensitivity to power disturbances achievable by this decentralized approach (dependency from f_e is implicit for a more compact notation):

$$\lim_{\Gamma \to +\infty} M_d(\Gamma) = \frac{W_+^e + W_-^e}{(W_+^e + W_-^e)(k + 2\alpha_1 + 2\alpha_2 + \lambda_1^e + \lambda_2^e) - 2w(\omega_+^e + \omega_-^e)}$$

2.4.2 Rejection of Wind Torque Variations

It has been assumed so far that the wind torque acting on the turbines is constant in time. It is interesting to evaluate what are the effects of variations of w on the system frequency f when the proposed controller is adopted. Similarly to the previous case, the analysis is conducted by linearizing the closed-loop system equations (2.5) and (2.9). In this case the input of the system is $w(t) = w^e + \bar{w}(t)$, where w^e represents the value at equilibrium and $\bar{w}(t)$ is an additional time-varying component. If one assumes that the derivative of the switching functions at f_e is equal to (2.15), it holds:

$$\dot{\bar{\pi}}_+ = -(\lambda_1(f^e) + \lambda_2(f^e))\bar{\pi}_+ - \Gamma\bar{f}$$

$$\dot{\bar{\omega}}_+ = -(\alpha_1 + \beta + \lambda_1(f^e))\bar{\omega}_+ + \lambda_2(f^e)\bar{\omega}_- + w^e\bar{\pi}_+ - \Gamma\left(\omega_+^e + \omega_-^e\right)\bar{f} + \pi_+^e\bar{w}$$

$$\dot{\bar{\omega}}_- = -(\alpha_2 + \beta + \lambda_2(f^e))\bar{\omega}_- + \lambda_1(f^e)\bar{\omega}_+ - w^e\bar{\pi}_+ + \Gamma\left(\omega_+^e + \omega_-^e\right)\bar{f} + (1 - \pi_+^e)\bar{w}$$

$$\dot{\bar{W}}_+ = -(2\alpha_1 + 2\beta + \lambda_1(f^e))\bar{W}_+ + \lambda_2(f^e)\bar{W}_- + 2w^e\bar{\omega}_+ - \Gamma\left(W_+^e + W_-^e\right)\bar{f} + 2\omega_+^e\bar{w}$$

$$\dot{\bar{W}}_- = -(2\alpha_2 + 2\beta + \lambda_2(f^e))\bar{W}_- + \lambda_1(f^e)\bar{W}_+ + 2w^e\bar{\omega}_- + \Gamma\left(W_+^e + W_-^e\right)\bar{f} + 2\omega_-^e\bar{w}$$

$$\dot{\bar{f}} = -k\bar{f} + k_1(NK(\alpha_1\bar{W}_+ + \alpha_2\bar{W}_-) + \bar{d})$$

$$(2.18)$$

We denote now by W_{wf} the transfer function between $\bar{w}$ and the frequency variation $\bar{f}$, considered as an output of the system. The magnitude response for increasing values of Γ, adopting the parameters in (2.16), is shown in Fig. 2.5. As in the case of variations on the power balance d, letting Γ tend to infinity is considered a good approximation of the discontinuous switching functions presented in (2.14). It can be noticed that, in general, a consistent attenuation is achieved for increasing values of Γ. The main difference with respect to the previous case is that the resonance peak, albeit still present, tends to

zero when Γ goes to infinity. If one introduces $M_w(\Gamma) = \max_\omega |W_{wf}(j\omega, \Gamma)|$, explicit calculations show the following:

$$\lim_{\Gamma \to +\infty} M_w(\Gamma) = 0$$
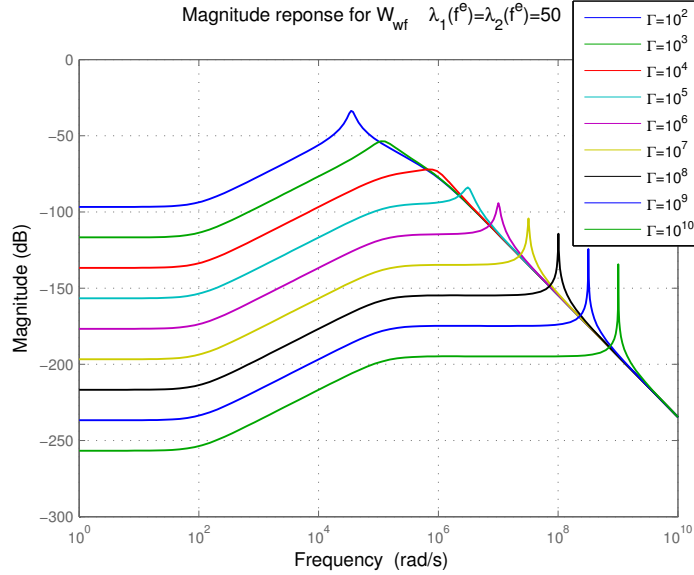
FIGURE 2.5: Magnitude Bode plot of W_{wf} for increasing values of Γ.

2.5 Simulation Results

In order to validate the design approach presented in this chapter, the performance of the distributed controller is evaluated in simulation. We consider turbines with power rating $P_r = 2MW$, generated at the optimal operation mode ($\alpha_1 = \beta$) at equilibrium. The wind farm is composed by 1000 elements and operates within an electric network where, at the initial time $t = 0$ of simulation, the total power generation from other sources amounts to $10GW$ and the power balance d is equal to zero.

2.5.1 Scenario 1a - Frequency Drop in Stable Configuration

In this scenario a loss of $90MW$ in the generation (or an equivalent increase of demand) occurs in the system at $t = 0.1s$, when 90% of the turbines are working at the suboptimal operating point with $\pi_+(0.1) = 0.1$ and $\pi_-(0.1) = 0.9$. A stable configuration has been chosen ($\alpha_2 < \alpha_1$), using the parameters considered in (2.16) and assuming $\Lambda_1 = \Lambda_2 = 15$. The network frequency f, the total power balance $d + P_{TOT}$ in the network and the

wind-generated power P_{TOT} are shown in Fig. 2.6. Note that the stochastic controller is able to compensate the frequency drop resulting from the generation loss in about $0.3s$, properly varying the power generated by the wind farm.
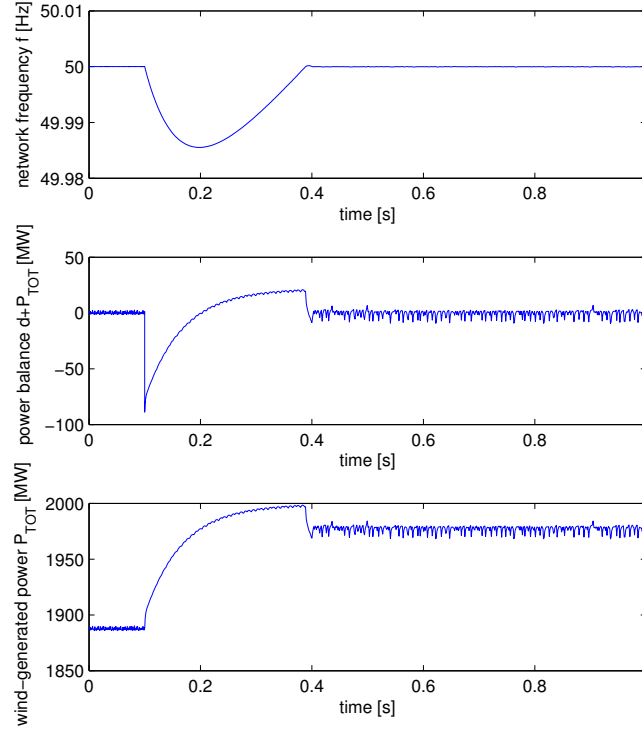
FIGURE 2.6: Simulation of a power loss for the system in stable configuration.

2.5.2 Scenario 1b - Frequency Drop in Unstable Configuration

The same event of Scenario 1a is simulated with an unstable configuration: the values of the parameters correspond to the ones in (2.16), with the exceptions of $\gamma = 1.8$ and consequently $\alpha_2 = 1013 > \alpha_1$. The results in Fig. 2.7 show that, coherently with the analysis of Section 2.3.2, the system has a periodic solution for $\alpha_2 > \alpha_1$.

2.5.3 Scenario 2 - Rejection of Disturbances on Power Balance

In this case the capability of the controller to reject variations of the power balance d has been tested. A sinusoid $d_d(t) = 50sin(2\pi t)MW$ has been added to the constant signal d^e when the fraction of turbines that are initially operating at the optimal and suboptimal point is equal ($\pi_+(0) = \pi_-(0) = 0.5$). The results in Fig. 2.8 show that a consistent rejection is achieved and the oscillations introduced by the disturbance d_d on the network frequency are minimal.
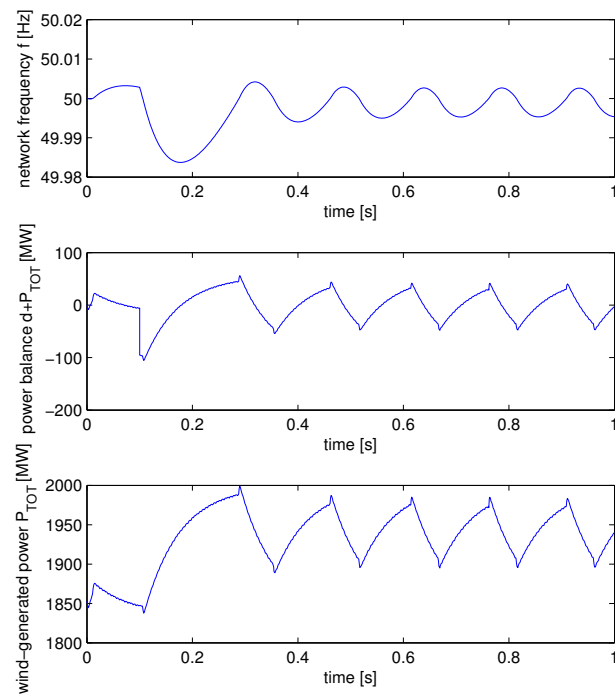
FIGURE 2.7: Simulation of a power loss for the system in unstable configuration.
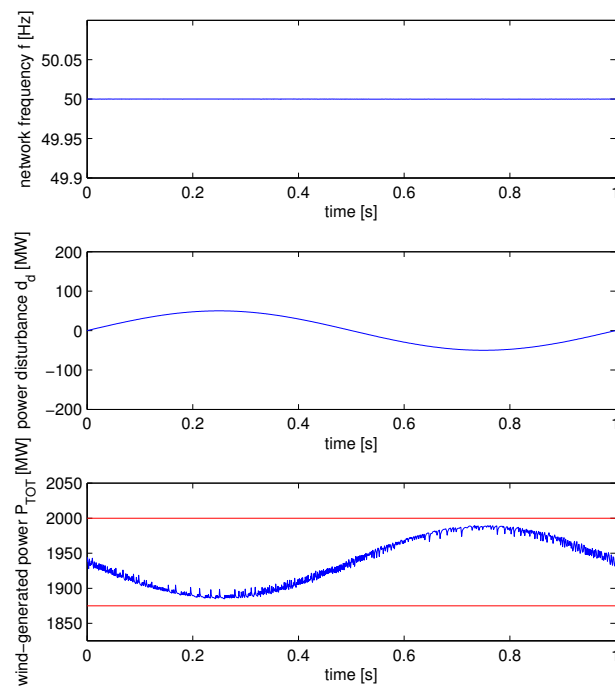
FIGURE 2.8: Simulation of a sinusoidal disturbance d_d on the power balance d (in red the minimum and maximum power that the wind farm is able to generate for the considered constant wind torque).

2.6   Conclusions

A distributed approach is proposed for frequency control with wind turbines. This choice allows to overcome some disadvantages of deterministic control strategies, avoiding synchronization of the generators and undesired frequency overshoots. The single generator is modelled as a stochastic hybrid system that can operate in two discrete states, to which correspond different levels of efficiency and generated power. The transitions between these states are random and driven by frequency dependent switching functions. In this way the behaviour of the individual generators is stochastic, while large populations of turbines perform deterministically, changing the total generated power in response to frequency variations. Furthermore, the implementation of the control strategy does not require any additional communication infrastructure. The robust stability and the disturbance rejection of the proposed control strategy have firstly been theoretically proved and then showed in simulations.

Chapter 3

Scheduling of Wind Turbines for Frequency Response

In this chapter the provision of frequency response from variable-speed wind turbines is obtained through temporary overproduction. The turbines move from the steady-state operating point of maximum efficiency, reducing the rotor angular speed and releasing part of their kinetic energy. Two different approaches are considered, assuming that the electric torque of the generators follows two given expressions or can instead be arbitrarily set. In both cases the scheduling of the turbines is determined in order to guarantee extra power production following a fault in the power system, maximizing the time of frequency support provision or reducing energy losses. Finally, the recovery problem is analyzed, determining the optimal control strategy which brings back the turbines to the original working point of maximum efficiency after having provided frequency response.

3.1 Introduction

The problem of frequency control with variable-speed wind turbines is tackled with a deterministic approach. As in the previous chapter, the control effort is distributed among the whole turbines population. The aim is to increase the power provided by the wind farm after the trip of a large generating plant in order to reduce the resulting frequency fall. The control strategy is designed as a constrained optimization, maximizing the time of frequency response provision of the wind farm or minimizing the energy losses of the generators. Differently from Chapter 2, where a fraction π_- of turbines was operating, in steady-state, at a suboptimal working point, it is now assumed that in normal operative conditions all generators are running at maximum efficiency. Following a fault in the network, the resulting frequency response is an increase in power

47

generation, obtained by slowing down the turbines and releasing part of the kinetic energy stored in their rotating shafts. A different model is introduced to characterize the mechanical dynamics of the generators and take into account the relationship between the rotor speed of the turbine and the corresponding efficiency of power absorption from the wind. Two different approaches are then considered: one assumes that, in order to provide extra power, the turbines can switch to an overproduction mode, applying an extra torque step. The switching rate to the second mode and the permanence time of the generators in this state become the control inputs of the turbine scheduling and are designed in order to maximize the time of frequency response. A second possibility is to assume that the generated power of each machine can be arbitrarily set (within the operational limits of the generator): in this case the scheduling minimizes the energy losses caused by the turbines slowing down and reducing their efficiency. Finally, the inverse problem of recovery is considered: after having provided frequency response and reduced their kinetic energy, the turbines are brought back to their operating point of maximum efficiency.

The rest of this Chapter is structured as follows: the model for the turbine dynamics and power absorption from the wind is described in Section 3.2. The two approaches for the scheduling of wind turbines are presented respectively in Section 3.3 and 3.4 while the problem of recovery is tackled in Section 3.5.

3.2 Modelling

The single wind turbine has been modelled in its mechanical part as a rotating mass, describing its angular speed ω by the swing equation:

$$\dot{\omega} = \frac{1}{J}(T_m - T_e) \tag{3.1}$$

where J is the total moment of inertia, T_m is the mechanical torque extracted from the wind and T_e is the electric torque used to generate power. The electrical dynamics of the turbine are much faster than the mechanical ones and therefore have been neglected. The additional control loop which determines the electrical quantities of rotor and stator in order to achieve a certain torque T_e is not considered and T_e directly represents the control input of the system. If we denote by v the wind speed, by R the radius of the rotor and by μ the air density, the power of the wind P_w and the corresponding mechanical torque acting on the turbine are:

$$P_w = \frac{\mu \pi R^2 v^3}{2} \qquad T_m = \frac{P_w \bar{C}(\lambda, \theta)}{\omega} \tag{3.2}$$

The power coefficient $\bar{C}$ represents the fraction of wind power which is captured by the turbine and is dependent on the tip-speed ratio $\lambda = \frac{\omega R}{v}$ and the blades pitch angle θ. For instance, in the simulation section, the formulation proposed by [41] will be considered:

$$\bar{C}(\lambda, \theta) = 0.22 \left(\frac{116}{\lambda_i} - 0.4\theta - 5 \right) e^{-\frac{12.5}{\lambda_i}} \qquad \frac{1}{\lambda_i} = \frac{1}{\lambda + 0.08\theta} - \frac{0.035}{\theta^3 + 1} \qquad (3.3)$$

For the wind speed v and the pitch angle θ, the following assumptions are introduced:

Assumption 3.1. *Given the relatively short time interval to be considered for the frequency response of the turbines, it is reasonable to assume that the wind speed v is constant in time. Furthermore, if one excludes high wind conditions, pitch angle actions are not applied and the angle θ is constant and equal to zero. In this scenario, the power coefficient can be defined exclusively as a function of the rotor speed ω and wind speed v:*

$$C(\omega, v) = \bar{C} \left(\frac{\omega R}{v}, 0 \right) \qquad (3.4)$$

A diagram of the wind turbine model, with a representation of the current assumptions, is presented in Figure 3.1. The Optimal Power Point Tracking block (OPPT) is the controller which is used in normal operation and determines the reference of electric torque $T_{e_{ref}}$ in order to achieve maximum efficiency. The frequency control strategies presented in the next sections will bypass this block and directly determine T_e when a frequency event occurs.
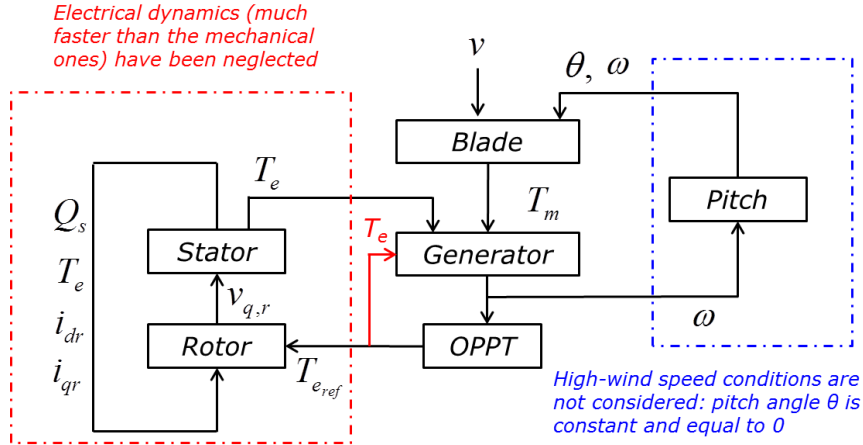
FIGURE 3.1: Block representation of the individual wind turbine. Source: [2].

3.3 Two-modes Scheduling

In this first formulation each turbine can only operate in two modes, one corresponding to maximum power extraction at steady state and one characterized by a slower suboptimal

equilibrium. By switching to the second mode, the wind turbine reduces its kinetic energy and is able to temporarily generate more power. This policy can be desirable if one wants to slow down only a fraction of the wind farm while waiting for secondary response services to take over. In this case, in order to coordinate the switching of each generator between the two modes, centralized management of the turbines is required.

For a constant wind speed v (assumed equal for all turbines), the two modes correspond to different choices of the electrical torque T_e. In one case it is desirable to operate at the rotor speed ω_{ss} (and at the resulting tip-speed ratio $\lambda_{ss} = \omega_{ss}R/v$) that optimizes the C coefficient and guarantees maximum efficiency. This is done by setting the electric torque T_e equal to the reference $T_{e_{ref}}$ of the OPPT controller, which can be described by the following function T_+ [22]:

$$T_+(\omega) = \frac{\mu\pi R^5 C(\omega_{ss}, v)}{2\lambda_{ss}^3}\omega^2 = K_T\omega^2 \tag{3.5}$$

Denoting by ω_+ the rotor speed in the first operation mode and replacing (3.2) and (3.5) in the swing equation (3.1), we obtain:

$$\dot{\omega}_+ = \frac{P_w}{J}\frac{\omega_{ss}^3 C(\omega_+, v) - \omega_+^3 C(\omega_{ss}, v)}{\omega_{ss}^3\omega_+} \tag{3.6}$$

It is straightforward to verify that ω_{ss} is an equilibrium point for (3.6) and it can be easily proved, by linearization of the system, that such equilibrium is locally asymptotically stable. The wind turbines are able to provide frequency response by switching to the second operation mode, where an additional torque T_f is applied, slowing down the turbine and releasing part of its kinetic energy to the network:

$$\dot{\omega}_- = \frac{P_w}{J}\frac{\omega_{ss}^3 C(\omega_-, v) - \omega_-^3 C(\omega_{ss}, v)}{\omega_{ss}^3\omega_-} - \frac{T_f}{J} \tag{3.7}$$

Remark 3.1. Several factors must be taken into account when choosing T_f: operative constraints on the rotor speed ω can be satisfied by setting the additional torque in such a way that the suboptimal equilibrium speed for (3.7) is acceptable. High values of T_f must also be avoided, in order to limit the mechanical stress on the switching turbines.

Given their particular structure and the complicated expression of C, it has not been possible to solve the equations (3.6) and (3.7) analytically, however, their solutions are straightforward to obtain numerically. If we denote by $\phi_+(\omega_{IN}, t)$ and $\phi_-(\omega_{IN}, t)$, respectively, the solutions of (3.6) and (3.7) at time t with initial condition $\omega(0) = \omega_{IN}$, the corresponding power generated by the turbine in the two modes is:

$$P_+(\omega_{IN}, t) = K_T\phi_+^3(\omega_{IN}, t) \qquad P_-(\omega_{IN}, t) = K_T\phi_-^3(\omega_{IN}, t) + T_f\phi_-(\omega_{IN}, t) \tag{3.8}$$

We consider a population of turbines where the single generator, at each time instant, can operate according to (3.6) or (3.7). All turbines are initially in the first mode (with $+$ subscript) and the control input $\rho(t)$ determines the rate at which they commute to the second operation mode (with $-$ subscript) at time t. Generators switching to the second mode at t will operate according to (3.7) for $\Theta(t)$ seconds, where Θ is a second control input, and then switch back and remain in the first mode (further transitions are not considered). For large populations, one can assume that the switching rate $\rho(t)$ can be set to any positive value, provided that the fraction of available turbines in the first mode, at time t, is greater than 0. Notice that turbines switching at the same time are constrained to commute back to the original mode simultaneously. This hypothesis makes the analysis of the system easier and does not limit its performance, as shown later on.

3.3.1 Maximization of Frequency Support Time

We want to understand what is the choice of $\rho(\cdot)$ and $\Theta(\cdot)$ that guarantees the best frequency response. We will do so by considering the following scenario: a frequency drop is detected at $t = 0$ and a fraction ρ_0 of turbines instantly switches to the second mode. The aggregate power P_{TOT} generated by the turbines population instantly increases from P_0 to $P_0 + \Delta P$. If one considers the positive constant K as a rescaling factor, the power increase is equal to $\Delta P = K T_f \omega_{ss} \rho_0$. This scenario of extra power generation can be modelled by a switching function $\rho(t)$ that presents a Dirac pulse of amplitude ρ_0 at $t = 0$. Our optimality criterion will be the maximization of the time interval $[0, T_{END}]$ during which it is possible to provide the extra generation ΔP or, equivalently, impose that $\dot{P}_{TOT}(t) = 0$ for all $t \in (0, T_{END}]$. Denoting by $\mathbb{D}$ the set of integrable distributions with non negative values, the optimization problem corresponds to:

$$\max_{\rho(\cdot), \Theta(\cdot), T_{END}} T_{END}$$

$$\text{s.t.} \quad \int_{0+}^{T_{END}} \rho(t) \, dt = 1 - \rho_0 \tag{3.9}$$

$$\dot{P}_{TOT}(t) = 0 \qquad \forall t \in (0, T_{END}]$$

$$\rho(\cdot) \in \mathbb{D}$$

To calculate the optimal $\rho^*(\cdot)$ and $\Theta^*(\cdot)$ for (3.9), a slightly different problem is initially studied, removing the integral constraint on ρ and fixing the final time T_{END}:

$$\min_{\rho(\cdot), \Theta(\cdot)} \int_{0+}^{T_{END}} \rho(t) \, dt$$

$$\text{s.t.} \quad \dot{P}_{TOT}(t) = 0 \qquad \forall t \in (0, T_{END}] \tag{3.10}$$

$$\rho(\cdot) \in \mathbb{D}$$

Some additional notation and properties, required for the resolution of these two problems, are detailed next while the main results are provided in Section 3.3.3.

3.3.2 Preliminary Operations

The power generated by a single turbine at time t, if this has switched to the second mode at $t = 0$ and switched back to the first mode at $t = \theta$, is denoted by $P_G(t, \theta)$ and has the following expression:

$$
P_G(t, \theta) = \begin{cases} P_-(\omega_{ss}, t) & \text{if } t < \theta \\\\ P_+(\phi_-(\omega_{ss}, \theta), t - \theta) & \text{if } t \geq \theta \end{cases} \tag{3.11}
$$

A graphical representation is provided using the parameters presented in the simulation section. The generated power $P_G(t, 5)$ and the resulting rotor speed ω (blue) are compared in Fig. 3.2 with the corresponding quantities of a turbine that always operates in the first mode (red). In the time interval which goes from $t = 0$ to $t = \theta = 5s$, the turbine in the second mode generates more power, at the cost of a reduction of its rotor speed. When the generator switches back to the first mode, the extra torque step T_f is no longer applied: the electric torque (and consequently the generated power) instantly decrease, causing an acceleration of the turbine.
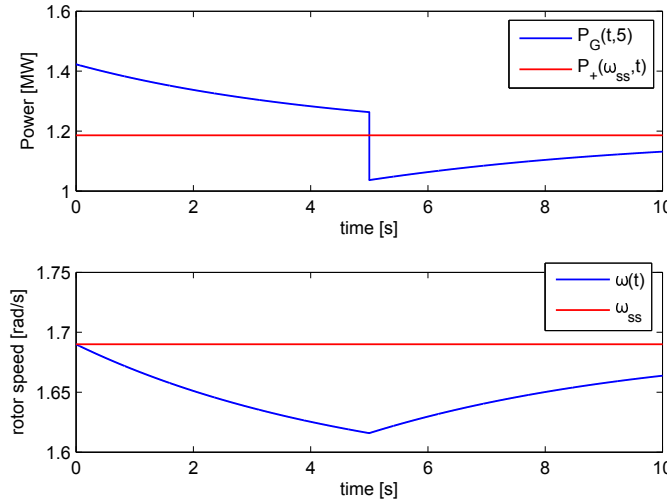
FIGURE 3.2: Comparison of generated power and rotor speed between a turbine that remains in mode 1 (red) and one that switches to the second mode at $t = 0s$ and switches back at $t = \theta = 5s$ (blue)

It is straightforward to derive from (3.11) the rate of switching $\eta(t, \theta)$ that compensates the power variation introduced at time t by a unitary fraction of turbines ($\rho_0 = 1$)

switching at $t = 0$ and undergoing a switch back to the initial mode after θ seconds. Considering that the time derivative of $P_G(t, \theta)$ is defined everywhere except for $t = \theta$ and denoting as δ the Dirac delta, we deduce:

$$\eta(t, \theta) = \begin{cases} -\dfrac{1}{T_f \omega_{ss}} \dfrac{\partial P_G(t, \theta)}{\partial t} & \text{if} \quad t \neq \theta \\ \dfrac{\phi_-(\omega_{ss}, \theta)}{\omega_{ss}} \delta(t - \theta) & \text{if} \quad t = \theta \end{cases} \tag{3.12}$$

Remark 3.2. It is important to point out that, when (3.10) is considered, $\rho(t)$ is unequivocally defined by the constraint $\dot{P}_{TOT}(t) = 0$ and the choice of $\Theta(\cdot)$. Given that turbines remaining in the first mode have constant power derivative, at each time instant t the switching rate ρ must be determined in order to compensate the power variations of the generators that have switched to the second mode in the time interval $[0, t)$:

$$\rho(t) = \int_0^{t_-} \eta(t - \tau, \Theta(\tau)) \rho(\tau) \, d\tau \tag{3.13}$$

Furthermore, given the considered initial switching, ρ presents a Dirac delta of amplitude ρ_0 at $t = 0$ and the following equivalent expression can be provided:

$$\rho(t) = \eta(t, \Theta(0)) \rho_0 + \int_{0+}^{t_-} \eta(t - \tau, \Theta(\tau)) \rho(\tau) \, d\tau \tag{3.14}$$

This means that solution of problem (3.10) amounts to optimally select $\Theta(\cdot)$. In this respect, it is useful to extend our notation and, for a given $\Theta(\cdot)$, denote by $\bar{\rho}(t, s)$ the switching rate after t seconds if a unitary fraction of turbines switches at time s (corresponding to a Dirac delta in $\bar{\rho}(t, s)$ at $t = 0$) and the power is kept constant thereafter. Since, at each t, $\bar{\rho}(t, s)$ must compensate the power variations introduced by all turbines that have switched in $[s, s + t)$, we can derive:

$$\bar{\rho}(t, s) = \int_0^{t_-} \eta(t - \tau, \Theta(s + \tau)) \bar{\rho}(\tau, s) \, d\tau = \eta(t, \Theta(s)) + \int_{0+}^{t_-} \eta(t - \tau, \Theta(s + \tau)) \bar{\rho}(\tau, s) \, d\tau \tag{3.15}$$

An alternative representation of $\bar{\rho}(t, s)$ can be obtained considering that, at each time instant t, two different components must be taken into account:

1. Compensation of the initial power variation: $\eta(t, \Theta(s))$

2. Compensation of the cascaded losses introduced at each time instant $\tau < t$ by the first component above: $\eta(\tau, \Theta(s)) \bar{\rho}(t - \tau, s + \tau)$

The resulting expression for $\bar{\rho}(t, s)$ is:

$$\bar{\rho}(t, s) = \eta(t, \Theta(s)) + \int_{0+}^{t_-} \eta(\tau, \Theta(s)) \bar{\rho}(t - \tau, s + \tau) \, d\tau = \int_{0+}^{t} \eta(\tau, \Theta(s)) \bar{\rho}(t - \tau, s + \tau) \, d\tau \tag{3.16}$$

A similar dual definition can be introduced for the integral $\bar{\rho}_I(t, s)$, defined as the cumulative fraction of turbines that switch in the interval $(s, s + t]$, for a given $\Theta(\cdot)$, if a unitary fraction of turbines undergoes switching at s and the total generated power is to be kept constant:

$$\bar{\rho}_I(t, s) = \int_{0+}^{t} \bar{\rho}(\tau, s) \, d\tau \tag{3.17}$$

Proposition 3.1. *The cumulative fraction $\bar{\rho}_I$ satisfies the following integral condition:*

$$\bar{\rho}_I(t, s) = \int_{0+}^{t} \eta(\tau, \Theta(s)) \left[1 + \bar{\rho}_I(t - \tau, s + \tau)\right] ds \tag{3.18}$$

Proof. To show the equivalence of the two expressions for $\bar{\rho}_I$, we initially replace (3.16) in the right-hand side of (3.17):

$$\bar{\rho}_I(t, s) = \int_{0+}^{t} \eta(\tau, \Theta(s)) d\tau + \int_{0+}^{t} \int_{0+}^{\tau-} \eta(x, \Theta(s)) \bar{\rho}(\tau - x, s + x) \, dx \, d\tau$$

By switching the order of integration in the second term and introducing the change of variable $\tilde{\tau} = \tau - x$, we obtain:

$$\bar{\rho}_I(t, s) = \int_{0+}^{t} \eta(\tau, \Theta(s)) \, d\tau + \int_{0+}^{t} \int_{0+}^{t-x} \eta(x, \Theta(s)) \bar{\rho}(\tilde{\tau}, s + x) \, d\tilde{\tau} \, dx$$

It is easy to realize that, moving $\eta(x, \Theta(s))$ out of the integral over $\tilde{\tau}$, the resulting expression is equivalent to (3.18). $\qquad\square$

3.3.3 Optimal Switching Time

It is now possible to provide the following result for the integral minimization problem presented in Section 3.3.1:

Theorem 3.1. *The optimal switching profile $\tilde{\Theta}(\cdot)$ for the optimization problem (3.10) can be defined as follows:*

$$\tilde{\Theta}(t) = \underset{\theta \in (0, T_{END} - t]}{\arg\min} \left[\int_{0+}^{T_{END} - t} \eta(s, \theta) \left[1 + \tilde{\rho}_I(t + s)\right] ds \right] \tag{3.19}$$

where $\tilde{\rho}_I$ satisfies an integral equation solved backwards in time (with $\tilde{\rho}_I(T_{END}) = 0$):

$$\tilde{\rho}_I(t) = \int_{0+}^{T_{END} - t} \eta(s, \tilde{\Theta}(t)) \left[1 + \tilde{\rho}_I(t + s)\right] ds \tag{3.20}$$

Proof. Since the switching rate $\rho(t)$ is linear with respect to the initial fraction ρ_0 of switched turbines, the objective function in (3.10) is equal to $\rho_0 \bar{\rho}_I(T_{END}, 0)$, which in turn is a function of the switching time profile $\Theta(\cdot)$. When this is equal to $\tilde{\Theta}(\cdot)$, it

holds $\tilde{\rho}_I(t) = \bar{\rho}_I(T_{END} - t, t)$. It is now necessary to show that $\rho_0 \tilde{\rho}_I(0)$ is the minimum for the considered optimization problem. In order to so, we introduce a different switching profile $\hat{\Theta}(\cdot)$ which does not satisfy condition (3.19) on a set $\mathcal{T} \subseteq [0, T_{END}]$ of positive measure. Similarly to $\tilde{\rho}_I$, we denote by $\hat{\rho}_I(t)$ the cumulative fraction of turbines $\bar{\rho}_I(T_{END} - t, t)$ when $\Theta = \hat{\Theta}$. It is straightforward to derive the following expression:

$$\hat{\rho}_I(t) = \int_{0+}^{T_{END}-t} \eta(s, \hat{\Theta}(t)) \left[1 + \hat{\rho}_I(t+s)\right] ds \tag{3.21}$$

Consider that, when the switching profile $\hat{\Theta}(\cdot)$ is applied, the objective function in (3.10) is equal to $\rho_0 \hat{\rho}_I(0)$. To show the suboptimality of this choice, we introduce the difference $\rho_D^A(t) = \hat{\rho}_I(t) - \tilde{\rho}_I(t)$ and prove that, under the considered assumptions, it is always positive. Subtracting (3.20) from (3.21) yields:

$$\begin{aligned}
\rho_D^A(t) &= \int_{0+}^{T_{END}-t} [\eta(s, \hat{\Theta}(t)) - \eta(s, \tilde{\Theta}(t))] \left[1 + \tilde{\rho}_I(t+s)\right] ds \\
&+ \int_{0+}^{T_{END}-t} \eta(s, \hat{\Theta}(t)) \rho_D^A(t+s) \, ds \\
&= \rho_D^0(t) + \int_{0+}^{T_{END}-t} \eta(s, \hat{\Theta}(t)) \rho_D^A(t+s) \, ds
\end{aligned} \tag{3.22}$$

It follows from the definition of $\tilde{\Theta}$ in (3.19) that $\rho_D^0(t) \geq 0 \; \forall t \in \mathcal{T}$ and $\rho_D^0(t) = 0$ elsewhere. An equivalent expression for the difference $\hat{\rho}_I(t) - \tilde{\rho}_I(t)$ is given by ρ_D^B:

$$\rho_D^B(t) = \int_t^{T_{END}} \bar{\rho}_D(t, s) \, ds \tag{3.23}$$

where $\bar{\rho}_D(t, s)$ represents the component of $\rho_D^B(t)$ resulting by different values of $\tilde{\Theta}$ and $\hat{\Theta}$ at time s:

$$\bar{\rho}_D(t, s) = \rho_D^0(t)\delta(t - s) + \int_{0+}^{s-t} \eta(\tau, \hat{\Theta}(t))\bar{\rho}_D(t+\tau, s) \, d\tau \tag{3.24}$$

For $s \notin \mathcal{T}$ and $t \leq s$ we have that $\bar{\rho}_D(t, s) = 0$ is a solution of (3.24). To prove the equivalence of ρ_D^A and ρ_D^B we initially notice that they are equal for $t = T_{END}$ and then we show that ρ_D^B satisfies the integral condition in (3.22):

$$\begin{aligned}
\rho_D^B(t) &= \rho_D^0(t) + \int_{t+}^{T_{END}} \bar{\rho}_D(t, s) \, ds = \rho_D^0(t) + \int_{t+}^{T_{END}} \int_{0+}^{s-t} \eta(\tau, \hat{\Theta}(t))\bar{\rho}_D(t+\tau, s) \, d\tau \, ds \\
&= \rho_D^0(t) + \int_{0+}^{T_{END}-t} \int_{t+\tau}^{T_{END}} \eta(\tau, \hat{\Theta}(t))\bar{\rho}_D(t+\tau, s) ds d\tau \\
&= \rho_D^0(t) + \int_{0+}^{T_{END}-t} \eta(\tau, \hat{\Theta}(t))\rho_D^B(t+\tau) \, d\tau
\end{aligned}$$

Consider that $\bar{\rho}_D(t, s)$ fulfils the same kind of integral equation as (3.16) for $\bar{\rho}(s - t, t)$

which, under the considered overproduction regime, is always positive. We can conclude that $\bar\rho_D(t,s) \geq 0$ when $s \in \mathcal{T}$. It follows from $\bar\rho_D(\cdot,s) = 0 \; \forall s \notin \mathcal{T}$ that $\rho_D^B(0) \geq 0$ and therefore $\rho_0 \tilde\rho_I(0)$, obtained applying $\tilde\Theta$ in (3.19), is the minimum for the cost function in (3.10). $\square$

The result of Theorem 3.1 can be interpreted as follows: $\tilde\rho_I(t)$ represents the minimum fraction of turbines which is required to maintain a constant power on the interval $[t, T_{END}]$ if a unit fraction of turbines undergoes switching at time t. Furthermore, $\tilde\rho_I(t)$ is defined by the integral of its values for $s > t$, weighted by the function η. This means that the solution of (3.10), which is proportional to $\tilde\rho_I(0)$, can be obtained by choosing the minimizing switching time $\tilde\Theta$ defined in (3.19) for decreasing values of time. Regarding the integral equation that defines $\tilde\rho_I$ the following result can be provided:

Proposition 3.2. *If $\Theta(\cdot)$ is a positive increasing function of t, there exists one and only one solution for the following integral equation:*

$$x_I(t) = \int_0^{T_{END}-t} \eta(s, \Theta(t)) \left[1 + x_I(t+s)\right] ds \qquad x_I(T_{END}) = 0 \qquad (3.25)$$

Proof. Introducing $\hat t = T_{END} - t$ and $\hat x_I(\hat t) = x_I(T_{END} - \hat t)$ yields:

$$\hat x_I(\hat t) = \int_0^{\hat t} \eta(s, \Theta(T_{END} - \hat t))[1 + \hat x_I(\hat t - s)] \, ds \qquad (3.26)$$

Considering $\hat s = \hat t - s$ we have:

$$\hat x_I(\hat t) = \int_0^{\hat t} \eta(\hat t - \hat s, \Theta(T_{END} - \hat t))[1 + \hat x_I(\hat s)] \, d\hat s \qquad (3.27)$$

Notice from (3.12) that the function $\eta(s, \Theta(t))$, for a fixed t, can be defined as the sum of two contributes: a piecewise continuous function $-\frac{1}{T_f \omega_{ss}} \frac{\partial P_G(s, \Theta(t))}{\partial s}$ (with a discontinuity for $s = \Theta(t)$) and a Dirac pulse for $s = \Theta(t)$. If we introduce $\hat\Theta(\hat t) = \Theta(T_{END} - \hat t)$, equation (3.27) can be rewritten as follows:

$$
\begin{aligned}
\hat x_I(\hat t) \;=\; & \int_0^{\hat t} -\frac{1}{T_f \omega_{ss}} \frac{\partial P_G(\hat t - \hat s, \hat\Theta(\hat t))}{\partial t}[1 + \hat x_I(\hat s)] \, d\hat s \\[2mm]
& + \left[\frac{\phi_-(\omega_{ss}, \hat\Theta(\hat t))}{\omega_{ss}}[1 + \hat x_I(\hat t - \hat\Theta(\hat t))] \right] \cdot \mathbb{1}_{[\hat\Theta(\hat t), T_{END}]}(\hat t)
\end{aligned}
\qquad (3.28)
$$

The function $L(\hat t) = \hat t - \hat\Theta(\hat t)$ is introduced, denoting by L^i the $i-th$ iterate of L. Given the monotonicity assumption on $\Theta(\cdot)$, the function $L(\hat t)$ is monotonic increasing. Considering also that $L(0) < 0$ (the switching time Θ is always greater than 0), it is

possible to partition $[0, T_{END}]$ in n subsets Φ_i defined as follows:

$$\Phi_i = \left\{ \hat{t} : L^i(\hat{t}) < 0 \wedge L^{i-1}(\hat{t}) \geq 0 \right\} \qquad i = 1 \ldots n \tag{3.29}$$

When $\hat{t} \in \Phi_1$ the second term in (3.28) is equal to zero and it is possible to write the equation as a standard Volterra integral equation of the second kind:

$$\hat{x}_I(\hat{t}) = \int_0^{\hat{t}} -\frac{1}{T_f \omega_{ss}} \frac{\partial P_G(\hat{t} - \hat{s}, \hat{\Theta}(\hat{t}))}{\partial t} [1 + \hat{x}_I(\hat{s})] \, d\hat{s} = K_1(\hat{t}) + \int_0^{\hat{t}} K_2(\hat{t}, \hat{s}) \hat{x}_I(\hat{s}) \, d\hat{s} \tag{3.30}$$

where K_1 and K_2 are defined as follows:

$$K_1(\hat{t}) = \int_0^{\hat{t}} -\frac{1}{T_f \omega_{ss}} \frac{\partial P_G(\hat{t} - \hat{s}, \hat{\Theta}(\hat{t}))}{\partial t} \, d\hat{s} \quad K_2(\hat{t}, \hat{s}) = -\frac{1}{T_f \omega_{ss}} \frac{\partial P_G(\hat{t} - \hat{s}, \hat{\Theta}(\hat{t}))}{\partial t}$$

The terms $K_1(\hat{t})$ and $K_2(\hat{t}, \hat{s})$ are bounded and continuous since the point of non differentiability for P_G is outside the integration interval. This implies that (3.30) and therefore (3.25) have one and only one (continuous) solution for $\hat{t} \in \Phi_1$. When $\hat{t} \in \Phi_2$, we can write:

$$\begin{aligned} \hat{x}_I(\hat{t}) &= K_1(\hat{t}) + \int_0^{\hat{t}} K_2(\hat{t}, \hat{s}) \hat{x}_I(\hat{s}) \, d\hat{s} + \left[\frac{\phi_-(\omega_{ss}, \hat{\Theta}(\hat{t}))}{\omega_{ss}} [1 + \hat{x}_I(\hat{t} - \hat{\Theta}(\hat{t}))] \right] \\ &= \bar{K}_1(\hat{t}) + \int_0^{\hat{t}} K_2(\hat{t}, \hat{s}) \hat{x}_I(\hat{s}) \, d\hat{s} \end{aligned} \tag{3.31}$$

In this case $\hat{t} - \hat{\Theta}(\hat{t}) \in \Phi_1$ and, from previous results, $\hat{x}_I(\hat{t} - \hat{\Theta}(\hat{t}))$ is a well defined quantity. It is then possible to group the elements outside the integral in the function $\bar{K}_1(\hat{t})$. By noticing that $K_2(\hat{t}, \hat{s})$ is continuous everywhere except for $\hat{s} = \hat{t} - \Theta(\hat{t})$ and considering that $\bar{K}_1$ has a finite number of discontinuities, we can conclude applying Theorem 1 in [42] (and verifying that the other technical assumptions are satisfied) that (3.31) has one and only one solution when $\hat{t} \in \Phi_1 \cup \Phi_2$ and the same holds for (3.25). By repeating the same procedure for increasing values of i, it is possible to prove existence and uniqueness of the solution in all the other partitions Φ_i with $i = 3 \ldots n$. $\qquad \square$

Additional properties can now be presented for the proposed scheduling, justifying the choice of equal switching time $\Theta(t)$ for turbines that commute to the second mode at some time instant t and allowing to provide results for the original optimization problem (3.9).

Remark 3.3. The hypothesis that the time $\Theta(t)$ of permanence in mode 2 is equal for all turbines is not restrictive. Assume that, for $t = \bar{t}$, the turbines are divided in two groups of size k_1 and k_2 that switch back for $\Theta_1(\bar{t})$ and $\Theta_2(\bar{t})$, which may differ in general. The switching times are determined as the arguments of the minimum for the

following optimization:

$$\min_{\theta_1,\theta_2} \left[\int_{0+}^{T_{END}-\bar{t}} k_1\eta(s,\theta_1) \cdot [1 + \tilde{\rho}_I(t+s)] + k_2\eta(s,\theta_2) \cdot [1 + \tilde{\rho}_I(t+s)] \, ds \right]$$

The solution can be obtained by separately solving two minimization problems of the same form:

$$\min_{\theta_1} \left[k_1 \int_{0+}^{T_{END}-\bar{t}} \eta(s,\theta_1) \cdot [1 + \tilde{\rho}_I(t+s)] \right]$$

$$\min_{\theta_2} \left[k_2 \int_{0+}^{T_{END}-\bar{t}} \eta(s,\theta_2) \cdot [1 + \tilde{\rho}_I(t+s)] \right]$$

Hence they will yield the same results and this shows that considering a unique switching policy does not degrade the optimal solution.

Remark 3.4. We denote by $\tilde{I}(T_{END})$ and $\tilde{\Theta}_S(T_{END}, \cdot)$, respectively, the optimal value and optimal switching times for (3.10) as functions of the final time instant T_{END}. If the minimization is performed for a certain $T_{END} = T_1$ by solving (3.19) and (3.20) backwards in time, the solutions for all $T_2 < T_1$ are also obtained:

$$\tilde{I}(T_2) = \rho_0 \cdot \tilde{\rho}_I(T_1 - T_2) \qquad \tilde{\Theta}_S(T_2, t) = \tilde{\Theta}_S(T_1, t + T_1 - T_2) \tag{3.32}$$

Moreover, one can assume that, under the considered overproduction regime, the function $\tilde{I}(T)$ is strictly monotonic increasing: a larger fraction of turbines will be required to switch to the second mode if extra power must be generated for longer times. For the same reasons, fixed a certain T_{END} as final time, $\tilde{\rho}_I(t)$ in (3.20) is strictly monotonic decreasing and always positive in $[0, T_{END}]$ since $\tilde{\rho}_I(T_{END}) = 0$.

Remark 3.5. For the optimization problem (3.10) with $\rho_0 < 1$, given previous considerations, there exists T_N such that $\tilde{I}(T_N) = 1 - \rho_0$. Furthermore, solving (3.10) for a sufficiently large T_{END} with $T_N < T_{END}$ yields:

$$\rho_0 \cdot \tilde{\rho}_I(T_{END} - T_N) = \tilde{I}(T_N) = 1 - \rho_0 \tag{3.33}$$

Notice that, if problem (3.10) is directly solved for $T_{END} = T_N$, the resulting minimum fraction of turbines required to switch in order to guarantee the extra power generation (corresponding to an initial fraction ρ_0 of switched turbines at $t = 0$) is equal to $1 - \rho_0$ and therefore corresponds to the utilization of all available generators. We can now provide the following result for the original problem of time maximization:

Theorem 3.2. *The optimal switching profile $\Theta^*(\cdot)$ for the maximization problem (3.9) can be computed according to the following formula:*

$$\Theta^*(t) = \underset{\theta \in (0, T_N - t]}{\arg \min} \left[\int_{0^+}^{T_N - t} \eta(s, \theta) \left[1 + \tilde{\rho}_I(t + s)\right] ds \right] \tag{3.34}$$

where $\tilde{\rho}_I$ is defined by an integral equation solved backwards in time (with $\tilde{\rho}_I(T_N) = 0$):

$$\tilde{\rho}_I(t) = \int_{0^+}^{T_N - t} \eta(s, \Theta^*(t)) \left[1 + \tilde{\rho}_I(t + s)\right] ds \tag{3.35}$$

Proof. If Θ^* is not optimal, there exists a feasible $\hat{\Theta}$ and corresponding switching rate $\hat{\rho}$ that guarantee $\dot{P}_{TOT}(t) = 0 \; \forall t \in (0, \hat{T}_{END}]$, with final time $\hat{T}_{END} > T_N$ and such that:

$$1 - \rho_0 = \int_{0^+}^{\hat{T}_{END}} \hat{\rho}(t) \, dt \tag{3.36}$$

This is impossible since Θ^* is the optimal switching time for the integral maximization (3.10) with $T_{END} = T_N$ and the following must hold from Remark 3.4:

$$\int_{0^+}^{\hat{T}_{END}} \hat{\rho}(t) \, dt \geq \tilde{I}(\hat{T}_{END}) > \tilde{I}(T_N) = 1 - \rho_0 \tag{3.37}$$

$\square$

In conclusion, the duration of the frequency response from the wind turbines population can be maximized by adopting the scheduling introduced in Theorem 3.1 for the integral minimization problem, calculated considering T_N as final time instant. This corresponds to the maximum utilization of the available generators, since $\tilde{I}(T_N) = 1 - \rho_0$.

3.3.4   Simulation Results

The performance of the control strategy described in Section 3.3.3 has been evaluated in simulations. The function $\eta(t, \theta)$ has been calculated at discretized values, considering different steps and intervals for its two variables. The step $\Delta t = 0.01s$ has been chosen for t in order to properly capture the dynamics of the switching turbines, evaluating η for $t \in [0, T_{END}]$. For the variable θ, to reduce the computational burden, a larger step $\Delta \theta = 0.5s$ has been used. For the same reason, a restricted interval of values has been considered, excluding the time instants that were too close to T_{END} and that, after direct verification, represented suboptimal switching times for the turbines. The solution $(\tilde{\Theta}(\cdot), \tilde{\rho}(\cdot))$ of problem (3.10) for $T_{END} = 500s$ has been calculated through numerical

integration of (3.19) and (3.20), using the parameters in [41]:

$$R = 37.5m \qquad v = 10m/s \qquad T_{ss} = K_T\omega_{ss}^2 = 7.02 \cdot 10^5 Nm$$
$$J = 5.9 \cdot 10^6 Kg \cdot m^2 \quad \omega_{ss} = 1.69 rad/s \qquad P_{ss} = K_T\omega_{ss}^3 = 1.18 \cdot 10^6 W \tag{3.38}$$

The quantity $\tilde{\rho}_I(t)$ has been evaluated by integrating backward in time (3.20), obtaining $\tilde{\Theta}(t)$, at each time step, through the minimization problem (3.19). The corresponding switching rate $\rho(t)$, for $\rho_0 = 4.3 \cdot 10^{-4}$, is compared in Fig. 3.3 with the case $\Theta(t) = T_{END}\,\forall t \in [0,T]$, characterized by switching rate $\rho^C(t)$. The most significant difference is represented by the spikes of $\rho(t)$, caused by the cascaded compensations of the initial fraction of turbines ρ_0 switching back to mode 1. The corresponding fractions of switched turbines (respectively $\rho_I(t) = \int_{0^+}^t \rho(s)\,ds$ and $\rho_I^C(t) = \int_{0^+}^t \rho^C(s)\,ds$) are shown in Fig. 3.4. The integral $\rho_I(t)$ (blue) is initially bigger, since some of the turbines are returning to mode 1 and require higher power compensation. When T_{END} is approaching the turbines stop switching back and, given that some of them are again in mode 1 (with higher efficiency) $\rho_I(t)$ increases more slowly. At final time T_{END}, as expected, the integral ρ_I is lower than ρ_I^C. The optimal switching profile $\tilde{\Theta}(t)$ for different torque steps T_f (considered as fractions of $T_{ss} = K_T\omega_{ss}^2$, the steady-state torque in mode 1) are shown in Fig. 3.5. In all cases $\tilde{\Theta}(t)$ increases with time: at lower time instants, turbines switch back to the first mode since the instantaneous increase of $\rho(t)$ is compensated over time by the increasing efficiency. There exists a threshold after which it is not possible to perform such compensation and turbines remain in the second state ($\tilde{\Theta}(t) = T_{END}$). The maximum frequency response duration T_N for (3.9) is shown in Fig. 3.6 as a function of the power increase ratio $\Delta P/P_0$, for different torque steps T_f. Considering that $\rho_0 = \frac{\Delta P}{KT_f\omega_{ss}}$, it appears that higher values of T_N are achieved in a certain range of ρ_0: when ΔP is lower, low values of T_f are preferable and vice versa.
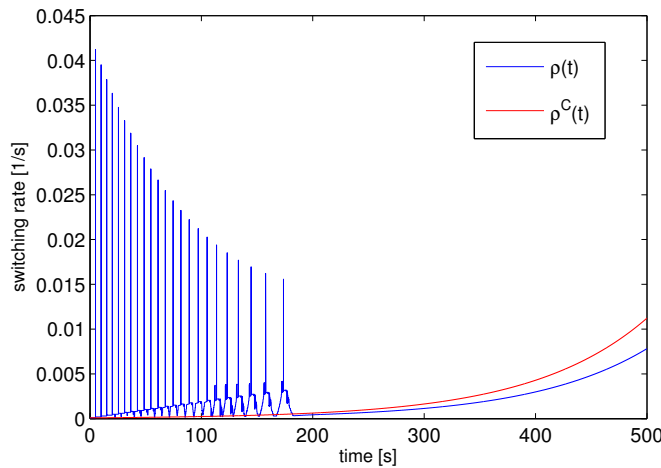
FIGURE 3.3: Switching rates $\rho(t)$ (blue) when $\Theta(t) = \tilde{\Theta}(t)$ and $\rho^C(t)$ (red) when $\Theta(t) = T_{END}$.
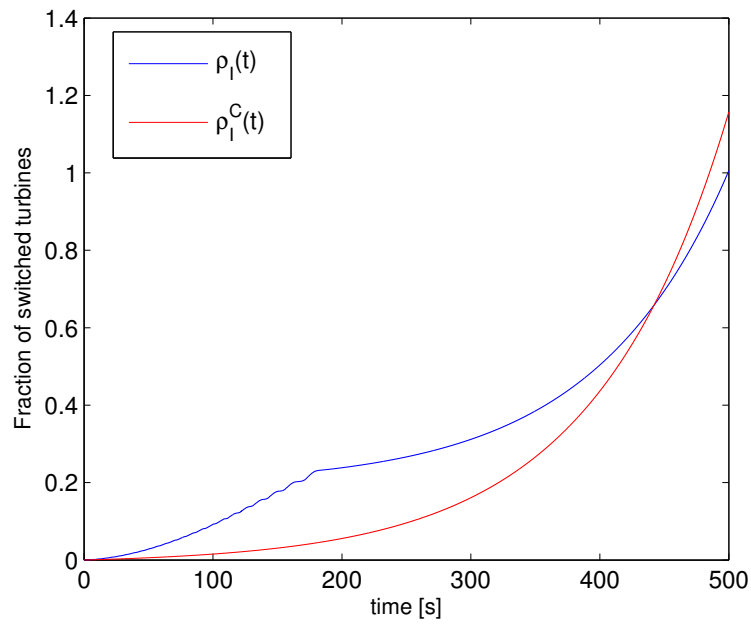
FIGURE 3.4: Fractions of switched turbines $\rho_I(t)$ (blue) when $\Theta(t) = \tilde{\Theta}(t)$ and $\rho_I^C(t)$ (red) when $\Theta(t) = T_{END}$.
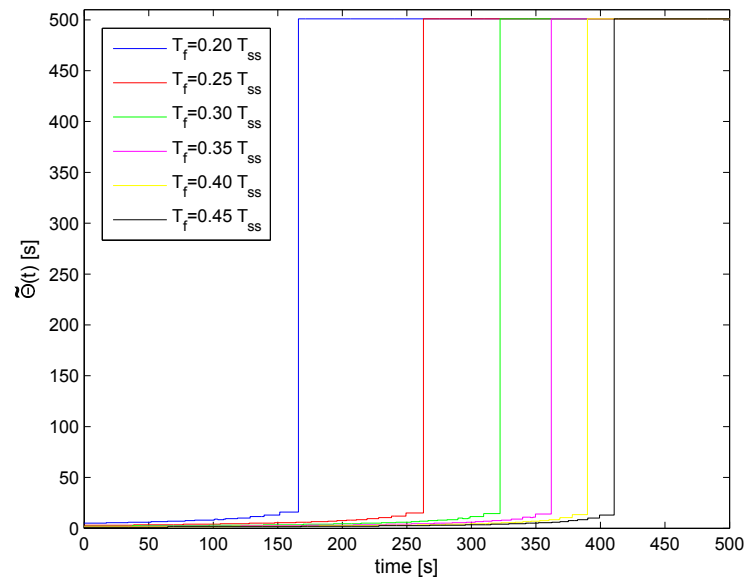
FIGURE 3.5: Optimal switching time $\tilde{\Theta}(t)$ for different torque steps, with $T_{END} = 500s$.
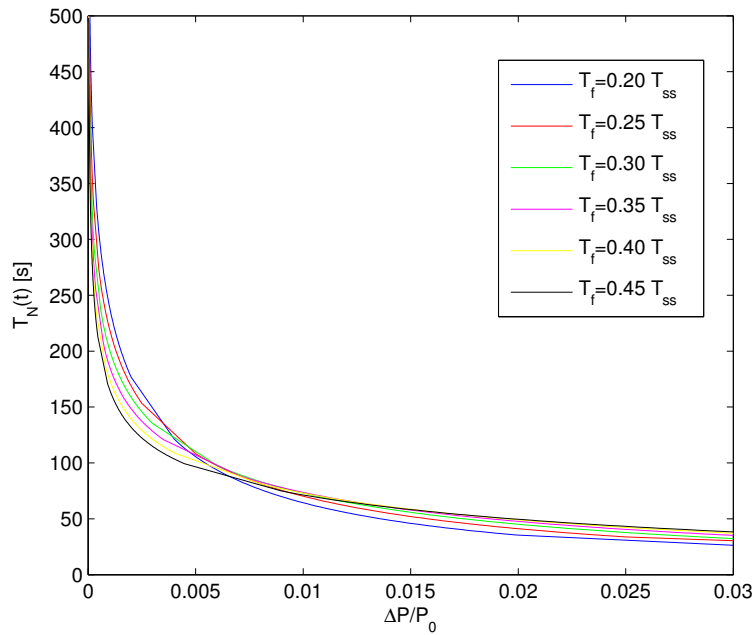
FIGURE 3.6: Maximum time T_N of frequency response provision as a function of percentage increase in power, for different torque steps T_f.

3.4   Optimal Inertial Response

In this section it is assumed that the wind turbines are not constrained to operate in the two modes presented in Section 3.3 but it is instead possible to consider their electric torque T_e as a control input. Following a frequency drop, a set-point is introduced for the aggregate extra generation that must be provided by the wind farm, calculating the power profile of each turbine in order to minimize the resulting losses of kinetic energy. In this case, the application of the classical tools of optimal control is prevented by the complicated expression that describes the power extraction from the wind and the large number of considered generators. For this reason, the optimal power profile of the turbines is obtained by exploiting particular monotonicity properties that arise if one considers the kinetic energy dynamics and their relationship with the efficiency of the generators. The problem is initially solved for the simplified case without constraints on generated power, using the results as a starting point for the more realistic analysis in which the power provided by each turbine cannot exceed some technical limits. It is worth noticing that the optimal power profiles are straightforward to calculate numerically. In practical implementations, in case of frequency events, they can be used to determine the torque reference $T_{e_{ref}}$, replacing the values calculated by the OPPT controller (see Fig. 3.1). A similar approach can be used to study the energy recovery problem: after having provided frequency response, the aggregate power set-point is

reduced and turbines are brought back to the operating state with maximum efficiency. With the same tools, it is possible to determine which power references are feasible for a given energy state and calculate the power profiles which allow to perform the recovery in minimal time.

3.4.1 Wind Turbine Dynamics and Power Extraction

The dynamics of the individual wind turbine are described by the swing equation (3.1) presented in Section 3.2 and Assumption 3.1 is still valid. The wind speed is assumed constant in time but, in this case, is in general different for each turbine. Furthermore, on the basis of the expressions of $\bar{C}$ proposed in the literature, the following assumptions are introduced for the corresponding coefficient $C(\omega, v) = \bar{C}(\omega R/v, 0)$, obtained for pitch angle $\theta = 0$:

Assumption 3.2. *For a fixed wind speed v, it is assumed that the power coefficient $C(\omega, v)$ has a unique maximum for $\omega = \omega_{ss}(v)$, is a monotonic increasing function in some interval $[\omega_L(v), \omega_{ss}(v)]$ and is strictly concave for $\omega > \omega_L(v)$.*

In order to study the optimal control problem to be defined in the next subsection, it is convenient to introduce a change of coordinates, describing the state evolution of a single turbine by considering its kinetic energy $E = \frac{1}{2}J\omega^2$ (rather than its angular speed). It is straightforward, using (3.2) and (3.4), to express the mechanical power $P_m = T_m \cdot \omega$ as a function Γ that depends only on E and v:

$$P_m = P_w C(\omega, v) = P_w C\left(\sqrt{\frac{2E}{J}}, v\right) = \Gamma(E, v) \tag{3.39}$$

Values of Γ at different wind speeds, for the turbine parameters considered in the simulation section, are shown in Fig. 3.7.

The state equation in the new coordinate becomes:

$$\dot{E} = J\omega\dot{\omega} = P_m - P_e = \Gamma(E, v) - P_e \tag{3.40}$$

The term $P_e = T_e \cdot \omega$ in (3.40) represents the electrical power generated by the turbine. Assuming that the rotor speed ω can be measured without uncertainties, P_e can be considered as the new control input of the system. To account for physical constraints of the turbine, the kinetic energy E is limited to some interval $\mathcal{E} = [E_{MIN}, E_{MAX}]$.

Remark 3.6. The properties of C introduced in Assumption 3.2 are closely related to the function Γ. For a fixed v, the mechanical power $\Gamma(E, v)$ has a unique maximum for $E = E_{ss}(v) = \frac{1}{2}J\omega_{ss}^2(v)$ and is monotone increasing in the interval $[E_L(v), E_{ss}(v)]$.
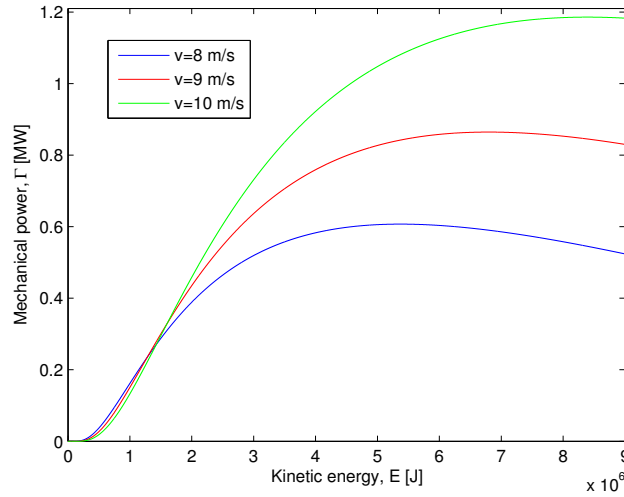
FIGURE 3.7: Mechanical power Γ as a function of kinetic energy E, for different wind speeds v.

Assumption 3.3. *Given the expressions for the coefficient C and the specifications of the turbines found in the literature, it is reasonable to assume that $\Gamma(E,v)$ is strictly concave on $[E_L(v), E_{MAX}]$ and the energy E of the single generator, in the overproduction regime of the frequency response, is always within the concavity region of Γ:*

$$E_L(v) \leq E_{MIN} \leq E \leq E_{ss}(v) \leq E_{MAX}$$

3.4.2   Scheduling in the Case of Unconstrained Power

A population of N wind turbines is considered and the kinetic energy, electrical power and wind speed of the i-th generator are denoted respectively by E_i, P_i and v_i. All turbines are initially operating in steady-state at the kinetic energy $E_{ss}(v_i)$ which guarantees the maximum efficiency, with the following equality holding for the mechanical and electrical power:

$$\Gamma(E_{ss}(v_i), v_i) = P_i(0) \qquad i = 1 \ldots N$$

When a frequency drop occurs in the network at time $t = 0$, the wind turbine population can increase its aggregate generated power by releasing part of the kinetic energy stored in the rotating shafts. In particular, a reference $P_r(\cdot)$ is set on the time interval $[0, T]$, requiring an aggregate power which is greater than the one at steady state:

$$P_r(t) > \sum_{i=1}^{N} \Gamma(E_{ss}(v_i), v_i) = P_0 \qquad \forall t \in [0, T] \tag{3.41}$$

Our aim is to determine the power profile $P_i(\cdot)$ of each turbine in order to satisfy the following:

$$\sum_{i=1}^{N} P_i(t) = P_r(t) \qquad \forall t \in [0, T]$$

$$E_i(t) \in [E_{MIN}, E_{MAX}] \qquad i = 1 \dots N$$

(3.42)

In general there exist multiple choices of P_i which are feasible for (3.42) and it is therefore important to introduce some optimality criterion in the calculation of the power profiles. In this respect a logical choice is to define as optimal the set of $P_i(\cdot)$ which maximizes the total final energy $\sum_i E_i(T)$ of the turbines. This choice takes into account the following recovery phase of the generators that, after having provided frequency response, are brought back to their working point of maximum efficiency. Furthermore, it will be shown that the resulting power profiles guarantee feasibility for the largest class of power references P_r.

The simpler case in which no constraints are imposed on the generated power P_i of the turbines is initially analysed. The corresponding optimization problem is:

$$\begin{aligned}
\max_{P_i(\cdot), i=1\dots N} \quad & \sum_{i=1}^{N} E_i(T) \\
\text{s. t.} \quad & \sum_{i=1}^{N} P_i(t) = P_r(t) & \left(\begin{array}{c} \forall i = 1, \dots, N \\ \forall t \in [0, T] \end{array} \right) \\
& E_i(0) = E_i^0 \\
& \dot{E}_i(t) = \Gamma(E_i(t), v_i) - P_i(t) \\
& E_i(t) \in [E_{MIN}, E_{MAX}]
\end{aligned}$$

(3.43)

In this scenario, given any state vectors E^a and E^b in $\mathcal{E}^N$ of equivalent total energy (viz. such that $\sum_{i=1}^{N} E_i^a = \sum_{i=1}^{N} E_i^b$), it is possible to transfer between turbines the amount of energy required so as to achieve an instantaneous switch between the two states. This is true since all P_i are unconstrained and (as we are neglecting power losses) the total power required for the switch is zero. Therefore, indications on the solution of (3.43) can be obtained by solving, at each time instant t, a static optimization problem. In particular, the kinetic energy E_{TOT} of the wind farm is distributed among the turbines in order to obtain the maximum derivative $h(E_{TOT})$ of the total mechanical power extracted from the wind:

$$h(E_{TOT}) = \max_{x_i, i=1\dots N} \sum_{i=1}^{N} \Gamma(x_i, v_i)$$

(3.44a)

$$\text{s.t.} \sum_{i=1}^{N} x_i = E_{TOT}$$

(3.44b)

$$x_i \in [E_{MIN}, E_{MAX}]$$

(3.44c)

In order to solve (3.44) it is useful to introduce the partial derivative $\Gamma_E(E, v) = \frac{\partial \Gamma(E,v)}{\partial E}$ and its inverse function with respect to the energy E when $v = v_i$, which can be denoted as $\Gamma_{E_i}^{-1} : [0, \Gamma_E(E_{MIN}, v_i)] \to [E_{MIN}, E_{ss}(v_i)]$. Given the strict concavity of Γ established in Assumption 3.3, this inverse function is always well defined and monotonic. It is now possible to provide the following preliminary result:

Proposition 3.3. *For any value of total energy $E_{TOT} \in [NE_{MIN}, \sum_i E_{ss}(v_i)]$ there exists one and only one κ, that we denote by $K(E_{TOT})$, such that the following holds:*

$$\sum_{i=1}^{N} \Gamma_{E_i}^{-1}\left(\min(\kappa, \Gamma_E(E_{MIN}, v_i))\right) = E_{TOT} \tag{3.45}$$

Proof. Existence and uniqueness of $K(E_{TOT})$ are straightforward to verify if one considers that the function $K^{-1}(\kappa)$, which denotes the left-hand-side of (3.45), is monotonic decreasing, continuous and its image includes the interval $[NE_{MIN}, \sum_i E_{ss}(v_i)]$:

$$K^{-1}(0) = \sum_{i=1}^{N} E_{ss}(v_i) \qquad K^{-1}\left(\max_{i \in \{1,\dots,N\}} (\Gamma_E(E_{MIN}, v_i))\right) = NE_{MIN}$$

$\square$

This result allows to determine the solution of the static optimization problem:

Theorem 3.3. *If $E_{TOT} \in [NE_{MIN}, \sum_i E_{ss}(v_i)]$, under Assumption 3.3 for the function Γ, there exists a unique solution $x^* = [x_1^* \dots x_N^*]'$ for problem (3.44) and the single component x_i^* is defined as follows:*

$$x_i^* = \Gamma_{E_i}^{-1}\left(\min(K(E_{TOT}), \Gamma_E(E_{MIN}, v_i))\right) \qquad i = 1, \dots, N \tag{3.46}$$

Proof. The feasibility of x^* is straightforward to verify: the constraint (3.44b) is satisfied from equation (3.45) while for (3.44c) it is sufficient to notice that, for the considered values of E_{TOT}, the result of the function $\Gamma_{E_i}^{-1}$ is always in the interval $[E_{MIN}, E_{ss}(v_i)]$ with $E_{ss}(v_i) < E_{MAX}$ from Assumption 3.3. The optimality of the candidate solution is now proved through Karush-Kuhn-Tucker (KKT) conditions. In this particular case such conditions are necessary and sufficient since the inequality constraints are convex, equation (3.44b) is affine and the objective function is strictly concave [43]. To see this, consider that the Hessian of the objective function $H = \text{diag}(\Gamma_{EE}(x_1, v_1), \dots, \Gamma_{EE}(x_N, v_N))$ is negative definite since the second derivative $\Gamma_{EE} = \partial^2 \Gamma(E, v)/\partial E^2$ is negative from the strict concavity of Γ established in Assumption 3.3. For the proposed solution the constraint on the maximum energy E_{MAX} is never active (the corresponding multiplier will always be equal to 0) and only the inequality in the opposite sense $x_i \geq E_{MIN}$ must

be considered when deriving the KKT conditions. Therefore, the vector x^* is optimal if and only if there exists κ and $\mu = [\mu_1, \ldots, \mu_N]$ such that:

$$\Gamma_E(x_i^*, v_i) = -\mu_i + \kappa$$
$$\mu_i \geq 0 \qquad\qquad i = 1, \ldots, N$$
$$\mu_i \cdot (E_{MIN} - x_i^*) = 0$$

In particular these conditions are satisfied if one chooses the multipliers as follows:

$$\kappa = K(E_{TOT})$$
$$\mu_i = \begin{cases} 0 & \text{if} \quad \Gamma_E(E_{MIN}, v_i) > \kappa \\ \kappa - \Gamma_E(E_{MIN}, v_i) & \text{if} \quad \Gamma_E(E_{MIN}, v_i) \leq \kappa \end{cases}$$

Notice also that uniqueness of the optimal solution follows from its existence and the strict concavity of the function to maximize. □

For a better understanding of the structure of the solution for (3.44), a graphical representation is provided in Fig. 3.8 for the simple case with $N = 3$. Three different values of total energy $[\tilde{E}_1, \tilde{E}_2, \tilde{E}_3]$ are considered, associating to each $\tilde{E}_j$ a function $p_j(E) = K(\tilde{E}_j)$, represented in the figure as a black/grey dashed line. For the generator with index i, if $K(\tilde{E}_j) < \Gamma_E(E_{MIN}, v_i)$, the optimal value x_i^* for $E_{TOT} = \tilde{E}_j$ is given by the projection on the x axis of the intersection between $p_j(\cdot)$ and the function $\Gamma_E(\cdot, v_i)$ (see for example the projections of the red curve). If, on the other hand, $K(\tilde{E}_j) \geq \Gamma_E(E_{MIN}, v_i)$, the corresponding x_i^* is equal to E_{MIN} (for example the x-value of the curve in green). The optimal energy values are in the same colour of the corresponding Γ_E curves (blue: $v_i = 7m/s$, green: $v_i = 8.5m/s$, red: $v_i = 10m/s$). They are displayed as circles when $E_{TOT} = \tilde{E}_1 = 10MJ$, as squares when $E_{TOT} = \tilde{E}_2 = 7.5MJ$ and as crosses when $E_{TOT} = \tilde{E}_3 = 5.4MJ$.

The following property of the function $h(\cdot)$, as defined in (3.44), will be crucial for determining optimality of the proposed solution to problem (3.43):

Proposition 3.4. *The maximum $h(E_{TOT})$ of (3.44) is strictly concave and Lipschitz continuous with respect to E_{TOT} in the interval $[NE_{MIN}, \sum_{i=1}^{N} E_{ss}(v_i)]$.*

Proof. Consider that the right hand side in (3.44a) is a strictly concave function of x and the compact-valued continuous correspondence $D(E_{TOT})$ which returns the set of feasible x for a given E_{TOT} has a convex graph. It is therefore possible to apply the maximum theorem 9.17 in [44], considering E_{TOT} as a parameter of the optimization and concluding that h is strictly concave with respect to E_{TOT}. Notice now that, following the concavity properties introduced in Assumption 3.3, the definition of the derivative
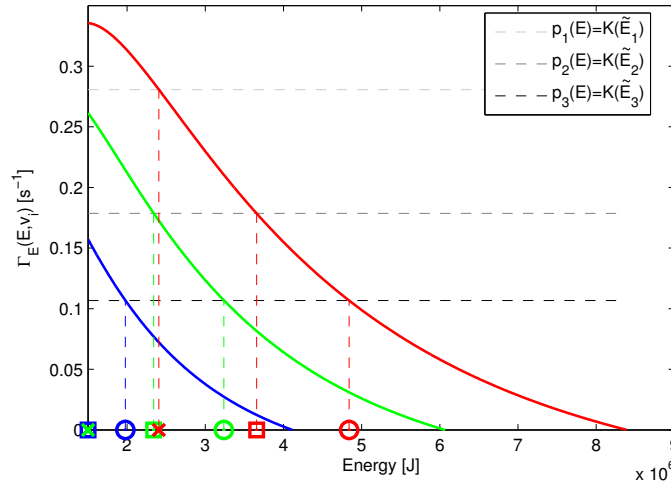
FIGURE 3.8: Solution of the static maximization problem (3.44) for different values of E_{TOT}.

inverse $\Gamma_{E_i}^{-1}$ can be extended to the interval $[\Gamma_E(E_{MAX}, v_i), \Gamma_E(E_L(v_i), v_i)]$. It is also possible to define the domain of h as the interval $\mathcal{E}_D = \left[\sum_{i=1}^{N} E_L(v_i), \sum_{i=1}^{N} E_R(v_i)\right]$ which satisfies the following property:

$$\left[NE_{MIN}, \sum_{i=1}^{N} E_{ss}(v_i)\right] \subset \mathcal{E}_D \subset \left[\sum_{i=1}^{N} E_L(v_i), NE_{MAX}\right]$$

where $E_R(v_i) < E_{MAX}$ is the maximum value for the optimal energy of the i-th turbine, for which it holds:

$$\Gamma_E(E_R(v_1), v_1) = \cdots = \Gamma_E(E_R(v_N), v_N) < 0$$

Such domain definition is possible if one considers that in each $[E_L(v_i), E_R(v_i)]$ the monotonicity and concavity properties mentioned in the previous remarks still hold. It is therefore sufficient to extend the results of Proposition 3.3 and Theorem 3.3, repeating the steps of the corresponding proofs for the new interval $\mathcal{E}_D$. From the concavity of h with respect to E_{TOT} we can then conclude that it is also Lipschitz continuous in the same variable on the interval $[NE_{MIN}, \sum_{i=1}^{N} E_{ss}(v_i)] \subset \mathcal{E}_D$. $\qquad \square$

Given the results of Proposition 3.4, assuming continuity of P_r and applying the Picard-Lindelöf theorem, it is possible to define $E_{TOT}^*(\cdot)$ as the unique solution of:

$$\dot{E}_{TOT}(t) = h(E_{TOT}(t)) - P_r(t) \qquad E_{TOT}(0) = \sum_{i=1}^{N} E_i^0 \qquad (3.47)$$

providing the following constructive solution for the problem of final energy maximization:

Theorem 3.4. *The functions $E_i^*(\cdot)$, $i = [1, \ldots, N]$, defined as the solution at each time $t \in [0, T]$ of problem (3.44) for $E_{TOT} = E_{TOT}^*(t)$, are optimal state trajectories for the final state maximization problem (3.43).*

Proof. For the feasibility of E^* notice that, at any time instant $t \in [0, T]$, it holds:

$$\dot{E}_{TOT}^*(t) = h(E_{TOT}^*(t)) - P_r(t) = \left(\sum_{i=1}^{N} \Gamma(E_i^*(t), v_i) \right) - P_r(t) = \sum_{i=1}^{N} \dot{E}_i^*(t).$$

Taking into account that individual power P_is are unconstrained, it is always possible to determine input profiles $P_i^*(t)$, with $i = [1, \ldots, N]$, which satisfy the constraint on the state derivative $\dot{E}_i^*(t) = \Gamma(E_i^*(t), v_i) - P_i^*(t)$ and such that $\sum_{i=1}^{N} P_i^*(t) = P_r(t)$. Consider now an arbitrary state trajectory $\bar{E}(\cdot)$ which is feasible for (3.43) and define, at each time instant t, the corresponding total energy $\bar{E}_{TOT}(t) = \sum_{i=1}^{N} \bar{E}(t)$. Such function is differentiable since it holds:

$$\dot{\bar{E}}_{TOT}(t) = \sum_{i=1}^{N} \Gamma(\bar{E}_i(t), v_i) - P_r(t)$$

From the definition of h, it follows:

$$\dot{\bar{E}}_{TOT}(t) \le h(\bar{E}_{TOT}(t)) - P_r(t) \ \forall t \in [0, T]$$

Given that $\bar{E}_{TOT}(0) = E_{TOT}^*(0)$, applying the comparison theorem in [45] we can conclude that $\bar{E}_{TOT}(t) \le E_{TOT}^*(t)$ for all $t \ge 0$ including $t = T$ and therefore $E^*(\cdot)$ is optimal for problem (3.43). $\qquad\square$

Since the optimal trajectory E^*, at each time instant, is the solution of the static optimization problem (3.44), evaluating the min function in the expression of x^*, provided in Theorem 3.3, yields:

$$E_i^*(t) = \begin{cases} \Gamma_{E_i}^{-1} \left(K \left(E_{TOT}^*(t) \right) \right) & \text{if} \quad i \in \mathcal{P}_1(t) \\[2ex] E_{MIN} & \text{if} \quad i \in \mathcal{P}_2(t) \end{cases} \tag{3.48}$$

where $E_{TOT}^*(t) = \sum_{i=1}^{N} E_i^*(t)$ and the two sets $\mathcal{P}_1(t)$ and $\mathcal{P}_2(t)$ are defined as follows:

$$\mathcal{P}_1(t) = \{i : \Gamma_E(E_{MIN}, v_i) > K \left(E_{TOT}^*(t) \right) \} \qquad \mathcal{P}_2(t) = \{1, 2, \ldots, N\} \backslash \mathcal{P}_1(t)$$

Remark 3.7. At any time t the components of $E^*(t)$ can be divided in two groups: the ones in $\mathcal{P}_2(t)$ will have minimum energy E_{MIN} while the remaining ones will be

characterized by equal derivatives $\Gamma_E(E_i^*(t), v_i) = K(E_{TOT}^*(t))$. Given (3.48) and the definitions of $\mathcal{P}_1$ and $\mathcal{P}_2$, it also holds:

$$\Gamma_E(E_i^*(t), v_i) \geq \Gamma_E(E_j^*(t), v_j) \qquad \forall\, i \in \mathcal{P}_1(t) \qquad \forall\, j \in \mathcal{P}_2(t) \tag{3.49}$$

We are now interested in determining the power profiles P^* which generate the optimal state trajectories. The analysis will consider the case in which it is not necessary to perform an instantaneous energy switch since the initial state corresponds to the optimal solution at time $t = 0$:

$$E_i^0 = E_i^*(0) \qquad i = 1, \ldots, N \tag{3.50}$$

If this is not the case, it is sufficient to consider in the expression of P_i^* an additional impulsive term $(E_i^0 - E_i^*(0)) \cdot \delta(t)$. For the calculation of the power profiles the following feedback law is introduced:

$$\varphi_i(E, t) = \begin{cases} \Gamma(E_i, v_i) - f_i(E, t) & \text{if } E_i > E_{MIN} \\[2mm] \Gamma(E_{MIN}, v_i) & \text{if } E_i = E_{MIN} \end{cases} \tag{3.51}$$

where the function f_i is obtained by differentiating the expression in (3.48) when $i \in \mathcal{P}_1(t)$, evaluated at an arbitrary state E:

$$f_i(E, t) = \frac{d}{d\kappa} \Gamma_{E_i}^{-1} \left(K \left(\sum_{i=1}^{N} E_i \right) \right) K' \left(\sum_{i=1}^{N} E_i \right) \left[\sum_{i=1}^{N} \Gamma(E_i, v_i) - P_r(t) \right] \tag{3.52}$$

Proposition 3.5. *If (3.50) holds for the initial state E^0, the optimal power profile P^* for (3.43) is equal to the feedback φ evaluated along the optimal trajectory E^*:*

$$P_i^*(t) = \varphi_i \left(E^*(t), t \right) \tag{3.53}$$

Proof. It is sufficient to show that the derivative for E_i^* defined in (3.48) corresponds to the dynamics (3.40) of the single turbine when P^* is applied. Notice that, for $E_i = E_{MIN}$, the feedback law is discontinuous. In this case, taking into account that, if $E_i^*(t) = E_{MIN}$, it holds $E_i^*(\bar{t}) = E_{MIN}$ for $\bar{t} > t$, the right derivative (equal to 0) can be considered. The following general expression can then be provided:

$$\frac{d}{dt} E_i^*(t) = f_i(E^*(t), t) \cdot \text{sign}(E_i^*(t) - E_{MIN}) = \Gamma(E_i^*(t), v_i) - P_i^*(t) \tag{3.54}$$

The first equality holds by definition of f_i, the second is obtained by replacing (3.51) in the expression (3.53) of P_i^*. Proof is concluded by verifying that the last member

in (3.54) is equal to the state equation (3.40) evaluated at $E = E_i^*(t)$, $P_e = P_i^*(t)$ and $v = v_i$.   □

Proposition 3.6. *The power profile defined by (3.53) satisfies the constraint on the total generated power, with $\sum_i P_i^*(t) = P_r(t)$ for all $t \in [0, T]$.*

Proof. Consider that, for the sum of the components of $P^*(t)$, it holds:

$$\sum_{i=1}^{N} P_i^*(t) = \sum_{i=1}^{N} \Gamma(E_i^*(t), v_i) - \sum_{i \in \mathcal{P}_1(t)} f_i(E_i^*(t), t) \tag{3.55}$$

The derivative of the function K in (3.52) can be written as follows:

$$
\begin{aligned}
K'\left(\sum_{i=1}^{N} E_i\right) &= \left(\frac{d}{d\kappa} K^{-1}(\kappa)\right)^{-1} \\
&= \left(\frac{d}{d\kappa} \sum_{i=1}^{N} \Gamma_{E_i}^{-1}(\min(\kappa, \Gamma_E(E_{MIN}, v_i)))\right)^{-1} \\
&= \left(\frac{d}{d\kappa} \sum_{\{i : E_i > E_{MIN}\}} \Gamma_{E_i}^{-1}(\kappa)\right)^{-1}
\end{aligned} \tag{3.56}
$$

To prove that $\sum_i P_i^*(t) = P_r(t)$, it is sufficient to replace E with $E^*(t)$ in (3.56), substituting the resulting expression in (3.52) and obtaining the following for the last sum in (3.55):

$$\sum_{i \in \mathcal{P}_1(t)} f_i(E_i^*(t), t) = \sum_{i=1}^{N} \Gamma(E_i^*(t), v_i) - P_r(t)$$

□

In conclusion, if one considers (3.48) and (3.54), it can be seen that the optimal scheduling, in the case of unconstrained power, is achieved by controlling the turbines in two different ways. The kinetic energy of the generators with $E_i^*(t) > E_{MIN}$ is reduced by imposing $\dot{E}_i^*(t) = f_i(E^*(t), t)$ so that the following holds:

$$\Gamma_E(E_i^*(t), v_i) = K(E_{TOT}^*(t)) \qquad \forall i \in \mathcal{P}_1(t)$$

Once the i-th turbine reaches the minimum energy E_{MIN}, it remains in that state ($\dot{E}_i^*(t) = 0$) and the energy reduction is performed with the same criterion on the remaining ones.

It is now possible to further discuss the choice of providing frequency response with a scheduling of the turbines which maximizes the total kinetic energy at the final time T.

Proposition 3.7. *For a given initial state E^0, the solution of problem (3.43) guarantees feasibility of (3.42) for the largest class of aggregate power set-points P_r.*

Proof. To show this, consider a reference $\tilde{P}_r : [0, T] \to \mathbb{R}_+$ for which (3.43) is unfeasible. Assuming $\tilde{P}_r$ is bounded, since the generated power of the individual turbine is unconstrained, there exist $\tilde{t} < T$ defined as the maximum t such that (3.43) is feasible for $\tilde{P}_r$ restricted on the interval $[0, t]$. In the considered overproduction regime this implies that, for the corresponding optimal state trajectories, it holds $E_1^*(\tilde{t}) = \cdots = E_N^*(\tilde{t}) = E_{MIN}$. Consider now an arbitrary power profile $\bar{P}$ with $\sum_i \bar{P}_i = \tilde{P}_r$. For the corresponding energy vector $\bar{E}$ it will hold $\sum_i \bar{E}_i(\tilde{t}) \leq \sum_i E_i^*(\tilde{t}) = NE_{MIN}$. This means that $\bar{E}(\tilde{t}) = E^*(\tilde{t})$ or there exists at least one i such that $\bar{E}_i(\tilde{t}) < E_{MIN}$. We can conclude that there is no power profile $P(\cdot)$ such that (3.42) is satisfied for $P_r = \tilde{P}_r$. $\qquad\square$

3.4.3 Optimal Response with Constraints on Generated Power

The analysis is now extended in order to consider the case of wind turbines which have a limited power output in the interval $[P_{MIN}, P_{MAX}]$. The corresponding control problem becomes:

$$
\begin{aligned}
\max_{P_i(\cdot), i=1\ldots N} \quad & \sum_{i=1}^N E_i(T) \\
\text{s.t.} \quad & \sum_{i=1}^N P_i(t) = P_r(t) \\
& E_i(0) = E_i^0 \\
& \dot{E}_i(t) = \Gamma(E_i(t), v_i) - P_i(t) \quad \left(\begin{array}{c} \forall i = 1, \ldots, N \\ \forall t \in [0, T] \end{array} \right) \\
& E_i(t) \in [E_{MIN}, E_{MAX}] \\
& P_i(t) \in [P_{MIN}, P_{MAX}]
\end{aligned}
\tag{3.57}
$$

It is important to notice that, under some conditions, the optimality results of the previous section can be extended to the present case. In particular, it is possible to state the following:

Remark 3.8. If we denote by $(E^{\bar{*}}, P^{\bar{*}})$ the solution of the unconstrained problem (3.43), this is feasible and optimal also for (3.57) if the following conditions are fulfilled:

$$
E_i^0 = E_i^{\bar{*}}(0) \qquad\qquad i = 1, \ldots, N \tag{3.58a}
$$

$$
P_{MIN} \leq P_i^{\bar{*}}(t) \leq P_{MAX} \qquad\qquad t \in [0, T] \tag{3.58b}
$$

The equation on the initial state E^0 guarantees that $P^{\bar{*}}$ is bounded since it is not necessary to perform an impulsive energy switching at $t = 0$, while (3.58b) verifies that the additional power constraints are satisfied.

The optimal scheduling problem is now solved for the cases in which condition (3.58a) does not hold. In this respect, it is useful to provide a preliminary result:

Proposition 3.8. *If a power profile $P^*(\cdot)$ is optimal for (3.57), it is also a solution to all the sub-problems which only consider a subset $\mathcal{S}$ of turbines in the time interval $[t_0, T]$:*

$$\{P_i^*(\cdot) : i \in \mathcal{S}\} = \underset{P_i(\cdot), i \in \mathcal{S}}{\arg\max} \sum_{i \in \mathcal{S}} E_i(T)$$

$$s.\ t.\ \sum_{i \in \mathcal{S}} P_i(t) = \sum_{i \in \mathcal{S}} P_i^*(t) = P_{\mathcal{S},r}(t)$$

$$E_i(t_0) = E_i^*(t_0)$$

$$\dot{E}_i(t) = \Gamma(E_i(t), v_i) - P_i(t) \qquad \left(\begin{array}{c} \forall i \in \mathcal{S} \\ \\ \forall t \in [t_0, T] \end{array} \right) \qquad (3.59)$$

$$E_i(t) \in [E_{MIN}, E_{MAX}]$$

$$P_{MIN} \le P_i(t) \le P_{MAX}$$

Proof. If the proposition statement is not verified, there exists $\bar{P}_i(\cdot)$ with $i \in \mathcal{S}$ such that, for the corresponding state trajectory $\bar{E} : [t_0, T] \to \mathcal{E}^{|\mathcal{S}|}$ with $\bar{E}(t_0) = E^*(t_0)$, it holds $\sum_{i \in \mathcal{S}} \bar{E}_i(T) > \sum_{i \in \mathcal{S}} E_i^*(T)$. It is now possible to define the following control function for the optimization problem (3.57):

$$\tilde{P}_i(t) = \begin{cases} \bar{P}_i(t) & \text{if} \quad i \in \mathcal{S} \wedge t \ge t_0 \\ \\ P_i^*(t) & \text{otherwise} \end{cases}$$

For the resulting state trajectory $\tilde{E}$, it holds:

$$\sum_{i=1}^{N} \tilde{E}_i(T) = \sum_{i \in \mathcal{S}} \bar{E}_i(T) + \sum_{i \notin \mathcal{S}} E_i^*(T) > \sum_{i=1}^{N} E_i^*(T)$$

which contradicts the optimality of P^* for (3.57). $\qquad\qquad \square$

This result is now applied to a set of turbines $\mathcal{S}$ and its subset of generators with minimum initial energy $\mathcal{S}_{MIN} = \{i : i \in \mathcal{S}, E_i(t_0) = E_{MIN}\}$ which satisfy the following at time t_0:

$$\Gamma_E(E_i(t_0), v_i) = \Gamma_E(E_j(t_0), v_j) \qquad i, j \notin \mathcal{S}_{MIN}$$

$$\qquad\qquad\qquad (3.60)$$

$$\Gamma_E(E_i(t_0), v_i) \le \Gamma_E(E_j(t_0), v_j) \qquad i \in \mathcal{S}_{MIN}, j \notin \mathcal{S}_{MIN}$$

In this case, for an arbitrary reference function $P_{\mathcal{S},r}$ one may attempt to solve (3.59) as an unconstrained problem, neglecting the inequalities $P_{MIN} \leq P_i(t) \leq P_{MAX}$:

$$
\begin{aligned}
\max_{P_i(\cdot), i \in \mathcal{S}} \quad & \sum_{i \in \mathcal{S}} E_i(T) \\
\text{s. t.} \quad & \sum_{i \in \mathcal{S}} P_i(t) = P_{\mathcal{S},r}(t) \\
& E_i(t_0) = E_i^*(t_0) \qquad\qquad\quad \left(\begin{array}{c} \forall i \in \mathcal{S} \\ \forall t \in [t_0, T] \end{array} \right) \\
& \dot{E}_i(t) = \Gamma(E_i(t), v_i) - P_i(t) \\
& E_i(t) \in [E_{MIN}, E_{MAX}]
\end{aligned}
\tag{3.61}
$$

In fact, if one considers the state optimality condition (3.48) and Remark 3.7, it is possible to verify that (3.60) corresponds to (3.58a) for the initial time instant (in this case t_0). Therefore, the unconstrained solution does not involve impulsive transfers of power at time t_0. Moreover, from Remark 3.8, the solution $P_{\mathcal{S}}^{\bar{*}}$ of the unconstrained problem (3.61) is feasible and optimal also for the constrained case (3.59) if the equivalent of (3.58b) holds:

$$
P_{MIN} \leq P_{\mathcal{S},i}^{\bar{*}}(t) \leq P_{MAX} \quad \forall\, i \in \mathcal{S} \quad t \in [t_0, T]
\tag{3.62}
$$

This means that when solving (3.57) we need to calculate, for a set $\mathcal{S}$ of the kind defined above, only the optimal aggregate profile $\sum_{i \in \mathcal{S}} P_i^*$, determining the power P_i^* of the individual turbine by solving (3.61), with $P_{\mathcal{S},r} = \sum_{i \in \mathcal{S}} P_i^*$. This approach can be applied to a more general situation by partitioning the turbines in subsets $\mathcal{S}_i$ that present similar properties as the ones detailed in (3.60).

Remark 3.9. To an arbitrary state vector $E \in \mathcal{E}^N$ it is always possible to associate $N-k$ distinct sets $\mathcal{S}_1, \ldots, \mathcal{S}_{N-k}$ with cardinality $\nu_i = |\mathcal{S}_i| \geq 1$ and such that the following holds for $i = 1, \ldots, N-k$:

$$
\begin{aligned}
\Gamma_E(E_j, v_j) &= \Gamma_E(E_l, v_l) & j, l &\notin \mathcal{S}_{MIN_i} \\
\Gamma_E(E_j, v_j) &\leq \Gamma_E(E_l, v_l) & j &\in \mathcal{S}_{MIN_i}\,,\ l \notin \mathcal{S}_{MIN_i}
\end{aligned}
\tag{3.63}
$$

where $\mathcal{S}_{MIN_i} = \{j : j \in \mathcal{S}_i, E_j = E_{MIN}\}$ with $|\mathcal{S}_{MIN_i}| = \nu_{MIN_i}$ and k is the difference between the state dimension N and the number of sets. Denoting the maximum derivative of Γ in each subset i as $\gamma_i = \max_{j \in \mathcal{S}_i} \Gamma_E(E_j, v_j)$, the following additional condition can be imposed:

$$
\gamma_1 > \gamma_2 > \cdots > \gamma_{N-k}
\tag{3.64}
$$

Given a vector E and the corresponding sets $\mathcal{S}_1, \ldots, \mathcal{S}_{N-k}$ described in Remark 3.9, the reduced state vector $\phi^{(k)} \in \mathbb{R}^{N-k}$ is introduced:

$$\phi_i^{(k)}(E) = \sum_{j \in \mathcal{S}_i} E_j \qquad i = 1, \ldots, N - k \tag{3.65}$$

Accordingly, the following dynamics and input constraints can be considered:

$$\dot{\phi}_i^{(k)}(E) = \sum_{j \in \mathcal{S}_i} \Gamma\left(g_{i,j}\left(\phi_i^{(k)}(E)\right), v_j\right) - \psi_i^{(k)}(P) \tag{3.66}$$

$$\nu_i P_{MIN} \leq \psi_i^{(k)}(P) \leq \sum_{j \in \mathcal{S}_{MIN_i}} \Gamma(E_{MIN}, v_j) + (\nu_i - \nu_{MIN_i}) P_{MAX} \tag{3.67}$$

where $\psi^{(k)}(P)$, to be regarded as the input vector of the reduced system, is defined as follows:

$$\psi^{(k)}(P) = \left[\sum_{j \in \mathcal{S}_1} P_j, \ldots, \sum_{j \in \mathcal{S}_{N-k}} P_j, \right] \tag{3.68}$$

The system reduction applies the results of Proposition 3.8 to sets $\mathcal{S}_1, \ldots, \mathcal{S}_{N-k}$ for which the solution of sub-problem (3.59) is equal to the unconstrained one $(E_{\mathcal{S}_i}^{\bar{*}}, P_{\mathcal{S}_i}^{\bar{*}})$ for (3.61), assuming that (3.62) holds on each subset $\mathcal{S}_i$. The function $g_{i,j}$ in (3.66) returns the energy repartition in the original coordinate E_j of the aggregate state $\phi_i^{(k)}$. Since we are assuming that the state trajectories of the turbines in $\mathcal{S}_i$ correspond to the optimal ones of the unconstrained problem (3.61), following Theorem 3.4 it is possible to define $g_{i,j}$ as the energy component of the j-th turbine in the solution of (3.44) for $E_{TOT} = \phi_i^{(k)}$. This reduces the number of control inputs to be determined from $P \in \mathbb{R}^N$ to $\psi^{(k)} \in \mathbb{R}^{N-k}$: for each set $\mathcal{S}_i$, once the aggregate power $\psi_i^{(k)}$ has been determined, the individual power P_j with $j \in \mathcal{S}_i$ can be calculated by considering (3.53) of the unconstrained sub-problem. The choice to model the aggregate state $\phi_i^{(k)}$ as the sum of the individual turbine energies in $\mathcal{S}_i$ is used to introduce monotonicity, as it will be shown next, and allows to consider the sum $\psi_i^{(k)}(P) = \sum_{j \in \mathcal{S}} P_j$ as an explicit input of the new system. Notice also that, for sets $\mathcal{S}_i = \{l\}$ with $\nu_i = 1$, the corresponding inputs ($\psi_i^{(k)}$ and P_l) and states ($\phi_i^{(k)}$ and E_l) in the two systems coincide.

A change of coordinates is now introduced:

$$\hat{\phi}_i^{(k)}(E) = \sum_{j=1}^{i} \phi_j^{(k)}(E) \qquad \hat{\psi}_i^{(k)}(P) = \sum_{j=1}^{i} \psi_j^{(k)}(P) \tag{3.69}$$

$$\dot{\hat{\phi}}_i^{(k)}(E) = \sum_{j=1}^{i} \sum_{l \in \mathcal{S}_j} \Gamma(g_{j,l}(\phi_j^{(k)}(E)), v_l) - \hat{\psi}_i^{(k)}(P) \tag{3.70}$$

with the following expressions for state and output in the original coordinates:

$$\phi_i^{(k)}(E) = \begin{cases} \hat{\phi}_1^{(k)}(E) & \text{if} \quad i = 1 \\ \hat{\phi}_i^{(k)}(E) - \hat{\phi}_{i-1}^{(k)}(E) & \text{if} \quad i > 1 \end{cases} \tag{3.71}$$

$$\psi_i^{(k)}(E) = \begin{cases} \hat{\psi}_1^{(k)}(E) & \text{if} \quad i = 1 \\ \hat{\psi}_i^{(k)}(E) - \hat{\psi}_{i-1}^{(k)}(E) & \text{if} \quad i > 1 \end{cases} \tag{3.72}$$

Proposition 3.9. *The system defined by (3.69) and (3.70), for partitions that satisfy the conditions in Remark 3.9, is monotone for the orders induced from orthant $\mathbb{R}_{\geq 0}^{N-k}$ for the state $\hat{\phi}^{(k)}$ and $\mathbb{R}_{\leq 0}^{N-k}$ for the control $\hat{\psi}^{(k)}$.*

Proof. The monotonicity can be proved by considering Corollary III.3 in [46]. Notice in particular that the function on the right hand side of (3.70), which defines the state derivative, is continuously differentiable (from maximum theorem in the proof of Proposition 3.4) and the sets of admissible states and controls (denoted respectively by $\hat{\Phi}$ and $\hat{\Psi}$) are convex since they are defined by a set of linear inequalities. This means that the system is monotone if, for the following partial derivatives, it holds:

$$\begin{aligned} \frac{\partial \dot{\hat{\phi}}_i}{\partial \hat{\phi}_j}(\hat{\phi}, \hat{\psi}) &\geq 0 & i \neq j & & \hat{\phi} \in \hat{\Phi}, \hat{\psi} \in \hat{\Psi} \\ \frac{\partial \dot{\hat{\phi}}_i}{\partial \hat{\psi}_j}(\hat{\phi}, \hat{\psi}) &\leq 0 & \begin{matrix} i = 1 \dots N - k \\ j = 1 \dots N - k \end{matrix} & & \phi \in \hat{\Phi}, \hat{\psi} \in \hat{\Psi} \end{aligned} \tag{3.73}$$

Notice that dependency from E, P and the reduction parameter k are not explicitly shown in the proof for a more compact notation. It is straightforward to verify that the derivatives with respect to $\hat{\psi}$ are negative while, for the ones with respect to the state $\hat{\phi}$, two different cases have to be considered. The following expression can be provided for $i = 1$ by substituting (3.71) in (3.70):

$$\frac{\partial \dot{\hat{\phi}}_1}{\partial \hat{\phi}_j} = \begin{cases} \displaystyle\sum_{l \in \mathcal{S}_1} \Gamma_E \left(g_{1,l}\left(\hat{\phi}_1\right), v_l \right) \cdot \frac{dg_{1,l}\left(\hat{\phi}_1\right)}{d\phi} & \text{if } j = 1 \\ 0 & \text{if } j > 1 \end{cases} \tag{3.74}$$

In the same way, it is possible to verify that for $i > 1$ and $j > i$ the partial derivatives are equal to zero while, for the case $i > 1$ and $j < i$, it holds:

$$\begin{aligned} \frac{\partial \dot{\hat{\phi}}_i}{\partial \hat{\phi}_j} = &\sum_{l \in \mathcal{S}_j} \Gamma_E \left(g_{j,l}\left(\hat{\phi}_j - \hat{\phi}_{j-1}\right), v_l \right) \cdot \frac{dg_{j,l}\left(\hat{\phi}_j - \hat{\phi}_{j-1}\right)}{d\phi} \\ &- \sum_{l \in \mathcal{S}_{j+1}} \Gamma_E \left(g_{j+1,l}\left(\hat{\phi}_{j+1} - \hat{\phi}_j\right), v_l \right) \cdot \frac{dg_{j,l}\left(\hat{\phi}_{j+1} - \hat{\phi}_j\right)}{d\phi} = \dots \end{aligned}$$

$$\cdots \quad = \quad \sum_{l \in \mathcal{S}_j} \Gamma_E \left(g_{j,l} \left(\phi_j \right), v_l \right) \cdot \frac{dg_{j,l} \left(\phi_j \right)}{d\phi} - \sum_{l \in \mathcal{S}_{j+1}} \Gamma_E \left(g_{j+1,l} \left(\phi_{j+1} \right), v_l \right) \cdot \frac{dg_{j,l} \left(\phi_{j+1} \right)}{d\phi}$$

$$(3.75)$$

Notice now that $g_{j,l}(\phi_j)$ is defined as the optimal energy of the l-th turbine in the solution of (3.44) for $E_{TOT} = \phi_j$. Considering that $\sum_{l \in \mathcal{S}_j} g_{j,l}(\phi_j) = \phi_j$, for the sum of derivatives we have:

$$\sum_{l \in \mathcal{S}_j} \frac{dg_{j,l}(\phi_j)}{d\phi} = 1 \qquad (3.76)$$

Furthermore, given the definition of the sets $\mathcal{S}_j$ provided in Remark 3.9, two different cases have to be analysed. If $\mathcal{S}_{MIN_j} = \mathcal{S}_j$ only positive variations of ϕ_j must be considered. From Remark 3.7 on the optimal state in the unconstrained problem, the components which are equal to E_{MIN} must always have a derivative Γ_E which is lower or equal than the remaining ones. This means that in the present case the energy increase must be performed only on the sets of turbines $\mathcal{S}_{\gamma_j}$, defined as follows:

$$\mathcal{S}_{\gamma_j} = \{l : l \in \mathcal{S}_j, \Gamma_E(g_{j,l}(\phi_j), v_l) = \gamma_j\}$$

From the total sum (3.76) for the derivatives of g, the following holds:

$$\frac{dg_{j,l}(\phi_j)}{d\phi} = 0 \ \forall l \notin \mathcal{S}_{\gamma_j} \qquad \sum_{l \in \mathcal{S}_{\gamma_j}} \frac{dg_{j,l}(\phi_j)}{d\phi} = 1$$

When $\mathcal{S}_{MIN_j} \subset \mathcal{S}_j$, one can directly consider the derivative with respect to $E_{TOT}^*(t)$ of the optimal state $E_i^*(t)$ defined in (3.48) for the unconstrained case, obtaining the following:

$$\frac{dg_{j,l}(\phi_j)}{d\phi} = 0 \ \forall l \in \mathcal{S}_{MIN_j} \qquad \sum_{l \in \mathcal{S}_j \setminus \mathcal{S}_{MIN_j}} \frac{dg_{j,l}(\phi_j)}{d\phi} = 1$$

In conclusion, for both cases, $dg_{j,l}(\phi_j)/d\phi$ is different from zero only for a subset of turbines whose derivatives Γ_E are all equal to γ_j. If we consider that (3.76) holds for the total sum, the following equivalent expression can be provided for (3.75):

$$\frac{\partial \dot{\hat{\phi}}_i}{\partial \hat{\phi}_j} = \gamma_j - \gamma_{j+1} > 0$$

where the inequality is verified if one considers (3.64) in the definition of the sets $\mathcal{S}_i$. $\quad \square$

Following Proposition 3.8 and subsequent comments, the calculation of the optimal solution of (3.57) can be characterized analytically and computed through numerical integration of suitable ODEs if we constrain our analysis to a particular class of signals $\mathbb{E}$.

Definition 3.1. Consider a feasible state trajectory $\bar{E}(\cdot) : [0, T] \to \mathcal{E}^N$, denoting by $\bar{P}(\cdot)$ the corresponding power profile and defining, for each $t \in [0, T]$, a subset repartition $\{\mathcal{S}_1(t), \ldots, \mathcal{S}_{N-k(t)}(t)\}$ which satisfies (3.63) for $E = \bar{E}(t)$. It holds $\bar{E}(\cdot) \in \mathbb{E}$ if the following condition is satisfied:

$$\bar{P}_{\mathcal{S}_i(t)}(t) = P_{\mathcal{S}_i(t)}^{\bar{*}}(t) \qquad \begin{array}{c} i = 1, \ldots, N - k(t) \\ \forall t \in [0, T] \end{array} \tag{3.77}$$

where $\bar{P}_{\mathcal{S}_i(t)}(t)$ is the vector of the j-th components of $\bar{P}(t)$ such that $j \in \mathcal{S}_i(t)$ while $P_{\mathcal{S}_i(t)}^{\bar{*}}$ is the solution of the unconstrained optimization problem (3.61) with $\mathcal{S} = \mathcal{S}_i(t)$, $t_0 = t$ and $P_{\mathcal{S},r}(s) = \sum_{j \in \mathcal{S}_i(s)} \bar{P}_j(s)$:

$$
\begin{aligned}
P_{\mathcal{S}_i(t)}^{\bar{*}} = \; & \underset{P_j(\cdot), j \in \mathcal{S}_i(t)}{\arg\max} \; \sum_{j \in \mathcal{S}_i(t)} E_j(T) \\
\text{s. t. } & \sum_{j \in \mathcal{S}_i(t)} P_j(s) = \sum_{j \in \mathcal{S}_i(t)} \bar{P}_j(s) \\
& E_j(t) = \bar{E}_j(t) \\
& \dot{E}_j(s) = \Gamma(E_j(s), v_j) - P_j(s) \\
& E_j(s) \in [E_{MIN}, E_{MAX}]
\end{aligned}
\qquad
\left(
\begin{array}{c}
\forall j \in \mathcal{S}_i(t) \\
\\
\forall s \in [t, T]
\end{array}
\right)
\tag{3.78}
$$

In other words, the class of signals $\mathbb{E}$ corresponds to the state trajectories $\bar{E}(\cdot)$ whose power profiles $\bar{P}(\cdot)$ are equal to the optimum of the unconstrained subproblem (3.61) for any configuration which at time t satisfies (3.58a) and therefore does not require impulsive switching. This implies that, for all $t \in [0, T]$, the power profiles of the individual turbines in $\mathcal{S}_i(t)$ can be defined exclusively on the basis of their current kinetic energy and of their aggregate power value. It is therefore possible to associate to $\bar{E}(\cdot) \in \mathbb{E}$ a reduced system description with state $\phi^{(k(t))}(\bar{E})$ and input $\psi^{(k(t))}(\bar{P})$, defined as in (3.65)-(3.68). The partitioning of the state E at each time instant can then be performed by simply joining at time t existing subsets i, j which present equal maximum derivative $\gamma_i(t) = \gamma_j(t)$. This can be achieved by the following procedure, which also preserves at each t the ordering in (3.64) and therefore the monotonicity of the reduced system described in Proposition 3.9:

1. At time $t = 0$ introduce the partition $\mathcal{S}_1^{\langle 0 \rangle}, \ldots, \mathcal{S}_{N-k_0}^{\langle 0 \rangle}$ following Remark 3.9 for $E = E^0$. The corresponding maximum derivative over time are denoted by $\gamma_1^{\langle 0 \rangle}(t), \ldots, \gamma_{N-k_0}^{\langle 0 \rangle}(t)$ and defined as follows:

$$\gamma_i^{\langle 0 \rangle}(t) = \max_{j \in \mathcal{S}_i^{\langle 0 \rangle}} \Gamma_E(E_j(t), v_j) \tag{3.79}$$

2. Set $l = 0$ and $t_l = 0$.

3. At each time $t > t_l$ verify if there exist indexes $i, j \in \{1, \ldots, N - k_l\}$ for which the following holds:

$$\gamma_i^{\langle l \rangle}(t) = \gamma_j^{\langle l \rangle}(t) \tag{3.80}$$

- If (3.80) is never satisfied, then $\mathcal{S}_i(t) = \mathcal{S}_i^{\langle l \rangle}$ and $k(t) = k_l$ for all $t \in (t_l, T]$ and $i = 1, \ldots, N - k_l$. Set $L = l$ and exit the procedure.

- If (3.80) holds for $t = \bar{t}$, go to step 4.

4. Define $\mathcal{S}_i(t) = \mathcal{S}_i^{\langle l \rangle}$ and $k(t) = k_l$ for $i = 1, \ldots, N - k_l$ and for all $t \in (t_l, \bar{t}]$. Set $l = l + 1$ and $t_l = \bar{t}$.

5. Set $\mathcal{S}^{IN} = \mathcal{S}^{\langle l-1 \rangle}$ and perform the following:

    (a) Denote by q the dimension of $\mathcal{S}^{IN}$ and by $\gamma_1^{IN}, \ldots, \gamma_q^{IN}$ the maximum derivative in each of its subsets.

    (b) Find the minimum $m \in \{1, \ldots, q\}$ such that it yields $\gamma_m^{IN} = \gamma_{m+1}^{IN}$.

    (c) If m does not exist set $\mathcal{S}^{\langle l \rangle} = \mathcal{S}_{IN}$ and $k_l = N - q$, define $\gamma_1^{\langle l \rangle}, \ldots, \gamma_{N-k_l}^{\langle l \rangle}$ as in (3.79) and go to step 3. If m exists, define $\mathcal{S}_{FIN}$ as follows:

$$\mathcal{S}_i^{FIN} = \begin{cases} \mathcal{S}_i^{IN} & \text{if} \quad i < m \\ \mathcal{S}_m^{IN} \cup \mathcal{S}_{m+1}^{IN} & \text{if} \quad i = m \\ \mathcal{S}_{i+1}^{IN} & \text{if} \quad i > m \end{cases}$$

Set $\mathcal{S}^{IN} = \mathcal{S}^{FIN}$ and go to step 5.a.

With the proposed procedure it is possible to partition the time interval $[0, T]$ in the following way:

$$[0, T] = [t_0, t_1] \cup (t_1, t_2] \cdots \cup (t_L, T] = \tau_1 \cup \tau_2 \cdots \cup \tau_L$$

Furthermore, the order reduction parameter k is a function of time and is constant on each of the time subinterval:

$$k(t) = k_l \qquad \forall t \in \tau_l$$

with $k_1 < k_2 < \cdots < k_L$. Notice also that the proposed algorithm unifies two partition subsets $\mathcal{S}_i^{\langle l \rangle}(t)$ and $\mathcal{S}_{i+1}^{\langle l \rangle}(t)$ every time it holds $\gamma_i^{\langle l \rangle}(t) = \gamma_{i+1}^{\langle l \rangle}(t)$. If we consider that the derivative Γ_E is continuous in time and the initial partition at $t = 0$ is performed according to Remark 3.9, the following inequality is satisfied for all $l \in \{1, \ldots, L\}$ and $t \in \tau_l$:

$$\gamma_1^{\langle l \rangle}(t) > \cdots > \gamma_{N-k_l}^{\langle l \rangle}(t)$$

The main result for the final state maximization problem (3.57) can now be provided:

Theorem 3.5. *Consider a state trajectory $E^*(\cdot)$ and the corresponding power profile $P^*(\cdot)$ which are feasible for (3.57), where $E^*(\cdot) \in \mathbb{E}$ as specified in Definition 3.1 and therefore admits a reduced system $(\phi^{(k)}(E^*), \psi^{(k)}(P^*))$. The control P^* is optimal for problem (3.57) if the following holds for any other feasible $\bar{P}$:*

$$\hat{\psi}_i^{(k(t))}(P^*(t)) \leq \hat{\psi}_i^{(k(t))}(\bar{P}(t)) \qquad \begin{array}{c} \forall t \in [0, T] \\ i = 1, \ldots, N - k(t) \end{array} \tag{3.81}$$

where $\hat{\phi}^{(k)}(E^*)$ and $\hat{\psi}^{(k)}(P^*)$ represent respectively state and control of the reduced system when the change of coordinate described by (3.69) is applied.

Proof. It follows from (3.70) and inequality (3.81) that the power profile P^* maximizes the derivative of each state component $\hat{\phi}_i^{(k(t))}(E^*(t))$ of the reduced system. If one considers the time interval $\tau_L = (t_L, T]$, following the monotonicity of the reduced system introduced in Proposition 3.9, for $i = 1, \ldots, N - k_L$ it holds:

$$\hat{\phi}_i^{(k_L)}(E^*(T)) = \max_{\hat{\psi}^{(k_L)}(\cdot)} \hat{\phi}_i^{(k_L)}(E(T))$$

$$\text{s. t.} \quad \begin{array}{l} \sum_{i=1}^{N} P_i = P_r(t) \\ \hat{\phi}_i^{(k_L)}(E(t_L)) = \hat{\phi}_i^{(k_L)}(E^*(t_L)) \qquad \forall t \in (\tau_L, T] \\ P_i(t) \in [P_{MIN}, P_{MAX}] \end{array} \tag{3.82}$$

For the same monotonicity properties, the maximized state $\hat{\phi}_i^{(k_L)}(E^*(T))$ is monotonically increasing with respect to each component of $\hat{\phi}^{(k_L)}(E^*(t_L))$. It also holds $\hat{\phi}^{(k_L)}(E^*(t_L)) \subset \hat{\phi}^{(k_{L-1})}(E^*(t_L))$: in fact, a new subset repartition is always obtained by unifying sets with adjacent indexes and $\hat{\phi}_i^{(k)}$ is defined as the sum of the variables $\phi_j^{(k)}$ for $j = 1, \ldots, i$. With similar steps, one can verify that $\hat{\phi}^{(k_{L-1})}(E^*(t_L))$ is the maximum of (3.82) for k_{L-1}, τ_{L-1} and t_{L-1}. By repeating the same considerations for decreasing values of l and corresponding order reductions k_l, time intervals τ_l and final times t_l until $l = 0$, it is possible to show that, for the given initial condition E^0, P^* maximizes $\hat{\phi}_i^{(k_L)}(E(T))$ for $i = 1, \ldots, N - k_L$. Proof is concluded by considering that the objective function in (3.57) is the last state component of the reduced system in the changed coordinates:

$$\sum_{i=1}^{N} E_i(T) = \hat{\phi}_{N-k_L}^{(k_L)}(E(T))$$

$\square$

The numerical calculation of the optimal profile P^* is straightforward and can be performed, starting from 0 and for increasing values of t, in two separate steps:

1. Given the current state repartition $\{\mathcal{S}_1, \ldots, \mathcal{S}_{N-k(t)}\}$ calculate the values of $\psi^{(k(t))}$ which satisfy (3.81) for the corresponding $\hat{\psi}^{(k(t))}$ and the constraint in (3.57) on the aggregate power, with $\sum_{i=1}^{N-k(t)} \psi_i^{(k(t))} = P_r(t)$. Notice from (3.69) that each $\psi_j^{(k)}$ appears in the expression of all $\hat{\psi}_i^{(k)}$ with $i \geq j$. This means that (3.81) can be satisfied by choosing the maximum feasible value for $\psi_{N-k(t)}^{(k(t))}$, doing the same on all the others $\psi_i^{(k(t))}$ for decreasing indexes i until the aggregate power $P_r(t)$ has been allocated.

2. Determine $P^*(t)$ which returns the desired $\psi^{(k(t))}$. For each partition subset $\mathcal{S}_i(t)$, with $i = 1, \ldots, N - k(t)$, two different cases must be considered:

    (a) If $\nu_i = |\mathcal{S}_i(t)| = 1$ and $\mathcal{S}_i(t) = \{l\}$, one can verify that $P_l^*(t) = \psi_i^{(k(t))}$.

    (b) If $\nu_i > 1$, the unconstrained sub-problem (3.61) is solved for $\mathcal{S} = \mathcal{S}_i(t)$, $t_0 = t$ and $P_{\mathcal{S},r} = \psi_i^{k(t)}$. The values of $P_l^*(t)$ with $l \in \mathcal{S}_i(t)$ will correspond to the unconstrained solution $P_{\mathcal{S}_i(t)}^{\bar{*}}(t)$.

From Theorem 3.5 and the procedure for the calculation of the optimal control, it can be seen that the final aggregate kinetic energy is maximized by allocating maximum power on the turbines with lower derivative Γ_E. When a group of turbines $\mathcal{S}$ have equal derivative, this configuration is considered as the initial condition of an unconstrained problem whose solution $P^{\bar{*}}$ is feasible for the original maximization if (3.62) holds.

Remark 3.10. Notice that in some cases condition (3.62) may not be satisfied. In particular, given the expressions (3.51) and (3.53) for the optimal power in the unconstrained case, it can be seen that this is in general different for each turbine and it depends on the wind speed v_i. Consider now a subset $\mathcal{S}(\bar{t})$ of turbines with cardinality S: if the assigned power reference $P_{\mathcal{S}(\bar{t}),r}$ is sufficiently close to $S \cdot P_{MAX}$, the resulting unconstrained optimal power profiles $P_{\mathcal{S}(\bar{t}),i}^{\bar{*}}$ will not be feasible. In this case, under the specified constraints, the initial ordering of the maximum derivative γ of the turbine subsets cannot be preserved and the results of Theorem 3.5 no longer apply. Notice that this does not happen when equal wind speeds are considered since, in this case, equal Γ_Es correspond to equal P^*s.

It is also worth pointing out that, for scenarios with different wind speeds, it is possible to find a possibly suboptimal solution by the following heuristic approach. In particular, a new repartition for which (3.64) holds can be introduced. Starting from $\bar{t}$, the resulting state vector $\hat{\phi}^{(k(\bar{t}))}$ (which still includes in its last component the total kinetic energy of the wind farm) can be maximized over the interval $[\bar{t}, T]$. For simulations run with standard turbine parameters, whose results are shown in the next section, the feasibility of $P^{\bar{*}}$ for the constrained problem has always been verified.

3.4.4 Simulation Results

The performance of the proposed scheduling has been evaluated in simulations. The turbine parameters presented in [41] have been adopted, converting the operative interval of the rotor speed to the corresponding kinetic energy values:

$$
\begin{aligned}
R &= 37.5m & J &= 5.9 \cdot 10^6 Kg \cdot m^2 \\
P_{MIN} &= 0MW & P_{MAX} &= 2MW \\
E_{MIN} &= 2.62 \cdot 10^6 J & E_{MAX} &= 1.43 \cdot 10^7 J
\end{aligned}
\tag{3.83}
$$

A first analysis focuses on the case of turbines with unconstrained power, considering a population of $N = 20$ generators. A qualitative representation of the considered scenario is presented in Fig. 3.9: initially all generators are operating at the point of maximum efficiency $E_i(0) = E_{ss}(v_i)$ with different wind speeds in the interval $[8m/s, 10m/s]$ and equal derivatives $\Gamma_E(E_1(0), v_1) = \cdots = \Gamma_E(E_N(0), v_N) = 0$. The total power provided by the wind farm is equal to P_0, as defined in (3.41). At time $t = 0$, supposing a frequency event occurs, the reference for the aggregate generated power is increased:

$$
P_r(t) = 1.3 \sum_{i=1}^{N} \Gamma(E_{ss}(v_i), v_i) = 1.3 P_0
$$

After having provided frequency response, the turbines move to a recovery phase: they reduce power generation in order to increase their kinetic energy and reach the operating point of maximum efficiency which characterizes normal operation. The recovery problem is studied in detail in Section 3.5.
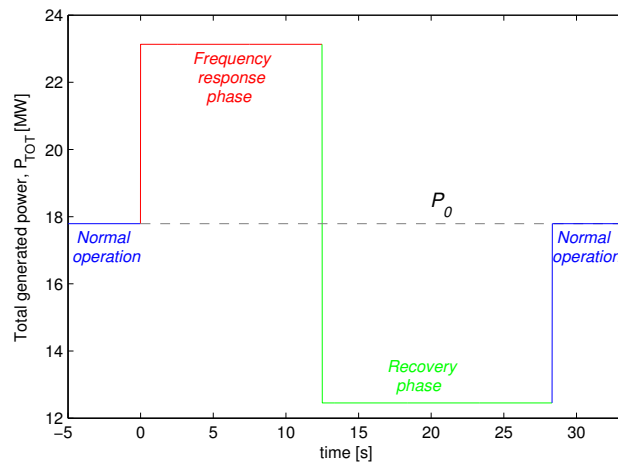
FIGURE 3.9: Total power generated by the wind turbines population at different operational modes.

The optimal scheduling is calculated with a time step $\Delta t = 0.05s$, solving the static optimization problem (3.44) at each time instant $l \cdot \Delta t$. The optimal energy trajectories E^* for each turbine are shown in Fig. 3.10. It can be seen that the kinetic energy is reduced across time in all generators in order to maintain an equal derivative Γ_E. The corresponding optimal power profiles P^* are shown in Fig. 3.11: at first the generated power is approximatively constant for all turbines. When the slowest turbine (let it be turbine i) reaches the minimum energy E_{MIN}, its power generation is instantaneously reduced to $\Gamma(E_{MIN}, v_i)$ and the control effort is redistributed among the remaining generators which, as a consequence, increase their individual power output considerably in order to meet overall power requirements. Since turbines have equal derivatives Γ_E at time $t = 0$ and therefore satisfy (3.50), there is no impulsive energy switch. The optimal power in the unconstrained case is finite and, in this example, it is also within the operational limit $P_{MIN} < P < P_{MAX}$ of the turbines except for the very last part of the frequency response when the power output of some turbines is indirectly limited by the fact that they have reached the minimum feasible energy E_{MIN}.
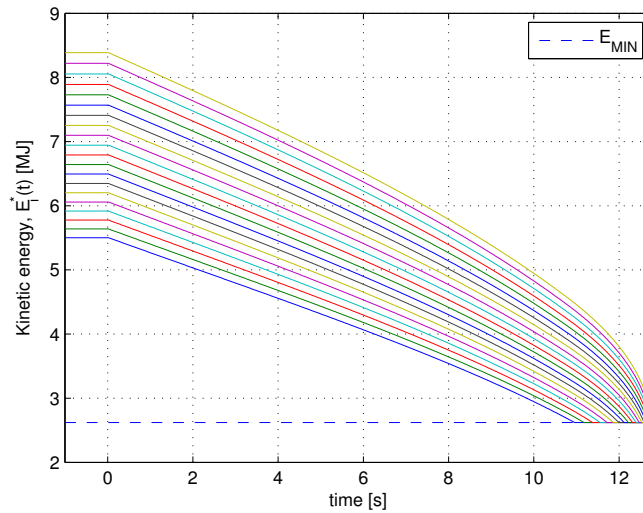
FIGURE 3.10: Kinetic energy of the individual wind turbines when providing frequency response in the unconstrained power case.

A similar scenario is now simulated when constraints on the generated power P are considered: in this case it is assumed that turbines have different derivative Γ_E at $t = 0$, with wind speed and initial state defined as follows for $j = 1, \ldots, 20$:

$$v_j = 8 + 0.1 \cdot j \qquad E_j(0) = E_{ss}(v_j) \cdot (1.02 - 0.02 \cdot j) \tag{3.84}$$

The optimal state trajectories, generated power profiles and partial derivatives Γ_E of the individual turbines are shown respectively in Fig. 3.12, 3.13 and 3.14. Three different
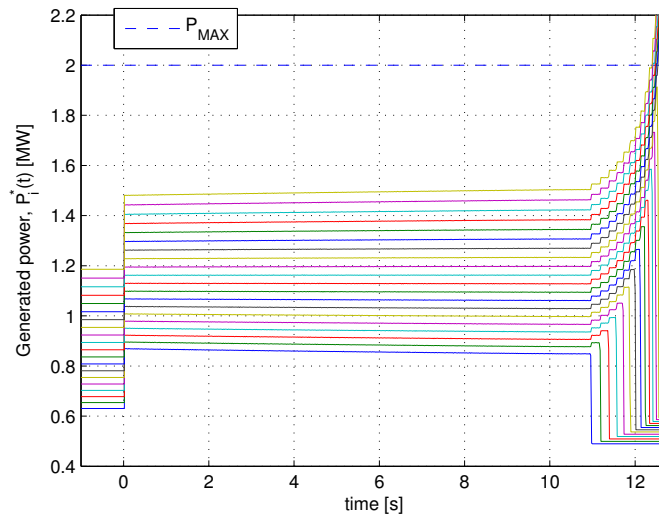
FIGURE 3.11: Optimal power profiles P_i^* for turbine scheduling in the unconstrained case.

time intervals can be analysed separately, on the basis of the values of Γ_E. At the beginning of the frequency response (from 0 to 1 second) the power derivatives are distinct: the aggregate power P_r is allocated by setting $P_i^*(t) = P_{MAX}$ for the turbines that have lower Γ_E which, as a result, are slowed down. Since P_r is not an integer multiple of P_{MAX}, one of these turbines will generate a power which is lower than the maximum. Gradually the generators will converge to equal values of Γ_E: every time this happens, one turbine moves from maximum (or minimum) generation to some intermediate value and the power of the turbines with the same derivative is adjusted accordingly. In a second time interval (approximatively from 1 to 6 seconds), all turbines have equal values of Γ_E and therefore the results are similar to the ones of the unconstrained case: energy is gradually reduced, the derivative Γ_E increases over time and the power P_i^* of each generator remains almost constant. In the last interval, when turbines start reaching the minimum energy value E_{MIN}, their power is reduced to $P_i^*(t) = \Gamma(E_{MIN}, v_i)$ and such variation is compensated by increasing the power on the remaining ones until feasibility can be guaranteed.

Finally, for the considered values of initial energy and wind speed, it is supposed that a certain time T of frequency response is required from the turbines. The maximum power increase factor $\Delta P/P_0$ which can be obtained with the proposed scheduling by setting $P_r(t) = P_0 + \Delta P$ for all $t \in [0, T]$ is shown in Fig. 3.15. Notice that, at lower values of T (and higher power increase factors), the power reduction is more significant. This can be explained considering that, in this case, turbines are generating more power, moving away faster from their initial operating point and introducing a larger reduction of efficiency.
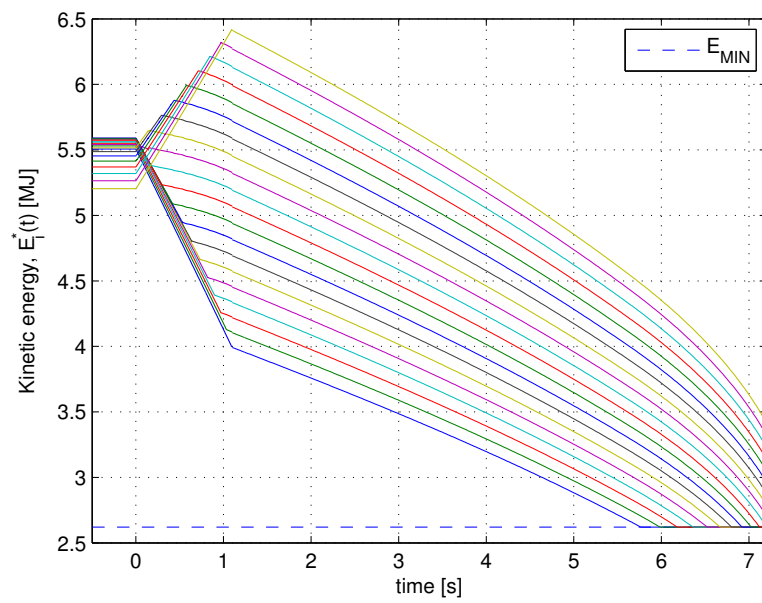
FIGURE 3.12: Kinetic energy of the individual wind turbines when providing frequency response in the constrained power case.
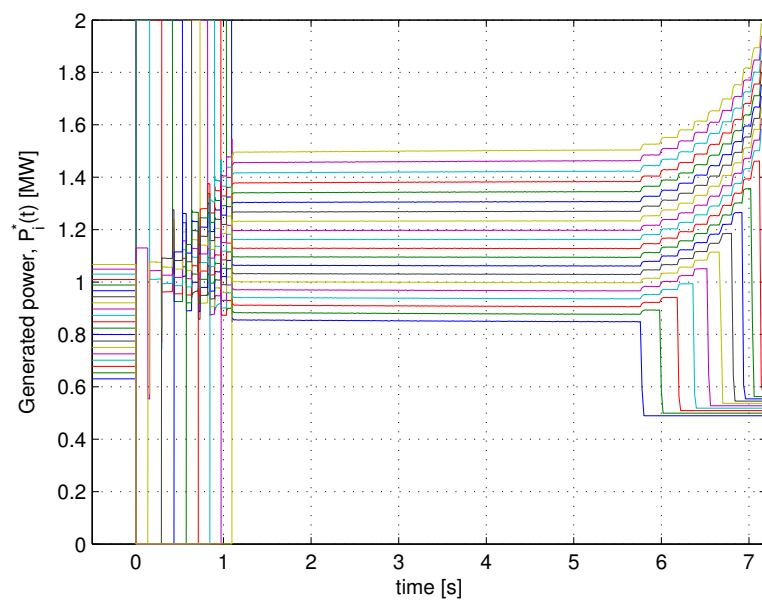
FIGURE 3.13: Optimal power profiles P_i^* for turbine scheduling with constraints on generated power.
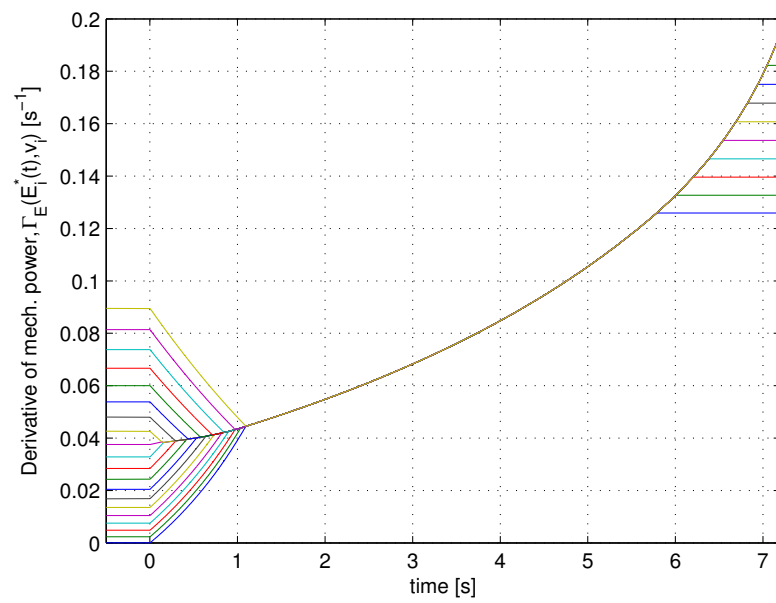
FIGURE 3.14: Partial derivative $\Gamma_E(E_i^*(t), v_i)$ for the optimal scheduling with constraints on generated power.
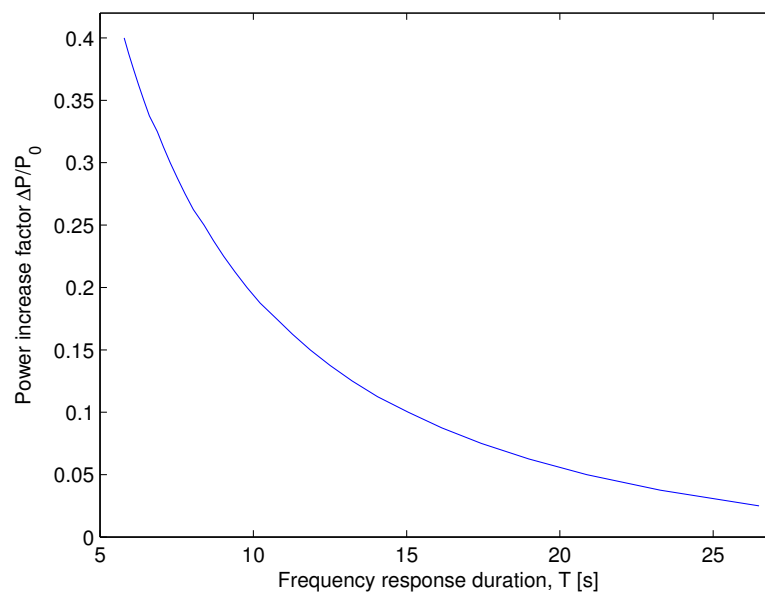
FIGURE 3.15: Maximum percentage increase $\Delta P/P_0$ of total generation that can be achieved with the proposed scheduling when T seconds of frequency response are required.

3.5 Optimal Energy Recovery

When turbines provide frequency response they release part of their kinetic energy and, as a result, they move away from their operation point of maximum efficiency. Therefore, after the frequency support has been provided, it is desirable to bring back the turbines to their optimal rotor speed (and corresponding kinetic energy). The recovery is approached as an optimal control problem, imposing a minimum value P_L of aggregate generated power and calculating the power profiles P_i which minimize the time required to restore the original configuration of maximum production in the wind farm:

$$
\begin{aligned}
\min_{T, P_i(\cdot), i=1\ldots N} \quad & T \\
\text{s. t.} \quad & \sum_{i=1}^{N} P_i(t) \geq P_L \\
& E_i(0) = E_i^0 \\
& E_i(T) = E_{ss}(v_i) \\
& \dot{E}_i(t) = \Gamma(E_i(t), v_i) - P_i(t) \\
& E_i(t) \in [E_{MIN}, E_{ss}(v_i)] \\
& P_i(t) \in [P_{MIN}, P_{MAX}]
\end{aligned}
\qquad
\left(
\begin{array}{c}
\forall i = 1, \ldots, N \\
\forall t \in [0, T]
\end{array}
\right)
\tag{3.85}
$$

The feasibility of the problem is initially assessed, determining the values of P_L in the interval $[NP_{MIN}, NP_{MAX}]$ for which a solution exists. A preliminary assumption is made for the constraints on the generated power P_i of the single turbine:

Assumption 3.4. *For any feasible value E_i, it is always possible to increase or reduce the kinetic energy of the turbine:*

$$
0 \leq P_{MIN} < \Gamma(E_i, v_i) < P_{MAX}
\qquad
\begin{array}{c}
i = 1, \ldots, N \\
E_i \in [E_{MIN}, E_{ss}(v_i)]
\end{array}
\tag{3.86}
$$

A first feasibility result can now be provided with the following sufficient condition:

Proposition 3.10. *Under Assumption 3.4, given the initial state E^0, problem (3.85) is feasible for a certain value P_L of minimum total generated power if:*

$$
P_L < \sum_{i=1}^{N} \Gamma\left(E_i^0, v_i\right) = \Gamma_{TOT}\left(E^0\right)
\tag{3.87}
$$

where Γ_{TOT} denotes the aggregate mechanical power extracted by the wind turbines as a function of their kinetic energy.

Proof. We show that, if (3.87) holds, there exists at least one power profile $\bar{P}(\cdot)$ that satisfies the constraints in (3.85). In order to construct $\bar{P}$, denote the set of turbines

which have reached the desired terminal state by $\mathcal{F}(E) := \{i : E_i = E_{ss}(v_i)\}$. The power profile can now be defined through the following feedback law for $i = 1, \dots N$:

$$\bar{\varphi}_i(E) = \begin{cases} \Gamma(E_{ss}(v_i), v_i) & i \in \mathcal{F}(E) \\ \\ \max\left(\Gamma(E_i, v_i) \cdot r(E), P_{MIN}\right) & i \notin \mathcal{F}(E) \end{cases} \tag{3.88}$$

where the function $r(E)$ is defined as follows:

$$r(E) = \frac{P_L - \sum_{i \in \mathcal{F}(E)} \Gamma(E_{ss}(v_i), v_i)}{\Gamma_{TOT}(E) - \sum_{i \in \mathcal{F}(E)} \Gamma(E_{ss}(v_i), v_i)} = \frac{P_L - \sum_{i \in \mathcal{F}(E)} \Gamma(E_{ss}(v_i), v_i)}{\sum_{i \notin \mathcal{F}(E)} \Gamma(E_i, v_i)} \tag{3.89}$$

It is straightforward to verify that $\bar{\varphi}$ satisfies the constraint on the minimum total generated power. In fact, for an arbitrary E, it holds:

$$\sum_{i \notin \mathcal{F}(E)} \bar{\varphi}_i(E) \geq \sum_{i \notin \mathcal{F}(E)} \Gamma(E_i, v_i) \cdot r(E) = P_L - \sum_{i \in \mathcal{F}(E)} \bar{\varphi}_i(E) \tag{3.90}$$

We define now $\bar{E}(\cdot)$ as the unique solution, for $i = 1, \dots, N$, of the following system of differential equations:

$$\dot{E}_i(t) = \Gamma(E_i(t), v_i) - \varphi_i(E(t)) \qquad E_i(0) = E_i^0 \tag{3.91}$$

The corresponding power profile will be equal to the feedback law $\bar{\varphi}$ evaluated along $\bar{E}$, with $\bar{P}_i(t) = \bar{\varphi}_i(\bar{E}(t))$ for $i = 1, \dots, N$. To show that $\bar{E}$ satisfies the final state condition in (3.85), considering that $\dot{\bar{E}}_i(t) = 0$ if $\bar{E}_i(t) = E_{ss}(v_i)$, it is sufficient to verify the following:

$$\dot{\bar{E}}_i(0) > 0 \qquad \forall i \notin \mathcal{F}(E^0) \tag{3.92}$$

$$\frac{\partial \zeta_i(E)}{\partial E_j} > 0 \qquad \begin{matrix} \forall i, j \notin \mathcal{F}(E) \\ \forall E \in \prod_i \left(E_i^0, E_{ss}(v_i)\right] \end{matrix} \tag{3.93}$$

where $\zeta_i(E)$ denotes the time derivative of the i-th component of E when the feedback $\bar{\varphi}$ is applied. Specifically, for $i \notin \mathcal{F}(E)$, it holds:

$$\zeta_i(E) = \begin{cases} \Gamma(E_i, v_i)\left[1 - r(E)\right] & \text{if} \quad \Gamma(E_i, v_i) \cdot r(E) > P_{MIN} \\ \\ \Gamma(E_i, v_i) - P_{MIN} & \text{if} \quad \Gamma(E_i, v_i) \cdot r(E) \leq P_{MIN} \end{cases} \tag{3.94}$$

For the inequality in (3.92) notice that $\dot{\bar{E}}_i(0) = \zeta_i(E^0)$. If one replaces E^0 in (3.94), for the case $\Gamma(E_i, v_i) \cdot r(E) > P_{MIN}$ it is sufficient to consider that $r(E^0) < 1$ since $P_L < \Gamma_{TOT}(E^0)$. The inequality in the other case is verified from (3.86). For condition (3.93), this is always satisfied when $\Gamma(E_i, v_i) \cdot r(E) \leq P_{MIN}$ since $\Gamma_E > 0$. In the opposite

case, it holds $r(E) > 0$ since $\Gamma(E_i, v_i)$ and P_{MIN} are both nonnegative quantities. Furthermore, for the considered E, we have $P_L < \Gamma_{TOT}(E_0) < \Gamma_{TOT}(E)$ and therefore $r(E) < 1$. From expression (3.94) and the positivity of Γ_E, condition (3.93) holds if the following inequality is satisfied:

$$\frac{\partial r(E)}{\partial E_j} = -\frac{\Gamma_E(E_j, v_j)\left[P_L - \sum_{i \in \mathcal{F}(t)} \Gamma(E_{ss}(v_i), v_i)\right]}{\left[\Gamma_{TOT}(\bar{E}(t)) - \sum_{i \in \mathcal{F}(t)} P_i(t)\right]^2} < 0$$

This is true since the positivity of $\left[P_L - \sum_{i \in \mathcal{F}(t)} \Gamma(E_{ss}(v_i), v_i)\right]$ follows from the fact that $r(E)$ and its denominator in (3.89) are both greater than zero. The proof is concluded by noticing that also the constraints in (3.85) on the single power $\bar{P}_i$ are satisfied since $\varphi_i(E) \geq P_{MIN}$ by definition and $r(E) < 1$. □

If the sufficient condition (3.87) does not hold, there is no power profile which allows to instantly increase the energies E_i of all turbines. It is still possible, on the other hand, to provide milder conditions for the feasibility of the recovery problem, which in this case are necessary and sufficient:

Proposition 3.11. *For a given initial state E^0 and minimum aggregate generation P_L, problem (3.85) is feasible if and only if there exists a time $\tau \geq 0$ and a power profile $\bar{P}(\cdot)$ such that, for the corresponding energy vector $\bar{E}$, it holds:*

$$\sum_{i=1}^{N} \Gamma(\bar{E}_i(\tau), v_i) = \Gamma_{TOT}(\bar{E}(\tau)) > P_L \tag{3.95}$$

Proof. If τ specified in the claim does not exist, it follows that the derivative of the total energy stored in the turbines is always negative and therefore, since $E_i(0) < E_{ss}(v_i)$ $\forall i$, problem (3.85) is infeasible. If, on the other hand, (3.95) is satisfied, the feasibility is guaranteed by Proposition 3.10, considering τ as the initial time instant. □

This means that the feasibility of problem (3.85) can be determined by solving the following problem for increasing values of τ and comparing its solution with P_L:

$$
\begin{aligned}
\max_{P_i(\cdot), i=1...N} \quad & \Gamma_{TOT}(E(\tau)) \\
\text{s. t.} \quad & \sum_{i=1}^{N} P_i(t) \geq P_L \\
& E_i(0) = E_i^0 \\
& \dot{E}_i(t) = \Gamma(E_i(t), v_i) - P_i(t) \quad \left(\begin{array}{c} \forall i = 1, \ldots, N \\ \forall t \in [0, \tau] \end{array}\right) \\
& E_i(t) \in [E_{MIN}, E_{ss}(v_i)] \\
& P_i(t) \in [P_{MIN}, P_{MAX}]
\end{aligned}
\tag{3.96}
$$

In this respect, it is possible to extend previous optimization results:

Remark 3.11. If a power profile $P^*(\cdot)$ is optimal for problem (3.57) with $P_r(t) = P_L$ and $T = \tau$, it is also a solution for (3.96). To show this, it is sufficient to apply the state repartition presented in Remark 3.9 to the present case, considering the corresponding reduced system with the change of coordinates (3.69). Notice now that $\Gamma_{TOT}(E(t))$ corresponds to $\hat{\phi}_{N-k(t)}^{(k(t))} + P_r(t)$ which, from Proposition 3.9, has positive partial derivatives with respect to all the state components $\hat{\phi}_i^{(k(t))}$ with $i = 1 \ldots, N - k(t)$. Since, from the proof of Theorem 3.5, such components are maximized at final time $T = \tau$ by $P^*(\cdot)$, this is optimal also for problem (3.96).

The results provided in Section 3.4.3 can also be used to solve the current problem of time minimization:

Theorem 3.6. *Consider a state trajectory $E^*(\cdot)$ and the corresponding input profile $P^*(\cdot)$ which are feasible for (3.85), where $E^*(\cdot) \in \mathbb{E}$ as specified in Definition 3.1 and therefore admits a reduced system $(\phi^{(k)}(E^*), \psi^{(k)}(P^*))$. The input P^* (and the corresponding final time T^*) are optimal for problem (3.85) if, at each time instant $t \in [0, T^*]$, the following holds for any feasible $\bar{P}(t)$ such that $\sum_j \bar{P}_j(t) \geq P_L$, for $i = 1, \ldots, N - k(t)$:*

$$\hat{\psi}_i^{(k(t))}(P^*(t)) \leq \hat{\psi}_i^{(k(t))}(\bar{P}(t)) \tag{3.97}$$

where $\hat{\phi}^{(k)}(E^*)$ and $\hat{\psi}^{(k)}(P^*)$ represent respectively state and control of the reduced system when the change of coordinate described by (3.69) is applied.

Proof. Considering Theorem 3.5, P^* is the solution of (3.57) with $E_{MAX} = E_{ss}(v_i)$ and $P_r(t) = P_L \ \forall t \in [0, T^*]$. From the proof of such theorem, it follows that P^* maximizes the total amount of kinetic energy at each time instant $t \in [0, T^*]$. Furthermore, taking into account the constraints on the energy E_i of the single turbine, the following holds for the total kinetic energy over time:

$$\sum_{i=1}^{N} E_i^*(t) < \sum_{i=1}^{N} E_i^*(T^*) = \sum_{i=1}^{N} E_{ss}(v_i) \ \forall t \in [0, T^*) \tag{3.98}$$

If P^* is not optimal for (3.85), there exists a feasible power profile $\bar{P}$ and the corresponding energy vector $\bar{E}$ such that, for $\bar{T} < T^*$, it holds $\bar{E}_i(\bar{T}) = E_{ss}(v_i)$ with $i = 1, \ldots, N$. As a result, the following must hold at $t = \bar{T}$:

$$\sum_{i=1}^{N} \bar{E}_i(\bar{T}) = \sum_{i=1}^{N} E_{ss}(v_i) > \sum_{i=1}^{N} E_i^*(\bar{T})$$

but this contradicts the optimality of P^* for problem (3.57) with final time $\bar{T}$. $\qquad \square$

The time-minimizing control P^* can be calculated in the same way of problem (3.57): at each time instant t the aggregate power is allocated starting with the turbines which have lower Γ_E, solving the unconstrained energy problem for group of turbines which have equal derivatives. The feasibility conditions and the optimal scheduling for the energy recovery problem have been tested in simulations adopting the same parameters (3.83) used in Section 3.4.4. In particular, the feasibility conditions presented in Proposition 3.10 and 3.11 have been applied to the simple case of $N = 3$ turbines with different wind speeds $v = [8m/s, 9m/s, 10m/s]$ and a power reference $P_L = 2.5MW$. The borders of the feasibility regions with respect to the initial energy E_i^0 of each turbine are shown in Fig. 3.16. The border B_1 (in red) delimits the initial energy values for which a recovery scheduling exists (from Proposition 3.11) while the border B_2 (in blue) denotes the smaller area, defined by Proposition 3.10, in which is possible to initially accelerate all turbines at the same time.
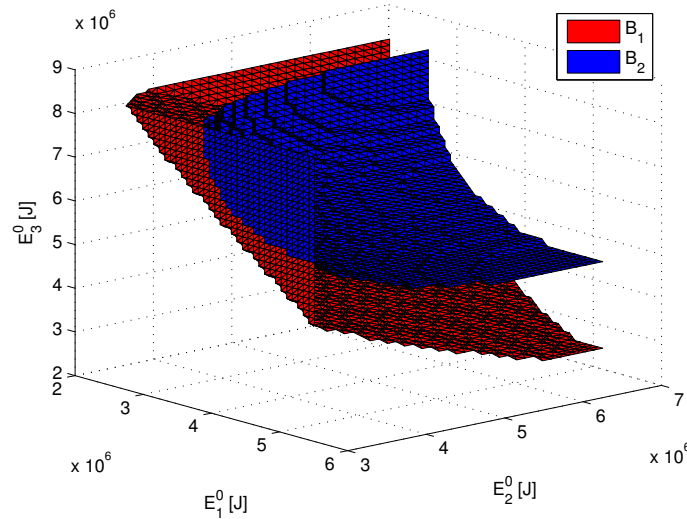
FIGURE 3.16: Borders of the feasibility region of the recovery problem with respect to initial state E_0, as defined by Prop. 3.10 (blue) and Prop. 3.11 (red) in the case of $N = 3$ turbines.

The proposed scheduling is also compared with the recovery of the turbines when a standard optimum power point tracking (OPPT) is used and the power generated by the i-th turbine is defined as a function of the rotor speed ω_i [22]:

$$\bar{P}_i(\omega_i) = \frac{\mu \pi R^5 \bar{C}(\lambda_{ss}(0), 0)}{2\lambda_{ss}^3(0)}\omega_i^3 = K_T \omega_i^3 \tag{3.99}$$

where $\lambda_{ss}(0)$ denotes the tip-speed ratio which maximizes the power coefficient $\bar{C}(\lambda, \theta)$ when $\theta = 0$. The aggregate power profile P_{TOT} generated with this controller is then used as reference for the optimal recovery problem (extended to consider time-varying P_L). The kinetic energies of the turbines in the two cases are compared in Fig. 3.17. Notice

that, with the proposed scheduling, only some turbines are initially accelerated and then, when equal values of Γ_E are obtained, the solution of the unconstrained problem is applied. The total kinetic energy of the turbines in the two cases (respectively $\bar{E}_{TOT}$ and E^*_{TOT}) is shown in Fig. 3.18: as expected, the proposed scheduling is able to achieve, for the same aggregate generated power, a faster recovery of the wind farm.
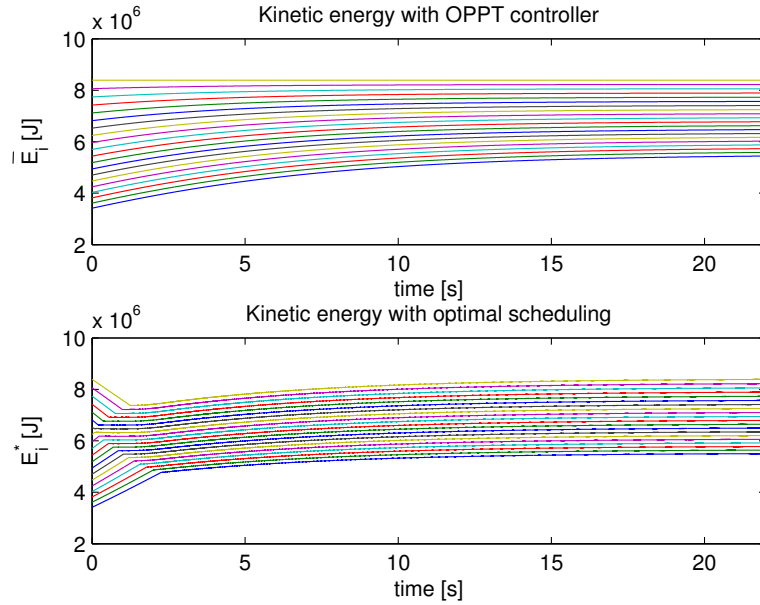
FIGURE 3.17: Kinetic energy of each wind turbine during recovery when a standard OPPT controller is used (top) and when the optimal scheduling is applied (bottom).
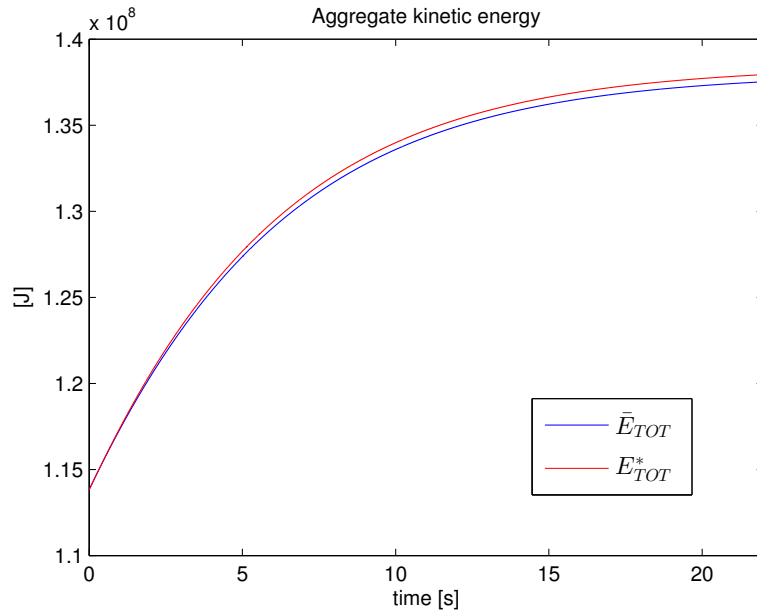
FIGURE 3.18: Comparison between the aggregate energy $\bar{E}_{TOT}$ obtained with standard OPPT controller (blue) and the total energy E^*_{TOT} resulting from the application of the optimal scheduling (red).

3.6   Conclusions

New techniques for the provision of frequency response through variable-speed wind turbines have been presented. In particular, the extra power generation that follows a frequency event is distributed among the individual turbines in order to optimize some global criteria: maximization of the frequency response duration or minimization of the energy losses. Two different approaches are considered, assuming respectively that turbines can switch to a second mode with an additional torque step or directly determining (within the operational constraints of the devices) the generated power of each turbine. The performance of the proposed control strategies is evaluated in simulations and then extended to consider the similar recovery problem, determining the optimal power profiles that, in minimum time, bring back the turbines to their original working point of maximum efficiency. We point out that the control strategies proposed in this chapter are open-loop policies. These can be implemented in closed-loop by solving a sequence of optimal control problems in a receding horizon framework.

Chapter 4

Distributed Control of Micro-storage Devices with Mean Field Games

This chapter provides a general overview of the principal benefits and challenges related to micro-storage and dynamic demand, describing the main approaches presented in the literature for the management of large populations of agents in the power system. A distributed control strategy is then proposed for micro-storage devices that perform energy arbitrage and maximize their profit by optimally charging/discharging energy on the basis of its price throughout the day. For large populations of appliances, the problem can be approximated as a differential game with infinite players (mean field game). Through the resolution of coupled partial differential equations, it is possible to determine, as a fixed point, the optimal feedback strategy for each player and the resulting price of energy if that strategy is applied. A decentralized implementation is straightforward to obtain and it is possible to extend the original model in order to consider additional elements such as cyclic constraints, multiple populations of devices and uncertainties on demand.

4.1   Introduction

One of the key features of the smart grid paradigm, which represents the conceptual vision of future power systems, is the increasing participation of end customers in system operation. In particular, the growing diffusion of flexible loads (i.e. "smart appliances" [47] and electric vehicles [48]) and the development of new storage technologies [49] will allow users, in the near future, to have an active role in the electricity market [50]. This section provides a general overview of the main control challenges that arise from this

95

scenario, describing the principal approaches and mathematical tools which have been proposed in the literature to solve them.

4.1.1 Distributed Storage and Energy Arbitrage

Energy storage in a traditional power system is usually constituted by large scale pumped-hydro systems. Recent technological developments are making possible its implementation on a smaller scale and with different technologies. The potential advantages of this scenario have been widely analysed [51] and include absorption of wind power variability [52], [53], load levelling [54] and primary frequency regulation [55]. The recent introduction of micro-storage devices like the ones presented in [56] and [57] has increased the interest in energy arbitrage with storage on a distributed scale. It is reasonable to assume that, in the near future, batteries will be installed in private households in the order of millions. These devices will determine their operation strategy in order to maximize their profit by trading energy with the system at different prices during the day. This, in principle, would correspond to a profit for the individual customer and positive effects for the power system in the form of reduced prices and improved reliability. The main challenge is the coordination of the devices: a greedy optimization from the single agents could result in synchronicity phenomena, when devices all charge/discharge at the same time, altering the original price function and resulting in suboptimality of their operation strategy. This problem is tackled in the subsequent sections of this chapter using mean field games, introduced in Section 4.1.4.

4.1.2 Flexible Demand: Challenges and Potential Benefits

The increasing number of flexible loads in the power system will give customers the possibility to partially schedule their power consumption and have an active role in the management of the network. The impact and potential benefits of this development have been widely investigated [58], [59], [60]: the individual customers will reduce the cost of their electricity bill with a minimum impact on their comfort. At the same time, the power system will achieve an improved reliability and will benefit from a reduction in the peak demand and in the reliance on fossil fuel peaking plants. Participation of flexible demand has usually been considered with two different approaches:

1. Incentive-Based Programs [61]: the customers stipulate a contract with the system operator and are compensated for providing services such as interruptibility, emergency response and ancillary services.

2. Price-Based Programs [62]: a price signal is broadcast to the devices which determine independently their power consumption, operating during the hours of the day characterized by lower energy prices.

When the latter policy is applied, one must consider the global effect that the power scheduling of the appliances has on the aggregate demand and the resulting energy price: for example, if all devices operate when energy is cheaper, the peak demand will simply be shifted. Equilibrium conditions and decentralized control strategies for this problem will be provided in Chapter 5.

4.1.3 Management of Flexible Loads and Storage

The difficulties of coordinating large populations of agents acting in a competitive framework are very similar if one considers storage devices or flexible demand. For this reason, the most common solutions proposed in the literature for the two cases are presented in a unified manner.

Two main approaches have been proposed to model the interactions of a large number of devices with the energy market and design suitable control techniques. Centralized mechanisms tackle this problem by considering a global optimization which is solved by the market operator on the basis of the data provided by generators and consumers, as proposed in [63] and [64]. Given the complexity of this problem for high number of appliances, privacy concerns and the traditional tendency of customers to have full control of their energy consumption, distributed approaches have also been considered. For example, [65] proposes an adaptive pricing scheme for the energy suppliers, broadcasting the price of energy to the devices in advance of each daily period, in order to better predict the global storage behaviour. Similarly, [66] adopts the concept of congestion pricing and proposes a control technique based on price feedbacks. A game theory approach is used in [67] to calculate the performance bounds of the storage devices, which are then used as benchmark for the proposed adaptive strategy. Game theory has also been applied to the similar case of electric vehicles, calculating a cost-minimizing scheduling which fills the valleys in electric load profiles. In [68] the mean behaviour of the vehicles population is used to determine the charging profile of each agent, achieving a Nash equilibrium that coincides with the globally optimal strategy if the vehicles are identical. Similarly, [69] proposes an iterative strategy where each agent minimizes its own cost function (which takes into account the result of the previous iteration), reaching an equilibrium with certain valley-filling properties. A different approach is adopted in [70] to integrate flexible demand in the electricity market, using a two-level iterative process with Lagrange relaxation.

4.1.4 Mean Field Games

The main challenges in the management of flexible appliances and micro-storage are represented by the high number of devices and the difficulty to model and predict their behaviour. One way to address these problems is to approximate the population size as infinite and consider a differential game with an infinite number of players. The theory for this approach has been independently developed by Huan-Caines-Malhamé [71], [72] and Lasry-Lions [73], who introduced the term Mean Field Games (MFG) for games with a continuum of players. In their basic formulation they are described by two coupled Partial Differential Equations (PDEs): one Hamilton-Jacobi-Bellman (HJB) equation, which returns the optimal control of the agents, and one Fokker-Planck (FP) equation which describes their distribution. An introduction to the subject, starting with toy models and gradually presenting the mathemathical concepts, is given in [74] while [75] provides some fundamental results of existence and unicity of solutions. Current theoretical research focuses on extending the original framework, for example considering cases with minor-major agents [76] or a limited number of players [77]. Consistent research work is also being carried out on integration schemes and the numerical resolution of the coupled PDEs [78], [79]. Mean field games are currently being used in several fields such as crowd dynamics [80], [81], economics [82], [83], and consensus dynamics [84]. Many applications have also been considered for the new smart grid paradigm: [85] models electric vehicles as infinitesimal agents and calculates the charging profiles that minimizes generation costs while [86] applies a similar approach to consider large-scale real-time bidding with a high number of suppliers and consumers. Large populations of electrical heating or cooling appliances are controlled in [87] to guarantee desynchronization and improve power network resilience.

In Section 4.2 the problem of energy arbitrage with storage is presented as a competitive game for the case of a finite number of players, modelling the dynamics of the single device and the energy market. The analysis is then extended in Section 4.3 to consider an infinite number of agents, deriving the coupled PDEs of the corresponding mean field game. The iterative resolution procedure, the chosen numerical methods and the simulative results are presented in Section 4.4 while Section 4.5 contains some extensions to the original model.

4.2 Differential Game with Finite Number of Players

4.2.1 Modelling of the Storage Devices

The energy arbitrage with a finite number N of devices is initially considered in a competitive game framework: each device (agent) exchanges energy with the network aiming at maximizing its own profit. The i-th storage is described by the following set of equations:

$$\begin{aligned} \dot{E}_s^{(i)}(t) &= u_s^{(i)}(t) \\ y_s^{(i)}(t) &= u_s^{(i)}(t) + \gamma_s u_s^{(i)^2}(t) \end{aligned} \tag{4.1}$$

The derivative of the stored energy E_s is equal to the charging power u_s which represents the control input of the device. In order to take into account the storage efficiency, quadratic losses parametrized by the positive quantity γ_s are introduced in the expression of y_s, which denotes the power exchanged by the device with the network. It is important to notice that, with an appropriate choice of the parameter γ_s, the introduction of $y_s^{(i)}$ can be considered a reasonable approximation of the traditional efficiency model with linear losses, where the power z_s exchanged with the network has the following expression:

$$z_s = u_s + \eta |u_s| \tag{4.2}$$

A representation of the differences between u_s, y_s and z_s is provided in Fig. 4.1.
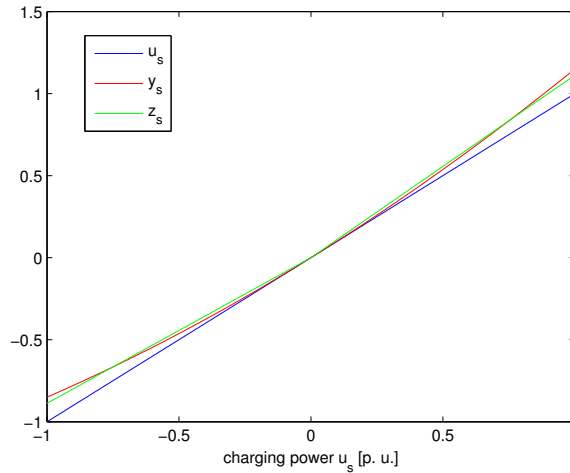
FIGURE 4.1: Qualitative comparison between the rate of charge u_s and the power exchanged with the network, modelled with quadratic (y_s) and linear (z_s) losses.

The physical limitations of the storage devices are also taken into account. If one denotes respectively by E_r and P_r the energy and power rating of the devices, the stored energy E_s and the charging power u_s are subject to the following constraints

within the considered time interval $[0, T]$:

$$0 \le E_s^{(i)}(t) \le E_r \qquad \qquad \forall\, t \in [0, T]$$
$$u_s^{MIN} = -P_r \le u_s^{(i)}(t) \le P_r = u_s^{MAX} \qquad i = 1, \dots, N \tag{4.3}$$

The efficiency of the devices can alternatively be expressed through the parameter k_s, defined such that the linear loss $k_s u_s$ is equal to the chosen quadratic one for $u_s = u_s^{MIN}$:

$$-\gamma_s \left(u_s^{MIN} \right)^2 = k_s u_s^{MIN} \to k_s = -\gamma_s u_s^{MIN}$$

Remark 4.1. The power constraints are such that $u_s^{MIN} < 0$ and $u_s^{MAX} > 0$. Furthermore, if one considers the physical meaning of y_s, i.e. the power that the storage device exchanges with the network for a certain rate of charge u_s, it is reasonable to assume that y_s is monotonic increasing with respect to u_s. This is equivalent to impose $u_s^{MIN} > -\frac{1}{2\gamma_s}$ or, alternatively, $k_s < \frac{1}{2}$.

Remark 4.2. Homogeneity of storage is initially assumed: all devices have the same parameters γ_s, E_s^{MAX}, u_s^{MIN} and u_s^{MAX}. In Section 4.5.2 the possibility to extend the results obtained under this assumption to the case of multiple typologies of devices will be investigated.

4.2.2 Energy Market and Objective Function of the Appliances

The electricity market has been abstracted with the monotonic increasing function $\Pi : [d_{MIN}, +\infty] \to [\pi_{MIN}, +\infty]$ where d_{MIN} and π_{MIN} are fixed positive quantities. This function associates, to a given value of aggregate demand $D(t)$, the corresponding energy price $p(t) = \Pi(D(t))$. The power demand D will be given by two different components: the inflexible demand D_i and the contribution D_s of the storage population. The inflexible profile is modelled with the function $D_i(t)$, initially assumed to be known without uncertainties, while the storage component D_s is defined as the total power exchanged by the devices:

$$D_s(t) = \sum_{i=1}^{N} y_s^{(i)}(t) = \sum_{i=1}^{N} u_s^{(i)}(t) + \gamma_s u_s^{(i)^2}(t) \tag{4.4}$$

We denote by $u_s^{(\bar{i})}$ the vector of control inputs for all players except i and we introduce the cost function $J_s^{(i)}$ that the i-th agent aims to minimize. By implicitly considering the dependency of $J_s^{(i)}$ from $u_s^{(i)}$ through the price function $\Pi(D_i(t) + D_s(t))$, it holds:

$$J_s^{(i)} \left(E_s^{(i)}(0), u_s^{(i)}, u_s^{(\bar{i})} \right) = \int_0^T \Pi(D_i(t) + D_s(t))[u_s^{(i)}(t) + \gamma_s u_s^{(i)^2}(t)]\, dt + \Psi(E_s^{(i)}(T)) \tag{4.5}$$

The integral component of $J_s^{(i)}$ represents the cost sustained by the device while charging/discharging energy during the considered time interval $[0, T]$ while the terminal cost function Ψ is used to take into account the final energy value and avoid, for example, the total discharge of the device. The main objective is to determine a Nash Equilibrium for the non cooperative game described by (4.1), (4.3) and (4.5). To this end, we denote by $\bar{\mathcal{U}}_s^{(i)}$ the set of open-loop feasible strategies for the i-th player and introduce the corresponding product set $\bar{\mathcal{U}}_s = \bar{\mathcal{U}}_s^{(1)} \times \cdots \times \bar{\mathcal{U}}_s^{(N)}$. Given a vector of initial energies $E_s(0)$, we want to determine if there exists $u_s^*(\cdot) = \left[u_s^{(1)^*}(\cdot), \ldots, u_s^{(N)^*}(\cdot) \right] \in \bar{\mathcal{U}}_s$ for which the following holds:

$$J_s^{(i)} \left(E_s^{(i)}(0), u_s^{(i)^*}, u_s^{(\bar{i})^*} \right) \le J_s^{(i)} \left(E_s^{(i)}(0), u_s^{(i)}, u_s^{(\bar{i})^*} \right) \quad \forall u_s^{(i)} \in \bar{\mathcal{U}}_s^{(i)} \quad i = 1 \ldots N$$

(4.6)

4.2.3 Existence Results

The existence of a Nash equilibrium for the differential game with a finite number of players is now investigated, replacing the terminal cost function Ψ with the constraint $E_s^{(i)}(0) = E_s^{(i)}(T)$ for $i = 1, \ldots, N$.

Assumption 4.1. *The price function Π is considered to be linear with respect to the aggregate power demand (with constant parameter $\Gamma > 0$):*

$$\begin{aligned} \Pi(D_i(t) + D_s(t)) &= \Gamma \left[D_i(t) + D_s(t) \right] = \Gamma \left[D_i(t) + \sum_{i=1}^{N} \left(u_s^{(i)}(t) + \gamma_s u_s^{(i)^2}(t) \right) \right] \\ &= c(t) + \Gamma \sum_{i=1}^{N} \left(u_s^{(i)}(t) + \gamma_s u_s^{(i)^2}(t) \right) \end{aligned}$$

(4.7)

Assumption 4.2. *The variation on the price $p(t) = \Pi(D(t))$ introduced by the charge profile of the single device is assumed to be negligible. If one denotes by $l^{(i)}$ the Lagrangian of the functional in (4.5), the following approximation can be considered:*

$$\frac{\partial l^{(i)}(t, u_s)}{\partial u_s^{(i)}} \simeq \Pi(D(t)) \left(1 + 2\gamma_s u_s^{(i)} \right) = \left[c(t) + \Gamma \sum_{i=1}^{N} \left(u_s^{(i)} + \gamma_s u_s^{(i)^2} \right) \right] \left(1 + 2\gamma_s u_s^{(i)} \right)$$

Assumption 4.3. *The constraints (4.3) on stored energy E_s and charged power u_s are initially neglected.*

It is now possible to provide the following result for the existence of equilibria in the case of finite players.

Theorem 4.1. *Consider the differential game characterized by the following optimization problem for the i-th player:*

$$\min_{u_s^{(i)}(\cdot)} \quad \int_0^T p(t)[u_s^{(i)}(t) + \gamma_s u_s^{(i)^2}(t)]\, dt$$
$$s.\ t. \quad \dot{E}_s^{(i)}(t) = u_s^{(i)}(t) \qquad\qquad i = 1, \ldots, N \tag{4.8}$$
$$E_s^{(i)}(0) = E_s^{(i)}(T)$$

where the price function $p(t) = \Pi(D_i(t) + D_s(t))$ is defined as in (4.7). Under Assumptions 4.1, 4.2 and 4.3 there exists one and only one open-loop Nash equilibrium if:

$$\Gamma N - 4\gamma_s c(t) \leq 0 \quad \forall t \in [0, T] \tag{4.9}$$

Proof. Following the definition of open-loop Nash equilibrium provided for example in [88], the theorem statement can be verified under the specified assumptions by applying the Pontryagin Minimum Principle (PMP) to the optimization problem of each player. If one replaces $p(\cdot)$ in (4.8) with an arbitrary positive price function $\pi(\cdot)$, the corresponding Hamiltonian $H^{(i)}$ for the i-th player is equal to:

$$H^{(i)}(t, E_s^{(i)}(t), u_s^{(i)}(t), \lambda^{(i)}(t)) = \pi(t)[u_s^{(i)}(t) + \gamma_s u_s^{(i)^2}(t)] + \lambda^{(i)}(t)u_s^{(i)}(t)$$

Considering Assumption 4.2, the necessary conditions for the optimal control $u_s^{(i)^*}$ and costate $\lambda^{(i)^*}$ are:

$$u_s^{(i)^*}(t) = -\frac{\pi(t) + \lambda_s^{(i)^*}(t)}{2\gamma_s \pi(t)} \qquad \dot{\lambda}_s^{(i)^*}(t) = 0 \qquad \int_0^T u_s^{(i)^*}(t)\, dt = 0 \tag{4.10}$$

Since $H^{(i)}$ does not depend on state $E_s^{(i)}$ and is convex with respect to $u_s^{(i)}$, it is possible to conclude from [89] that such conditions are also sufficient. For a positive $\pi(\cdot)$, given that $u_s^{(i)^*}(t)$ is strictly decreasing with respect to $\lambda_s^{(i)^*}$ at each t, there exists at most one constant costate $\lambda_s^{(i)}(t) = \tilde{\lambda}_s^{(i)}$ for which the third condition (fixed terminal state) in (4.10) is verified. Given the special structure of the problem, the optimal control $u_s^{(i)^*}$ is independent from the initial state $E_s^{(i)}(0)$ and therefore equal for all agents. It follows that the theorem is verified if there exist $(\bar{\pi}(\cdot), \bar{u}(\cdot), \bar{\lambda})$ such that:

$$\bar{u}(t) = -\frac{\bar{\pi}(t) + \bar{\lambda}}{2\gamma_s \bar{\pi}(t)} \qquad \bar{\pi}(t) = c(t) + \Gamma N\left[\bar{u}(t) + \gamma_s \bar{u}^2(t)\right] \qquad \int_0^T \bar{u}(t)\, dt = 0 \tag{4.11}$$

An equivalent representation of the first two conditions is obtained by replacing the expression of $\bar{u}$ in $\bar{\pi}$:

$$\bar{\pi}(t) = c(t) + \Gamma N\left[-\frac{\bar{\pi}(t) + \bar{\lambda}}{2\gamma_s \bar{\pi}(t)} + \gamma_s \frac{(\bar{\pi}(t) + \bar{\lambda})^2}{4\gamma_s^2 \bar{\pi}^2(t)}\right] = c(t) + \Gamma N\left[\frac{-\bar{\pi}^2(t) + \bar{\lambda}^2}{4\gamma_s \bar{\pi}^2(t)}\right] \tag{4.12}$$

By rearranging the terms, considering the price as a variable π and the costate λ as a free parameter, a cubic equation is obtained:

$$4\gamma_s\pi^3 + \left[\Gamma N - 4\gamma_s c(t)\right]\pi^2 - \Gamma N\lambda^2 = 0 \tag{4.13}$$

Consider that the price π must be a real positive quantity. If (4.9) holds, the discriminant Δ for the cubic function (4.13) is negative, therefore there exist one real root and two complex conjugate roots. Furthermore, by the sign alternance of the coefficients, the real root, denoted by $\tilde{\pi}(t,\lambda)$, is positive. It follows that the equivalent (4.12) of the first two conditions in (4.11) is satisfied for $\bar{\pi}(t) = \tilde{\pi}(t,\bar{\lambda})$. In order to prove the existence of the Nash equilibrium, it is sufficient to show that also the integral condition in (4.11) is satisfied and there always exists $\bar{\lambda}$ such that:

$$\int_0^T \bar{u}(t)\,dt = \int_0^T -\frac{\tilde{\pi}(t,\bar{\lambda})+\bar{\lambda}}{2\gamma_s\tilde{\pi}(t,\bar{\lambda})}\,dt = -\frac{T}{2\gamma_s} - \frac{1}{2\gamma_s}\int_0^T \frac{\bar{\lambda}}{\tilde{\pi}(t,\bar{\lambda})} = 0 \tag{4.14}$$

Explicit calculations show the following for $\lambda/\tilde{\pi}(t,\lambda)$:

$$\frac{\partial\left(\frac{\lambda}{\tilde{\pi}(t,\lambda)}\right)}{\partial\lambda} > 0 \ \forall\lambda\in\mathbb{R} \qquad \lim_{\lambda\to-\infty}\frac{\lambda}{\tilde{\pi}(t,\lambda)} = -\infty \qquad \lim_{\lambda\to+\infty}\frac{\lambda}{\tilde{\pi}(t,\lambda)} = +\infty \tag{4.15}$$

All these properties naturally extend to the function $\int_0^T \lambda/\bar{\pi}(t,\lambda)\,dt$ which is continuous, strictly monotonic increasing and with image equal to $\mathbb{R}$. This means that there exists a unique $\bar{\lambda}$ such that $\int_0^T \frac{\bar{\lambda}}{\bar{\pi}(t,\lambda)} = -T$ and therefore satisfies (4.14). We can conclude that the price $\bar{\pi}$ and the control $\bar{u}$ for which the equilibrium conditions (4.11) hold are given by:

$$\bar{\pi}(t) = \tilde{\pi}(t,\bar{\lambda}) \qquad \bar{u}(t) = -\frac{\tilde{\pi}(t,\bar{\lambda})+\bar{\lambda}}{2\gamma_s\tilde{\pi}(t,\bar{\lambda})} \qquad \forall t\in[0,T]$$

The charge profiles of the devices at equilibrium are: $u_s^{(1)*} = \cdots = u_s^{(N)*} = \bar{u}$. $\qquad\square$

Existence and uniqueness of the Nash equilibrium are preserved when constraints on the charging power $u_s^{(i)}$ are introduced. In particular:

Proposition 4.1. *Under Assumptions 4.1 and 4.2, if (4.9) holds, a unique open-loop Nash equilibrium exists for the differential game given by (4.8) when the following additional constraints are introduced:*

$$u_s^{MIN} \le u_s^{(i)}(t) \le u_s^{MAX} \qquad \forall t\in[0,T] \qquad i = 1,\dots,N$$

Proof. In the case of constraints on the charging power u_s, the set $\mathcal{P}(t)$ of feasible energy prices at the time instant t is equal to a closed interval. From (4.7), if one denotes by

$y_s^{MIN} = u_s^{MIN} + \gamma_s u_s^{MIN2}$ the minimum power exchanged by the single device and defines similarly the maximum y_s^{MAX}, it follows:

$$\mathcal{P}(t) = \left[c(t) + \Gamma N y_s^{MIN}, c(t) + \Gamma N y_s^{MAX} \right] = \left[p^{MIN}(t), p^{MAX}(t) \right]$$

Note that p^{MIN} and p^{MAX} correspond to the prices obtained when all devices are respectively discharging and charging at maximum rate. Considerations in the proof of Theorem 4.1 on the convexity of the Hamiltonian for the optimization of the single player and its independence from the state E_s still apply. This means that the proposition is verified if there exist $(\bar{\pi}_c(\cdot), \bar{u}_c(\cdot), \bar{\lambda}_c)$ such that it holds:

$$\bar{u}_c(t) = \underset{\mathcal{U}_s}{\mathrm{sat}} \left[-\frac{\bar{\pi}_c(t) + \bar{\lambda}_c}{2\gamma_s \bar{\pi}_c(t)} \right] \qquad \bar{\pi}_c(t) = c(t) + \Gamma N \left[\bar{u}_c(t) + \gamma_s \bar{u}_c^2(t) \right] \qquad \int_0^T \bar{u}_c(t) \, dt = 0 \tag{4.16}$$

where $\mathcal{U}_s$ is the interval $[u_s^{MIN}, u_s^{MAX}]$ of feasible controls. As in the previous case, an equivalent expression for the first two conditions can be obtained by replacing the expression for $\bar{u}_c$ in $\bar{\pi}_c$:

$$\bar{\pi}_c(t) = c(t) + \Gamma N \left(\underset{\mathcal{U}_s}{\mathrm{sat}} \left[-\frac{\bar{\pi}_c(t) + \bar{\lambda}_c}{2\gamma_s \bar{\pi}_c(t)} \right] + \gamma_s \underset{\mathcal{U}_s}{\mathrm{sat}} \left[-\frac{\bar{\pi}_c(t) + \bar{\lambda}_c}{2\gamma_s \bar{\pi}_c(t)} \right]^2 \right) \tag{4.17}$$

Notice now that the unique positive solution $\tilde{\pi}(t, \lambda)$ of (4.13) presented in the proof of Theorem 4.1, for a fixed t, is monotonic decreasing and admits an inverse $\tilde{\pi}^{-1}(t, p)$ with respect to λ. Consider in fact that (4.12), evaluated at $\bar{\lambda} = \lambda$, is satisfied for $\bar{\pi}(t) = \tilde{\pi}(t, \lambda)$. Partial derivation with respect to λ on both sides of the equation yields:

$$\frac{\partial \tilde{\pi}(t, \lambda)}{\partial \lambda} = \frac{\Gamma N}{2\gamma_s} \frac{\lambda}{\tilde{\pi}(t, \lambda)} \frac{\partial(\lambda / \tilde{\pi}(t, \lambda))}{\partial \lambda}$$

Since the costate λ must be negative in order to satisfy the integral constraint in (4.16) (price $\bar{\pi}_c$ and parameter γ_s are always positive), we can conclude from (4.15) that $\frac{\partial \tilde{\pi}(t, \lambda)}{\partial \lambda}$ is negative. One can then introduce λ^{MIN} and λ^{MAX}, which represent the costate values at which the saturation constraints on $\bar{u}_c$ are active:

$$\lambda^{MIN}(t) = \tilde{\pi}^{-1}(t, p^{MAX}(t)) \qquad \lambda^{MAX}(t) = \tilde{\pi}^{-1}(t, p^{MIN}(t))$$

Considering that control $\bar{u}_c$ and price $\bar{\pi}_c$, at a certain t, take the same values for all $\bar{\lambda}_c \leq \lambda^{MIN}(t)$ (the same property holds in the opposite sense with $\lambda^{MAX}(t)$), one can provide the following definition for $\tilde{\pi}_c$ which satisfies (4.17):

$$\tilde{\pi}_c(t, \lambda) = \begin{cases} \tilde{\pi}(t, \lambda) & \text{if} \quad \lambda^{MIN}(t) \leq \lambda \leq \lambda^{MAX}(t) \\ \tilde{\pi}(t, \lambda^{MIN}(t)) & \text{if} \quad \lambda < \lambda^{MIN}(t) \\ \tilde{\pi}(t, \lambda^{MAX}(t)) & \text{if} \quad \lambda > \lambda^{MAX}(t) \end{cases}$$

The proof is concluded by verifying that there exists a unique $\bar{\lambda}_c$ that satisfies the integral condition in (4.16), which can be rewritten as follows:

$$\int_0^T \bar{u}_c(t)\,dt = \int_0^T \underset{\mathcal{U}_s}{\mathrm{sat}} \left[-\frac{\tilde{\pi}_c(t,\bar{\lambda}_c) + \bar{\lambda}_c}{2\gamma_s \tilde{\pi}_c(t,\bar{\lambda}_c)} \right] = 0$$

To see this, $\bar{\lambda}^{MIN}$ and $\bar{\lambda}^{MAX}$ are introduced:

$$\bar{\lambda}^{MIN} = \min_{t\in[0,T]} \lambda^{MIN}(t) \quad \bar{\lambda}^{MAX} = \max_{t\in[0,T]} \lambda^{MAX}(t)$$

We now have that $\Lambda = \left[\bar{\lambda}^{MIN}, \bar{\lambda}^{MAX}\right]$ contains all possible values of λ which returns different results for the integral $\tilde{u}_I(\lambda) = \int_0^T \tilde{u}(t,\lambda)\,dt$, with $\tilde{u}(t,\lambda) = \mathrm{sat}_{\mathcal{U}_s}\left[-\frac{\tilde{\pi}_c(t,\lambda)+\lambda}{2\gamma_s\tilde{\pi}_c(t,\lambda)}\right]$. The integral condition is verified if one considers that $u_I(\lambda)$ is a continuous monotonic decreasing function of λ in Λ and the following holds:

$$\tilde{u}_I(\bar{\lambda}_{MIN}) = Tu_s^{MAX} \geq 0 \geq \tilde{u}_I(\bar{\lambda}_{MAX}) = Tu_s^{MIN}$$

$\square$

4.3 Energy Arbitrage with Mean Field Games

4.3.1 Infinite Number of Players

It is in general difficult to extend the results of the previous section when constraints on the state E_s are considered and the optimal control u_s^* is different for each device, depending on their initial energy. A possible way to approach the problem and also explicitly account for Assumption 4.2 is to consider that the contribution of the single device to the total value of D_s (and to the corresponding price $p = \Pi(D_i + D_s)$) is reduced by increasing values of N. If the number of devices is very high, it can be approximated as infinite: the contribution of the single device to the total demand becomes negligible and it is necessary to consider only the effect of the whole storage population (mean field). Furthermore, such population can be described as a continuum, introducing the following equations for the single agent:

$$\dot{E}(t) = u(t) \qquad y(t) = u(t) + \gamma u^2(t) \tag{4.18}$$

In this case the variables E and u represent respectively the state of charge of the device (between 0 and 1) and the rate of charge. The physical constraints of the devices in

these new variables can be represented as follows:

$$0 \leq E(t) \leq 1$$

$$u^{MIN} = -\frac{P_r}{E_r} \leq u(t) \leq \frac{P_r}{E_r} = u^{MAX} \qquad \forall \, t \in [0, T] \qquad (4.19)$$

Remark 4.3. All the results provided in this section can be rescaled and used to approximate the scenario with a finite number of players N. In this case, assuming E_r and P_r equal for all devices, the stored energy E_s, the charging power u_s and the efficiency coefficient k_s can be defined as follows:

$$E_s = E_r \cdot E \qquad u_s = E_r \cdot u \qquad k_s = -\gamma u^{MIN} = k \qquad (4.20)$$

The energy distribution within the storage population is denoted by m: given two arbitrary values E_1 and E_2 for the state of charge, $\int_{E_1}^{E_2} m(t, E) \, dE$ will correspond to the fraction of devices for which $E_1 \leq E(t) \leq E_2$. Since the optimal control is going to be calculated in feedback form, it is assumed that the charging rate of the devices $u(t, E)$ is a function of time and current state of charge. By considering the aggregate energy capacity $E^{TOT} = N \cdot E_r$ as a rescaling factor, the variation to total demand introduced by the storage population can now be defined:

$$D_s(t) = E^{TOT} \int_0^1 m(t, E) \left[u(t, E) + \gamma u^2(t, E) \right] \, dE = E^{TOT} \int_0^1 m(t, E) y(t, E) \, dE \qquad (4.21)$$

We finally introduce the cost J to be minimized by each agent:

$$\begin{aligned} J(E(0), u(\cdot)) &= \int_0^T \Pi \left(D_i(t) + D_s(t) \right) \left[u(t) + \gamma u^2(t) \right] dt + \Psi(E(T)) \\ &= \int_0^T p(t) y(t) \, dt + \Psi(E(T)) \end{aligned}$$

As in (4.5), the different devices interact between each other by varying the value of D_s and therefore the price of energy. It is significant that, with this approach, such variations do not depend on the single device but on the charge distribution of the whole population.

4.3.2 Derivation of the Coupled PDEs

It is now possible to derive the partial differential equations that describe the mean field game and are used to determine the decentralized control. In order to calculate the optimal rate of charge u^* which minimizes J, if one denotes by $\mathcal{U} = [u^{MIN}, u^{MAX}]$ the

set of admissible controls, a Hamilton-Jacobi-Bellman equation can be considered:

$$-\partial_t V(t, E) = \min_{u \in \mathcal{U}} \left[p_m^*(t)(u + \gamma u^2) + \partial_E V(t, E)u \right]$$

$$V(T, E) = \Psi(E)$$

(4.22)

In particular, the function p_m^* represents the price of energy resulting from all devices (with distribution m) applying the optimal charging profile u^*. If one denotes by $\mathcal{E} = [0, 1]$ the interval of feasible states, it holds:

$$p_m^*(t) = \Pi \left(D_i(t) + E^{TOT} \int_{\mathcal{E}} m(t, E) \left[u^*(t, E) + \gamma u^{*^2}(t, E) \right] dE \right)$$

(4.23)

Note that (4.22) is a PDE in the unknown function V which corresponds to the value function of the optimization problem:

$$\left\{ V(t, x) = \min_{u(\cdot)} \int_t^T p_m^*(t)[u(t) + \gamma u^2(t)] \, dt + \Psi(E(T)) \right\} \Bigg|_{\dot{E}=u} \qquad E(t) = x$$

(4.24)

The optimal control u^*, at each time instant, is the argument of the minimum in (4.22) and therefore must satisfy the following:

$$u^*(t, E) = \operatorname*{sat}_{\mathcal{U}} \left[-\frac{p_m^*(t) + \partial_E V(t, E)}{2\gamma p_m^*(t)} \right]$$

(4.25)

Since p_m^* depends on u^*, there is no closed expression for the optimal control. On the other hand, it is possible to provide the following result:

Theorem 4.2. *Consider an arbitrary $t \in [0, T]$ and m which belongs to the space of probability measures on $\mathcal{E}$ and assume that the partial derivative $\partial_E V(t, \cdot)$ exists and is bounded. If Π is a Lipschitz continuous and monotonic increasing function, there exists a unique $u^*(t, \cdot)$ which satisfies equations (4.23) and (4.25).*

Proof. At an arbitrary time instant t the control which satisfies (4.25) for a given price p is denoted by $f(E, p)$:

$$f(E, p) = \operatorname*{sat}_{\mathcal{U}} \left[-\frac{p + \partial_E V(E)}{2\gamma p} \right] = \operatorname*{sat}_{\mathcal{U}} \left[-\frac{1}{2\gamma} - \frac{\partial_E V(E)}{2\gamma p} \right]$$

where the dependency from time t is not denoted explicitly for a more compact notation. The function g which is obtained by considering $u^*(E) = f(E, p)$ in the right-hand side of (4.23) has the following expression:

$$g(p) = \Pi \left(D_i + E^{TOT} \int_{\mathcal{E}} m(E) \left[f(E, p) + \gamma f(E, p)^2 \right] dE \right)$$

The theorem statement corresponds to existence and uniqueness of a fixed point for the function g under the same assumptions. Since D_i and the demand variation introduced by storage are bounded and their sum is always positive, $g(p)$ is defined on a closed interval $[p^{MIN}, p^{MAX}]$ (with p^{MIN} equal to a strictly positive quantity) and takes values in the same set. From Brouwer's fixed point theorem [90], if g is continuous, a fixed point exists. To show this, the function $\tilde{f}(E, p)$ is introduced:

$$\tilde{f}(E, p) = -\frac{p + \partial_E V(E)}{2\gamma p} = -\frac{1}{2\gamma} - \frac{\partial_E V(E)}{2\gamma p}$$

The continuity of $\tilde{f}$ with respect to p can be proven by showing that, for any couple (p_1, p_2) such that $p_1, p_2 \in [p^{MIN}, p^{MAX}]$ and $||p_1 - p_2||_1 = c$, the following holds:

$$||\tilde{f}(E, p_1) - \tilde{f}(E, p_2)||_1 = \left| \frac{\partial_E V(E)}{2\gamma p_1 p_2}(p_1 - p_2) \right| \leq \frac{|\partial_E V(E)|}{2\gamma p^{MIN^2}} c$$

It is straightforward to prove that also the function f is continuous, for example verifying with a case by case inspection that:

$$||f(E, p_1) - f(E, p_2)||_1 \leq ||\tilde{f}(E, p_1) - \tilde{f}(E, p_2)||_1 \leq \frac{|\partial_E V(E)|}{2\gamma p^{MIN^2}} c \qquad (4.26)$$

In order to prove the continuity of g, given the current assumptions, it is sufficient to show that the function l, presented below, is continuous:

$$l(p) = D_i + E^{TOT} \int_{\mathcal{E}} m(E) \left[f(E, p) + \gamma f(E, p)^2 \right] dE$$

For any (p_1, p_2) with $p_1, p_2 \in [p^{MIN}, p^{MAX}]$ and $||p_1 - p_2||_1 = c$, bringing the absolute value in the integral in l and considering that $|f(E, p)| \leq u^{MAX} = -u^{MIN}$ yields:

$$||l(p_1) - l(p_2)||_1 \leq E^{TOT} \int_{\mathcal{E}} |m(E)[f(E, p_1) - f(E, p_2)][1 + \gamma(f(E, p1) + f(E, p2))]| \, dE$$

$$\leq E^{TOT} \max_E \left((1 + 2\gamma u^{MAX}) \frac{|\partial_E V(E)|}{2\gamma p^{MIN^2}} c \right) = \max_E (|\partial_E V(E)|) E^{TOT} \frac{1 + 2\gamma u^{MAX}}{2\gamma p^{MIN^2}} c$$

Since l is Lipschitz continuous, we can conclude that g is also continuous and therefore, from previous considerations, has a fixed point. For the uniqueness of such fixed point, considering Remark 4.1 and (4.20), it is sufficient to show that for $k < \frac{1}{2}$ the function f and therefore g are monotonic decreasing with respect to p. In this respect, notice that $\tilde{f}(E, p)$ is monotonic decreasing and always greater than $-\frac{1}{2\gamma}$ if $\partial_E V(E) < 0$. On the other hand, if $\partial_E V(E) > 0$, the function $\tilde{f}$ is monotonic increasing and always lesser than $-\frac{1}{2\gamma}$. This second case is always excluded in f by the saturation, since from

Remark 4.1 it holds $k = k_s < \frac{1}{2}$ or, equivalently, $-\frac{1}{2\gamma} < u^{MIN}$. $\qquad\square$

It has been shown how the optimal control u^* depends on the charge distribution m through the energy price p_m^* but an analogue relationship also holds in the opposite sense. In particular, m depends on the charge profile of the devices through the following transport equation:

$$\partial_t m(t, E) = -\partial_E \left[u^*(t, E) m(t, E) \right]$$
$$m(0, E) = m_0(E) \tag{4.27}$$

The solution to the arbitrage problem as a mean field game consists then in the couple (V, m) (and the corresponding (u^*, m)), which represents a fixed point for equations (4.22) and (4.27). In other words, it is necessary to determine an optimal u^* which minimizes the cost J for a given distribution m and, at the same time, induces such distribution. For practical implementations, the MFG solution can be calculated in a centralized manner following the procedure detailed in the next section. Once this has been determined, a distributed control can be implemented with a one-way communication channel: the resulting energy price p_m^* is broadcast to the devices, which will only need to solve their individual optimization to determine their charge profile.

Remark 4.4. Existence and uniqueness for the solution of the MFG described by equations (4.22) and (4.27) have not been proved theoretically: current mathematical literature on the topic provides results in this sense only for much simpler classes of systems [91]. In the rest of this chapter it is assumed that such solution exists and is approximated by the result of the numerical procedure described next.

4.4   Numerical Integration of the MFG Equations

For the calculation of the MFG solution it is important to consider that not only the two equations (4.22) and (4.27) are interdependent, but they are also integrated in two different directions. In fact, for the dynamic programming principle, the HJB equation must be integrated backward in time while the transport equation is integrated forward. In this respect, two different approaches are usually analysed in the literature: one possibility, described for example in [78] and [79], is to approximate the MFG solution by finite difference methods of the mean field model. In particular, the coupled PDEs are solved at once applying a Newton method and solving the corresponding systems of nonlinear equations through an iterative procedure. The application of this method in the present case is complicated by the presence of the additional fixed point described by (4.23) and (4.25). The use of discrete Semi-Lagrangian scheme is presented in [92], which solves iteratively the two coupled PDEs until convergence to a solution.

4.4.1 Iterative Strategy

A similar approach is used for the numerical resolution of the energy arbitrage MFG, solving one equation at a time and using the result as a starting point for the next integration. All steps of the numerical resolution are detailed below:

1. The initial guess for the energy distribution and the demand variation introduced by storage are denoted respectively by $\tilde{m}$ and $\tilde{D}_s$ and are defined as follows:

$$\begin{aligned} \tilde{m}(t, E) &= m_0(E) \\ \tilde{D}_s(t) &= 0 \end{aligned} \qquad \forall\, t \in [0, T] \qquad (4.28)$$

2. The HJB equation (4.22) is integrated backwards starting from $V(T, E) = \Psi(E)$ and assuming $m = \tilde{m}$. At each time step t the fixed point for equations (4.23) and (4.25), which corresponds to the optimal control u^* and related price p_m^*, is calculated according to steps a) to d):

   (a) The energy price is initially assumed equal to $\tilde{p}(t) = \Pi(D_i(t))$.

   (b) Optimal control estimate $\bar{u}(t, \cdot)$ is obtained with equation (4.25), where $p_m^*(t)$ is replaced with $\tilde{p}(t)$.

   (c) The new price estimate $\bar{p}$ is calculated as:

$$\bar{p}(t) = \Pi\left(D_i(t) + E^{TOT} \int \tilde{m}(t, E) \left[\bar{u}(t, E) + \gamma \bar{u}^2(t, E) \right]\, dE \right) \qquad (4.29)$$

   (d) The quantity $|\bar{p}(t) - \tilde{p}(t)|$ is evaluated. Given a certain price error tolerance ϵ_p, if $|\bar{p}(t) - \tilde{p}(t)| < \epsilon_p$ the iterations are stopped and step 3 is executed. If the condition is not satisfied, the initial price estimation is reset with $\tilde{p}(t) = \bar{p}(t)$ and steps 2.b-c are repeated.

3. A new estimate $\bar{m}$ is obtained integrating forward equation (4.27) while considering $u^* = \bar{u}$. The resulting demand variation $\bar{D}_s(t)$ introduced by storage is calculated by replacing $\bar{m}$ and $\bar{u}$ in (4.21).

4. The following function norm is evaluated:

$$\|\bar{D}_s - \tilde{D}_s\|_1 = \int_0^T \left| \bar{D}_s(t) - \tilde{D}_s(t) \right|\, dt$$

For a certain demand error tolerance ϵ_D, if $\|\bar{D}_s - \tilde{D}_s\|_1 < \epsilon_D$ step 5 is executed. Otherwise, the estimates in (4.28) are updated with $\tilde{m} = \bar{m}$ and $\tilde{D}_s = \bar{D}_s$ and steps 2-3 are repeated.

5. The solution of the MFG corresponds to the results of the last iteration:

$$u^* = \bar{u} \qquad\qquad m = \bar{m}$$

4.4.2   Numerical Methods

The numerical integration of the coupled PDEs has been performed using finite difference schemes. The time and state of charge steps Δt and ΔE are chosen and the corresponding vectors are partitioned:

$$t_i = i \cdot \Delta t \qquad\qquad E_j = j \cdot \Delta E$$

The value of a function $f(t, E)$ in $(i\Delta t, j\Delta E)$ will be hereby denoted as f_j^i.

It is important to point out that the adopted numerical method for the integration of the HJB equation is based on dynamic programming techniques for discretized systems. Heuristically, the results are regarded to be consistent with the boundary conditions that the constraints on the state E introduce in the PDE of the continuous problem [93]. In particular, the following expression is considered for the optimal control u^*:

$$u_j^{*i} = \arg\min_{u \in \mathcal{U}(E_j)} \left[p_m^{*i}(u + \gamma u^2) + (\partial_E V)_j^i \cdot u \right]$$

Minimization is performed over the set $\mathcal{U}(E)$ of feasible controls for a given state E:

$$\mathcal{U}(E) = \begin{cases} \left[0, u^{MAX}\right] & \text{if} & E = 0 \\ \left[u^{MIN}, u^{MAX}\right] & \text{if} & 0 < E < 1 \\ \left[u^{MIN}, 0\right] & \text{if} & E = 1 \end{cases}$$

The control $\bar{u}$ in step 2.b of the iterative strategy can then be determined as:

$$\bar{u}_j^i = \operatorname*{sat}_{\mathcal{U}(E_j)} \left[-\frac{\tilde{p}^i + \frac{V_{j+1}^i - V_{j-1}^i}{2\Delta E}}{2\gamma\tilde{p}^i} \right]$$

The integration of the HJB equation (4.22) at the time step $i - 1$ is performed with an upwind scheme [94]:

$$
\begin{aligned}
V_j^{i-1} &= \Delta t \cdot \bar{u}_j^i \left[\frac{1 + sign(\bar{u}_j^i)}{2} \frac{(V_{j+1}^i - V_j^i)}{\Delta E} \right] + \Delta t \cdot \bar{u}_j^i \left[\frac{1 - sign(\bar{u}_j^i)}{2} \frac{(V_j^i - V_{j-1}^i)}{\Delta E} \right] \\
&+ \Delta t \cdot \bar{p}^i \left[\bar{u}_j^i + \gamma \left(\bar{u}_j^i \right)^2 \right] + V_j^i
\end{aligned}
$$

$$(4.30)$$

With this approach, the calculation of the partial derivative $\partial_E V$ at the state boundaries is straightforward: when $j = 1$ the forward derivative, calculated using V_1^i and V_2^i, is always adopted and the same holds for the backward derivative when $j = 1/\Delta E$. The transport equation (4.27) has been integrated with a Lax-Friedrich method [95]. An artificial viscosity with coefficient ϵ is introduced, adopting the following numerical scheme:

$$\bar{m}_j^{i+1} = \bar{m}_j^i - \frac{\Delta t}{2\Delta E} \left[\bar{u}_{j+1}^i \bar{m}_{j+1}^i - \bar{u}_{j-1}^i \bar{m}_{j-1}^i \right] + \epsilon \left[\bar{m}_{j+1}^i - 2\bar{m}_j^i + \bar{m}_{j-1}^i \right] \qquad (4.31)$$

Equation (4.31) can be easily extended to the energy boundaries ($j = 1$ and $j = 1/\Delta E$) by taking into account that the sum of the viscosity term over j must be equal to 0.

4.4.3 Simulation Results

The presented iterative strategy and numerical methods are now used to simulate the scenario of a large population of storage devices performing energy arbitrage in the British power system. Regarding the parameters of the network, the inflexible demand D_i has been chosen equal to a 24-h UK demand profile [96] shown in Fig. 4.2. The price function $\Pi(D)$ has been defined on the basis of the values used in [97] and is shown in Fig. 4.3.
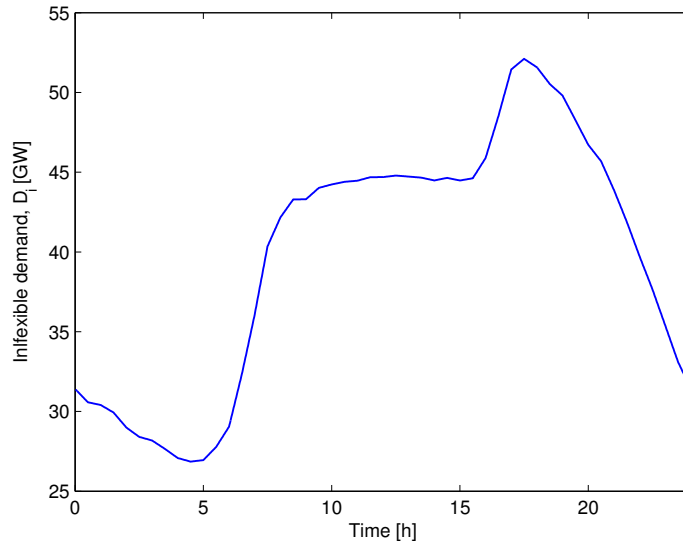
FIGURE 4.2: Chosen values of D_i over a time interval of 24h.

In this case study a population of $N = 10^6$ devices has been considered, with the following parameters:

$$P_r = 2.5 KW \qquad E_r = 25 KWh \qquad k = 0.25$$
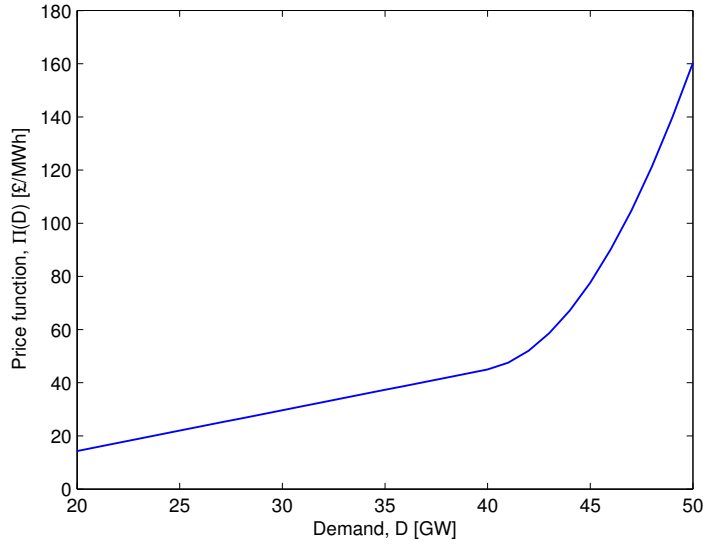
FIGURE 4.3: Energy price $\Pi(D)$ with respect to aggregate demand D.

The approximation with infinite players is then introduced, defining the boundary conditions of the PDEs: m_0 has been chosen as a gaussian distribution and Ψ as a quadratic function which penalizes final values of E different from $1/2$:

$$m_0(E) = \frac{1}{\sqrt{2\pi}\sigma}e^{-\frac{\left(E-\frac{1}{2}\right)^2}{2\sigma^2}} \qquad \Psi(E) = c_E\left(E - \frac{1}{2}\right)^2 \qquad (4.32)$$

The chosen parameters, including time and state of charge step, are:

$$\Delta t = 0.02h \qquad \sigma = 0.1 \qquad \epsilon_p = 0.5\pounds$$
$$\Delta E = 0.004 \qquad c_E = 1000 \qquad \epsilon_D = 1GWh$$

Consider that, once the mean field game has been solved, the results for a finite number of devices can be obtained following Remark 4.3: the energy level E_s and the charging power u_s for the single device can be calculated by multiplying E and u by E_r. In a similar way, it is possible to obtain their energy distribution m_s, optimal power profile u_s^* and cost function J_s. A numerical solution to the mean field game described by (4.22) and (4.27) is now obtained by following the procedure detailed at the beginning of this section. Simulations have been run in a MATLAB environment on a HP Z600 machine equipped with an Intel Xeon CPU (frequency of $2.4GHz$) and 12 GB of RAM. The whole resolution procedure is completed, for the specified parameters, in about 7 seconds. The inflexible demand profile D_i and the aggregate demand $D_i + D_s$, at each iteration of the backward/forward integration, are shown in Fig. 4.4. The proposed resolution strategy, for the chosen demand error tolerance ϵ_D, converges in 3 iterations. Furthermore, the presence of storage devices performing energy arbitrage introduces in the aggregate demand a considerable peak shaving/valley filling. The optimal power

profile $u_s^*(t, E_s) = u^*(t, \frac{E_s}{E_r})E_r$ is shown in Fig. 4.5. The resolution of the HJB equation returns an optimal control in feedback form: since the charge profile is not only a function of time but it also depends on the current energy of the device, greater robustness is guaranteed. The energy stored in the devices across time, for different values of $E_s(0)$, is shown in Fig. 4.6: notice that, in general, the trajectories have similar trends across time and charging occurs in the first hours of the day when energy prices are low. Devices with high values of $E_s(0)$ represent the only exception: in this case the initial charging is limited by the constraint on the maximum energy E_r. Moreover, it is important to point out that the whole population, given the particular choice of Ψ (equal for all devices), converges at time T towards the energy value $\frac{E_r}{2}$. The possibility to introduce different terminal conditions, for example imposing that devices must have the same initial and final energy, is considered in the next section. In Fig. 4.7 the original price of energy $p(t) = \Pi(D_i(t))$ is compared to $p_m^*(t)$, obtained when the storage population applies the optimal charge profile u^*. Following the variations introduced in the aggregate demand profile (shown in Fig. 4.4) and considering the chosen price function Π, the proposed operation strategy achieves a considerable price reduction during peak times. From expression (4.24) of the value function V, the profit $G_s = -J_s$ of the single device as a function of its initial energy $E_s(0)$ can be defined as follows:

$$G_s(E_s(0)) = -V\left(0, \frac{E_s(0)}{E_r}\right) \cdot E_r$$

and it is shown, for the last iteration, in Fig. 4.8. As previously mentioned, in the current formulation all devices will tend towards the same final value $\frac{E_r}{2}$ of stored energy. This means that G_s will be bigger for devices with higher values of $E_s(0)$ that have more energy available to exchange.
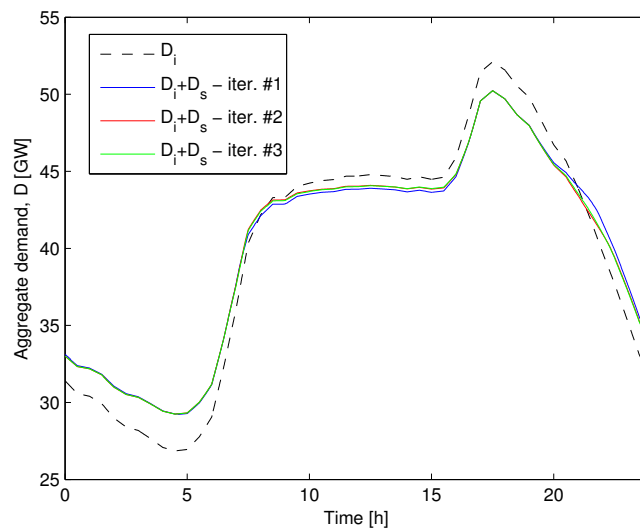
FIGURE 4.4: Aggregate demand profile at each iteration of the MFG-solving procedure.
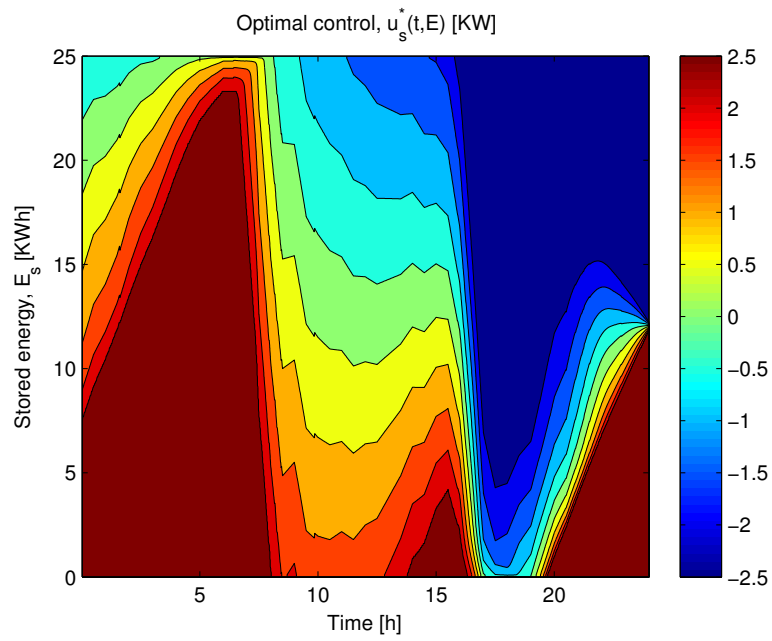
FIGURE 4.5: Optimal power u_s^* as a function of time and current stored energy E_s.
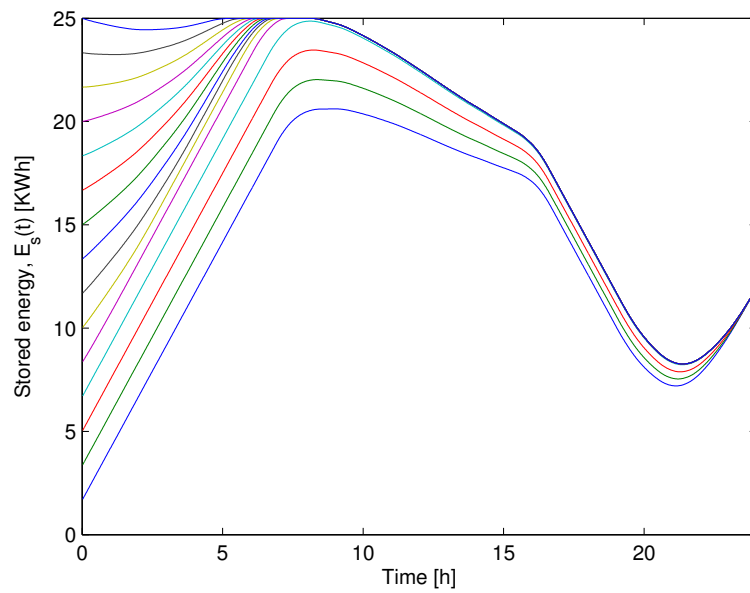
FIGURE 4.6: Stored energy $E_s(t)$ of the single device across time for different initial values $E_s(0)$.
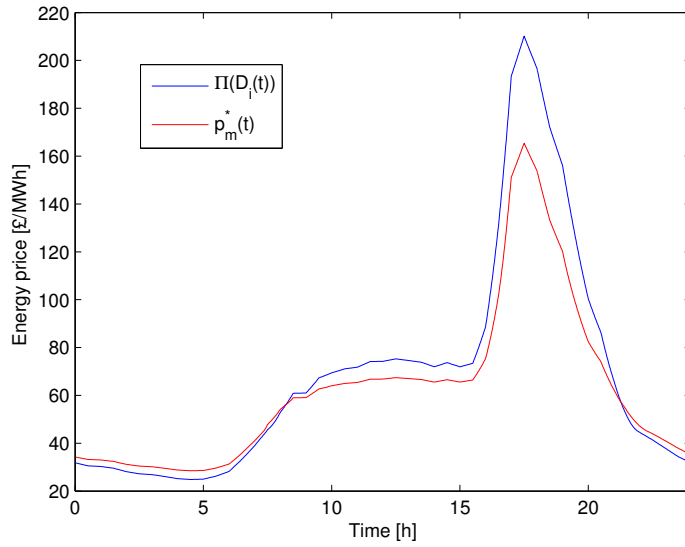
FIGURE 4.7: Comparison between the original energy price $\Pi(D_i(t))$ (blue) and p_m^* (red), resulting from the solution of the mean field game.
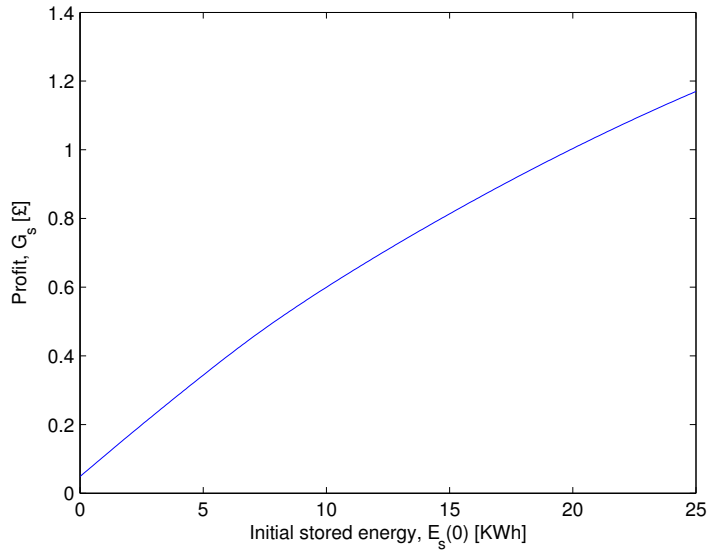
FIGURE 4.8: Profit G_s of the single device as a function of the initial stored energy.

4.5 Model Extensions

The energy arbitrage problem with an infinite number of devices, described by the mean field game with equations (4.22) and (4.27), is extended in this section in order to consider additional elements or different constraints.

4.5.1 Cyclic Constraints

In the original formulation the terminal cost function $\Psi(E)$ is the same for all devices, which in turn induces convergence towards similar values of E_s at $t = T$. It might be desirable to impose, for each device, a cyclic constraint $E_s(0) = E_s(T)$. In order to do so, we introduce an additional state variable I_s, defined as follows:

$$I_s(t) = \int_0^t u_s(\tau) \, d\tau \qquad -E_r \leq I_s(t) \leq E_r \tag{4.33}$$

Notice that $I_s(t)$ represents the total variation of stored energy in the interval $[0, t]$ and the condition $E_s(0) = E_s(T)$ is equivalent to require $I_s(T) = 0$. For the case of infinite players, the equivalent state variable $I(t) = \int_0^t u(\tau) \, d\tau$ (in p.u.) is introduced in the mean field game equations. For the transport equation, taking into account that the optimal control will depend on time and the two state variables, it holds:

$$\begin{aligned} \partial_t m(t, E, I) &= -\partial_E \left[u^*(t, E, I) m(t, E, I) \right] - \partial_I \left[u^*(t, E, I) m(t, E, I) \right] \\ m(0, E, I) &= m_0(E, I) \end{aligned} \tag{4.34}$$

Similarly, for the HJB equation:

$$\begin{aligned} -\partial_t V(t, E, I) &= \min_{u \in \mathcal{U}} \left[p_m^*(t)(u + \gamma u^2) + (\partial_E V(t, E, I) + \partial_I V(t, E, I)) \, u \right] \\ V(T, E, I) &= \Psi(E, I) \end{aligned} \tag{4.35}$$

In this case the demand variation D_s introduced by the storage population and considered in the calculation of p_m^* corresponds to:

$$D_s(t) = E^{TOT} \int \int m(t, E, I)[u^*(t, E, I) + \gamma u^{*^2}(t, E, I)] \, dI \, dE$$

Regarding the boundary conditions of the PDEs, for the transport equation (4.34) it is sufficient to specify for E the initial energy distribution of the devices, with $I = 0$. For the previous case study, considering (4.32) and denoting by δ the Dirac delta, it holds:

$$m_0(E, I) = \frac{1}{\sqrt{2\pi}\sigma} e^{-\frac{\left(E - \frac{1}{2}\right)^2}{2\sigma^2}} \cdot \delta(I)$$

The cyclic condition $E(0) = E(T)$ can be introduced as a soft constraint, choosing Ψ in order to penalize, for example quadratically with parameter c_I, final values of I different from 0:

$$\Psi(E, I) = c_I \cdot I^2$$

As in the previous case, the coupled PDEs (4.34) and (4.35) have been solved numerically, using the algorithm described in Section 4.4.1. The main difference is that the additional

state variable increases considerably the computational complexity of the integration schemes. For this reason, different numerical methods are considered. The step Δu is introduced and the admissible controls are defined as:

$$u_l = l \cdot \Delta u \qquad l = \frac{u^{MIN}}{\Delta u}, \frac{u^{MIN}}{\Delta u} + 1, \ldots, 0, \ldots, \frac{u^{MAX}}{\Delta u} - 1, \frac{u^{MAX}}{\Delta u} \qquad (4.36)$$

The time and state of charge steps are chosen in such a way that the state variation introduced by u_l is a multiple of ΔE, with $\Delta E = \Delta u \cdot \Delta t = \Delta I$. A notation similar to the one presented in Section 4.4.2 is adopted for the numerical schemes, denoting as $f^i_{j,k}$ the value of a function $f(t, E, I)$ at $(i\Delta t, j\Delta E, k\Delta I)$. The HJB equation can be integrated considering a dynamic programming problem:

$$V^{i-1}_{j,k} = \min_{l \in \mathcal{L}(E_i, I_j)} \left[\bar{p}^i \left[u_l + \gamma u_l^2 \right] \Delta t + V^i_{j+\Delta_l, k+\Delta_l} \right] \qquad (4.37)$$

where $\Delta_l = u_l \frac{\Delta t}{\Delta E}$ corresponds to the energy index variation introduced by u_l and $\mathcal{L}(E, I)$ is the set of admissible input indexes for a certain state (E, I). Given the control $\bar{u}^i_{j,k}$ and the resulting energy index variation $\bar{\Delta}^i_{j,k} = \bar{u}^i_{j,k} \frac{\Delta t}{\Delta E}$, the integration of the transport equation can be easily implemented by initializing $\bar{m}^{i+1}$ at 0 and iterating the following over j and k:

$$\bar{m}^{i+1}_{j+\bar{\Delta}^i_{j,k}, k+\bar{\Delta}^i_{j,k}} = \bar{m}^{i+1}_{j+\bar{\Delta}^i_{j,k}, k+\bar{\Delta}^i_{j,k}} + \bar{m}^i_{j,k}$$

The scenario described in the previous section has been simulated with the following parameters:

$$P_r = 2.5KW \qquad E_r = 25KWh \qquad k = 0.25 \qquad c_I = 10^5$$
$$\Delta u = 0.0125/h \qquad \Delta t = 0.32h \qquad \Delta E = \Delta I = \Delta u \cdot \Delta t = 0.004 \qquad (4.38)$$

The algorithm for the resolution of the MFG converges, as in the previous case, in about three iterations and, given the additional variable I introduced in the problem, for the parameters in (4.38) requires about 4 hours to be completed. By choosing a larger step $\Delta u = 0.025/h$, it is possible to complete the same calculations in 1 hour, with a difference in the results which is not significant. The profile of total demand obtained in simulation is very similar to the one in Fig. 4.4. The corresponding energy trajectories for different values of $E(0)$ are shown in Fig. 4.9. As expected, each device charges/discharges on the basis of the current price of energy, returning at its initial state of charge for $T = 24h$. In this case the profit G_s of the single device as a function of its initial energy $E_s(0)$ is equal to $-V\left(0, \frac{E_s(0)}{E_r}, 0\right) E_r$. A sensitivity analysis has been carried out, evaluating G_s for different values of E_r (while keeping unaltered the other parameters). The results are shown in Fig. 4.10. One can see that to higher energy ratings correspond higher profits. Furthermore, the arbitrage is in general more profitable for the devices which

start with a low state of charge and are therefore able to charge more energy during the first hours of the day, when energy price is lower. A further consideration can be made for the scenario with $E_r = 25KWh$: in this case the highest profit is achieved by devices with initial state of charge within a certain interval. It can be noticed from Fig. 4.9 that these devices are the ones for which the constraints on minimum and maximum energy are not active in the considered time horizon.
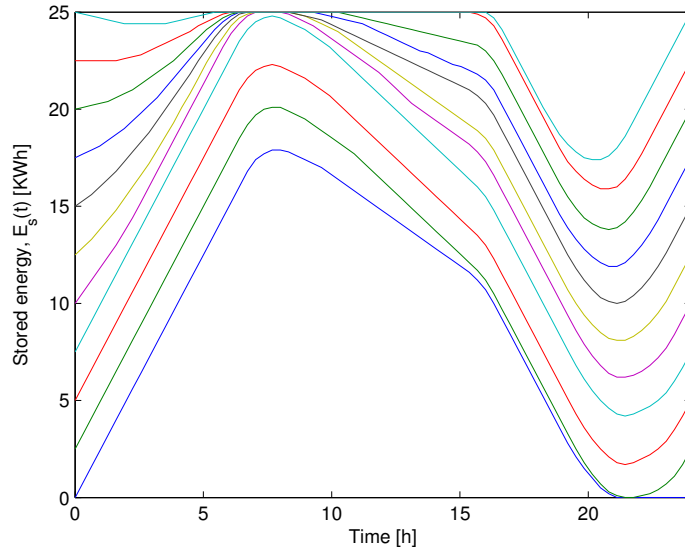
FIGURE 4.9: Stored energy of the devices across time for different values of $E(0)$, with energy rating $E_r = 25KWh$.
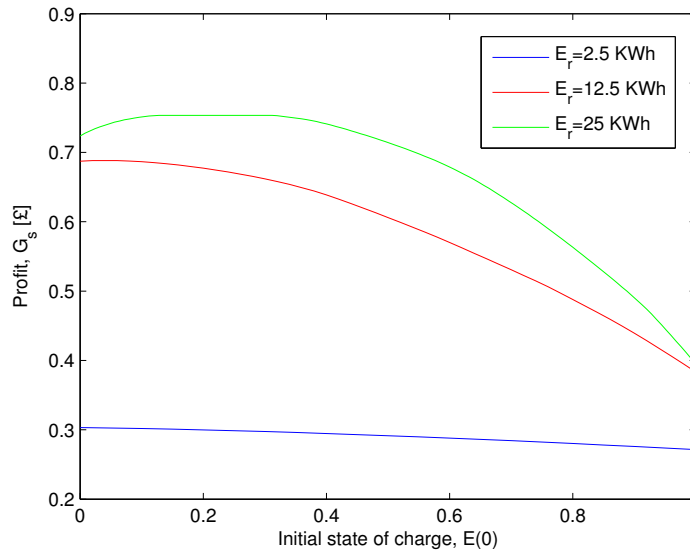
FIGURE 4.10: Profit G_s of the single device as a function of the initial state of charge $E(0)$, for different energy ratings.

4.5.2 Multiple Populations of Devices

A preliminary hypothesis in the formulation of the arbitrage problem as a mean field game has been the homogeneity of the devices: all agents have the same efficiency, capacity and maximum rate of charge. It is possible, in principle, to introduce in the model a parameter α which varies in the population, considering it as an additional state variable and imposing $\dot{\alpha} = 0$. The main problem with this approach is that it increases considerably the complexity of the problem. An acceptable trade-off can be obtained if, instead of parameters that vary continuously, we consider a finite number of populations, each with devices of the same kind. In fact, for the considered arbitrage problem, these distinct groups of agents will interact only through the energy price $\Pi(D_i + D_s)$. This particular case can be approached by solving in parallel a set of coupled PDEs (4.34) and (4.35), one for each population, that share the same price function. The same resolution procedure is followed, with a different expression for the demand variation introduced by storage. Denoting with subscript j the energy distribution, total capacity and optimal control for the j-th population, it holds:

$$D_s(t) = \sum_{j=1}^{M} E_j^{TOT} \int \int m_j(t, E, I) \left[u_j^*(t, E, I) + \gamma_j u_j^{*2}(t, E, I) \right] dE \, dI \qquad (4.39)$$

In the case of a finite number M of populations, characterized by different sets of parameters, M coupled PDEs are solved in parallel, with a computational complexity that increases linearly with respect to M. This extension is particularly significant if one considers practical implementations of the proposed control algorithm. In fact, in order to obtain the solution of the mean field game, the centralized entity that performs this calculation must know the initial energy distribution of the devices and the corresponding characteristics (energy/power rating and efficiency). In this respect, it is reasonable to assume that a finite number of device typologies (with known parameters) will be available for commercial purposes. In the proposed formulation, to each kind of device will correspond one of the M populations considered above.

A scenario with two distinct groups of storage devices (A and B) performing energy arbitrage has been simulated, with the following choice of parameters:

$$N_A = 5 \cdot 10^5 \qquad E_{r_A} = 20KWh \qquad P_{r_A} = 2KW$$

$$N_B = 5 \cdot 10^5 \qquad E_{r_B} = 30KWh \qquad P_{r_B} = 3KW$$

The corresponding MFG equations with cyclic constraints have been integrated using the same boundary conditions and numerical methods presented in the previous subsection. With the hardware/software specifications provided in Section 4.4.3, the simulation is

completed in about 4 hours. As in the previous case, the simulation time is sensibly reduced if one increases the discretization step Δu of the control u. The aggregate demand at each iteration of the backward/forward integration is shown in Fig. 4.11. Convergenge to the solution is achieved in 3 steps when $\epsilon_D = 1GWh$ and the peak shaving/valley filling introduced by storage is comparable to the one achieved when a single population is considered. The profit of the devices as a function of their initial state of charge is compared in Fig. 4.12 for the two groups. Notice in particular that for the devices of population A, with a lower power rating, the corresponding profit G_{s_A} is sensibly lower. Furthermore, the considerations on Fig. 4.10 about the effect of the initial state of charge on the profit G_s can be extended to the present case.
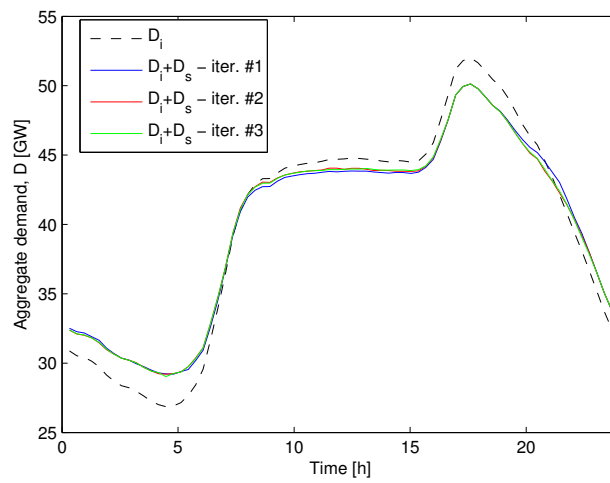
FIGURE 4.11: Comparison between inflexible and aggregate demand at each iteration of the MFG-solving procedure.
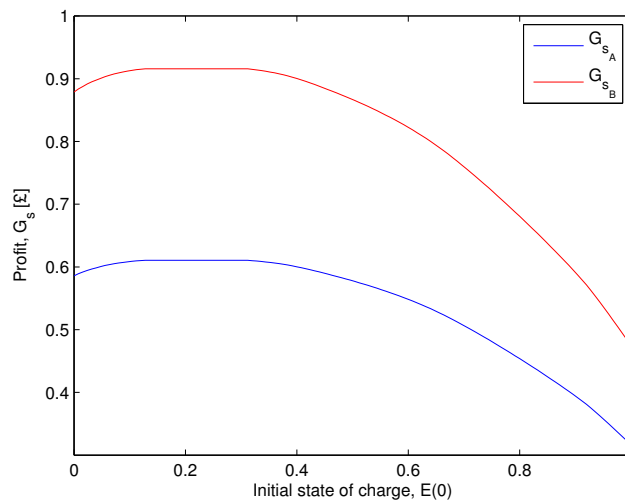
FIGURE 4.12: Profit G_s of the single device as a function of the initial state of charge, for population A (blue) and B (red).

4.5.3 Uncertainty in Demand

Another assumption in the formulation of the mean field game presented in Section 4.3 is that the inflexible demand profile D_i is known without uncertainties. It is possible to consider error in the demand forecast $\tilde{D}_i$ by introducing the following expression:

$$\tilde{D}_i(t) = D_i(t) + \eta(t)$$

where D_i is the actual inflexible demand and η is a stochastic process. One possible way to take into account demand uncertainty is to use a receding horizon control:

1. At time t the actual demand $D_i(t)$ is measured and the forecast $\tilde{D}_i$ is estimated over the interval $[t, t+T]$.

2. Based on the current distribution $m(t, \cdot)$, the terminal cost function Ψ is updated:

$$\bar{E}(t) = \int_{\mathcal{E}} m(t, E) E \, dE$$
$$\Psi(E) = c_E \cdot \left(E - \bar{E}(t) \right)^2$$

3. The coupled PDEs (4.22) and (4.27) are solved considering $\tilde{D}_i$ as profile of inflexible demand.

4. The optimal u^* is applied only at the current time step.

5. Steps 1-4 are repeated for $t + \Delta t$.

This approach allows to implicitly incorporate uncertainty in the model but, on the other hand, increases the computational complexity by a factor of $T/\Delta t$ since the equations of the mean field game must now be solved at each time step. For the simulation presented next, the dynamics of η are defined as follows:

$$d\eta_t = \sigma_f \cdot dW_t \tag{4.40}$$

where W denotes the Wiener process. The forecast error η is characterized, similarly to what is shown for example in [98], by mean value $\mu_\eta(t) = 0$ and standard deviation $\sigma_\eta(t) = \sigma_f \sqrt{t}$. The performance of the receding horizon strategy has been evaluated for the case study described in Section 4.4.3, with a higher time step $\Delta t = 0.2h$. The average daily profit $\bar{G}_s$ of the single device over 200 days has been calculated for different values of σ_f and it is shown in Fig. 4.13. The simulation time for each σ_f amount to about 80 minutes. Notice that, in practical implementations, calculations would be gradually

performed during the whole time interval and not entirely at the beginning. As expected, there is a reduction of $\bar{G}_s$ for increasing values of σ_f. On the other hand, such reduction is not very significant: by solving the MFG at each time step, with updated forecasts on demand, the impact of uncertainties on the final result can be considerably reduced.
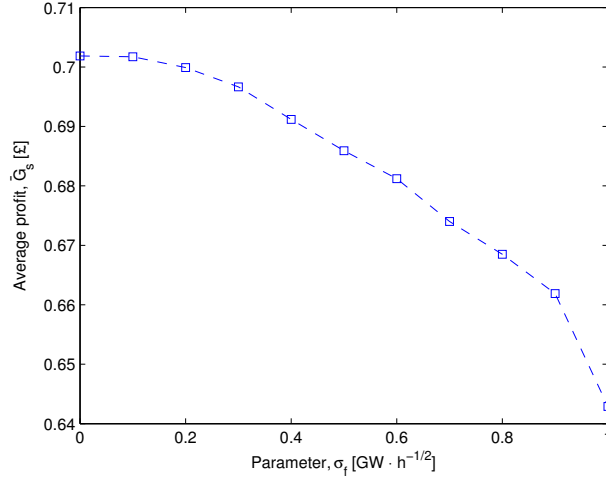
FIGURE 4.13: Average daily profit $\bar{G}_s$ of the single device (over 200 days) as a function of the parameter σ_f when the receding horizon control is applied.

4.5.4 Multi-Area Systems

In the initial model presented in Section 4.3 it is assumed that all generators, loads and storage devices belong to the same area and there is no limit to the power that can be exchanged within the network. To consider a more realistic framework, the power system can be divided in different areas, introducing transmission constraints. In each area k the generation cost $C_k(G)$, the demand D_k and the installed storage capacity E_k^{TOT} are different. To calculate the price at which storage devices will exchange energy in the different areas, an optimal power flow problem must be solved. On the basis of the current values of demand, storage charge profiles and transmission constraints, the generated power is distributed among the different areas in order to minimize the total generation cost. For a system with n_A areas, if we denote by $\bar{F}_{kl}$ the capacity constraint between areas k and l and by F_{kl} the actual power flow, we have:

$$\begin{aligned}
\min_{G} \quad & \sum_{k=1}^{n_A} C_k(G_k) \\
\text{s.t.} \quad & G_k = D_k + \sum_{j=1,j\neq k}^{n_A} F_{kj} \quad k = 1 \ldots n_A \\
& |F_{kl}| \leq \bar{F}_{kl} \; \forall (k,l)
\end{aligned} \tag{4.41}$$

The optimization problem is approached by considering as decision variables the net inflows I_k and the voltage angles θ_k. Under the standard assumptions for DC power flow, (4.41) can now be written as [99]:

$$
\begin{aligned}
\min_{I,\theta} \quad & \sum_{i=1}^{n_A} C_k(G_k) \\
\text{s.t.} \quad & G_k = D_k + I_k \quad k = 1 \ldots n_A \\
& I = Y\theta \\
& |F_{kl}| = \left| \frac{1}{x_{kl}}(\theta_k - \theta_l) \right| \leq \bar{F}_{kl} \quad \forall \, (k,l)
\end{aligned}
\tag{4.42}
$$

where I and θ denote respectively the vectors of net inflows and voltage angles, Y is the admittance matrix of the system and x_{kl} is the reactance of line kl. Each demand D_k in (4.42) has two components, the known inflexible profile D_{i_k} and the contribution of storage D_{s_k}. The prices p_k at which the storage devices in area k exchange energy are given by the value of the Lagrange multiplier associated with the equality constraint $I_k = Y_k\theta$. The MFG equations for the population of devices in area k are a straight derivation of (4.22) and (4.27):

$$
-\partial_t V_k(t, E_k) = \min_{u_k \in \mathcal{U}_k} \left[p_k(t)[u_k + \gamma u_k^2] + \partial_{E_k} V_k(t, E_k) u_k \right]
\tag{4.43}
$$
$$
\partial_t m_k(t, E_k) = -\partial_{E_k} \left[m_k(t, E_k) u_k^*(t, E_k) \right]
$$

The coupled PDEs (one for each area k) can be solved in parallel with the procedure described in Section 4.4.1. The only difference is that the price $\bar{p}$ at step 2.c is not calculated with equation (4.29) but it is obtained solving problem (4.42), considering the following expression for the demand D_k in each area:

$$
D_k(t) = D_{i_k}(t) + E_k^{TOT} \int_{\mathcal{E}} \bar{m}_k(t, E) \bar{y}_k(t, E) \, dE
\tag{4.44}
$$

Furthermore, the convergence conditions in step 2.d and 4 have to be verified for prices and demand in each area.

Simulations have been run for the 3-area power system shown in Fig. 4.14, with the following choice of parameters:

$$
\begin{aligned}
& x_{12} = 0.2 \text{ p.u.} && x_{13} = 0.1 \text{ p.u.} && x_{23} = 0.2 \text{ p.u.} \\
& \bar{F}_{12} = 8GW && \bar{F}_{13} = 8GW && \bar{F}_{23} = 4.3GW \\
& E_1^{TOT} = 15GWh && E_2^{TOT} = 15GWh && E_3^{TOT} = 7.5GWh
\end{aligned}
\tag{4.45}
$$

Generation costs increase from Area 1 to Area 3 ($C_1(G) > C_2(G) > C_3(G)$) and the inflexible demand profile in each area is a repartition of the function D_i shown in Fig. 4.2:

$$D_{i_1} = \frac{1}{2}D_i \qquad D_{i_2} = \frac{1}{3}D_i \qquad D_{i_3} = \frac{1}{6}D_i \tag{4.46}$$
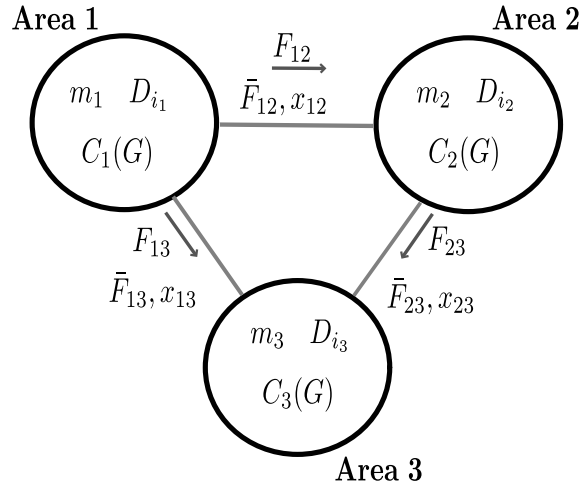
FIGURE 4.14: Three area system considered in the numerical resolution of the MFG.
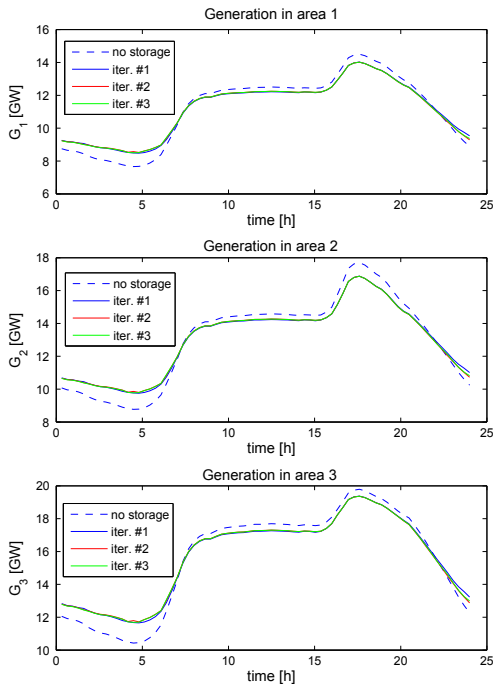
FIGURE 4.15: Generation in the 3-area system.
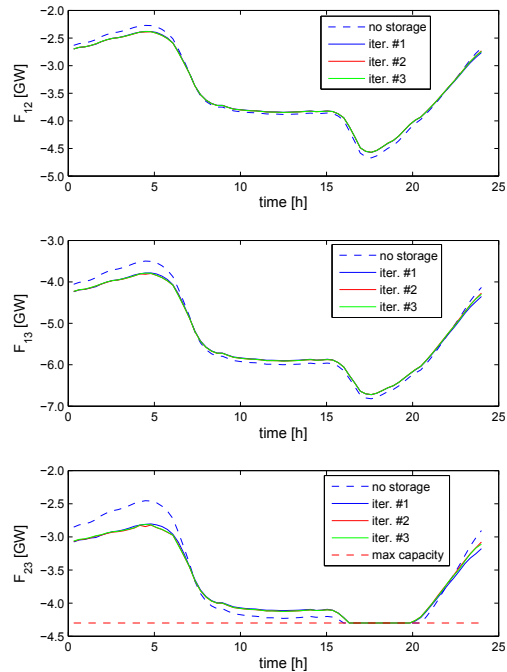
FIGURE 4.16: Power flows in the 3-area system.

The numerical procedure for the integration of (4.43) converges, as in the previous cases, in 3 iterations. The values of generation in each of the 3 areas are shown in Fig. 4.15. It can be seen that, as in the other case studies, the energy arbitrage performed by the storage devices introduces a significant valley filling. A similar trend can be noticed in the power flows, shown in Fig. 4.16: the presence of storage reduces their variation during the day and restricts the time interval during which the line 2-3 operates at full capacity. The prices at which the devices exchange energy are in Fig. 4.17. It is interesting to notice that prices are equal in all areas except when a capacity constraint is active and energy becomes more expensive in areas 1 and 2.
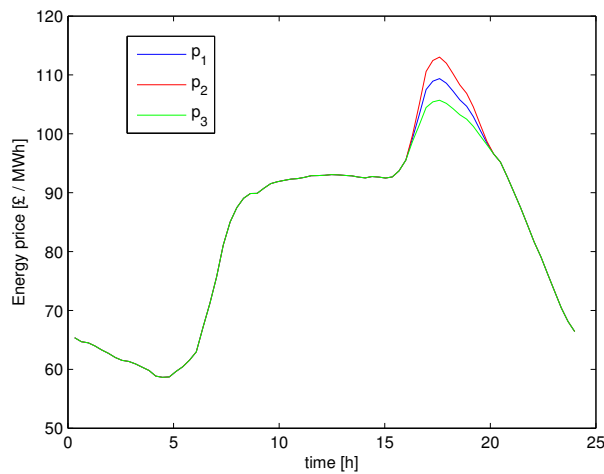
FIGURE 4.17: Nodal prices in the three areas.

4.6 Conclusions

A new methodology is presented for distributed control of storage devices performing energy arbitrage. The problem is formulated in a competitive game framework, considering initially a finite number of players and providing some preliminary existence results. In order to properly account for the changes in the total power demand and energy price introduced by the devices, the storage population is modelled as a continuum and the problem is approached as a differential game with infinite players (mean field game). Once the game is solved by numerical integration of coupled PDEs, an updated energy price can be communicated to the devices, which are able to calculate their optimal charge profile in a decentralized manner. The methodology is tested through simulations and then expanded to account for additional elements such as cyclic constraints, uncertainty on demand and multi-area systems.

Chapter 5

Decentralized Scheduling of Flexible Demand in the Electricity Market

This chapter deals with large populations of flexible appliances which, in order to minimize their energy cost, greedily determine their daily profile of power consumption on the basis of a broadcast price signal. By approximating the population size as infinite and describing its behaviour as a continuum, it is possible to provide necessary and sufficient conditions for the existence of a Nash equilibrium in the energy market. These conditions can be extended introducing proportional constraints on the absorbed power of the devices, limiting the impact of the population on the energy price at critical time instants. The described framework is tested in simulation and extended in order to consider partial flexibility of the appliances.

5.1 Introduction

Flexible demand is an important aspect of the smart grid paradigm for the future power system. As mentioned in Section 4.1.2, it is expected that in the next few years there will be a consistent number of devices (e.g. "smart" domestic appliances and electric cars) that would be able to schedule their power consumption throughout the day. In particular, it is reasonable to assume that the scheduling will be determined in order to minimize the total operating cost. As in the previous chapter, which considers micro-storage devices, the demand variations introduced by the aggregate power consumption of the population modify the resulting price of energy and must therefore be taken into account. The main difference with respect to the storage case is that the flexible

appliances can only absorb energy from the system. This implies that it is no longer necessary to impose constraints on the state of the devices (which in the previous chapter corresponds to their state of charge): each appliance will only need to specify the total amount of energy to be consumed during the considered time horizon.

The problem is analysed within a game-theory framework: the appliances are considered as competing agents which schedule their power consumption in order to minimize their energy cost, on the basis of a broadcast price signal received by some central entity. Existence and uniqueness of a Nash equilibrium are investigated, determining under which conditions all the appliances have no unilateral interest in changing their operation strategy, formulated on the basis of the broadcast signal, when the energy price of the resulting aggregate demand profile is considered. A significant element of novelty with respect to most of the distributed control strategies presented in Section 4.1.3 is that, instead of operating iteratively by updating in turn the broadcast price and the strategies of the players, necessary and sufficient conditions are provided for convergence to equilibrium in one step. This is achieved by approximating the population size as infinite and accounting for its parameters distribution through a *power density of task durations* which describes the valley-filling capability of the appliances. Similarly, the inflexible demand profile is described by the *negotiable valley capacity*, a function that is related to the measure of its different sublevel sets and quantifies the amount of flexible demand that can be allocated while preserving an equilibrium. By comparing these two functions, it is possible to verify whether an equilibrium exists and show that, if this is the case, it can be achieved by simply broadcasting to the devices the price of the inflexible demand. When the equilibrium conditions are not satisfied, the problem is approached by introducing a time-varying proportional constraint (equal for all appliances) in order to limit the power absorption at critical time instants. Such constraint is designed in order to achieve a Nash equilibrium and, at the same time, minimize the operation time of all the appliances. It is possible to show that the proposed control strategy is optimal also for some global index that quantifies the flattening of aggregate demand and, in some cases, achieves Pareto optimality. The proposed algorithms are then evaluated in simulations and extended to consider partial flexibility of the devices. In particular, assuming that each agent can operate only after a certain time instant, the analysis focuses on a specific class of broadcast signals which can be parametrized as valleys. A design method is provided in order to calculate, if there exists, a demand/price function that can be broadcast to the devices and induce an equilibrium under the additional time constraint.

The rest of this chapter is structured as follows: Section 5.2 models the flexible appliances population and their optimization strategy with respect to a broadcast price. The

necessary and sufficient conditions for a Nash equilibrium are derived in Section 5.3 and extended, through the addition of time-varying proportional constraints, in Section 5.4. Simulation results are presented in Section 5.5 while Section 5.6 describes the global optimality properties of the proposed control strategy and Section 5.7 details the case of appliances with partial flexibility.

5.2 Flexible Demand and Optimization Strategies

The existence of Nash equilibria in the electricity market is investigated considering a large number of flexible appliances, such as "smart" domestic loads and electric cars, that must complete a certain task within a specified time interval $[0, T]$, at minimum cost. Each of them communicates to a central entity the total amount of energy E_{tot} that needs to consume and the minimum time t_{min} required to do so by operating at rated power P_r. If the number of appliances is sufficiently large to be described by a continuum, it is possible to derive the unnormalized distribution $m(t, E)$ of these parameters, where $\int_{t_1}^{t_2} \int_{E_1}^{E_2} m(t, E) \, dE \, dt$ will denote the number of devices for which $E_1 \leq E_{tot} \leq E_2$ and $t_1 \leq t_{min} \leq t_2$. For the purposes of the present work, the properties of the appliances population can be summarized by the function $f(t)$, which denotes the aggregate amount of energy required by the appliances with $t_{min} \leq t$, and its derivative f'. Denoting by $\mathcal{E}$ an interval which includes all broadcast values of E_{tot}, they can be defined as follows:

$$f(t) := \int_0^t \int_{\mathcal{E}} m(\tau, E) E \, dE \, d\tau \qquad f'(t) := \int_{\mathcal{E}} m(t, E) E \, dE \qquad (5.1)$$

Assumption 5.1. *The derivative f' is assumed of compact support with $\mathcal{F} = \mathrm{supp}(f') = [q_{min}, q_{max}]$. In general this can correspond to a scenario of heterogeneous appliances with different parameters t_{min} and E_{tot} but can also represent the case of homogeneous devices which, at the beginning of the considered time interval $[0, T]$, are performing distinct tasks that require different amounts of time or energy to be completed.*

The energy price $p(t)$ (generally varying in time) is modelled as a static function of the aggregate demand D_a at the same instant, viz. $p(t) = \Pi(D_a(t))$, for some monotonically increasing function $\Pi : [0, +\infty) \to [0, +\infty)$. The aggregate demand, in turn, is given by two different components: the inflexible demand D_i, assumed to be known a priori, and the contribution D_f of the flexible appliances. These appliances receive from the mentioned central entity a certain demand profile $D(t)$ (or equivalently the price $p(t) = \Pi(D(t))$) and determine their power consumption u by minimizing their

own resulting total energy cost:

$$\min_{u(\cdot)} \quad \int_0^T \Pi(D(t)) \cdot u(t)\, dt$$
$$\text{s. t} \quad 0 \le u(t) \le \frac{E_{tot}}{t_{min}} \tag{5.2}$$
$$\int_0^T u(t)\, dt = E_{tot}$$

It is straightforward to verify that the solution of (5.2) corresponds to operate, at rated power $P_r = \frac{E_{tot}}{t_{min}}$, during the t_{min} hours characterized by lowest demand (or equivalently lowest price). In order to provide a formal expression of the optimal power consumption profile u^*, the following definition is crucial:

Definition 5.1. Considering the continuous function $D : [0, T] \to [0, +\infty)$ as the broadcast profile, we define its *cumulative distribution* $Q_D : [d_{min}, d_{max}] \to [0, T]$ as:

$$Q_D(d) := \mu\left(\{\tau \in [0, T] : D(\tau) \le d\}\right) \tag{5.3}$$

where μ denotes the Lebesgue measure. Notice that $Q_D(d)$, which returns the measure of the sublevel sets of the profile D, is a monotone increasing function. Furthermore, it holds $Q_D(d_{min}) = 0$ and $Q_D(d_{max}) = T$ where d_{min} and d_{max} are defined as follows:

$$d_{min} := \inf_{t \in [0,T]} D(t) \qquad d_{max} := \sup_{t \in [0,T]} D(t) \tag{5.4}$$

Assumption 5.2. *There are no level sets of positive measure for the broadcast demand* D. *In particular, for any* $d \in [d_{min}, d_{max}]$, *it must hold:*

$$\mu\left(\{\tau \in [0, T] : D(\tau) = d\}\right) = 0. \tag{5.5}$$

Such assumption is not very restrictive and holds in general for typical profiles of inflexible demand, which will be considered later on when determining the equilibrium conditions. Furthermore, it guarantees continuity of the cumulative distribution Q_D and uniqueness (up to congruence in the ℓ_1 norm) of the optimal solution of (5.2). Consider in fact that, for all values of t_{min}, there exists a sublevel set of D of measure t_{min} that we denote by $\mathcal{S}_D(t_{min})$ and define as follows:

$$\mathcal{S}_D(t_{min}) = \{t \in [0, T] : Q_D(D(t)) \le t_{min}\}. \tag{5.6}$$

In particular, from (5.3) and Assumption 5.2, it holds:

$$D(t_1) < D(t_2) \qquad \forall t_1 \in \mathcal{S}_D(t_{min}) \quad \forall t_2 \in [0, T] \backslash \mathcal{S}_D(t_{min}) \tag{5.7}$$

For a better understanding of the relationship between time t and the measure $Q_D(D(t))$, some comparisons are performed next. Examples of broadcast demand profiles are shown in Fig. 5.1 while Fig. 5.2 contains the corresponding functions $Q_D(D(t))$.
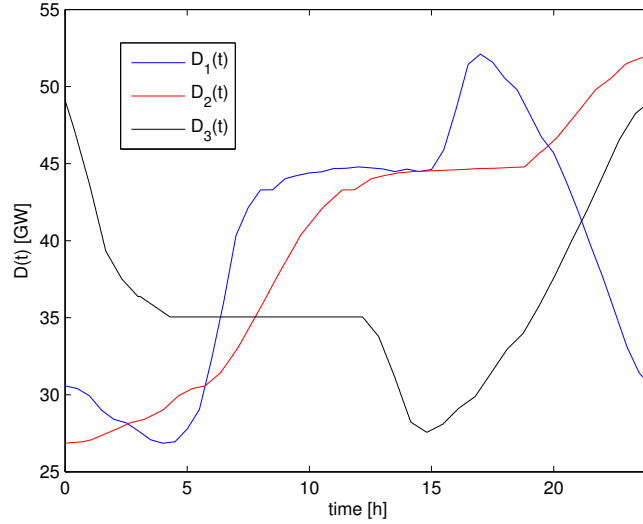
FIGURE 5.1: Examples of broadcast profiles D.
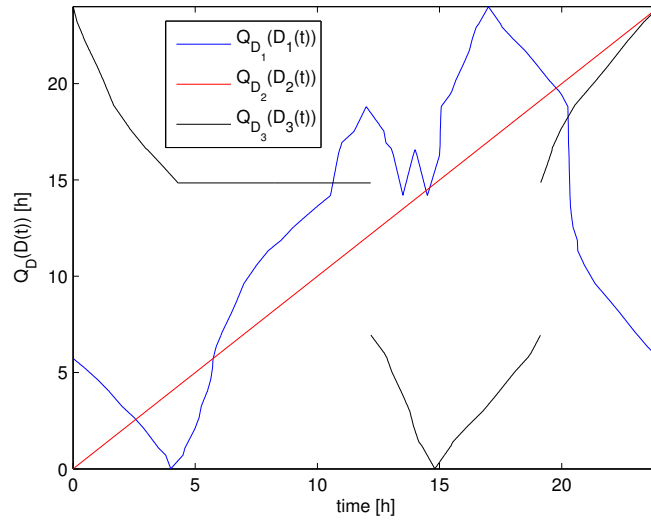
FIGURE 5.2: Measure function $Q_D(D(t))$ for the broadcast profiles shown in Fig. 5.1.

The blue curve D_1 in Fig. 5.1 is a typical 24h UK demand profile and the corresponding function Q_{D_1} in Fig. 5.2 shows the same monotonicity trends with values in the interval $[0, 24]$. The red curve D_2 represents an example of monotonically increasing profile to which, by definition, corresponds a linear function $Q_{D_2}(D_2(t)) = t$. The last considered curve D_3 is a profile which violates Assumption 5.2 and is constant over an interval of

positive measure. It is clear from Fig. 5.2 that this corresponds to discontinuities in the measure function Q_{D_3}.

The optimal power consumption profile u^* for devices with minimum time $t_{min} = s$ and total energy $E_{tot} = x$ can now be defined as:

$$u^*(t, s, x) = \begin{cases} \dfrac{x}{s} & \text{if} \quad t \in \mathcal{S}_D(s) \\[2ex] 0 & \text{if} \quad t \notin \mathcal{S}_D(s) \end{cases} \tag{5.8}$$

Consider that $t \in \mathcal{S}_D(s)$ if and only if $Q_D(D(t)) \leq s$. This means that u^* can be calculated as a function of the measure q returned by $Q_D(D(t))$. If the broadcast demand D satisfies Assumption 5.2, the following expression can be provided for the optimal power profile of the individual device with $t_{min} = s$ and $E_{tot} = x$:

$$\bar{u}^*(q, s, x) = \begin{cases} \dfrac{x}{s} & \text{if} \quad q \leq s \\[2ex] 0 & \text{if} \quad q > s \end{cases} \tag{5.9}$$

Furthermore, it is possible to define the aggregate power density $\bar{g}$ of the devices with $t_{min} = s$ as a function of q:

$$\bar{g}(q, s) = \int_{\mathcal{E}} \bar{u}^*(q, s, x) \cdot m(s, x) \, dx = \begin{cases} \dfrac{f'(s)}{s} & \text{if} \quad q \leq s \\[2ex] 0 & \text{if} \quad q > s \end{cases} \tag{5.10}$$

By taking the integral of $\bar{g}$ over the different minimum times t_{min}, one can derive the expression of the flexible demand $\bar{D}_f$ generated by the appliances population when D is broadcast:

$$\bar{D}_f(q) = \int_0^T \bar{g}(q, s) \, ds = \int_q^T \frac{f'(s)}{s} \, ds \tag{5.11}$$

Remark 5.1. The optimal power consumption profile u^*, its aggregation g and the flexible demand D_f can be calculated as functions of time by evaluating the corresponding expressions in the q variable at $q = Q_D(D(t))$:

$$u^*(t, s, x) = \bar{u}^*(Q_D(D(t)), s, x) \qquad g(t, s) = \bar{g}(Q_D(D(t)), s) \qquad D_f(t) = \bar{D}_f(Q_D(D(t))) \tag{5.12}$$

Remark 5.2. Since $\frac{f'(s)}{s}$ quantifies the aggregate rated power of the appliances with $t_{min} = s$, given expression (5.9) for the optimal power profile $\bar{u}^*$ and Assumption 5.1 on the support of f', it follows that, when D is broadcast, all devices will operate (at rated power) when $Q_D(D(t)) < q_{min}$ and will instead not operate when $Q_D(D(t)) > q_{max}$.

Having defined the flexible demand which results from broadcasting a certain D, the corresponding aggregate profile $D_{a,D}$ will have the following expression:

$$D_{a,D}(t) = D_i(t) + \bar{D}_f(Q_D(D(t))) \tag{5.13}$$

In the particular case in which $D = D_i$ (viz. inflexible demand is broadcast), the aggregate demand depends exclusively on the current broadcast value $d = D_i(t)$ through the function $K(d)$ defined below:

$$D_{a,D_i} = K(d) = \begin{cases} d & \text{if} & Q_{D_i}(d) > q_{max} \\ d + \int_{q_{min}}^{q_{max}} \dfrac{f'(s)}{s}\, ds & \text{if} & Q_{D_i}(d) < q_{min} \\ d + \int_{Q_{D_i}(d)}^{q_{max}} \dfrac{f'(s)}{s}\, ds & \text{if} & Q_{D_i}(d) \in \operatorname{supp}(f') \end{cases} \tag{5.14}$$

5.3 Conditions for Nash Equilibrium

It is desirable to understand under which conditions a Nash equilibrium is achieved in the energy market. In particular, we want to determine which are the broadcast profiles D such that the corresponding u^* are optimal power schedules also for the resulting aggregate demand $D_{a,D}$. In other words the devices, which have optimized their power consumption considering the broadcast D, will have no unilateral interest in changing their operation strategy in response to the variation of prices induced by considering the aggregate demand. The analysis of the equilibria will be carried out by comparing two different functions in the variable q which are related to the chosen broadcast profile and to the properties of the appliances population.

Consider that high penetration of flexible demand has the potential of transforming valleys of the broadcast demand signal into peaks of the aggregated demand profile. In this case the decentralized power scheduling computed by the appliances is suboptimal and constantly susceptible to renegotiation in a way that forbids convergence to a well defined power consumption profile. For a given profile D, it is possible to quantify the amount of flexible demand that can be greedily allocated by the appliances while preserving the existence of a Nash equilibrium. We name this quantity the *negotiable valley capacity*:

Definition 5.2. For a continuous demand profile $D : [0, T] \to [0, +\infty)$ fulfilling Assumption 5.2, the *negotiable valley capacity* is defined as the function $\Lambda_D : [0, T] \to [0, +\infty)$ presented below:

$$\Lambda_D(q) : q \to \frac{d}{dq} Q_D^{-1}(q).$$

Such definition is independent of the price of energy Π and quantifies the flexible power density allowed in the valleys of the broadcast signal D.

In a similar way, it is possible to describe how a certain population of appliances will allocate their power consumption u as a function of the sublevel set measure q, based on the distribution of the parameters t_{min} and E_{tot}. In particular, the following notion of power density at q can be introduced:

Definition 5.3. For a population of flexible appliances with parameters distribution m, we define the *power density of task durations* as the function $\Lambda_f : [q_{min}, q_{max}] \to [0, +\infty)$ given below:

$$\Lambda_f : q \to \frac{f'(q)}{q} = \frac{\int_{\mathcal{E}} E m(q, E) \, dE}{q}$$

Notice that $\Lambda_f(q) = \frac{f'(q)}{q}$ is a density function which quantifies the total rated power of the appliances with parameter $t_{min} = q$. Therefore, given $q_1, q_2 \in \text{supp}(f')$, the integral $\int_{q_1}^{q_2} \Lambda_f(\tau) \, d\tau$ is equal to the total rated power of the appliances with $t_{min} \in [q_1, q_2]$. It will be shown in the rest of this section how the existence of an equilibrium can be verified by comparing the values of Λ_f and Λ_{D_i} on the interval $[q_{min}, q_{max}]$.

If one initially considers the problem in the time variable t, an equilibrium exists if and only if the flexible demand scheduled on the basis of the a priori broadcast price signal $\Pi(D)$ is also optimal for the a posteriori price signal (viz. taking into account the sum $D_{a,D}$ of the inflexible and flexible demand). Hence, the following needs to hold for all $E_{tot} = x \in \mathcal{E}$ and $t_{min} = s \in [q_{min}, q_{max}]$:

$$
\begin{aligned}
\int_0^T \Pi(D_{a,D}(t)) u^*(t, s, x) dt = \quad &\min_{u(\cdot)} \quad \int_0^T \Pi(D_{a,D}(t))) u(t) \, dt \\
&\text{s. t} \quad 0 \le u(t) \le \frac{x}{s} \\
&\qquad \int_0^T u(t) \, dt = x
\end{aligned}
\tag{5.15}
$$

Given the optimality of the power profile u^* for (5.2) and its expression provided in (5.8), the following is verified for all $t_{min} \in \text{supp}(f')$:

$$D(t_1) < D(t_2) \quad \forall t_1 \in \mathcal{S}_D(t_{min}) \quad \forall t_2 \in [0, T] \backslash \mathcal{S}_D(t_{min}) \tag{5.16}$$

In the same way, u^* will be the solution of the minimization problem in (5.15) (when the aggregate profile $D_{a,D}$ is considered) if and only if a similar inequality holds for all $t_{min} \in \text{supp}(f')$:

$$D_{a,D}(t_1) \le D_{a,D}(t_2) \quad \forall t_1 \in \mathcal{S}_D(t_{min}) \quad \forall t_2 \in [0, T] \backslash \mathcal{S}_D(t_{min}) \tag{5.17}$$

(the "only if" direction being a consequence of continuity of the aggregate demand if Assumption 5.2 is fulfilled). These conditions are at the core of the following result which characterizes existence of a Nash equilibrium in the electricity market:

Theorem 5.1. *Consider a continuous profile of inflexible demand D_i fulfilling Assumption 5.2. The equilibrium condition (5.15) is satisfied for $D = D_i$ if and only if:*

$$\Lambda_f(q) \leq \Lambda_{D_i}(q) \qquad \forall q \in [q_{min}, q_{max}]. \tag{5.18}$$

Proof. Given definition (5.6) of the set $\mathcal{S}_D(t_{min})$ for $D = D_i$, the optimality condition (5.17) for D_{a,D_i} (equivalent to (5.15)) can alternatively be written, for all $t_{min} \in \text{supp}(f')$, as:

$$K(d_1) \leq K(d_2) \quad \forall d_1, d_2 : Q_{D_i}(d_1) \leq t_{min}, Q_{D_i}(d_2) > t_{min} \tag{5.19}$$

where K, defined in (5.14), is the function that returns the aggregate demand when the inflexible profile D_i is broadcast. A more general expression which accounts for all values of t_{min} can also be provided:

$$K(d_1) \leq K(d_2) \qquad \forall (d_1, d_2) \in \mathcal{D}_C : d_1 \leq d_2$$

In order to define the set $\mathcal{D}_C$, consider that the comparisons in (5.17) and (5.19) are performed between the demand values at some instant t_1, included in the interval $\mathcal{S}_{D_i}(t_{min})$ and some other t_2 not included in it. Since the inequality must hold for all $t_{min} \in \text{supp}(f')$, if one denotes by d_{min} and d_{max} the minimum and maximum values of inflexible demand, it is possible to give the following definition:

$$\mathcal{D}_C := ([d_{min}, d_{max}] \times [d_{min}, d_{max}]) \setminus (\mathcal{D}_{min} \cup \mathcal{D}_{max})$$

The sets $\mathcal{D}_{min}$ (and $\mathcal{D}_{max}$) correspond to pairs of demand values at which all devices are consuming power (respectively not consuming). From Remark 5.2, it holds:

$$\mathcal{D}_{min} = \{(d_1, d_2) : Q_{D_i}(d_1) < q_{min}, Q_{D_i}(d_2) < q_{min}\}$$

$$\mathcal{D}_{max} = \{(d_1, d_2) : Q_{D_i}(d_1) > q_{max}, Q_{D_i}(d_2) < q_{max}\}$$

Taking into account that $K(d)$ is monotonic increasing by definition in the intervals $[d_{min}, Q_{D_i}^{-1}(q_{min})]$ and $[Q_{D_i}^{-1}(q_{max}), d_{max}]$, conditions (5.17) and (5.19) correspond to K being monotonic increasing on $\mathcal{D}_{D_i} = [Q_{D_i}^{-1}(q_{min}), Q_{D_i}^{-1}(q_{max})]$ or equivalently:

$$K'(d) = 1 - \frac{f'(Q_{D_i}(d))}{Q_{D_i}(d)} Q'_{D_i}(d) \geq 0 \qquad \forall d \in \mathcal{D}_{D_i}$$

Dividing both terms of the inequality by $Q'_{D_i}(d)$ and letting q denote $Q_{D_i}(d)$ yields:

$$\Lambda_f(q) = \frac{f'(q)}{q} \leq \frac{d}{dq} Q_{D_i}^{-1}(q) = \Lambda_{D_i}(q) \qquad \forall q \in [q_{min}, q_{max}]$$

$\square$

From Theorem 5.1 it is possible to conclude that, if the power density Λ_f is lesser or equal than the negotiable valley capacity Λ_{D_i} on the support of f', the equilibrium can be achieved (in a one-step iteration) by simply broadcasting to the devices the profile D_i (or the associated price) of inflexible demand and letting each device schedule its power consumption at constant maximum rate within the sublevel set of D_i of appropriate measure, viz. corresponding to its own minimum time parameter t_{min}.

Remark 5.3. Condition (5.18) in Theorem 5.1 is equivalent to impose that the aggregate demand is monotonic increasing in the q variable. In fact, if one considers (5.11), the left hand side Λ_f in (5.18) represents the derivative of the flexible demand in the variable q changed in sign. Similarly, since $Q_{D_i}^{-1}(q)$ returns the value of D_i at a given q, the right hand side Λ_{D_i} in (5.18) represents the derivative of the inflexible demand with respect to q. The equilibrium condition (5.18) can then be rewritten as:

$$\bar{D}'_i(q) + \bar{D}'_f(q) \geq 0 \qquad \forall q \in [q_{min}, q_{max}] \tag{5.20}$$

where $\bar{D}_f(q)$ and $\bar{D}_i(q)$ denote respectively flexible and inflexible demand as a function of the measure q.

The next step is to understand if alternative profiles D could be broadcast in order to induce an equilibrium when condition (5.18) is violated. Namely, whether or not there exist other kinds of Nash equilibria, possibly under relaxed conditions and higher density of flexible demand. To this end, let us regard two broadcast profiles as equivalent if they induce (for almost all times) the same scheduling of flexible demand. The equivalence class $\mathcal{D}_i$ of the signal D_i can be characterized as in the definition below.

Definition 5.4. Let $\mathcal{D}_i$ denote the set of signals D_b for which the following conditions are satisfied for almost all $t \in [0, T]$:

$$Q_{D_b}(D_b(t)) \leq q_{min} \qquad \text{if} \quad Q_{D_i}(D_i(t)) \leq q_{min} \tag{5.21a}$$

$$Q_{D_b}(D_b(t)) \geq q_{max} \qquad \text{if} \quad Q_{D_i}(D_i(t)) \geq q_{max} \tag{5.21b}$$

$$Q_{D_b}(D_b(t)) = Q_{D_i}(D_i(t)) \quad \text{if} \quad q_{min} \leq Q_{D_i}(D_i(t)) \leq q_{max} \tag{5.21c}$$

From Remark 5.2 and expressions (5.11) and (5.12) for the flexible demand, condition (5.21a) is equivalent to impose that time intervals for which the flexible demand equals

its maximum value $\int_{q_{min}}^{q_{max}} \frac{f'(\tau)}{\tau} d\tau$ when D_b and D_i are broadcast coincide up to sets of zero measure. Similarly, condition (5.21b) ensures that the intervals for which flexible demand is equal to zero when D_b and D_i are broadcast differ for sets of zero measure. Finally, condition (5.21c) imposes equality of the flexible demand at all other time instants.

It is now possible to verify that an equilibrium can be achieved only with broadcast signals D that belong to $\mathcal{D}_i$.

Theorem 5.2. *The Nash equilibrium condition (5.15) is satisfied for a broadcast profile $D = D_b$ which fulfils Assumption 5.2 if and only if $D_b \in \mathcal{D}_i$ and inequality (5.18) holds.*

Proof. It is straightforward to verify the sufficient part of the theorem by noticing that, if $D_b \in \mathcal{D}_i$, the aggregate demand D_{a,D_b} and the optimal power profile u^* obtained with the broadcast D_b are equal almost everywhere to the corresponding quantities obtained when the inflexible demand D_i is broadcast. For the necessary part of the theorem, it can be shown that, if any condition in (5.21) is violated on a set of positive measure, the power absorption profiles calculated according to D_b are not optimal for the resulting aggregate demand. In this respect, it is useful to define the following sets associated to an arbitrary profile D:

$$\mathcal{T}_{min_D} := \{t : Q_D(D(t)) \leq q_{min}\} \quad \mathcal{T}_{max_D} := \{t : Q_D(D(t)) \geq q_{max}\} \tag{5.22}$$

and calculate the corresponding measures:

$$\mu(\mathcal{T}_{min_D}) = q_{min} \qquad \mu(\mathcal{T}_{max_D}) = T - q_{max}$$

Alternatively, $\mathcal{D}_i$ can be defined as the set of broadcast profiles D_b which satisfy the following conditions:

$$\mu\left(\mathcal{T}_{min_{D_b}} \backslash \mathcal{T}_{min_{D_i}}\right) = 0 \tag{5.23a}$$

$$\mu\left(\mathcal{T}_{max_{D_b}} \backslash \mathcal{T}_{max_{D_i}}\right) = 0 \tag{5.23b}$$

$$Q_{D_b}(D_b(t)) = Q_{D_i}(D_i(t)) \qquad \forall\, t \in [0,T] \backslash (\mathcal{T}_{max_{D_i}} \cup \mathcal{T}_{min_{D_i}}) \tag{5.23c}$$

Assume now that (5.23a) does not hold. Since $\mu(\mathcal{T}_{min_{D_i}}) = \mu(\mathcal{T}_{min_{D_b}}) = q_{min}$, it is possible to define t_1 and t_2 such that:

$$
\begin{aligned}
t_1 \in \mathcal{T}_{min_{D_b}} \quad & t_1 \notin \mathcal{T}_{min_{D_i}} \\
t_2 \notin \mathcal{T}_{min_{D_b}} \quad & t_2 \in \mathcal{T}_{min_{D_i}}
\end{aligned}
\tag{5.24}
$$

This means that, for all $t_{min} \in [q_{min}, Q_{D_b}(D_b(t_2)))$, it holds:

$$t_1 \in \mathcal{S}_{D_b}(t_{min}) \qquad t_2 \notin \mathcal{S}_{D_b}(t_{min}) \tag{5.25}$$

It follows from (5.24) that $D_i(t_2) < D_i(t_1)$. Moreover, if one considers the expressions of flexible demand in (5.11) and (5.12), since in the present case $Q_{D_b}(D_b(t_1)) < Q_{D_b}(D_b(t_2))$, it holds $D_f(t_2) < D_f(t_1)$. The following inequality is therefore verified for the aggregate demand:

$$D_i(t_1) + D_f(t_1) > D_i(t_2) + D_f(t_2)$$

This means that the Nash equilibrium condition (5.17) is violated for $D = D_b$ and $t_{min} \in [q_{min}, Q_{D_b}(D_b(t_2)))$.

A similar approach is followed when (5.23b) is not verified, defining t_1 and t_2 such that:

$$\begin{aligned} t_1 \notin \mathcal{T}_{max_{D_b}} & \quad t_1 \in \mathcal{T}_{max_{D_i}} \\ t_2 \in \mathcal{T}_{max_{D_b}} & \quad t_2 \notin \mathcal{T}_{max_{D_i}} \end{aligned} \tag{5.26}$$

Thus, for all $t_{min} \in [Q_{D_b}(D_b(t_1)), q_{max}]$, it holds:

$$t_1 \in \mathcal{S}_{D_b}(t_{min}) \qquad t_2 \notin \mathcal{S}_{D_b}(t_{min}) \tag{5.27}$$

Considering that $D_i(t_1) > D_i(t_2)$ from (5.26) and $Q_{D_b}(D_b(t_1)) < Q_{D_b}(D_b(t_2))$, we also have $D_f(t_1) > D_f(t_2)$. For the aggregate demand at the two time instants, it holds:

$$D_i(t_1) + D_f(t_1) > D_i(t_2) + D_f(t_2)$$

We can conclude that the Nash equilibrium condition (5.17) is not verified for $D = D_b$ when $t_{min} \in [Q_{D_b}(D_b(t_1)), q_{max}]$. We finally analyze the case when (5.23a) and (5.23b) hold but (5.23c) is violated. This means that the sets $\mathcal{T}_{min_D}$ and $\mathcal{T}_{max_D}$ coincide up to sets of measure 0 for the profiles D_i and D_b. Moreover, it is possible to define the following:

$$\mathcal{T}_M = [0, T] \backslash (\mathcal{T}_{max_i} \cup \mathcal{T}_{min_i}) = [0, T] \backslash (\mathcal{T}_{max_b} \cup \mathcal{T}_{min_b})$$

It is assumed that there exists $t_2 \in \mathcal{T}_M$ such that it holds:

$$Q_{D_i}(D_i(t_2)) < Q_{D_b}(D_b(t_2))$$

The proof can be easily extended to the case when the opposite inequality is verified. The following sets are now introduced:

$$\begin{aligned} \mathcal{T}_{i_-} &:= \{t : Q_{D_i}(D_i(t)) \leq Q_{D_i}(D_i(t_2)), \ t \in \mathcal{T}_M\} \\ \mathcal{T}_{b_-} &:= \{t : Q_{D_b}(D_b(t)) \leq Q_{D_b}(D_b(t_2)), \ t \in \mathcal{T}_M\} \end{aligned}$$

For the corresponding measures, it holds:

$$\mu(\mathcal{T}_{i_-}) = Q_{D_i}(D_i(t_2)) - q_{min} < Q_{D_b}(D_b(t_2)) - q_{min} = \mu(\mathcal{T}_{b_-})$$

Considering the assumptions on D_b, there exists $t_1 \in \mathcal{T}_{b_-} \backslash \mathcal{T}_{i_-}$ such that:

$$Q_{D_b}(D_b(t_1)) < Q_{D_b}(D_b(t_2)) \qquad Q_{D_i}(D_i(t_1)) > Q_{D_i}(D_i(t_2))$$

or equivalently:

$$D_b(t_1) < D_b(t_2) \qquad D_i(t_1) > D_i(t_2)$$

Notice now that, if the profile D_b is broadcast, for all $t_{min} \in [Q_{D_b}(t_1), Q_{D_b}(t_2))$ we have:

$$t_1 \in \mathcal{S}_{D_b}(t_{min}) \qquad t_2 \notin \mathcal{S}_{D_b}(t_{min})$$

This implies that $D_f(t_1) > D_f(t_2)$ and therefore the following holds for the aggregate demand:

$$D_i(t_1) + D_f(t_1) > D_i(t_2) + D_f(t_2) \tag{5.28}$$

We can conclude that in this case the equilibrium condition (5.17) with $D = D_b$ is violated for $t_{min} \in [Q_{D_b}(t_1), Q_{D_b}(t_2))$. $\qquad\qquad\qquad\square$

Theorem 5.1 and 5.2 provide (respectively) sufficient and necessary conditions for the existence of a Nash equilibrium in the sense described by (5.15): any broadcast profile in the set $\mathcal{D}_i$ will induce an equilibrium for the resulting aggregate demand if and only if the inequality (5.18) between negotiable valley capacity Λ_{D_i} and power density of task durations Λ_f holds. If this is not the case it is shown that, for all the other profiles $D \notin \mathcal{D}_i$ which fulfill Assumption 5.2, condition (5.15) is never satisfied.

5.4   Nash Equilibria through Saturated Flexible Demand

The possibility to extend the equilibrium conditions presented in the previous section is now investigated. When (5.18) does not hold the sublevel sets of the broadcast profile and of the resulting aggregate demand do not correspond. This means that the power absorption of the flexible appliances introduces peaks in the aggregate profile at time instants when the broadcast demand is particularly low (and therefore energy is considered cheap). The resulting high energy prices at such peaks make the original scheduled profiles suboptimal for the aggregate demand and prevent the existence of a Nash equilibrium. To avoid this and limit, at critical time instants, the demand variation introduced by the flexible appliances, we consider an additional constraint on

their maximum power absorption. For this purpose, the function $\alpha : [0, T] \rightarrow [0, 1]$ is introduced, defining a time-varying proportional constraint (equal for all the appliances) on the power u. For devices with minimum task time t_{min} and total energy E_{tot}, it must hold:

$$0 \leq u(t) \leq \alpha(t) \cdot \frac{E_{tot}}{t_{min}} \qquad \forall t \in [0, T] \tag{5.29}$$

With this formulation the maximum power of the devices is a fraction of the rated power $P_r = E_{tot}/t_{min}$. It is assumed that equal values of α correspond to equal values of broadcast demand D and therefore it is possible to define the proportional constraint as a function $\bar{\alpha}(q)$ of the measure q with $\alpha(t) = \bar{\alpha}(Q_D(D(t)))$. The main idea is to design $\bar{\alpha}$ in order to modify the global behaviour of the appliances population, shaping the profile of a new power density of task durations $\bar{\Lambda}_f$ which satisfies the inequality $\bar{\Lambda}_f(q) \leq \Lambda_{D_i}(q)$ for all values of q.

5.4.1   Optimal Power Profile and Equilibrium Conditions

The optimization problem solved by the flexible appliances when a profile D is broadcast and proportional constraints are introduced becomes:

$$\begin{aligned} \min_{u(\cdot)} \quad & \int_0^T \Pi(D(t)) \cdot u(t)\, dt \\ \text{s. t} \quad & 0 \leq u(t) \leq \alpha(t) \frac{E_{tot}}{t_{min}} \\ & \int_0^T u(t)\, dt = E_{tot} \end{aligned} \tag{5.30}$$

The optimal power profile of the devices with $E_{tot} = x$ and $t_{min} = s$ can be defined as a function of the measure $q = Q_D(D(t))$:

$$\bar{u}^*(q, s, x) = \begin{cases} \bar{\alpha}(q)\dfrac{x}{s} & \text{if} \quad \displaystyle\int_0^q \bar{\alpha}(\tau)\, d\tau \leq s \\[4mm] 0 & \text{otherwise} \end{cases} \tag{5.31}$$

Notice in fact that, similarly to (5.9), each appliance will operate (at maximum feasible power) at the lowest values of q until the total required energy x has been obtained. It follows that power absorption will be scheduled at a certain q only if the following condition is satisfied:

$$\int_0^q \bar{u}^*(\tau, s, x)\, d\tau \leq x, \tag{5.32}$$

This can equivalently be rewritten as $\int_0^q \bar{\alpha}(\tau)\frac{x}{s}\, d\tau \leq x$ and ultimately as $\int_0^q \bar{\alpha}(\tau)\, d\tau \leq s$. The aggregate power density $\bar{g}$ consumed by the devices with $t_{min} = s$ can be calculated

as $\bar{g}(q, s) = \int_{\mathcal{E}} \bar{u}^*(q, s, x) m(s, x) \, dx$, deriving the following expression:

$$\bar{g}(q, s) = \begin{cases} \bar{\alpha}(q) \dfrac{f'(s)}{s} & \text{if} \quad \displaystyle\int_0^q \bar{\alpha}(\tau) \, d\tau \leq s \\[4mm] 0 & \text{otherwise} \end{cases} \tag{5.33}$$

If one denotes by $\bar{\alpha}_I(q) = \int_0^q \bar{\alpha}(\tau) \, d\tau$ the integral of the constraint function $\bar{\alpha}$, the flexible demand $\bar{D}_f(q)$ can be defined as:

$$\bar{D}_f(q) = \int_0^T \bar{g}(q, s) \, ds = \bar{\alpha}(q) \int_{\bar{\alpha}_I(q)}^T \frac{f'(s)}{s} \, ds \tag{5.34}$$

Remark 5.4. Like in the unconstrained case, the optimal power profile, aggregate power density and flexible demand as functions of time can be obtained by evaluating the corresponding expressions in the q variable at $q = Q_D(D(t))$, as shown in (5.12).

To verify that $u^*(t) = \bar{u}^*(Q_D(D(t)))$ guarantees the total amount of required energy and to determine in general an useful relationship between the time t and the measure $q = Q_D(D(t))$, the following result is provided:

Lemma 5.1. *For an integrable function $\bar{f} : [0, T] \to \mathbb{R}$ and a profile D which satisfies Assumption 5.2, the following equality is always verified:*

$$\int_0^T \bar{f}(q) \, dq = \int_0^T \bar{f}\left(Q_D(D(t))\right) \, dt \tag{5.35}$$

Proof. Introducing the function $\bar{Q}_D(t) = Q_D(D(t))$ and recalling that μ denotes the Lebesgue measure, (5.35) is equivalent to:

$$\int_{[0,T]} \bar{f} \, d\mu = \int_{[0,T]} \bar{f} \circ \bar{Q}_D \, d\mu \tag{5.36}$$

Applying standard properties [100] of the Lebesgue integral, the right hand side in (5.36) can be written as:

$$\int_{[0,T]} \bar{f} \circ \bar{Q}_D \, d\mu = \int_{[0,T]} \bar{f} d\left(\bar{Q}_D^* \mu\right) \tag{5.37}$$

where $\bar{Q}_D^* \mu$ denotes the pushforward measure of μ induced by $\bar{Q}_D$ and it is such that, for any measurable set E, it holds $\bar{Q}_D^* \mu(E) = \mu(\bar{Q}_D^{-1}(E))$. From (5.37), the lemma is verified if the measures $\bar{Q}_D^* \mu$ and μ are equal and the following holds for any measurable set E:

$$\mu(\bar{Q}_D^{-1}(E)) = \mu(E) \tag{5.38}$$

Such condition is initially verified for a closed interval $X = [0, x_R]$ with $x_R \leq T$. In this case the set $\bar{Q}_D^{-1}(X)$ has the following expression:

$$\bar{Q}_D^{-1}([0, x_R]) = \left\{t : \bar{Q}_D(t) \leq x_R\right\} = \left\{t : \mu\left(\{s : D(s) \leq D(t)\}\right) \leq x_R\right\}$$

Given the monotonicity properties of Q_D, there exists $\bar{D}$ such that $Q_D(\bar{D}) = x_R$ and therefore it holds $\bar{Q}_D^{-1}([0, x_R]) = \left\{t : D(t) \leq \bar{D}\right\}$. For the corresponding measure, taking into account the definition of $\bar{D}$, the following expression can be provided:

$$\mu\left(\bar{Q}_D^{-1}([0, x_R])\right) = x_R = \mu([0, x_R])$$

Similarly, considering Assumption 5.2, it is possible to verify that (5.38) holds and $\mu(\bar{Q}_D^{-1}(X)) = x_R - x_L = \mu(X)$ for any arbitrary closed interval $X = [x_L, x_R] \subseteq [0, T]$:

$$\mu(\bar{Q}_D^{-1}[x_L, x_R]) = \mu\left(\{t : \bar{Q}_D(t) \leq x_R\}\right) - \mu\left(\{t : \bar{Q}_D(t) \leq x_L\}\right) = x_R - x_L$$

The equivalency of the measures can be extended to any measurable set X by considering the Vitali covering theorem [101] which guarantees that for any set X there exists an at most countable set of disjoint closed intervals I_j such that $\mu\left(X \setminus \cup_j I_j\right) = 0$. □

Applying Lemma 5.1 for $\bar{f} = \bar{u}^*$ and considering (5.32), it is straightforward to show:

$$\int_0^T u^*(t, s, x)\, dt = \int_0^T \bar{u}^*(Q_D(D(t)), s, x)\, dt = \int_0^T \bar{u}^*(q, s, x)\, dq = x$$

We are now interested in determining which constraint functions $\bar{\alpha}(\cdot)$ induce an equilibrium in the system when D_i is broadcast. The equilibrium condition is similar to the one presented in (5.15) and must hold for all $E_{tot} = x \in \mathcal{E}$ and $t_{min} = s \in [q_{min}, q_{max}]$:

$$\int_0^T \Pi(D_{a, D_i}(t)) u^*(t, s, x)\, dt = \min_{u(\cdot)} \int_0^T \Pi(D_{a, D_i}(t)) u(t)\, dt \tag{5.39}$$
$$\text{s. t. } 0 \leq u(t) \leq \alpha(t)\frac{x}{s}$$
$$\int_0^T u(t)\, dt = x$$

As in the unconstrained case, the aggregate demand $D_{a, D_i}(t) = D_i(t) + \bar{D}_f\left(Q_{D_i}(D_i(t))\right)$ obtained when D_i is broadcast can be defined as a function of the current broadcast demand value $d = D_i(t)$:

$$\begin{aligned} D_{a, D_i}(t) &= K(d) = d + \bar{D}_f(Q_{D_i}(d)) \\ &= d + \bar{\alpha}(Q_{D_i}(d)) \int_{\bar{\alpha}_I(Q_{D_i}(d))}^T \frac{f'(s)}{s}\, ds \end{aligned} \tag{5.40}$$

Similarly to what has been presented in the previous section, it is possible to provide conditions in the variable q for which (5.39) is satisfied.

Proposition 5.1. *For any integrable constraint function $\bar{\alpha}(\cdot)$ taking values in $[0, 1]$ and any broadcast demand $D = D_i$, the equilibrium condition (5.39) holds if:*

$$\bar{D}'_f(q) + \bar{D}'_i(q) \geq 0 \tag{5.41}$$

where $\bar{D}_f(q)$ and $\bar{D}_i(q)$ denote respectively flexible and inflexible demand as a function of the measure $q = Q_{D_i}(D_i(t))$ with $\bar{D}_i(Q_{D_i}(D_i(t))) = D_i(t)$, while primes denote derivation with respect to the argument q.

Proof. The interval of power consumption for devices with minimum time parameter t_{min}, when D_i is broadcast, can be defined as follows:

$$\mathcal{S}_{D_i}(t_{min}) = \{t : \bar{\alpha}_I(Q_{D_i}(D_i(t))) \leq t_{min}\} \tag{5.42}$$

Similarly to (5.17), the equilibrium condition (5.39) is verified if and only if the following holds for all $t_{min} \in \text{supp}(f')$:

$$D_{a,D_i}(t_1) \leq D_{a,D_i}(t_2) \quad \forall t_1 \in \mathcal{S}_{D_i}(t_{min}) \quad \forall t_2 \in [0, T] \backslash \mathcal{S}_{D_i}(t_{min}) \tag{5.43}$$

Notice now that the integral $\bar{\alpha}_I(q)$ is a monotonic increasing function since $\bar{\alpha}(q) \geq 0$. Given that $Q_{D_i}(d)$ has the same monotonicity properties and considering definition (5.42) of $\mathcal{S}_{D_i}(t_{min})$, for the values of inflexible demand at the time instants t_1 and t_2 considered above it holds $d_1 = D_i(t_1) \leq D_i(t_2) = d_2$. Therefore the inequalities in (5.43) are verified if:

$$K(d_1) \leq K(d_2) \quad \forall d_1, d_2 \in [d_{min}, d_{max}] : d_1 \leq d_2$$

This is equivalent to impose nonnegativity of $K'(d)$:

$$K'(d) = 1 + \bar{D}'_f(Q_{D_i}(d))Q'_{D_i}(d) \geq 0$$

Dividing both terms of the inequality by $Q'_{D_i}(d)$ and letting q denote $Q_{D_i}(d)$ yields:

$$0 \leq \left(\frac{d}{dq} Q_{D_i}^{-1}(q) \right) + \bar{D}'_f(q) = \bar{D}'_i(q) + \bar{D}'_f(q)$$

$\square$

5.4.2   Shaping of Power Density of Task Durations

The design of a constraint function $\bar{\alpha}$ which satisfies (5.41) is nontrivial since the relationship between $\bar{D}'_f$ and $\bar{\alpha}$ is not instantaneous:

$$\bar{D}'_f(q) = \bar{\alpha}'(q) \int_{\bar{\alpha}_I(q)}^{T} \frac{f'(s)}{s}\, ds - \bar{\alpha}^2(q) \frac{f'(\bar{\alpha}_I(q))}{\bar{\alpha}_I(q)}$$

For this reason, a desired profile of flexible demand that satisfies condition (5.41) will be initially calculated, deriving only as a second step the function $\bar{\alpha}$ needed to generate such profile. In particular, an additional function $\bar{F} : [0, T] \to \mathbb{R}^+$ and a reference $\bar{D}_r$ for the flexible demand are introduced with:

$$\bar{D}_r(q) = \int_{q}^{T} \bar{F}(\tau)\, d\tau \tag{5.44}$$

For a given function $\bar{F}(\cdot)$, it is possible to define the following dynamical system with states $\bar{\alpha}_I$ and $\bar{F}_I$:

$$\dot{\bar{\alpha}}_I(q) = \bar{\alpha}(q) = \frac{\int_{q}^{T} \bar{F}(\tau)\, d\tau}{\int_{\bar{\alpha}_I(q)}^{T} \frac{f'(\tau)}{\tau}\, d\tau} = \frac{F_{tot} - \bar{F}_I(q)}{\int_{\bar{\alpha}_I(q)}^{T} \frac{f'(\tau)}{\tau}\, d\tau} \qquad \bar{\alpha}_I(0) = 0$$

$$\dot{\bar{F}}_I(q) = \bar{F}(q) \qquad\qquad\qquad\qquad\qquad\qquad \bar{F}_I(0) = 0 \tag{5.45}$$

where $F_{tot} = \bar{F}_I(T) = \int_0^T \bar{F}(\tau)\, d\tau$ denotes the integral of $\bar{F}$ over the interval $[0, T]$. Given a feasible control profile $\bar{F}(\cdot)$, the unique solution of (5.45) will be denoted by $(\bar{\varphi}_\alpha(\cdot), \bar{\varphi}_F(\cdot))$. The definition of the derivative $\dot{\bar{\alpha}}_I(q)$ guarantees that the resulting flexible demand $\bar{D}_f$, defined in (5.34), is equal to $\bar{D}_r$. Furthermore, for $\bar{D}_f = \bar{D}_r$, the equilibrium condition (5.41) becomes:

$$\bar{D}'_i(q) \geq \bar{F}(q) \tag{5.46}$$

An alternative interpretation of (5.46) can be provided if one considers the power density of task durations Λ_f and the negotiable valley capacity Λ_{D_i} in the constrained case. Since it is not possible to modify Λ_{D_i}, which depends exclusively on the inflexible demand profile, the function F can be determined in order to change the behaviour of the appliances population and properly shape a new power density $\bar{\Lambda}_f$. In fact, if one imposes $\bar{D}_f = \bar{D}_r$ by choosing $\bar{\alpha}$ according to (5.45) and considers the results of Remark 5.3, condition (5.46) becomes:

$$\Lambda_{D_i}(q) = \bar{D}'_i(q) \geq \bar{F}(q) = -\bar{D}'_f(q) = \bar{\Lambda}_f(q)$$

This allows, rather than directly calculating $\bar{\alpha}$, to determine $\bar{F}(q)$ which satisfies (5.46) (and therefore guarantees an equilibrium) while obtaining the corresponding $\bar{\alpha}$ through

(5.45). In this respect, an additional constraint must be taken into account. Since $\bar{\alpha}(q)$ represents a proportional reduction in the maximum power of the devices, a certain state $(\bar{\alpha}_I(q), \bar{F}_I(q))$ will be feasible only if:

$$0 \leq \bar{\alpha}(q) = \frac{F_{tot} - \bar{F}_I(q)}{\int_{\bar{\alpha}_I(q)}^{T} \frac{f'(\tau)}{\tau} \, d\tau} \leq 1$$

When determining $\bar{F}$ we do not only seek to satisfy the equilibrium condition (5.46) but we also aim at optimizing some global properties of the system. In particular we are interested in minimizing the total time required by the appliances to perform their tasks. It will be shown later on that this minimization guarantees optimality properties for each single device and for some other global cost functions. Notice now that the time $\Gamma(t_{min})$ required by devices with parameter t_{min} to complete their task is equal to $\mu\left(\mathcal{S}_{D_i}(t_{min})\right)$. Considering definition (5.42) and the monotonicity of $\bar{\alpha}_I$, the following expression can be provided:

$$\Gamma(t_{min}) = \min_{q} \left\{ q : \bar{\alpha}_I(q) \geq t_{min} \right\} \tag{5.47}$$

Taking into account that $\mu\left(\mathcal{S}_{D_i}(t_{min_1})\right) \leq \mu\left(\mathcal{S}_{D_i}(t_{min_2})\right)$ if $t_{min_1} \leq t_{min_2}$, the total task duration corresponds to the one of the devices with $t_{min} = q_{max}$. The optimization problem can finally be defined as the minimization of $\Gamma(q_{max})$ or, alternatively:

$$
\begin{aligned}
\min_{\bar{F}(\cdot), F_{tot}} \quad & T_{END} \\
\text{s.t.} \quad & \bar{\alpha}_I(T_{END}) = q_{max} \qquad \bar{F}_I(T_{END}) = F_{tot} \\
& \dot{\bar{\alpha}}_I(q) = \frac{F_{tot} - \bar{F}_I(q)}{\int_{\bar{\alpha}_I(q)}^{T} \frac{f'(\tau)}{\tau} \, d\tau} \quad \dot{\bar{F}}_I(q) = \bar{F}(q) \\
& \bar{\alpha}_I(0) = 0 \qquad\qquad \bar{F}_I(0) = 0 \\
& 0 \leq \dot{\bar{\alpha}}_I(q) \leq 1 \qquad \bar{F}(q) \leq \bar{D}_i'(q)
\end{aligned}
\tag{5.48}
$$

Remark 5.5. Once the minimization problem has been solved, it is straightforward to obtain the corresponding values of α in the time variable t with $\alpha(t) = \bar{\alpha}(Q_{D_i}(D_i(t)))$. Since all devices complete their task for $q \leq T_{END}$ the values of $\bar{\alpha}(q)$ can be defined arbitrarily (for example equal to 1) when $q > T_{END}$.

5.4.3 Backward-integrated Dynamical System

One of the main challenges in the resolution of (5.48) is that the final value F_{tot} of the state $\bar{F}_I$, not known a priori, appears in the dynamics of $\bar{\alpha}_I(q)$. For this reason a different system is introduced in order to model the same dynamics of (5.45) in the opposite direction of integration. It will be shown that, for certain conditions on the

final state, the solutions of the two systems coincide and therefore it is possible to solve the optimization problem (5.48) without directly operating on (5.45). The new system is described by the following equations:

$$\dot{\tilde{\alpha}}_I^\epsilon(q) = \frac{\tilde{F}_I^\epsilon(q)}{\int_{q_{max}-\tilde{\alpha}_I^\epsilon(q)}^{q_{max}} \frac{f'(\tau)}{\tau} d\tau} = \frac{\tilde{F}_I^\epsilon(q)}{h(\tilde{\alpha}_I^\epsilon(q))} \qquad \tilde{\alpha}_I^\epsilon(0) = \epsilon$$

$$\dot{\tilde{F}}_I^\epsilon(q) = \tilde{F}(q) \qquad\qquad\qquad\qquad \tilde{F}_I^\epsilon(0) = 0$$

(5.49)

where the function $h(x) = \int_{q_{max}-x}^{q_{max}} \frac{f'(\tau)}{\tau} d\tau$ is used for a more compact expression of $\dot{\tilde{\alpha}}_I^\epsilon$. Notice that (5.49) defines a family of Cauchy problems parametrized by the initial condition ϵ of one of the state variables. Fixed a control profile $\tilde{F}(\cdot)$, the unique solution of (5.49) will be denoted by $(\tilde{\varphi}_\alpha^\epsilon(\cdot), \tilde{\varphi}_F^\epsilon(\cdot))$. Taking into account that the expression for $\dot{\tilde{\alpha}}_I^\epsilon$ is not well defined when $\left(\tilde{\alpha}_I^0(0), \tilde{F}_I^0(0)\right) = (0,0)$, we will consider decreasing values of ϵ, denoting by $(\tilde{\varphi}_\alpha(\cdot), \tilde{\varphi}_F(\cdot))$ the limit of solutions of (5.49) for ϵ which tends to zero. Such a limit exists and is unique as equation (5.49) defines a cooperative system (monotonicity with respect to initial conditions).

In order to show the relationship between solutions of (5.49) and (5.45), the function $\tilde{\varphi}_I^\epsilon$, representing the integral over q of the solution $\tilde{\varphi}_F^\epsilon$, is calculated:

$$\tilde{\varphi}_I^\epsilon(q) = \int_0^q \tilde{\varphi}_F^\epsilon(\tau) d\tau = \int_0^q \dot{\tilde{\varphi}}_\alpha^\epsilon(\tau) h(\tilde{\varphi}_\alpha^\epsilon(\tau)) d\tau = [\tilde{\varphi}_\alpha^\epsilon(\tau) h(\tilde{\varphi}_\alpha^\epsilon(\tau))]_0^q - \int_0^q \tilde{\varphi}_\alpha^\epsilon(\tau) h'(\tilde{\varphi}_\alpha^\epsilon(\tau)) d\tau$$

$$= [\tilde{\varphi}_\alpha^\epsilon(q) h(\tilde{\varphi}_\alpha^\epsilon(q)) - \epsilon h(\epsilon)] - \int_{g(\tilde{\varphi}_\alpha^\epsilon(q))}^{g(\epsilon)} g(\bar\tau) \frac{f'(\bar\tau)}{\bar\tau} d\bar\tau$$

$$= [\tilde{\varphi}_\alpha^\epsilon(q) - q_{max}] \int_{g(\tilde{\varphi}_\alpha^\epsilon(q))}^{g(\epsilon)} \frac{f'(\tau)}{\tau} d\tau + [\tilde{\varphi}_\alpha^\epsilon(q) - \epsilon] h(\epsilon) + \int_{g(\tilde{\varphi}_\alpha^\epsilon(q))}^{g(\epsilon)} f'(\tau) d\tau$$

(5.50)

where $g(x) = q_{max} - x$ and $\bar\tau = q_{max} - \tilde{\varphi}_\alpha^\epsilon(\tau)$ denotes a change of variable in the integral. When ϵ tends to zero the corresponding integral $\tilde{\varphi}_I^\epsilon(q)$ will have the following expression:

$$\tilde{\varphi}_I(q) = \lim_{\epsilon \to 0} \tilde{\varphi}_I^\epsilon(q) = [\tilde{\varphi}_\alpha(q) - q_{max}] \int_{q_{max}-\tilde{\varphi}_\alpha(q)}^{q_{max}} \frac{f'(\tau)}{\tau} d\tau + \int_{q_{max}-\tilde{\varphi}_\alpha(q)}^{q_{max}} f'(\tau) d\tau \quad (5.51)$$

It is now possible to provide a first result for the state trajectories of the discussed dynamical systems:

Proposition 5.2. *Consider any $\bar{F}(\cdot)$ defined on $[0, \tilde{T}]$, $\tilde{T} > 0$, which is feasible for (5.45) and such that, for the corresponding solution $(\bar\varphi_\alpha(\cdot), \bar\varphi_F(\cdot))$, it holds:*

$$\bar\varphi_\alpha(\tilde{T}) = q_{max} \qquad \bar\varphi_F(\tilde{T}) = F_{tot} \tag{5.52}$$

Denote now by $\tilde{F}(\cdot)$ the control input of system (5.49) defined by $\tilde{F}(q) = \bar{F}(\tilde{T} - q)$ for all $q \in [0, \tilde{T}]$. For the corresponding limiting solution $(\tilde{\varphi}_\alpha(\cdot), \tilde{\varphi}_F(\cdot))$ it holds:

$$\bar{\varphi}_\alpha(\tilde{T} - q) = q_{max} - \tilde{\varphi}_\alpha(q) \qquad \bar{\varphi}_F(\tilde{T} - q) = F_{tot} - \tilde{\varphi}_F(q) \tag{5.53}$$

Proof. The equality is straightforward for the states $\bar{\varphi}_F$ and $\tilde{\varphi}_F$:

$$
\begin{aligned}
\bar{\varphi}_F(\tilde{T} - q) &= \int_0^{\tilde{T}-q} \bar{F}(\tau)\,d\tau = F_{tot} - \int_{\tilde{T}-q}^{\tilde{T}} \bar{F}(\tau)\,d\tau = F_{tot} - \int_0^q \bar{F}(T - \bar{\tau})\,d\bar{\tau} \\
&= F_{tot} - \int_0^q \tilde{F}(\bar{\tau})\,d\bar{\tau} = F_{tot} - \tilde{\varphi}_F(q)
\end{aligned}
\tag{5.54}
$$

For the condition on the states $\bar{\varphi}_\alpha$ and $\tilde{\varphi}_\alpha$, the integral $\tilde{\varphi}_I(q)$ is evaluated. Considering (5.54) and the system equations (5.45) yields:

$$
\begin{aligned}
\tilde{\varphi}_I(q) &= \int_0^q \tilde{\varphi}_F(\tau)\,d\tau = \int_0^q F_{tot} - \bar{\varphi}_F(\tilde{T} - \tau)\,d\tau \\
&= \int_0^q \left[\dot{\bar{\varphi}}_\alpha(\tilde{T} - \tau) \int_{\bar{\varphi}_\alpha(\tilde{T}-\tau)}^{q_{max}} \frac{f'(s)}{s}\,ds \right] d\tau = \int_{\tilde{T}-q}^{\tilde{T}} \left[\dot{\bar{\varphi}}_\alpha(\bar{\tau}) \int_{\bar{\varphi}_\alpha(\bar{\tau})}^{q_{max}} \frac{f'(s)}{s}\,ds \right] d\bar{\tau}
\end{aligned}
$$

With algebraic steps similar to (5.50), the following expression can now be provided:

$$\tilde{\varphi}_I(q) = -\bar{\varphi}_\alpha(\tilde{T} - q) \int_{\bar{\varphi}_\alpha(\tilde{T}-q)}^{q_{max}} \frac{f'(\tau)}{\tau}\,d\tau + \int_{\bar{\varphi}_\alpha(\tilde{T}-q)}^{\bar{\varphi}_\alpha(\tilde{T})} f'(\tau)\,d\tau \tag{5.55}$$

The proof is concluded by noticing that $\tilde{\varphi}_I(q)$ as defined in (5.51) is a monotonic increasing function of $\tilde{\varphi}_\alpha(q)$ and therefore, considering that $\bar{\varphi}_\alpha(\tilde{T}) = q_{max}$, the two expressions (5.51) and (5.55) are equal if and only if $\bar{\varphi}_\alpha(\tilde{T} - q) = q_{max} - \tilde{\varphi}_\alpha(q)$. □

Similar results can be provided if one considers the correspondence between the two systems in the opposite direction:

Proposition 5.3. *Consider any $\tilde{F}(\cdot)$ defined on $[0, \tilde{T}]$ which is feasible for (5.49) and such that the corresponding solution $(\tilde{\varphi}_\alpha(\cdot), \tilde{\varphi}_F(\cdot))$ when ϵ tends to zero satisfies the following conditions:*

$$\tilde{\varphi}_\alpha(\tilde{T}) = q_{max} \qquad \tilde{\varphi}_F(\tilde{T}) = F_{tot} \tag{5.56}$$

If one denotes by $\bar{F}$ the control profile of system (5.45) such that $\bar{F}(q) = \tilde{F}(\tilde{T} - q)$ for all $q \in [0, \tilde{T}]$, it holds:

$$\tilde{\varphi}_\alpha(\tilde{T} - q) = q_{max} - \bar{\varphi}_\alpha(q) \qquad \tilde{\varphi}_F(\tilde{T} - q) = F_{tot} - \bar{\varphi}_F(q) \tag{5.57}$$

Proof. The equality for the states $\bar{\varphi}_F$ and $\tilde{\varphi}_F$ can be verified as follows:

$$
\begin{aligned}
\tilde{\varphi}_F(\tilde{T} - q) &= \int_0^{\tilde{T}-q} \tilde{F}(\tau)\,d\tau = F_{tot} - \int_{\tilde{T}-q}^{\tilde{T}} \tilde{F}(\tau)\,d\tau \\
&= F_{tot} - \int_0^q \tilde{F}(\tilde{T} - \tau)\,d\tau = F_{tot} - \bar{\varphi}_F(q)
\end{aligned}
$$

To check that also the first equation in (5.57) holds, the integral $\bar{\varphi}_I(q)$ is evaluated in two different ways:

$$
\bar{\varphi}_I(q) = \int_0^q F_{tot} - \bar{\varphi}_F(\tau)\,d\tau \qquad \bar{\varphi}_I(q) = \int_0^q \tilde{\varphi}_F(\tilde{T} - \tau)\,d\tau
$$

With algebraic steps similar to the ones used in the previous proof it is possible to show that the two expressions are equal if and only if $\tilde{\varphi}_\alpha(\tilde{T} - q) = q_{max} - \bar{\varphi}_\alpha(q)$. $\qquad \square$

The results of Proposition 5.2 and 5.3 determine the correspondence between the state trajectories of the dynamical systems introduced so far if certain conditions are verified for the states at the final time $\tilde{T}$. In the next subsection an optimization will be performed on the states of (5.49), using the equivalent for system (5.45) of the resulting optimal control to solve the time minimization problem (5.48) and induce a Nash equilibrium. The choice to operate on system (5.49) is motivated not only by the dependency of $\dot{\bar{\alpha}}_I$ in the original system (5.45) from the final state F_{tot} but also by its monotonicity properties:

Proposition 5.4. *The dynamical system described by (5.49) is cooperative.*

Proof. To show this, it is sufficient to consider the sign of the following partial derivatives:

$$
\begin{aligned}
\frac{\partial \dot{\tilde{\alpha}}_I^\epsilon}{\partial \tilde{F}_I^\epsilon} &= \frac{1}{h\left(\tilde{\alpha}_I^\epsilon\right)} \geq 0 & \frac{\partial \dot{\tilde{F}}_I^\epsilon}{\partial \tilde{\alpha}_I^\epsilon} &= 0 \\
\frac{\partial \dot{\tilde{\alpha}}_I^\epsilon}{\partial \tilde{F}} &= 0 & \frac{\partial \dot{\tilde{F}}_I^\epsilon}{\partial \tilde{F}} &= 1 > 0
\end{aligned}
\tag{5.58}
$$

$\qquad \square$

5.4.4 Task-time Minimizing Solution

The sets of admissible states $\left(\tilde{\alpha}_I^\epsilon, \tilde{F}_I^\epsilon\right)$ and controls $\tilde{F}(\cdot)$ for system (5.49), respectively $\mathcal{X}$ and $\mathcal{U}_{\tilde{T}}$, are defined as follows:

$$
\begin{aligned}
\mathcal{X} &= \left\{ \left(\tilde{\alpha}_I^\epsilon, \tilde{F}_I^\epsilon\right) : \tilde{F}_I^\epsilon \leq h\left(\tilde{\alpha}_I^\epsilon\right) \right\} \\
\mathcal{U}_{\tilde{T}} &= \{\tilde{F}(\cdot) : \tilde{F}(q) \in \left[0, \bar{D}_i'(\tilde{T} - q)\right] \; \forall q \in [0, \tilde{T}]\}
\end{aligned}
\tag{5.59}
$$

Given the monotonicity of (5.49), it is possible to maximize its state components by applying, at each q, the maximum feasible control. Each value of $\tilde{T}$ induces a corresponding maximizing solution. With the proper choice of the parameter $\tilde{T}$, it is then possible to satisfy (5.56) and apply Proposition 5.3, extending the same result to the forward system (5.45) and allowing to solve the original optimization problem (5.48). In order to so, the following feedback law as a function of q and current states $\tilde{\alpha}_I$ and $\tilde{F}_I$ is introduced:

$$\tilde{F}^*(q, \tilde{\alpha}_I, \tilde{F}_I) = \begin{cases} \bar{D}'_i(\tilde{T} - q) & \text{if } \tilde{F}_I < h(\tilde{\alpha}_I) \\ \\ \min\left(\bar{D}'_i(\tilde{T} - q), h'(\alpha_I)\right) & \text{if } \tilde{F}_I = h(\tilde{\alpha}_I) \end{cases} \tag{5.60}$$

We denote by $\Phi^{\tilde{T}}(x_0, q)$ the solution of (5.49) at 'time' q and from initial state x_0 $(q = 0)$ when the (time-varying and discontinuous) feedback law $\tilde{F}^*$ is applied. Subscripts F and α will be used to refer to the corresponding single state components. Define next the value function γ^ϵ of the following optimization problem:

$$\gamma^\epsilon(\tilde{T}) := \max_{\tilde{F}(\cdot) \in \mathcal{U}_{\tilde{T}}} \tilde{\alpha}^\epsilon_I(\tilde{T}) \tag{5.61}$$

Considering the monotonicity of the system and the fact that $\tilde{F}^*$ represents the maximum feasible control at any time instant and current state, for any $\tilde{T} \geq 0$ we have:

$$\gamma^\epsilon(\tilde{T}) = \Phi^{\tilde{T}}_\alpha([\epsilon, 0], \tilde{T}) \tag{5.62}$$

The next result introduces important properties of the above value function.

Proposition 5.5. *The function $\gamma^\epsilon(\tilde{T})$ is Lipschitz continuous and monotonically increasing.*

Proof. For any $T_1, T_2 \in [0, T]$ with $T_1 < T_2$, the maximum $\gamma^\epsilon(T_2)$ has the following expression:

$$\gamma^\epsilon(T_2) = \Phi^{T_2}_\alpha([\epsilon, 0], T_2) = \Phi^{T_1}_\alpha\left(\Phi^{T_2}([\epsilon, 0], T_2 - T_1), T_1\right). \tag{5.63}$$

To see this, it is sufficient to consider that the only dependency of $\Phi^{\tilde{T}}$ from the parameter $\tilde{T}$ is given by the maximum value $\bar{D}'_i(\tilde{T} - q)$ imposed for $\tilde{F}^*$ at each q. To prove the Lipschitz continuity of γ^ϵ, the following inequalities are considered for $|\gamma^\epsilon(T_2) - \gamma^\epsilon(T_1)|$:

$$\left|\Phi^{T_1}_\alpha\left(\Phi^{T_2}([\epsilon, 0], T_2 - T_1), T_1\right) - \Phi^{T_1}_\alpha([\epsilon, 0], T_1)\right|$$

$$\leq \left\|\Phi^{T_1}\left(\Phi^{T_2}([\epsilon, 0], T_2 - T_1), T_1\right) - \Phi^{T_1}([\epsilon, 0], T_1)\right\|_1 \tag{5.64}$$

$$\leq K_1 \left\|\Phi^{T_2}([\epsilon, 0], T_2 - T_1) - [\epsilon, 0]\right\|_1 \leq K_1 K_2 |T_2 - T_1|$$

where K_1 and K_2 are positive constants. The second inequality in (5.64) derives from the continuous differentiability of the solutions of (5.49) with respect to the initial conditions [102]. This can be verified by replacing $\tilde{F}^*$ in the expressions of (5.49) and noticing that the partial derivatives of the result with respect to each state component exist and are continuous (almost everywhere). The last inequality is a result of the boundedness of the state derivatives. For the monotonicity of the function γ^ϵ, it is sufficient to consider that for any $T_1, T_2 \in [0, T]$ with $T_2 > T_1$, following Proposition 5.4, it holds:

$$\Phi_\alpha^{T_1}\left(\Phi^{T_2}\left([\epsilon, 0], T_2 - T_1\right), T_1\right) \geq \Phi_\alpha^{T_1}\left([\epsilon, 0], T_1\right)$$

where the two sides of the inequality denote respectively $\gamma^\epsilon(T_2)$ and $\gamma^\epsilon(T_1)$ as shown in (5.62) and (5.63). $\qquad\square$

Given the properties of $\gamma^\epsilon(\tilde{T})$ introduced in the previous proposition and denoting by $\gamma(\tilde{T})$ the corresponding function when ϵ tends to 0, it is possible to provide the main result of this section, describing the solution of the optimization problem introduced in (5.48):

Theorem 5.3. *If problem (5.48) is feasible, there exists T^* defined as the minimum t such that $\gamma(t) = q_{max}$. Denote now by $\tilde{\psi}^*(q)$ the following signal:*

$$\tilde{\psi}^*(q) = \lim_{\epsilon \to 0} \tilde{F}^*\left(q, \Phi^{T^*}\left([\epsilon, 0], q\right)\right). \tag{5.65}$$

The control $\bar{F}^*$ defined below is feasible and optimal for (5.48):

$$\bar{F}^*(q) = \tilde{\psi}^*(T^* - q) \quad \forall q \in [0, T^*] \tag{5.66}$$

Proof. The existence of T^* is initially shown. In this respect, consider an arbitrary feasible control $\bar{F}$ for (5.48) such that, for the corresponding state trajectory of system (5.45), it holds $\bar{\varphi}_\alpha(T_{END}) = q_{max}$ at some $T_{END} \in [0, T]$. Applying the results of Proposition 5.2 for $\tilde{T} = T_{END}$, it is possible to define $\tilde{F}$ such that for the resulting limiting solution of (5.49), considering (5.53) at $q = \tilde{T} = T_{END}$, we have $\tilde{\varphi}_\alpha(T_{END}) = q_{max}$. Given the optimality of $\tilde{F}^*$ for the value function γ^ϵ defined in (5.61), we can conclude that $\gamma(T_{END}) \geq q_{max}$. It follows from the continuity and monotonicity of γ presented in Proposition 5.5 that there exists T^* as defined in the theorem statement. We show now that $\bar{F}^*$ in (5.66) is feasible for (5.48). Denoting by $\tilde{\varphi}^*$ the limiting solution of system (5.49) when $\tilde{\psi}^*$ is applied and ϵ tends to zero, considering (5.59) and definition (5.60) of $\tilde{F}^*$, we have:

$$\tilde{\psi}^*(q) \leq \bar{D}_i'(T^* - q) \qquad \frac{\tilde{\varphi}_F^*(q)}{h(\tilde{\varphi}_\alpha^*(q))} \leq 1 \qquad \forall q \in (0, T^*]$$

Given the results of Proposition 5.3 for the solution $\bar{\varphi}^*$ of system (5.45) when $\bar{F}^*$ is applied, the following holds at any $q \in [0, T^*)$:

$$\bar{F}^*(q) = \tilde{\psi}^*(T^* - q) \leq \bar{D}'_i(q) \qquad 0 \leq \dot{\bar{\varphi}}^*_\alpha(q) = \frac{F_{tot} - \bar{\varphi}^*_F(q)}{\int_{\bar{\varphi}^*_\alpha(q)}^{q_{max}} \frac{f'(\tau)}{\tau} d\tau} = \frac{\tilde{\varphi}^*_F(T^* - q)}{h(\tilde{\varphi}^*_\alpha(T^* - q))} \leq 1$$

Finally, to show the optimality of $\bar{F}^*$, we assume that there exists a control input $\bar{F}^\diamond$ which is feasible for (5.48) and such that, for the corresponding state trajectory $\bar{\varphi}$, it holds $\bar{\varphi}_\alpha(T^\diamond) = q_{max}$ with $T^\diamond < T^*$. If this were the case, it would be possible to define the corresponding control $\tilde{F}^\diamond$ for system (5.49) using the results of Proposition 5.2. For the same reasons detailed above for the final instant T_{END}, it would yield $\gamma(T^\diamond) \geq q_{max}$ with $T^\diamond < T^*$ which contradicts the definition of T^*. $\qquad\square$

From Theorem 5.3 we can conclude that the task-time minimizing profile of flexible demand in the q variable $\bar{D}_f(q)$ (and the function $\bar{\alpha}(q)$ that induces it when broadcast to the devices) can be calculated operating "backward". In particular, fixed a certain final instant T_{END} where we assume $\bar{D}_f(T_{END}) = 0$, the maximum increase $\tilde{F}(q)$ of flexible demand for decreasing values of q is calculated. Notice that two constraints must be taken into account when doing so: by imposing $\tilde{F}(q) = \bar{F}(T_{END} - q) \leq \bar{D}'_i(q)$ the equilibrium condition for the resulting aggregate demand profile is satisfied. Furthermore, it must be verified that the reference $\bar{D}_r$ for flexible demand is lesser or equal than the aggregate power that can be absorbed by the appliances population. At each q, taking into account the previous values of $\tilde{\alpha}$ through the integral $\tilde{\alpha}_I$, it must hold:

$$\tilde{F}_I(q) \leq \int_{q_{max}-\tilde{\alpha}_I(q)}^{q_{max}} \frac{f'(\tau)}{\tau} d\tau$$

For a certain final time instant ($T_{END} = T^*$ in the theorem statement), the allocation of flexible demand performed for decreasing q will be completed at $q = 0$. In this case the values of $\bar{F}$, considered for increasing q by setting $\bar{F}(q) = \tilde{F}(T_{END} - q)$, are optimal for problem (5.48). Moreover, since $\dot{\tilde{\alpha}}_I = \bar{\alpha}$ has been set in order to guarantee $\bar{D}_f = \bar{D}_r$ as defined in (5.44), the expression for the flexible demand induced by the optimal solution of (5.48) is:

$$\bar{D}_f^* = \int_q^{T^*} \bar{F}^*(s) \, ds \tag{5.67}$$

5.5 Simulation Results

The equilibrium conditions and the design method of the proportional constraint α presented in the previous sections are now tested in simulations. A typical 24h UK demand profile is considered (blue trace in Fig. 5.1), with a time discretization step of

$\Delta t = 0.01h$. Denoting by D_i^k the value of inflexible demand at $t = k \cdot \Delta t$, the function $Q_{D_i}\left(D_i^k\right)$ is approximated as $\left|\mathcal{S}^k\right| \cdot \Delta t$ where $\mathcal{S}^k$ is defined as follows:

$$\mathcal{S}^k = \left\{ j : D_i^j \le D_i^k \right\}$$

In the first case study we consider a population of flexible appliances described by a function f that satisfies condition (5.18) in Theorem 5.1 for the given D_i. The total energy required by the devices amounts to $55GWh$ and the corresponding f' is a truncated gaussian with mean equal to $8.2h$. This choice can represent heterogeneous devices that have different power ratings, but it can also model scenarios with only one type of device where each appliance needs to perform tasks that require different amounts of time or energy to be completed. The corresponding values of $\Lambda_f(q)$ and $\Lambda_{D_i}(q)$ are shown in Fig. 5.3. From the results of Theorem 5.1, since the density of task durations Λ_f (red) is always lesser or equal than the valley capacity Λ_{D_i} (blue), an equilibrium is achieved by broadcasting to the appliances the profile of inflexible demand D_i. The resulting demand components as functions of the measure q are shown in Fig. 5.4: given that $q = Q_D(D(t))$, when $D = D_i$ we expect $\bar{D}_i(q)$ to be a monotonic increasing function. Conversely, considering that all devices with $t_{min} < q$ perform their tasks in the interval $[0, t_{min}]$, the flexible demand $\bar{D}_f(q)$ will always be decreasing. From Remark 5.3, since in this case (5.18) is satisfied, the sum $\bar{D}_a(q)$ of the two demand components will be nondecreasing. The same quantities as functions of time are displayed in Fig. 5.5. The intervals of scheduled power consumption for the appliances with t_{min} equal to $5h$, $7h$ and $9h$ are represented by the blue shaded areas. As expected, the considered devices have no interest in changing their power profiles since they are operating (at rated power) during time intervals characterized by the lowest values of aggregate demand.
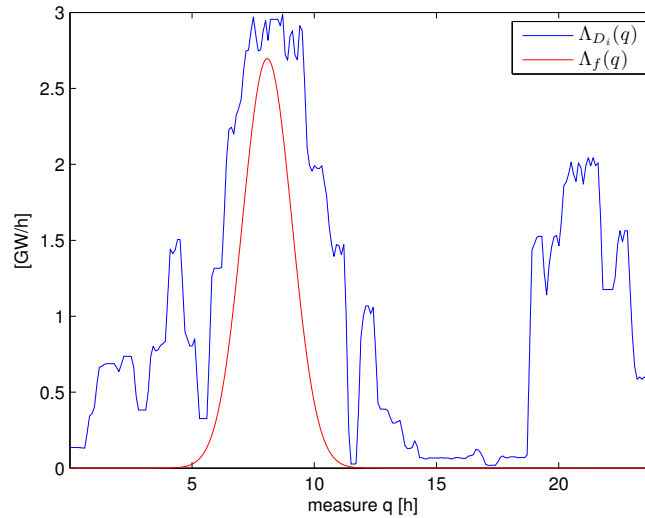
FIGURE 5.3: Graphical representation of the equilibrium condition (5.18).
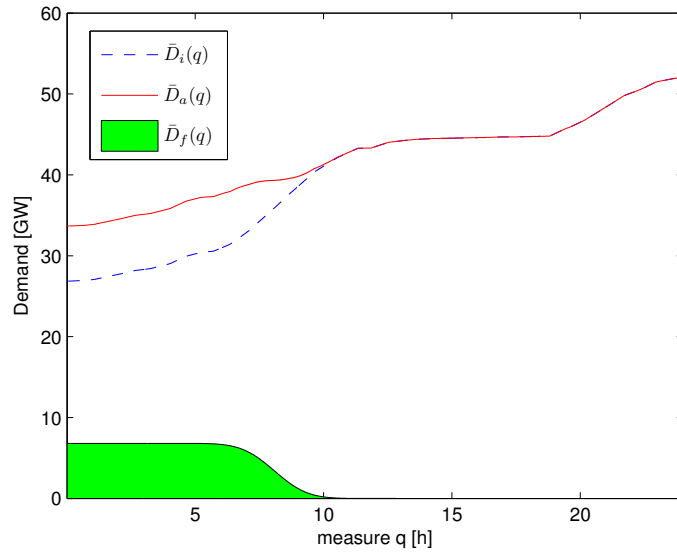
FIGURE 5.4: Profiles of inflexible, flexible and aggregate demand as a function of the measure $q = Q_{D_i}(D_i(t))$.
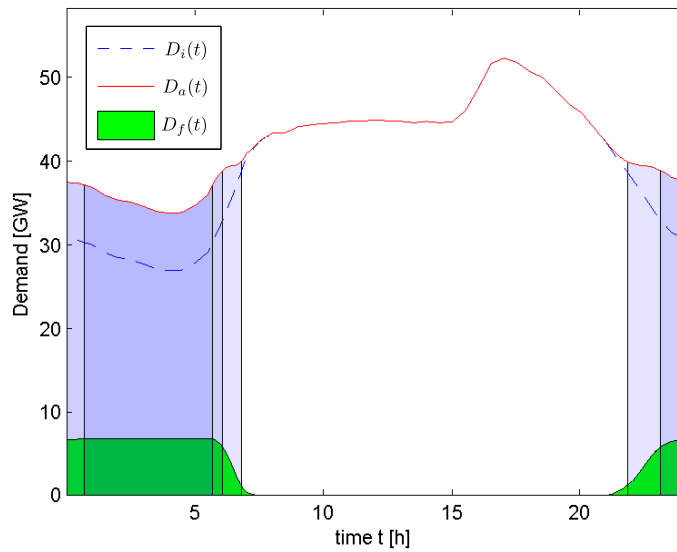
FIGURE 5.5: Profiles of inflexible, flexible and aggregate demand as a function of time.

A different case study is now simulated, considering an appliances population whose task duration profile Λ_f does not satisfy the equilibrium condition presented in Theorem 5.1. In particular, the function f' is defined as the sum of two truncated gaussians with mean equal to $4h$ and $8h$. This choice could model, for example, two distinct typologies of appliances (with different rated power), considering that devices in each group have different minimum times t_{min} for their tasks. The total energy required by the appliances, as in the previous case, amounts to $55GWh$. A graphical representation of the equilibrium condition of Theorem 5.1 applied to the present scenario is provided

in Fig. 5.6: it is straightforward to verify that an equilibrium cannot be achieved in the unconstrained case since $\Lambda_f(q) > \Lambda_{D_i}(q)$ in the interval which goes approximatively from $q = 2h$ to $q = 5h$. This can also be seen from the demand profiles shown in Fig. 5.7, obtained when $D = D_i$ is broadcast and no constraint α is imposed. In this case the shaded blue areas, which represent the scheduled interval of power consumption of devices with t_{min} equal to $2h$, $4h$ and $8h$, do not correspond to the lowest values of aggregate demand. For example, the appliances with $t_{min} = 2h$ could reduce their total cost by shifting part of their power consumption to the small valley of aggregate demand which appears around $t = 6h$. This means that the operation strategy formulated by the devices on the basis of the broadcast signal $D = D_i$ is not optimal for the induced aggregate demand and an equilibrium is not achieved.

The same scenario is approached by introducing a proportional constraint α on the power absorption, determined by solving the time minimization problem (5.48). The optimal $\bar{F}^*$ (and the corresponding α) are calculated according to Theorem 5.3. The value of T^* is determined through a bisection technique that exploits the monotonicity of the function γ. In particular, the following iterative procedure is followed:

1. Set $\tilde{T} = T/2$, $T_{min} = 0$ and $T_{max} = T$.

2. Calculate an approximation $\hat{\gamma}(\tilde{T})$ of the value function $\gamma(\tilde{T}) = \lim_{\epsilon \to 0} \gamma^\epsilon(\tilde{T})$. This can be done through integration of the system equations (5.49), considering a sufficiently small value of ϵ and applying the feedback control $\tilde{F}^*$ defined in (5.60).

3. Given a certain error tolerance $\delta > 0$, the following cases are considered:

   - If $|\hat{\gamma}(\tilde{T}) - q_{max}| < \delta$ it is assumed that the allocation of flexible demand is completed for $q = \tilde{T}$. Set $T^* = \tilde{T}$ and calculate the solution $\bar{F}^*$ of (5.48) according to (5.65) and (5.66). Exit the procedure.

   - If $\hat{\gamma}(\tilde{T}) + \delta < q_{max}$ the allocation of flexible demand is not completed. Set $\tilde{T}_{NEW} = (T_{max} + \tilde{T})/2$, $T_{min} = \tilde{T}$ and repeat steps 2 and 3 with $\tilde{T} = \tilde{T}_{NEW}$.

   - If $\hat{\gamma}(\tilde{T}) > q_{max} + \delta$ the allocation of flexible demand is completed for some smaller value of q. Set $\tilde{T}_{NEW} = (\tilde{T} + T_{min})/2$, $T_{max} = \tilde{T}$ and repeat steps 2 and 3 with $\tilde{T} = \tilde{T}_{NEW}$.

For the considered scenario this procedure converges, in 10 iterations, to $\tilde{T} = T^* = 12.8h$. The computational time, with an integration step of $0.01h$, amounts to about one minute. The resulting values of $\bar{F}^*$ (which corresponds to the reshaped task duration profile $\bar{\Lambda}_f$) are represented by the green dashed lines in Fig. 5.6 while the demand profiles and the proportional constraint $\bar{\alpha}$ as functions of the measure q are shown in Fig. 5.8.

Three different intervals, for decreasing values of q, can be considered. In particular, for $q > T^*$, it can be seen in Fig. 5.6 that $\bar{F}^*$ and the flexible demand $\bar{D}_f$ are equal to zero since all the appliances have already completed their tasks. In the interval which goes from approximatively $6h$ to T^*, the input $\bar{F}^*(q)$ corresponds to the function $\Lambda_f(q - \Delta)$ with Δ equal to about $2h$: the function α is equal to 1 and the resulting demand profile corresponds to the one obtained if all task times were increased by Δ. At about $q = 6h$ the function $\bar{F}^*$ intersects Λ_{D_i}: this means that a constraint must be introduced on the power rate of the appliances by setting $\bar{\alpha}(q) < 1$. This is done by imposing $\bar{F}^*(q) = \Lambda_{D_i}(q)$ which corresponds to a flat profile of aggregate demand in the q variable. The results in the time variable are shown in Fig. 5.9. Similarly to the previous case, the shaded blue areas represent the intervals of power consumption of devices with t_{min} equal to $2h$, $4h$ and $8h$. It is possible to verify that they correspond to the lowest values of $D_a(t)$ and therefore an equilibrium is achieved. On the other hand, given the introduction of the constraint α, the time required by the appliances to complete their task is larger than the corresponding one for the unconstrained case shown in Fig. 5.7. A comparison between the broadcast minimum time t_{min} and the actual task time $\Gamma(t_{min})$ is shown in Fig. 5.10. Notice in particular that the increase introduced in the task time of the appliances is larger for higher values of t_{min}. This can be explained if one considers that, for t_1, t_2 with $t_1 < t_2$, it holds $\mathcal{S}_{D_i}(t_1) \subset \mathcal{S}_{D_i}(t_2)$ and therefore appliances with higher values of t_{min} are limited by the constraint α on a larger interval.
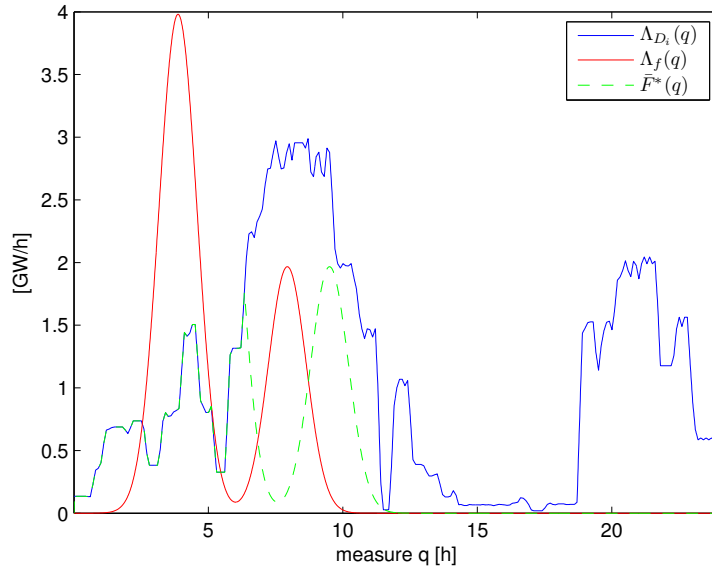
FIGURE 5.6: Graphical representation of the equilibrium condition (5.18) which, for the chosen function f' and corresponding Λ_f, is not satisfied.
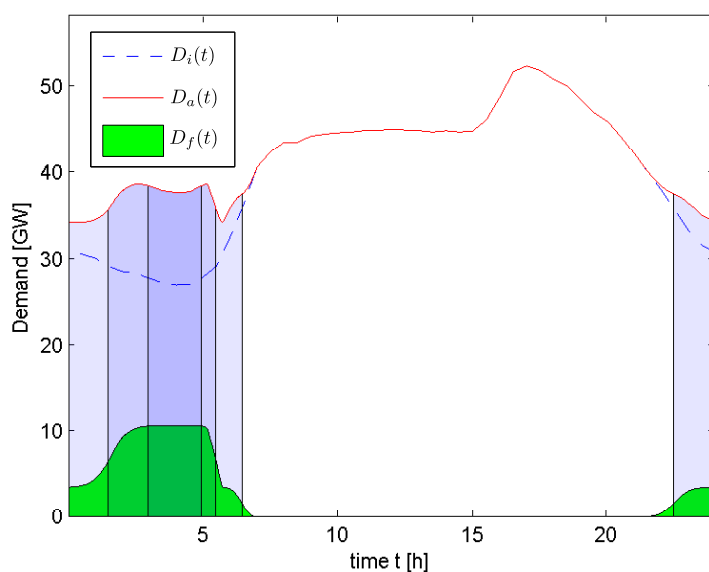
FIGURE 5.7: Profiles of inflexible, flexible and aggregate demand as a function of time, for Λ_f shown in Fig. 5.6 and with no constraint α on the maximum power of the appliances.
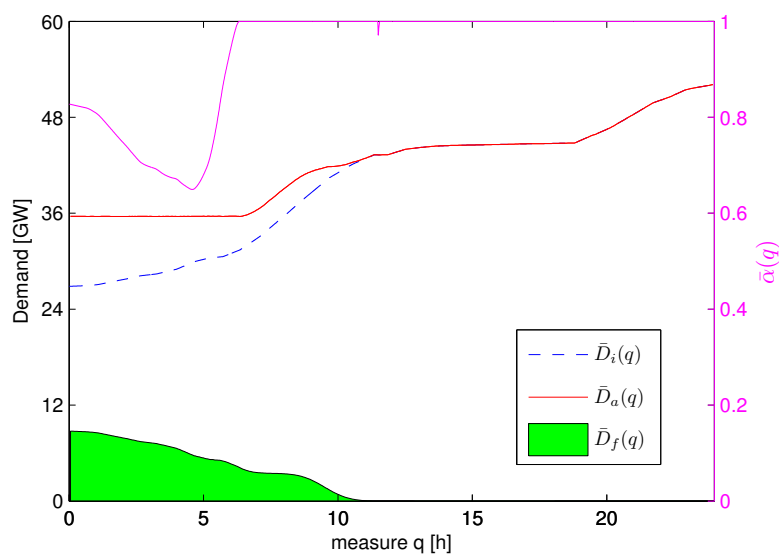
FIGURE 5.8: Profiles of inflexible, flexible and aggregate demand as a function of the measure q, for Λ_f shown in Fig. 5.6 and with the proportional constraint $\bar{\alpha}(q)$ (magenta).
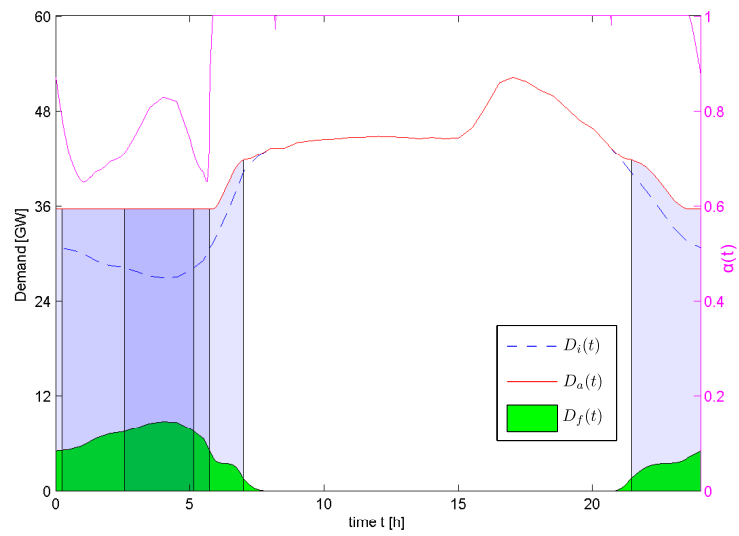
FIGURE 5.9: Profiles of inflexible, flexible and aggregate demand as a function of time, for Λ_f shown in Fig. 5.6 when the proportional constraint $\alpha(t)$ (magenta) is applied.
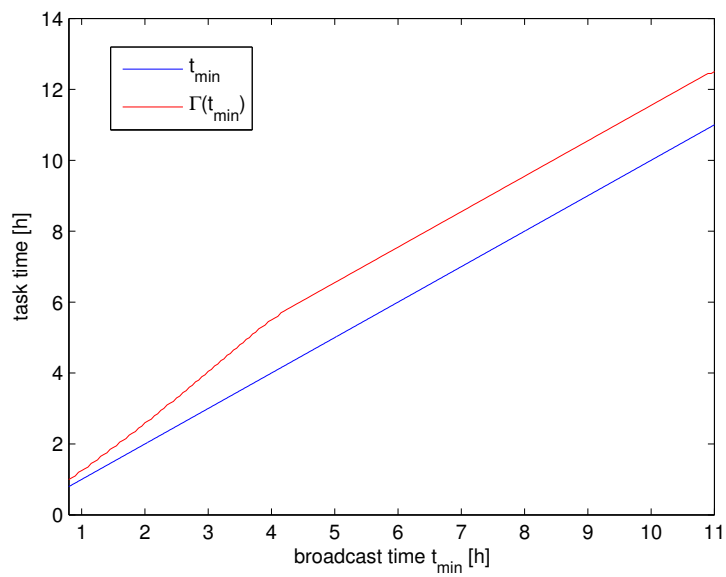
FIGURE 5.10: Comparison between the broadcast minimum time t_{min} and the actual task time $\Gamma(t_{min})$ of the appliances when the constraint α is introduced.

5.6   Properties of the Decentralized Control Strategy

In Section 5.3 necessary and sufficient conditions have been provided for the existence of a Nash equilibrium when the devices perform a selfish scheduling of their power consumption based on a broadcast demand signal. It is shown now that, under some additional conditions, such equilibrium is also Pareto optimal. Furthermore, for the constrained case presented in Section 5.4, the choice to design α which induces an equilibrium by minimizing the total task time of the population can be further justified by showing that additional optimality properties are guaranteed for the single appliances and from a global point of view. It is proved that the proposed control strategy minimizes the task time of the single appliance and is optimal for some index that quantifies the flattening of the aggregate demand profile.

5.6.1   Pareto Optimality

We want to investigate under which conditions the Nash equilibrium determined in Section 5.3 for the unconstrained scenario is also Pareto optimal. If this is not the case, there will exist power profiles different from u^* in (5.8) which allow to reduce the cost sustained by at least one device without increasing the costs of the other appliances. A different notation must be used in order to consider the more general case in which the power u is not obtained by a greedy optimization of the cost function on the basis of a broadcast signal D. This means that it is not possible to define u as a function of t_{min} and E_{tot} since, in general, appliances with equal parameters could have different power profiles. The set of devices is denoted by $\mathcal{V}$ while $\nu \in \mathcal{V}$ represents the single device with minimum task time $t_{min}(\nu)$ and total energy $E_{tot}(\nu)$. For a feasible power profile $u(\cdot, \nu)$ of the device ν, it must hold:

$$0 \le u(t, \nu) \le \frac{E_{tot}(\nu)}{t_{min}(\nu)} \qquad \forall t \in [0, T]$$
$$\int_0^T u(t, \nu)\, dt = E_{tot}(\nu)$$

The total costs sustained by the device ν when applying an arbitrary feasible profile $u(\cdot, \nu)$ and $u^*(\cdot, t_{min}(\nu), E_{tot}(\nu))$ are denoted respectively by $J(\nu)$ and $J^*(\nu)$:

$$J(\nu) = \int_0^T \Pi(D_i(t) + D_f(t)) u(t, \nu)\, dt$$
$$J^*(\nu) = \int_0^T \Pi(D_i(t) + D_f^*(t)) u^*(t, t_{min}(\nu), E_{tot}(\nu))\, dt$$

where $D_f(t) = \int_{\mathcal{V}} u(t, \nu)\, d\nu$ and $D_f^*(t)$ as defined in (5.12) are the flexible demand profiles introduced by the appliances when u and u^* are applied. If the Nash equilibrium

is Pareto optimal, there is no feasible $u(\cdot, \cdot)$ and $\tilde{\nu} \in \mathcal{V}$ for which the following holds:

$$J(\nu) \le J^*(\nu) \ \forall \nu \in \mathcal{V} \qquad J(\tilde{\nu}) < J^*(\tilde{\nu}). \tag{5.68}$$

The Pareto optimality will be verified by comparing the total costs of the appliances population (denoted respectively by J_{tot} and J_{tot}^*) when u and u^* are applied:

$$J_{tot} = \int_{\nu \in \mathcal{V}} J(\nu)\, d\nu = \int_0^T \Pi(D_i(t) + D_f(t)) D_f(t)\, dt$$

$$J_{tot}^* = \int_{\nu \in \mathcal{V}} J^*(\nu)\, d\nu = \int_0^T \Pi(D_i(t) + D_f^*(t)) D_f^*(t)\, dt$$

Assumption 5.3. *Define as $\mathcal{U}_q$ the set of feasible power profiles $u_q(\cdot, \cdot)$ such that, for the resulting flexible demand $D_{f,q}$, it holds:*

$$D_{f,q}(t_1) = D_{f,q}(t_2) \quad \forall(t_1, t_2) : D_i(t_1) = D_i(t_2) \tag{5.69}$$

For any feasible $u(\cdot, \cdot)$, there exists $u_q(\cdot, \cdot) \in \mathcal{U}_q$ to which corresponds a lower or equal value of total cost J_{tot}.

In other words, we are assuming that we can restrict our analysis to flexible demand profiles which are well defined in the variable $q = Q_{D_i}(D_i(t))$ since the function which minimizes J_{tot} will always be of such kind. Notice that such assumptions can be easily verified with standard optimal control techniques if one relaxes the constraints and minimizes J_{tot} over the positive flexible demand profiles with a given total integral.

It is now possible to provide the following result:

Theorem 5.4. *Denote by $\bar{D}_f^*$ the flexible demand in the variable q defined in (5.11) when the profile $D = D_i$ is broadcast and by $\bar{D}_a^*$ the corresponding aggregate demand. Assume that (5.18) is verified and therefore there exists a Nash equilibrium in the sense described by (5.15). For a monotonic increasing and convex price function Π, such equilibrium is Pareto optimal if the following holds for all $q \in [0, T]$:*

$$\bar{D}_a^{*'}(q) \left[\Pi''(\bar{D}_a^*(q)) \bar{D}_f^*(q) + \Pi'(\bar{D}_a^*(q)) \right] + \Pi'(\bar{D}_a^*(q)) \bar{D}_f^{*'}(q) \ge 0 \tag{5.70}$$

Proof. From Lemma 5.1, the cost J_{tot} for a power profile $u_q \in \mathcal{U}_q$ can be written as:

$$J_{tot} = \int_0^T \Pi(\bar{D}_i(q) + \bar{D}_f(q)) \bar{D}_f(q)\, dq = \int_0^T \Pi(\bar{D}_i(q) + \bar{D}_f^*(q) + l(q)) \left[\bar{D}_f^*(q) + l(q) \right] dq \tag{5.71}$$

where $\bar{D}_i$ and $\bar{D}_f$ represent respectively inflexible and flexible demand in the variable $q = Q_{D_i}(D_i(t))$ when u_q is applied. It follows from (5.9) that, when the control u^* which

induces the Nash equilibrium is chosen, the devices operate at maximum power at the lowest values of q and therefore, for any $u_q \in \mathcal{U}_q$, $\nu \in \mathcal{V}$ and $q \in [0, T]$, it holds:

$$\int_0^q u_q(s, \nu) \, ds \leq \int_0^q u^*(s, t_{min}(\nu), E_{tot}(\nu)) \, ds$$

By taking the integral over the whole population, it is possible to verify the same property for the demand profiles $\bar{D}_f$ and $\bar{D}_f^*$. We can conclude that the set $\mathcal{L}$ of feasible variations l to consider in (5.71) can be defined as:

$$\mathcal{L} := \left\{ l(\cdot) : \int_0^q l(s) \, ds \leq 0 \; \forall l \in [0, T], \int_0^T l(s) \, ds = 0 \right\} \tag{5.72}$$

The function $V(s, \tau) = \Pi(\bar{D}_i(s) + \bar{D}_f^*(s) + \tau) \left[\bar{D}_f^*(s) + \tau \right]$ is introduced, allowing to derive an alternative expression of the total cost J_{tot}:

$$\begin{aligned} J_{tot} &= \int_0^T V(s, 0) \, ds + \int_0^T \int_0^{l(s)} \frac{\partial V}{\partial \tau}(s, \tau) \, d\tau \, ds \\ &= J_{tot}^* - \int_{\mathcal{T}_-} \int_{l(s)}^0 \frac{\partial V}{\partial \tau}(s, \tau) \, d\tau \, ds + \int_{\mathcal{T}_+} \int_0^{l(s)} \frac{\partial V}{\partial \tau}(s, \tau) \, d\tau \, ds \end{aligned} \tag{5.73}$$

The sets $\mathcal{T}_-$ and $\mathcal{T}_+$ are defined as follows:

$$\mathcal{T}_- := \{s : l(s) < 0\} \qquad \mathcal{T}_+ := \{s : l(s) > 0\} \tag{5.74}$$

while for the partial derivative of V it holds:

$$\frac{\partial V}{\partial \tau}(s, \tau) = \Pi'(\bar{D}_i(s) + \bar{D}_f^*(s) + \tau) \left[\bar{D}_f^*(s) + \tau \right] + \Pi(\bar{D}_i(s) + \bar{D}_f^*(s) + \tau)$$

It is shown that, under the current assumptions, the partial derivative $\frac{\partial V}{\partial \tau}(s, \tau)$ is monotonically increasing with respect to τ and with respect to s when $\tau = 0$. The monotonicity with respect to τ is always verified since the price function Π is convex and monotonically increasing. For the monotonicity of $\frac{\partial V}{\partial \tau}(s, 0)$ in the variable s, explicit calculations show that the left hand side in (5.70) corresponds to $\frac{\partial^2 V}{\partial s \partial \tau}(q, 0)$ which is therefore positive for all $q \in [0, T]$. If one denotes by S_- and S_+ the following sets:

$$S_+ = \{(\tau, s) : l(s) \geq 0 \wedge \tau \in [0, l(s)]\}$$

$$S_- = \{(\tau, s) : l(s) \leq 0 \wedge \tau \in [l(s), 0]\}$$

it holds:

$$-\int_{S_-} d\tau \, ds + \int_{S_+} d\tau \, ds = \int_{\mathcal{T}_-} \int_0^{l(s)} d\tau \, ds + \int_{\mathcal{T}_+} \int_0^{l(s)} d\tau \, ds = \int_0^T l(s) \, ds = 0$$

Considering that $\int_0^q l(s)\, ds \leq 0$ and assuming that there only exist finitely many intervals $\{I_1, I_2, \ldots, I_n\}$ included in $[0, T]$ where $l(\cdot)$ is identically 0, it is possible to partition S_+ and S_- in n subsets $(S_+^1, \ldots, S_+^n)$ and $(S_-^1, \ldots, S_-^n)$ such that:

$$\int_{S_-^i} d\tau\, ds = \int_{S_+^i} d\tau\, ds \qquad s_1 \leq s_2 \qquad \tau_1 \leq 0 \leq \tau_2$$

where the inequalities are verified for all $(s_1, \tau_1) \in S_-^i$ and $(s_2, \tau_2) \in S_+^i$ with $i = 1, \ldots, n$. Such partition can be performed by choosing S_-^i as the connected components of S_-. We denote now as $t_+^1 \leq t_+^2 \leq \ldots \leq t_+^n \leq t_+^{n+1} = T$ the (minimal) values in $[0, T]$ such that:

$$\int_{S_-^i} d\tau ds = \int_{[t_+^i, t_+^{i+1}] \cap \mathcal{T}_+} \int_0^{l(s)} d\tau ds$$

The corresponding S_+^i can be defined as $([t_+^i, t_+^{i+1}] \times \mathbb{R}) \cap S_+$. Given the monotonicity properties of the partial derivative $\frac{\partial V}{\partial \tau}$, it also holds:

$$\frac{\partial V}{\partial \tau}(s_1, \tau_1) \leq \frac{\partial V}{\partial \tau}(s_1, 0) \leq \frac{\partial V}{\partial \tau}(s_2, 0) \leq \frac{\partial V}{\partial \tau}(s_2, \tau_2)$$

for all (τ_1, s_1) and (τ_2, s_2) as defined above. From the monotonicity of the integral, it follows:

$$\int_{S_-^i} \frac{\partial V}{\partial \tau}(s, \tau)\, d\tau ds \leq \int_{S_+^i} \frac{\partial V}{\partial \tau}(s, \tau)\, d\tau ds \qquad i = 1, \ldots, n \tag{5.75}$$

Adding up the inequalities (5.75) for i in $\{1, 2, \ldots, n\}$ yields:

$$\int_{\mathcal{T}_-} \int_{l(s)}^0 \frac{\partial V}{\partial \tau}(s, \tau)\, d\tau ds = \int_{S_-} \frac{\partial V}{\partial \tau}(s, \tau)\, d\tau ds$$
$$\leq \int_{S_+} \frac{\partial V}{\partial \tau}(s, \tau)\, d\tau ds = \int_{\mathcal{T}_+} \int_0^{l(s)} \frac{\partial V}{\partial \tau}(s, \tau)\, d\tau ds \tag{5.76}$$

Hence, the sum of the last two terms in (5.73) is positive and therefore $J_{tot} \geq J_{tot}^*$. Assumption 5.3 allows to extend this result from $u_q \in \mathcal{U}_q$ to any feasible u. The proof is concluded by noticing that (5.68) never holds if $J_{tot} \geq J_{tot}^*$. $\qquad\square$

It is of particular interest the application of Theorem 5.4 when an affine price function $\Pi(d) = a + b \cdot d$ is considered. In this case the inequality (5.70) corresponds to a relationship between the negotiable valley capacity Λ_{D_i} and the power density of task durations Λ_f:

$$-\bar{D}_f^{*\prime}(q) = \Lambda_f(q) \leq \frac{\Lambda_{D_i}(q)}{2} = \frac{\bar{D}_i'(q)}{2}$$

5.6.2 Minimization of Task Time for the Single Appliance

Consider the decentralized control in the constrained case that has been presented in Section 5.4. Recalling the definition of $\Gamma(t_{min})$ provided in (5.47) and the optimization (5.48) of the total task time, the problem of minimizing the time required by the single appliance (with parameter $t_{min} = s$) to complete its task can be written as:

$$
\begin{aligned}
\min_{\bar{F}(\cdot), F_{tot}} \quad & T_s \\
\text{s.t.} \quad & \bar{\alpha}_I(T_s) = s & & \bar{F}_I(T_{END}) = F_{tot} \\
& \dot{\bar{\alpha}}_I(q) = \frac{F_{tot} - \bar{F}_I(q)}{\int_{\bar{\alpha}_I(q)}^{T} \frac{f'(\tau)}{\tau} d\tau} & & \dot{\bar{F}}(q) = F(q) \\
& \bar{\alpha}_I(0) = 0 & & \bar{F}_I(0) = 0 \\
& 0 \le \dot{\bar{\alpha}}_I(q) \le 1 & & \bar{F}(q) \le \bar{D}_i'(q) \\
& \bar{\alpha}_I(T_{END}) = q_{max} & & T_{END} \le T
\end{aligned}
\tag{5.77}
$$

Similarly to (5.48), the considered constraints guarantee that an equilibrium is achieved for the resulting aggregate demand. Furthermore, the condition $\bar{\alpha}_I(T_{END}) = q_{max}$ with $T_{END} \le T$ is introduced to impose that the tasks of the whole population are performed within the considered time interval $[0, T]$. Note that the power absorption of the single device with $t_{min} = s$, in the q variable, is scheduled in the interval characterized by $\bar{\alpha}_I(q) \le s$. Considering the monotonicity of $\bar{\alpha}_I(q)$, it is sufficient to minimize T_s such that $\bar{\alpha}_I(T_s) = s$. It is now possible to provide the following result:

Theorem 5.5. *The control $\bar{F}^*$ defined in (5.66) and optimal for the problem (5.48) of global task time minimization, is the solution of (5.77) for all $s \in [q_{min}, q_{max}]$.*

Proof. Assume that $\bar{F}^*$ is not optimal and there exists another control $\bar{F}^\diamond$ which is feasible for (5.77) and such that, for the corresponding solution $(\bar{\varphi}_\alpha^\diamond, \bar{\varphi}_F^\diamond)$ of (5.45), it holds:

$$
\bar{\varphi}_\alpha^\diamond(T_s) = s > \bar{\varphi}_\alpha^*(T_s)
\tag{5.78}
$$

where $\bar{\varphi}^*$ denotes the solution of (5.45) when $\bar{F}^*$ is applied. Since $\bar{\varphi}_\alpha^\diamond(T_{END}) = q_{max}$, it is possible to apply Proposition 5.2 and calculate the equivalent control $\tilde{F}^\diamond$ for (5.49) to which corresponds the limiting solution $(\tilde{\varphi}_\alpha^\diamond, \tilde{\varphi}_F^\diamond)$ when ϵ tends to zero. The same operations are performed for the control $\bar{F}^*$ with final time T^*, obtaining the corresponding $\tilde{F}^*$ and the solution $(\tilde{\varphi}_\alpha^*, \tilde{\varphi}_F^*)$ for system (5.49). Considering the relationship (5.53) between trajectories in the two systems and the inequality in (5.78) yields:

$$
\tilde{\varphi}_\alpha^\diamond(T_{END} - T_s) < \tilde{\varphi}_\alpha^*(T^* - T_s) \qquad \tilde{\varphi}_\alpha^\diamond(T_{END}) = \tilde{\varphi}_\alpha^*(T^*) = q_{max}
\tag{5.79}
$$

with $T^* \leq T_{END}$ given the optimality of $\bar{F}^*$ for (5.48). Furthermore, $\tilde{\varphi}_I(q)$ defined in (5.51) can be considered as a strictly monotonic increasing function of $\tilde{\varphi}_\alpha(q)$. Denoting the value of $\tilde{\varphi}_I$ when $\tilde{F}^\diamond$ and $\tilde{F}^*$ are considered with the same superscript, we have:

$$\tilde{\varphi}_I^\diamond(T_{END} - T_s) < \tilde{\varphi}_I^*(T^* - T_s) \qquad \tilde{\varphi}_I^\diamond(T_{END}) = \tilde{\varphi}_I^*(T^*) = \int_0^{q_{max}} f'(\tau)\, d\tau \qquad (5.80)$$

It follows from $T^* \leq T_{END}$ and $\tilde{\varphi}_\alpha^*(0) = 0$, that $\tilde{\varphi}_\alpha^\diamond(T_{END} - T^*) \geq \tilde{\varphi}_\alpha^*(0)$. Given the inequality in (5.79) and the continuity of the solutions of system (5.49) there must exist $y \in [T_s, T^*]$ such that:

$$\tilde{\varphi}_\alpha^\diamond(T_{END} - y) = \tilde{\varphi}_\alpha^*(T^* - y) \qquad \dot{\tilde{\varphi}}_\alpha^\diamond(T_{END} - y) < \dot{\tilde{\varphi}}_\alpha^*(T^* - y) \qquad (5.81)$$

where the second condition in (5.81) corresponds to $\tilde{\varphi}_F^\diamond(T_{END} - y) < \tilde{\varphi}_F^*(T^* - y)$ from (5.49). Taking into account the monotonicity of system (5.49) with $\tilde{T} = y$ and the properties of $\tilde{F}^*$, considering as initial states $\tilde{\varphi}^\diamond(T_{END} - y)$ and $\tilde{\varphi}^*(T^* - y)$, we have:

$$\tilde{\varphi}_F^\diamond(T_{END} - T_s) \leq \tilde{\varphi}_F^*(T^* - T_s)$$

From the conditions (5.80) on the integral $\tilde{\varphi}_I$, there must exist an interval of positive measure $\mathcal{T} \subseteq [0, T_s]$ such that:

$$\tilde{\varphi}_F^\diamond(T_{END} - \tau) > \tilde{\varphi}_F^*(T^* - \tau) \; \forall \tau \in \mathcal{T}$$

Given the monotonicity properties of system (5.49) with $\tilde{T} = T_s$ and the fact that the control $\tilde{F}^*$ always maximizes the state derivatives, we can conclude that this is not possible. As a consequence, there is no $\bar{F}^\diamond$ for which (5.78) holds and therefore $\bar{F}^*$ is optimal for (5.77). □

5.6.3 Flattening of Aggregate Demand Profile

We are now interested in the global properties of the control strategy presented in Section 5.4. Similarly to what has been proposed in [69], we aim to quantify the flattening introduced in the aggregate demand by minimizing the following functional:

$$J\left(D_f(\cdot)\right) = \int_0^T U\left(D_i(t) + D_f(t)\right) dt = \int_0^T U\left(D_a(t)\right) dt \qquad (5.82)$$

where $U : [0, +\infty) \rightarrow \mathbb{R}^+$ is a positive convex function. It is desirable to perform such optimization on the class $\mathcal{D}_f$ of flexible demand profiles which result from a greedy optimization of the appliances on the basis of the broadcast signal $D = D_i$ and a proportional constraint on power consumption. We also require task completion for the

appliances population, fairness (the proportional constraint is equal for all the appliances) and equilibrium of the system in the sense specified by (5.39). Denote now as $\bar{\mathcal{D}}_f$ the set of flexible demand profiles in the variable q which are defined, given $(\bar{\alpha}_I, \bar{F}_I, \bar{F})$ which satisfy the constraints in (5.48), according to (5.34). From the results of Section 5.4, for each $D_f(\cdot) \in \mathcal{D}_f$ there exists $\bar{D}_f(\cdot) \in \bar{\mathcal{D}}_f$ such that:

$$
\begin{aligned}
D_f(t) &= \bar{D}_f(Q_{D_i}(D_i(t))) \\
D_a(t) &= \bar{D}_a(Q_{D_i}(D_i(t)))
\end{aligned}
\qquad \forall t \in [0, T]
\tag{5.83}
$$

where D_a and $\bar{D}_a$ denote respectively the resulting profiles of aggregate demand in the variables t and q. It is now possible to introduce the equivalent functional $\bar{J}$:

$$
\bar{J}(\bar{D}_f(\cdot)) = \int_0^T U\left(\bar{D}_i(q) + \bar{D}_f(q)\right) dq = \int_0^T U\left(\bar{D}_a(q)\right) dq
\tag{5.84}
$$

Remark 5.6. For any $D_f(\cdot) \in \mathcal{D}_f$ and $\bar{D}_f(\cdot) \in \bar{\mathcal{D}}_f$ which fulfil (5.83), as a direct result of Lemma 5.1, the following holds for the functionals defined in (5.82) and (5.84):

$$
\int_0^T U\left(D_i(t) + D_f(t)\right) dt = \int_0^T U\left(\bar{D}_i(q) + \bar{D}_f(q)\right) dq
\tag{5.85}
$$

This means that it is possible to minimize J by solving the equivalent optimization problem on $\bar{J}$. Since it is in general difficult to provide an analytical definition of $\bar{\mathcal{D}}_f$, a larger class of flexible demand profiles is introduced. If one considers $\bar{D}_f^*$ as defined in (5.67), which represents the flexible demand resulting from the optimal solution of (5.48), the set $\tilde{\mathcal{D}}_f$ can be defined as:

$$
\tilde{\mathcal{D}}_f := \left\{ \bar{D}_f(\cdot) : \bar{D}_f(q) = \bar{D}_f^*(q) + l(q) \ \forall q \in [0, T], l(\cdot) \in \mathcal{L} \right\}
\tag{5.86}
$$

where the set $\mathcal{L}$ of admissible variations is:

$$
\mathcal{L} := \left\{ l(\cdot) : \int_0^q l(s)\, ds \leq 0 \ \forall l \in [0, T], \int_0^T l(s)\, ds = 0 \right\}
\tag{5.87}
$$

Proposition 5.6. *The set of demand profiles $\bar{\mathcal{D}}_f$ and $\tilde{\mathcal{D}}_f$ defined in (5.86) are such that* $\bar{\mathcal{D}}_f \subseteq \tilde{\mathcal{D}}_f$.

Proof. To any profile $\bar{D}_f(\cdot) \in \bar{\mathcal{D}}_f$ must correspond task completion of the appliances population and therefore it must hold:

$$
\int_0^T \bar{D}_f(s)\, ds = \int_0^T \bar{D}_f^*(s)\, ds
\tag{5.88}
$$

This means that $\bar{\mathcal{D}}_f \subseteq \tilde{\mathcal{D}}$ if, for all $\bar{D}_f(\cdot) \in \bar{\mathcal{D}}_f$, the following holds at all $q < T$:

$$\int_0^q \bar{D}_f(s)\, ds \leq \int_0^q \bar{D}_f^*(s)\, ds \tag{5.89}$$

In fact, if this is true, there exists a function $l(\cdot) \in \mathcal{L}$ such that $\bar{D}_f = \bar{D}_f^* + l$. To verify (5.89), consider the solution $(\bar{\varphi}_\alpha, \bar{\varphi}_F)$ of (5.45) obtained applying the control $\bar{F}$ which induces the flexible demand $\bar{D}_f$. Denote by T_{END} the corresponding time required for total task completion of the population. From definition (5.44) of $\bar{D}_r = \bar{D}_f$, considering the state $(\tilde{\varphi}_\alpha, \tilde{\varphi}_F)$ of the backward system (5.49) obtained applying Proposition 5.2 for $\tilde{T} = T_{END}$, we have $\bar{D}_f(q) = \tilde{\varphi}_F(T_{END} - q)$. Denoting with the star subscript the corresponding quantities for $\bar{D}_f^*$ and considering T^* instead of T_{END} yields $\bar{D}_f^*(q) = \tilde{\varphi}_F(T^* - q)$. If one considers $\tilde{\varphi}_I(q) = \int_0^q \tilde{\varphi}_F(\tau)\, d\tau$, defined in (5.51), the inequality in (5.89) can be rewritten as:

$$D_I - \tilde{\varphi}_I(T_{END} - q) \leq D_I - \tilde{\varphi}_I^*(T^* - q) \tag{5.90}$$

The total demand integral $D_I = \int_0^T \bar{D}_f(q)\, dq = \int_0^T \bar{D}_f^*(q)\, dq$ is equal for the two cases, as shown in (5.88). Suppose now that (5.90) does not hold and there exist some $\bar{D}_f(\cdot) \in \bar{\mathcal{D}}_f$ and $q \in [0, T]$ such that $\tilde{\varphi}_I(T_{END} - q) < \tilde{\varphi}_I^*(T^* - q)$. If one considers that $\tilde{\varphi}_I(T_{END}) = \tilde{\varphi}_I^*(T^*) = D_I$, it is possible to show that this is impossible by following the steps detailed for (5.80) in the proof of Theorem 5.5. $\qquad\square$

The global cost (5.84), equivalent to (5.82), is minimized over $\tilde{\mathcal{D}}_f$ (which includes the set of feasible profiles $\bar{\mathcal{D}}_f$):

$$\min_{\bar{D}_f(\cdot) \in \tilde{\mathcal{D}}_f} \int_0^T U\left(\bar{D}_i(s) + \bar{D}_f(s)\right)\, ds \tag{5.91}$$

It can be shown that the task time minimizing solution presented in Section 5.4 is optimal also for the current problem. In particular:

Theorem 5.6. *The profile of flexible demand $\bar{D}_f^*$ induced by the optimal solution of (5.48) and defined in (5.67) is optimal for (5.91).*

Proof. For any $\bar{D}_f(\cdot) \in \tilde{\mathcal{D}}_f$ the cost function in (5.91), denoted as $\bar{J}$, can be written as:

$$\bar{J} = \int_0^T U\left(\bar{D}_i(s) + \bar{D}_f^*(s)\right) + \int_0^{l(s)} U'\left(\bar{D}_i(s) + \bar{D}_f^*(s) + \tau\right)\, d\tau\, ds$$
$$= \bar{J}^* - \int_{\mathcal{T}_-} \int_{l(s)}^0 U'\left(\bar{D}_i(s) + \bar{D}_f^*(s) + \tau\right)\, d\tau\, ds + \int_{\mathcal{T}_+} \int_0^{l(s)} U'\left(\bar{D}_i(s) + \bar{D}_f^*(s) + \tau\right)\, d\tau\, ds$$
$$\tag{5.92}$$

The term $\bar{J}^*$ denotes the cost function evaluated at $\bar{D}_f = \bar{D}_f^*$ while $\bar{D}_i$ represents the inflexible demand in the variable $q = Q_{D_i}(D_i(t))$ and the sets $\mathcal{T}_+$ and $\mathcal{T}_-$ are defined as follows:

$$\mathcal{T}_- := \{s : l(s) \leq 0\} \qquad \mathcal{T}_+ := \{s : l(s) \geq 0\} \tag{5.93}$$

Note that the derivative $U'\left(\bar{D}_i(s) + \bar{D}_f^*(s) + \tau\right)$ is monotonically increasing with respect to s and τ. The monotonicity in τ derives from the convexity of U and the same holds for s given that, from the definition of $\bar{D}_f^*$ and Remark 5.3, it follows $\bar{D}_i'(s) + \bar{D}_f'^*(s) \geq 0$. Notice also that, if one denotes by S_- and S_+ the following sets:

$$S_+ = \{(\tau, s) : l(s) \geq 0 \text{ and } \tau \in [0, l(s)]\}$$

$$S_- = \{(\tau, s) : l(s) \leq 0 \text{ and } \tau \in [l(s), 0]\}$$

it holds:

$$-\int_{S_-} d\tau\,ds + \int_{S_+} d\tau\,ds = \int_{\mathcal{T}_-}\int_0^{l(s)} d\tau\,ds + \int_{\mathcal{T}_+}\int_0^{l(s)} d\tau\,ds = \int_0^T l(s)\,ds = 0$$

Considering that $\int_0^q l(s)\,ds \leq 0$ and assuming that there only exist finitely many intervals $\{I_1, I_2, \ldots, I_n\}$ included in $[0, T]$ where $l(.)$ is identically 0, it is possible to partition S_+ and S_- in n subsets $(S_+^1, \ldots, S_+^n)$ and $(S_-^1, \ldots, S_-^n)$ such that:

$$\int_{S_-^i} d\tau\,ds = \int_{S_+^i} d\tau\,ds \qquad s_1 \leq s_2 \qquad \tau_1 \leq 0 \leq \tau_2$$

where the inequalities are verified for all $(s_1, \tau_1) \in S_-^i$ and $(s_2, \tau_2) \in S_+^i$ with $i = 1, \ldots, n$. These subsets can be determined as in the proof of Theorem 5.4, considering S_-^i as the connected components of S_-. We denote by $t_+^1 \leq t_+^2 \leq \ldots \leq t_+^n \leq t_+^{n+1} = T$ the (minimal) values in $[0, T]$ such that:

$$\int_{S_-^i} d\tau ds = \int_{[t_+^i, t_+^{i+1}] \cap \mathcal{T}_+}\int_0^{l(s)} d\tau ds.$$

The corresponding S_+^i can then be chosen as $([t_+^i, t_+^{i+1}] \times \mathbb{R}) \cap S_+$. Given the monotonicity properties of U', it also holds:

$$U'\left(\bar{D}_i(s_1) + \bar{D}_f^*(s_1) + \tau_1\right) \leq U'\left(\bar{D}_i(s_2) + \bar{D}_f^*(s_2) + \tau_2\right)$$

for all $(s_1, \tau_1) \in S_-^i$ and $(s_2, \tau_2) \in S_+^i$, with $i = 1, \ldots n$. Hence, by monotonicity of the integral, it follows:

$$\int_{S_-^i} U'\left(\bar{D}_i(s) + \bar{D}_f^*(s) + \tau\right) d\tau ds \leq \int_{S_+^i} U'\left(\bar{D}_i(s) + \bar{D}_f^*(s) + \tau\right) d\tau ds. \tag{5.94}$$

Adding up the inequalities (5.94) for i in $\{1, 2, \ldots, n\}$ yields:

$$\int_{S_-} U' \left(\bar{D}_i(s) + \bar{D}_f^*(s) + \tau \right) d\tau ds \leq \int_{S_+} U' \left(\bar{D}_i(s) + \bar{D}_f^*(s) + \tau \right) d\tau ds. \tag{5.95}$$

This shows:

$$\int_{\mathcal{T}_+} \int_0^{l(s)} U' \left(\bar{D}_i(s) + \bar{D}_f^*(s) + \tau \right) d\tau\, ds - \int_{\mathcal{T}_-} \int_{l(s)}^0 U' \left(\bar{D}_i(s) + \bar{D}_f^*(s) + \tau \right) d\tau\, ds$$

$$= \int_{S_+} U' \left(\bar{D}_i(s) + \bar{D}_f^*(s) + \tau \right) d\tau ds - \int_{S_-} U' \left(\bar{D}_i(s) + \bar{D}_f^*(s) + \tau \right) d\tau ds \geq 0$$

We can then conclude that the sum of the last two terms in (5.92) is positive and therefore $\bar{D}_f^*$ is optimal for (5.91) $\square$

5.7   Appliances with Partial Flexibility

It has been assumed so far that appliances can schedule their power consumption at any time instant within the considered interval $[0, T]$. It is possible to extend such formulation and account for devices that must operate with stricter time constraints. In particular, we will consider the case of appliances that must perform their tasks at $t \geq t_{st}$ where t_{st} ("*st*" standing for start) is an additional parameter of the individual device which is also communicated to the mentioned central entity. The distribution m of the parameters in the population will now have an additional variable: $\int_{t_1}^{t_2} \int_{\tau_1}^{\tau_2} \int_{E_1}^{E_2} m(t, \tau, E)\, dE\, d\tau\, dt$ will denote the number of devices for which $E_1 \leq E_{tot} \leq E_2$, $t_1 \leq t_{min} \leq t_2$ and also $\tau_1 \leq t_{st} \leq \tau_2$. Similarly, the function $f(t, \tau)$ in this case will represent the total amount of energy required by devices with $t_{st} = \tau$ and $t_{min} \leq t$:

$$f(t, \tau) := \int_0^t \int_{\mathcal{E}} E \cdot m(x, \tau, E)\, dE\, dx \tag{5.96}$$

It is now possible to define the derivative with respect to t of the function f with $f'(t, \tau) = \frac{\partial f(t, \tau)}{\partial t} = \int_{\mathcal{E}} E \cdot m(t, \tau, E)\, dE$.

Assumption 5.4. *For the derivative f', similarly to the previous analysis, we make an assumption of compact support. In particular:*

$$\mathrm{supp}(f') = [q_{min}, q_{max}] \times [\tau_{min}, \tau_{max}]$$

We also assume that $t_{min} + t_{st} \leq T$ for all $(t_{min}, t_{st}) \in \mathrm{supp}(f')$ as all appliances should be able to complete their task by operating at rated power within the specified availability interval $[t_{st}, T]$.

5.7.1   Optimal Power Profiles and Equilibrium Conditions

As in the case with total flexibility, the appliances minimize their individual cost on the basis of a broadcast demand profile D that satisfies Assumption 5.2. The optimization problem for the single device with $t_{min} = s$, $t_{st} = \tau$ and $E_{tot} = x$ is:

$$
\begin{aligned}
\min_{u(\cdot)} \quad & \int_\tau^T \Pi(D(t)) \cdot u(t)\, dt \\
\text{s. t} \quad & 0 \le u(t) \le \frac{x}{s} \\
& \int_\tau^T u(t)\, dt = x
\end{aligned}
\tag{5.97}
$$

In order to define the optimal power profile u^*, it is useful to provide the following preliminary result:

Proposition 5.7. *Given the sublevel set $\mathcal{S}_D$ defined in (5.6), for any $(s, \tau) \in \operatorname{supp}(f')$ there exists $\lambda \in [0, T]$, that we denote by $\Lambda(s, \tau)$, such that the following holds:*

$$
\lambda = \inf_x \left\{ x \in [0, T] : \mu\left([\tau, T] \cap \mathcal{S}_D(x)\right) = s \right\}
\tag{5.98}
$$

Proof. It is straightforward to verify that, under Assumption 5.2 for the broadcast D, the term $\mu\left([\tau, T] \cap \mathcal{S}_D(x)\right)$ in (5.98) is continuous and nondecreasing with respect to x. Furthermore, we have:

$$
\begin{aligned}
\mu\left([\tau, T] \cap \mathcal{S}_D(T)\right) &= \mu\left([\tau, T] \cap [0, T]\right) = T - \tau \\
\mu\left([\tau, T] \cap \mathcal{S}_D(0)\right) &= 0
\end{aligned}
\tag{5.99}
$$

Since, from Assumption 5.4, it holds $s \le T - \tau$ for all $(s, \tau) \in \operatorname{supp}(f')$, we can conclude that $\Lambda(s, \tau)$ exists as specified in the claim. $\qquad\square$

Notice that $\mathcal{S}_D(\Lambda(t_{min}, t_{st}))$ returns a time interval with the lowest values of broadcast demand D and whose intersection with $[t_{st}, T]$ has measure t_{min}. The solution to (5.97), for a device with $t_{min} = s$, $t_{st} = \tau$ and $E_{tot} = x$ can then be defined as follows:

$$
u^*(t, s, \tau, x) =
\begin{cases}
\dfrac{x}{s} & \text{if} \quad t \in \left([\tau, T] \cap \mathcal{S}_D(\Lambda(s, \tau))\right) \\[2ex]
0 & \text{if} \quad t \notin \left([\tau, T] \cap \mathcal{S}_D(\Lambda(s, \tau))\right)
\end{cases}
\tag{5.100}
$$

As in the previous analysis, considering the aggregate demand $D_{a,D}$ obtained by broadcasting the profile D to the appliances, an equilibrium is achieved if the following holds

for all $(t_{min}, t_{st}) = (s, \tau) \in \text{supp}(f')$ and $E_{tot} = x \in \mathcal{E}$:

$$
\int_\tau^T \Pi(D_{a,D}(t)))u^*(t, s, \tau, x)\, dt = \min_{u(\cdot)} \int_\tau^T \Pi(D_{a,D}(t))u(t)\, dt
$$
$$
\text{s. t} \quad 0 \le u(t) \le \frac{x}{s} \qquad\qquad (5.101)
$$
$$
\int_\tau^T u(t)\, dt = x
$$

In the case of appliances with partial flexibility, the concepts of negotiable valley capacity and power density of task durations are no longer applicable. In fact, it is in general not possible to provide an expression of flexible and aggregate demand simply as a function of the variable $q = Q_D(D(t))$. This is due to the fact that, following the additional constraint on the initial time of power consumption, equal values of D at different time instants do not correspond to equal values of D_f. On the other hand, it is possible to provide the following result:

Proposition 5.8. *A broadcast profile D induces a Nash equilibrium satisfying (5.101) if the following holds:*

$$
Q_D(D(t)) = Q_{D_{a,D}}(D_{a,D}(t)) \qquad \forall t \in [0, T] \qquad\qquad (5.102)
$$

Proof. To see this, it is sufficient to consider that the set $\mathcal{S}_D$ and the function Λ in (5.100) depend only on the measure $Q_D(D(t))$. This implies that, if (5.102) holds, the solution to the minimization problem in (5.101) can be achieved by adopting the power profile u^* which is optimal when considering the broadcast D in (5.97). $\qquad\square$

5.7.2 Parametrization of the Broadcast Signal

Since it is not possible to provide equilibrium conditions in the variable $q = Q_D(D(t))$, the problem is approached by restricting the analysis to a specific class $\mathcal{D}_m$ of broadcast signals $D : [0, T] \to [0, T]$ which are equal to their measure function Q_D. To define $\mathcal{D}_m$, consider the functions $\theta_L : [0, T] \to [0, T_0]$ and $\theta_R : [0, T] \to [T_0, T]$ with $T_0 \in [0, T]$ and such that, for all $q \in [0, T]$, it holds:

$$
\theta_R(q) - \theta_L(q) = q \qquad \dot\theta_L(q) < 0 \qquad \dot\theta_R(q) > 0 \qquad\qquad (5.103)
$$

Furthermore, the following conditions at $q = 0$ and $q = T$ are verified:

$$
\theta_L(0) = \theta_R(0) = T_0 \qquad \theta_L(T) = 0 \qquad \theta_R(T) = T \qquad\qquad (5.104)
$$

The class of profiles $\mathcal{D}_m$ will consist of the functions D for which there exist θ_L and θ_R which satisfy (5.103) and (5.104) and such that the following holds:

$$D(t) = \begin{cases} \theta_L^{-1}(t) & \text{if} \quad t \in [0, T_0] \\ \theta_R^{-1}(t) & \text{if} \quad t \in [T_0, T] \end{cases} \tag{5.105}$$

Notice that $D \in \mathcal{D}_m$ can be defined through (5.105) if one considers that the functions θ_L and θ_R are invertible and the union of their images is equal to $[0, T]$. Moreover, it holds $\text{Im}(\theta_L) \cap \text{Im}(\theta_R) = T_0$ with $\theta_L^{-1}(T_0) = \theta_R^{-1}(T_0) = 0$. The profiles $D \in \mathcal{D}_m$ can be visualized as valleys, with one decreasing profile θ_L^{-1} in the interval $[0, T_0]$ and an increasing one (θ_R^{-1}) on $[T_0, T]$.

Remark 5.7. Given (5.105), the following relationship holds for the broadcast profile $D \in \mathcal{D}_m$ evaluated at $\theta_L(q) \in [0, T_0]$ and $\theta_R(q) \in [T_0, T]$:

$$D(\theta_L(q)) = \theta_L^{-1}(\theta_L(q)) = q = \theta_R^{-1}(\theta_R(q)) = D(\theta_R(q)) \tag{5.106}$$

In order to provide equilibrium conditions under partial flexibility of the appliances, it is useful to introduce the following property:

Proposition 5.9. *For any $D \in \mathcal{D}_m$ the values of $Q_D(D(t))$ are equal to the profile itself:*

$$Q_D(D(t)) = \mu\left(\{s \in [0, T] : D(s) \leq D(t)\}\right) = D(t) \qquad \forall t \in [0, T] \tag{5.107}$$

Proof. Given definition (5.105) for $D \in \mathcal{D}_m$, the function Q_D can be written as follows:

$$\begin{aligned} Q_D(D(t)) &= \mu\left(\{s \in [0, T_0] : \theta_L^{-1}(s) \leq D(t)\}\right) + \mu\left(\{s \in [T_0, T] : \theta_R^{-1}(s) \leq D(t)\}\right) \\ &= \mu\left([\theta_L(D(t)), T_0]\right) + \mu\left([T_0, \theta_R(D(t))]\right) = \theta_R(D(t)) - \theta_L(D(t)) \end{aligned}$$

where the second equality holds for the monotonicity properties of the functions θ_L and θ_R (and consequentially of the inverse θ_L^{-1} and θ_R^{-1}). The proof is concluded by verifying that, following the equality in (5.103), it holds $\theta_R(D(t)) - \theta_L(D(t)) = D(t)$. $\square$

It is interesting to notice that, for $D \in \mathcal{D}_m$, the equilibrium condition (5.102) becomes:

$$D(t) = Q_{D_{a,D}}(D_{a,D}(t)) \qquad \forall t \in [0, T] \tag{5.108}$$

Furthermore, in the considered case, an important property holds also for the power consumption interval of the appliances:

Proposition 5.10. *If one considers a broadcast profile $D \in \mathcal{D}_m$, the power consumption of the single device with $t_{min} = s$, $t_{st} = \tau$ and $E_{tot} = x$ is scheduled (at maximum feasible*

rate x/s) during a compact interval $\bar{\mathcal{S}}_D(s, \tau)$:

$$
\bar{\mathcal{S}}_D(s, \tau) := \begin{cases} [\theta_L(s), \theta_R(s)] & \text{if } \tau \leq \theta_L(s) \\ \\ [\tau, \tau + s] & \text{if } \tau > \theta_L(s) \end{cases} \tag{5.109}
$$

Proof. For the interval in the first case of definition (5.109) it holds $[\theta_L(s), \theta_R(s)] \subseteq [\tau, T]$. Furthermore, considering (5.103) and (5.105), the following properties are satisfied:

$$
\mu\left([\theta_L(s), \theta_R(s)]\right) = s
$$

$$
D(t_1) < D(t_2) \qquad \forall t_1 \in [\theta_L(s), \theta_R(s)], t_2 \notin [\theta_L(s), \theta_R(s)]
$$

For the second case in (5.109), since D is monotonic increasing for $t > T_0$, it is sufficient to show the following:

$$
\tau + s > T_0 \tag{5.110}
$$

$$
D(t) \leq D(\tau + s) \ \forall t \in [\tau, \tau + s]
$$

Given that $\tau > \theta_L(s)$, it is possible to verify that $\tau + s > \theta_L(s) + s = \theta_R(s) > T_0$. For the second inequality in (5.110) two different cases have to be analyzed: if $t > T_0$ then $D(t) = \theta_R^{-1}(t) \leq \theta_R^{-1}(\tau + s) = D(\tau + s)$ from the monotonicity properties of θ_R^{-1}. If $t \in [\tau, T_0]$, from $\tau > \theta_L(s)$ and Remark 5.7, it follows:

$$
D(t) \leq D(\tau) < D(\theta_L(s)) = D(\theta_R(s)) < \theta_R^{-1}(\tau + s) = D(\tau + s)
$$

$\square$

It is now possible to provide the following expression for the optimal power profile at time t of appliances with $t_{min} = s$, $t_{st} = \tau$ and $E_{tot} = x$, when the profile $D \in \mathcal{D}_m$ is broadcast:

$$
\bar{u}^*(t, s, \tau, x) = \begin{cases} \dfrac{x}{s} & \text{if } t \in \bar{\mathcal{S}}_D(s, \tau) \\ \\ 0 & \text{if } t \notin \bar{\mathcal{S}}_D(s, \tau) \end{cases} \tag{5.111}
$$

Having derived the optimal power consumption, it is possible to calculate the resulting flexible demand $D_f(t)$ by evaluating the following integral:

$$
D_f(t) = \int_0^T \int_0^T \int_{\mathcal{E}} m(s, \tau, x) \bar{u}^*(t, s, \tau, x) \, dx \, d\tau \, ds = \int_0^T \int_0^T \frac{f'(s, \tau)}{s} \cdot \mathbb{1}_{\bar{\mathcal{S}}_D(s, \tau)}(t) \, d\tau \, ds \tag{5.112}
$$

Proposition 5.11. *The following expressions of D_f as a function of θ_L and θ_R hold:*

$$
\begin{aligned}
D_f(\theta_L(q)) &= \int_0^{\theta_L(q)} \int_q^T \frac{f'(s,\tau)}{s} \, ds \, d\tau \\
D_f(\theta_R(q)) &= \int_0^{\theta_L(q)} \int_q^T \frac{f'(s,\tau)}{s} \, ds \, d\tau + \int_{\theta_L(q)}^{\theta_R(q)} \int_{\theta_R(q)-\tau}^T \frac{f'(s,\tau)}{s} \, ds \, d\tau
\end{aligned}
\tag{5.113}
$$

Proof. To prove the equality for $D_f(\theta_L(q))$ it is useful to consider definition (5.109) of $\bar{\mathcal{S}}_D$ and notice that no appliance completes its task for $t < T_0$. This means that at time $\theta_L(q) \leq T_0$ the flexible demand can be determined by taking into account only the starting time of power consumption. For any appliance with initial time constraint $\tau < \theta_L(q)$, two cases must be considered: if the task duration at rated power $s \in (\theta_L^{-1}(\tau), T] \subset [q, T]$ then it holds $\tau > \theta_L(s)$ and from (5.109) the starting time is equal to $\tau \leq \theta_L(q)$. If instead $s \in [0, \theta_L^{-1}(\tau)]$, the starting time of power consumption is equal to $\theta_L(s)$ and only devices with task time $s \geq q$ must be accounted for in the computation of flexible demand. This proves the first expression in (5.113). For the expression of $D_f(\theta_R(q))$, the considered values of the parameter τ are lesser or equal than $\theta_R(q)$ and, from (5.109), the same holds for the starting time. The bounds of the integration in s when $\tau \leq \theta_L(q)$ can be determined similarly to the previous case, considering the final time of power consumption. If $\theta_L(q) < \tau \leq \theta_R(q)$ the only possible case to analyze in (5.109) is $\tau > \theta_L(s)$, when the interval of power consumption scheduled by the devices equals $[\tau, \tau + s]$. To account for the appliances that are operating at $t = \theta_R(q)$ it is sufficient to impose $\tau + s \geq \theta_R(q)$ and therefore $s \geq \theta_R(q) - \tau$. $\square$

It is straightforward to obtain an expression for the resulting aggregate demand $D_{a,D}$:

$$
\begin{aligned}
D_{a,D}(\theta_L(q)) &= D_i(\theta_L(q)) + D_f(\theta_L(q)) \\
D_{a,D}(\theta_R(q)) &= D_i(\theta_R(q)) + D_f(\theta_R(q))
\end{aligned}
\tag{5.114}
$$

5.7.3 Sufficient Conditions for Nash Equilibrium

Having calculated flexible and aggregate demand as functions of θ_L and θ_R corresponding to the broadcast $D \in \mathcal{D}_m$, it is possible to provide the following result:

Theorem 5.7. *The equilibrium condition (5.101) is satisfied for $D \in \mathcal{D}_m$ if, for the corresponding functions θ_L, θ_R and profile of aggregate demand $D_{a,D}$, it holds:*

$$
\begin{aligned}
&\frac{d}{dq} D_{a,D}(\theta_L(q)) > 0 \\
&\frac{d}{dq} D_{a,D}(\theta_L(q)) = \frac{d}{dq} D_{a,D}(\theta_R(q))
\end{aligned}
\qquad \forall q \in [0, T]
\tag{5.115}
$$

Proof. By the first equality in (5.104), $D_{a,D}(\theta_L(0)) = D_{a,D}(\theta_R(0)) = D_{a,D}(T_0)$. Therefore, the second condition in (5.115) is equivalent to:

$$D_{a,D}(\theta_L(q)) = D_{a,D}(\theta_R(q)) \quad \forall q \in [0, T].$$

Moreover, (5.115) and monotonicity of the functions θ_L and θ_R imply the following inequalities for all $q \in [0, T]$:

$$
\begin{aligned}
D_{a,D}(t) &\leq D_{a,D}(\theta_L(q)) = D_{a,D}(\theta_R(q)) & \text{if} \quad \theta_L(q) \leq t \leq \theta_R(q) \\
D_{a,D}(t) &> D_{a,D}(\theta_L(q)) = D_{a,D}(\theta_R(q)) & \text{otherwise}
\end{aligned}
\tag{5.116}
$$

To see this, consider t such that $\theta_L(q) \leq t \leq T_0$: by monotonicity and continuity of θ_L there exists $\bar{q} \leq q$ such that $\theta_L(\bar{q}) = t$ and therefore, from the inequality in (5.115):

$$D_{a,D}(t) = D_{a,D}(\theta_L(\bar{q})) \leq D_{a,D}(\theta_L(q))$$

Similarly, when $t < \theta_L(q)$, there exists $\bar{q} > q$ such that $\theta_L(\bar{q}) = t$ and $D_{a,D}(t) = D_{a,D}(\theta_L(\bar{q})) > D_{a,D}(\theta_L(q))$. The inequalities in (5.116) can be verified for $t > T_0$ in a similar manner, considering in this case the increasing function θ_R. It is now possible to provide the following expression for the measure function Q of the aggregate demand:

$$
\begin{aligned}
Q_{D_{a,D}}(D_{a,D}(\theta_R(q))) = Q_{D_{a,D}}(D_{a,D}(\theta_L(q))) &= \mu\left(\{s : D_{a,D}(s) \leq D_{a,D}(\theta_L(q))\}\right) \\
&= \theta_R(q) - \theta_L(q) = q
\end{aligned}
\tag{5.117}
$$

If one evaluates (5.117) at $q = D(t)$ with $t \leq T_0$, recalling that $\theta_L(D(t)) = t$ from (5.105), it holds:

$$Q_{D_{a,D}}(D_{a,D}(t)) = Q_{D_{a,D}}(D_{a,D}(\theta_L(D(t)))) = \theta_R(D(t)) - \theta_L(D(t)) = D(t)$$

The same result is obtained by considering $q = D(t)$ when $t > T_0$ and therefore $\theta_R(D(t)) = t$. We can then conclude that $Q_{D_{a,D}}(D_{a,D}(t)) = D(t)$ for all $t \in [0, T]$ and therefore (5.108), which is equivalent to the equilibrium condition (5.102) in Proposition 5.8, is satisfied. $\qquad\square$

Proposition 5.8 and Theorem 5.7 provide conditions for the existence of an equilibrium in the sense described by (5.101) by verifying that the optimal power profile of the devices, defined in (5.100), is identical when the broadcast D or the resulting aggregate demand $D_{a,D}$ are considered. Such conditions are only sufficient since the optimal power profile is unique and equal to (5.100) only if the broadcast signal satisfies Assumption 5.2. If such assumption holds not only for the function D but also for the resulting aggregate demand, the equilibrium conditions become also necessary.

5.7.4   Synthesis Technique and Simulations

Following the results of Theorem 5.7, it is also possible to provide a constructive technique which verifies, for a given D_i and f', if there exists a profile $D \in \mathcal{D}_m$ which satisfies (5.115) and allows to calculate it numerically. To do so, it is useful to derive expressions for the derivatives with respect to the variable q of the different demand components:

$$\frac{d}{dq}D_i(\theta_L(q)) = \frac{dD_i(t)}{dt}\bigg|_{t=\theta_L(q)} \dot{\theta}_L(q)$$

$$\frac{d}{dq}D_i(\theta_R(q)) = \frac{dD_i(t)}{dt}\bigg|_{t=\theta_R(q)} \dot{\theta}_R(q)$$

$$\frac{d}{dq}D_f(\theta_L(q)) = \int_q^T \frac{f'(s,\theta_L(q))}{s} ds \cdot \dot{\theta}_L(q) - \int_0^{\theta_L(q)} \frac{f'(q,\tau)}{q} d\tau = G_1(q) \cdot \dot{\theta}_L(q) - G_2(q)$$

$$\frac{d}{dq}D_f(\theta_R(q)) = \frac{d}{dq}D_f(\theta_L(q)) + \int_0^T \frac{f'(s,\theta_R(q))}{s} ds \cdot \dot{\theta}_R(q)$$

$$- \int_{\theta_R(q)-\theta_L(q)}^T \frac{f'(s,\theta_L(q))}{s} ds \cdot \dot{\theta}_L(q) - \int_{\theta_L(q)}^{\theta_R(q)} \frac{f'(\theta_R(q)-\tau,\tau)}{\theta_R(q)-\tau} d\tau \cdot \dot{\theta}_R(q)$$

$$= G_1(q) \cdot \dot{\theta}_L(q) - G_2(q) + G_3(q) \cdot \dot{\theta}_R(q) - G_4(q) \cdot \dot{\theta}_L(q) - G_5(q) \cdot \dot{\theta}_R(q)$$

$$\tag{5.118}$$

By replacing (5.118) in the equation of (5.115), it is possible to calculate $\theta_L(q)$ and $\theta_R(q)$ as the solution of the following dynamical system:

$$\dot{\theta}_L(q) = \frac{\frac{dD_i(t)}{dt}\bigg|_{t=\theta_R(q)} + G_3(q) - G_5(q)}{\frac{dD_i(t)}{dt}\bigg|_{t=\theta_L(q)} - \frac{dD_i(t)}{dt}\bigg|_{t=\theta_R(q)} - G_3(q) + G_4(q) + G_5(q)} \tag{5.119}$$

$$\dot{\theta}_R(q) = 1 + \dot{\theta}_L(q) \qquad \theta_L(0) = T_0 \qquad \theta_R(0) = T_0$$

If the solution satisfies the inequalities in (5.103) and (5.115) for some $T_0 \in [0,T]$, the corresponding $D \in \mathcal{D}_m$ defined according to (5.105) induces an equilibrium. To determine T_0, it is useful to consider the equality in (5.115), evaluated at $\theta_L(q) = \theta_R(q) = T_0$:

$$\dot{D}_{a,D}(T_0) - \dot{D}_{a,D}(T_0) = \left[\frac{dD_i(t)}{dt}\bigg|_{t=T_0} + \int_0^T \frac{f'(s,T_0)}{s} ds \right] = 0 \tag{5.120}$$

The described technique, given the hypothesis on the broadcast D and the fact that the power consumption of each appliance occurs during a compact time interval, is particularly suited for dealing with valleys in the inflexible demand. A qualitative example is now simulated with $T = 12h$, considering a parabolic profile for the inflexible demand

and an appliances population that requires $10GWh$ of total energy. The distribution of the parameter t_{st} has been modelled with a truncated gaussian with mean equal to $5h$ while the values of minimum task time t_{min} are in the range $[2h, 5h]$. The resulting function $f'(t_{min}, t_{st})$ is shown in Fig. 5.11. The initial condition T_0 for θ_L and θ_R has been calculated using (5.120) and is equal to $4.21h$. The equations in (5.119) have been integrated and the broadcast profile D has been obtained with (5.105). The corresponding measure Q_D is compared in Fig. 5.12 with the functions Q of the inflexible and aggregate demand. The comparison of the demand profiles is presented in Fig. 5.13. As expected, the measure $Q_{D_a,D}$ of the aggregate demand is equal to the function D and therefore an equilibrium is achieved according to (5.108). Notice also that D has a minimum at time $T_0 = 4.21h$ while the minimum in D_i is achieved at $t = 6h$. This is due to the time constraint t_{st}: the earlier power scheduling of devices with lower values of t_{st} (during a time interval which is not characterized by the lowest values of inflexible demand) will be balanced by the other appliances which are constrained to operate at later times.

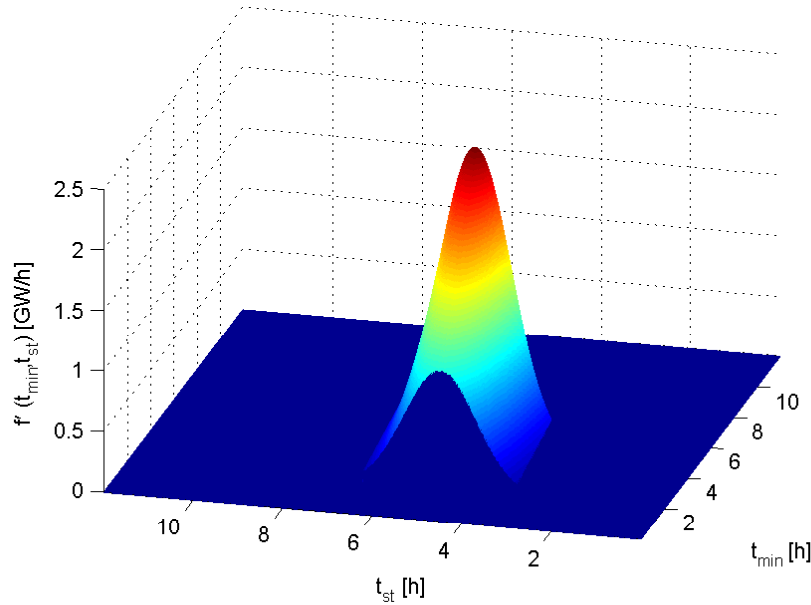FIGURE 5.11: Density f' of the considered population as a function of the minimum task time t_{min} and initial time constraint t_{st},
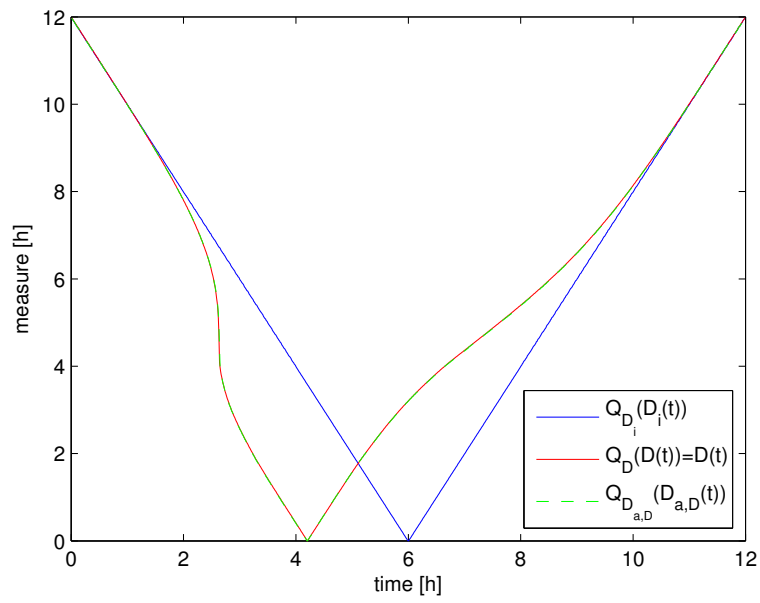
FIGURE 5.12: Comparison of the measure function Q for the inflexible demand D_i, broadcast signal D and resulting aggregate demand $D_{a,D}$.
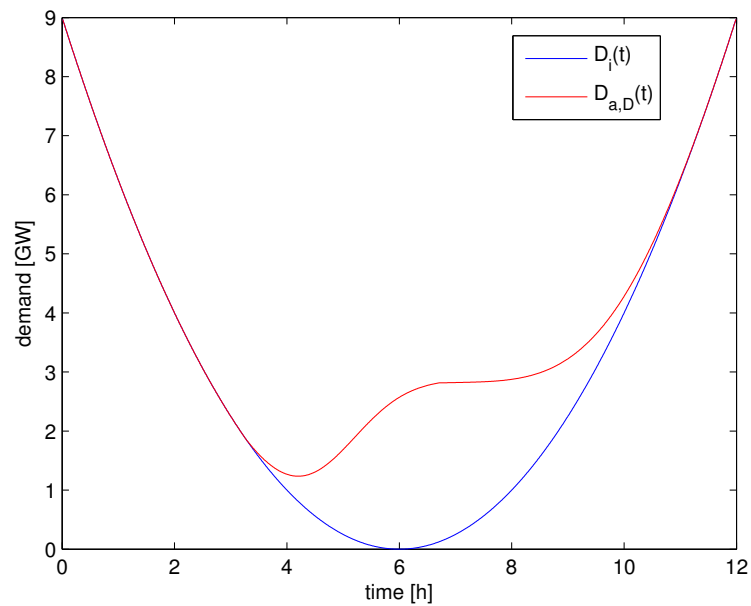

FIGURE 5.13: Values of inflexible demand D_i and aggregate profile $D_{a,D}$ obtained when the function D is broadcast.

5.8   Conclusions

This chapter describes a novel methodology for the management of large populations of flexible appliances which schedule their power consumption on the basis of a broadcast price signal. Necessary and sufficient conditions are presented for convergence to a Nash Equilibrium in one step. This is done by describing the devices population as a continuum, abstracting its valley-filling capabilities through a power density of task durations and then comparing this with the considered profile of inflexible demand, described by its negotiable valley capacity. The equilibrium conditions are then extended, introducing time-varying proportional constraints on the power of the devices. Such constraints are calculated in order to induce an equilibrium and, at the same time, minimize the task time of the appliances and optimize some global cost function. The case of partial flexibility of the devices is also considered, providing a design method for a broadcast signal which induces an equilibrium under additional time constraints.

Chapter 6

Conclusions and Future Research

6.1 Conclusions

This work has tackled some of the new challenges that arise in the context of the smart grid, proposing control strategies that are specifically designed for the management of a large number of agents. In particular, two main aspects of the future power system have been considered: frequency control with variable-speed wind turbines and management of large populations of price-responsive devices (storage and flexible appliances).

The first part of this thesis is focused on new methods for providing frequency response with wind generators. Initially, an overview is given of the frequency stability issues resulting from high penetration of wind turbines and corresponding reduction of system inertia. The main approaches proposed in the literature are described and a new distributed stochastic control strategy is presented. In particular, the single generator is modelled as a stochastic hybrid system that can operate in two discrete modes, which correspond to different levels of efficiency and generated power. Transitions between these two modes are random and are driven by frequency-dependent switching functions: the single turbine behaves stochastically and, at the same time, large populations perform deterministically, changing the aggregate generated power in response to frequency fluctuations. The main element of novelty is the stochastic repartition of the control effort among the individual generators: the responses of the single turbines are in general different, synchronicity of the generators is avoided and no additional communication infrastructure is required. The stability and robustness of the control strategy are shown theoretically and then evaluated in simulations.

The possibility to provide frequency response through temporary overproduction is also considered: following a fault in the system, the turbines can increase their generated

power by slowing down and releasing part of the kinetic energy stored in the rotating shafts. An optimal scheduling of the turbines is presented, determining the repartition of extra power among the single generators in order to optimize some global criterion. In particular, two different cases are considered, assuming respectively that the electric torque of the turbines can correspond to two distinct expressions or can be arbitrarily set. In this last scenario, the objective is to minimize the efficiency losses resulting from the overproduction, considering a wind speed different in general for each turbine and taking into account the physical limitations of the generators.

In the second part of the thesis, the coordination of large populations of micro-storage devices which perform energy arbitrage (charge/discharge on the basis of current energy prices) is considered. The main element of difficulty is that the charge profile of the appliances modifies the price of energy and therefore can prevent convergence to an equilibrium (i.e. all devices charge when price is low and peak demand is only shifted). The state of the art for this subject is discussed, presenting the different approaches investigated so far (centralized/distributed/game theory). The main idea for the novel proposed control strategy is to approximate the number of devices as infinite, describing the population as a continuum: the price variation introduced by the single agent becomes negligible and only the general behaviour of the population must be considered. The problem can then be modelled as a mean field game described by two coupled partial differential equations. Numerical resolution of these equations allows to determine a control strategy of the devices which is optimal for a certain price function and, at the same time, induces it when applied. A decentralized implementation can be obtained by broadcasting the mentioned price function to the devices, which are then able to perform their optimization independently. Extensions to the initial model are also considered, introducing cyclic constraints, multiple populations of appliances and uncertainties in the system.

The last section of this thesis deals with the similar problem of large populations of price-responsive flexible appliances that schedule their power consumption during the time intervals characterized by cheapest energy. As in the previous case, it is necessary to account for the change in energy prices that these devices introduce with their operation strategies. The presented analytic methods allow to derive necessary and sufficient conditions for the existence of a Nash equilibrium: all appliances, which have optimized their power consumption according to a broadcast price signal, have no interest in unilaterally changing their policy when the resulting price of aggregate demand is considered. These results are obtained by comparing two different functions which describe respectively the valley capacity of the inflexible demand and the global properties of the flexible devices. The equilibrium conditions can be extended by introducing time-varying proportional constraints on the maximum power of the appliances. The

case of partial flexibility is also studied, considering in particular devices which can only operate after a specified time instant.

6.2 Future Research Directions

6.2.1 Stochastic Distributed Control of Wind Turbines

One of the most promising extensions of the stochastic control strategy described in Chapter 2 for frequency response is the implementation of a more detailed model of the individual turbine. In particular, it could be considered that the power extracted from the wind is in general cubic with respect to the rotor speed, which also affects the efficiency of the generator. The first attempts in this sense have shown that it is not possible to provide a complete model of the turbines population with moments of finite orders like in the original case. This problem could be solved by introducing a moment truncation, verifying that the result is a reasonable approximation of the actual system and preserves the stability properties presented in the initial analysis.

6.2.2 Scheduling of Wind Generators for Frequency Response

For the scheduling of wind turbines presented in Chapter 3, it seems that the most promising research direction would be to extend the scenarios under which the proposed control algorithms can be applied. In particular, a wider range of wind speeds could be considered and the pitch angle of the turbines could be included as an additional actuator. Furthermore, one could provide frequency response with only a fraction of generators, using the remaining ones to support their recovery phase. In this way, after the frequency support, the resulting reduction of aggregate power from the turbines would be postponed, being easier to manage for the rest of the power system.

6.2.3 Energy Arbitrage with Micro-storage Devices

Regarding the distributed control of micro-storage devices, the following elements seem to be of particular importance:

- Theoretical results of existence and uniqueness for the solution of the mean field game equations. In particular, it would be interesting to understand if there is a maximum penetration of storage for which an equilibrium can be achieved. Furthermore, there may be some cases where multiple equilibria exist and one has

to determine which one corresponds to desired configuration of the system, for example evaluating some global performance index.

- Consider a model of the individual device where efficiency is accounted by introducing linear losses on the charging power. This would represent a more realistic representation of the storage devices which are currently being developed. On the other hand, the resulting optimal control of the devices in this case would be discontinuous, preventing the application of the numerical methods considered so far.

- Extensions of the current framework in order to account for devices which provide additional ancillary services. For example, the storage population could provide reserve: following errors in the demand forecast or unforeseen generation unavailability, the devices could contribute to compensate supply/demand imbalances. A possibility is to model these events stochastically, introducing a different cost function for the devices which perform this additional task.

- Account explicitly for demand uncertainties: instead of adopting a receding horizon strategy to deal with uncertainties on the inflexible demand profile, one could incorporate these forecast errors in the model, for example considering mean field games with major and minor players.

6.2.4 Equilibria in Energy Markets with Large Populations of Flexible Appliances

The most interesting extension of the equilibrium analysis presented in Chapter 5 is to remove the assumption that prescribes no level sets of positive measure for the broadcast demand. In this case the optimal control of the devices is in general not unique: the expression for the flexible demand and the equilibrium conditions provided so far do not longer apply. It is worth investigating whether other kinds of Nash equilibria exist and what is the level of coordination between the devices which is required to achieve them. Furthermore, a broader analysis for the case of devices with partial flexibility could be provided. In principle, one could consider appliances which can arbitrarily specify a time set during which they are available to operate. It would be interesting to understand how this limited flexibility impacts the fairness of the game and the pay-off of the individual player.

Bibliography

[1] O. Anaya-Lara, F. Hughes, N. Jenkins, and G. Strbac, "Contribution of DFIG-based wind farms to power system short-term frequency regulation," *IEE Proceedings - Generation, Trasmission and Distribution*, vol. 153, no. 2, pp. 164–170, 2006.

[2] S. Kuenzel, L. Kunjumuhammed, B. Pal, and I. Erlich, "Impact of wakes on wind farm inertial response," *IEEE Transactions on Sustainable Energy*, vol. 5, no. 1, pp. 237–245, 2014.

[3] Department of Energy & Climate Change. UK renewable energy roadmap. [Online]. Available: https://www.gov.uk/government/uploads/system/uploads/attachment_data/file/48128/2167-uk-renewable-energy-roadmap.pdf

[4] Parliament of the United Kingdom. Climate change act 2008. [Online]. Available: http://www.legislation.gov.uk/ukpga/2008/27/contents

[5] European Commission. Energy 2020 a strategy for competitive, sustainable and secure energy. [Online]. Available: http://eur-lex.europa.eu/legal-content/EN/TXT/?qid=1409650806265&uri=CELEX:52010DC0639

[6] European Commission. A policy framework for climate and energy in the period from 2020 to 2030. [Online]. Available: http://eur-lex.europa.eu/legal-content/EN/ALL/?uri=CELEX:52014DC0015

[7] "Pathways to high penetration of electric vehicles," Element Energy Limited, 20 Station Rd, Cambridge (UK), Tech. Rep., Dec. 2013.

[8] Department of Energy & Climate Change. The future of heating: A strategic framework for heat in the UK. [Online]. Available: https://www.gov.uk/government/uploads/system/uploads/attachment_data/file/48574/4805-future-heating-strategic-framework.pdf

[9] A. Ipakchi, "Grid of the future," *IEEE Power and Energy Magazine*, vol. 7, no. 2, pp. 52–62, 2009.

[10] European Commission. Smart Grids: from innovation to deployment. [Online]. Available: https://www.smartgrid.gov/sites/default/files/doc/files/Smart_Grids_From_Innovation_to_Deployment_201102.pdf

[11] P. Kundur, J. Paserba, V. Ajjarapu, G. Andersson, A. Bose, C. C. nizares, N. Hatziargyriou, D. Hill, A. Stankovic, C. Taylor, T. V. Cutsem, and V. Vittal, "Definition and classification of power system stability," *IEEE Transactions on Power Systems*, vol. 19, no. 2, pp. 1387–1401, 2004.

[12] P. Kundur, *Power System Stability and Control*. New York: Ed. McGraw-Hill, 1994.

[13] (2012) Department of Energy & Climate Change. [Online]. Available: http://www.decc.gov.uk/en/content/cms/meeting_energy/renewable_ener/renewable_ener.aspx/

[14] I. D. Margaris, A. D. Hansen, P. Sørensen, and Hatziargyriou, "Illustration of modern wind turbine ancillary services," *Energies*, vol. 3, no. 6, pp. 1290–1302, 2010.

[15] G. Lalor, A. Mullane, and M. O'Malley, "Frequency control and wind turbine technologies," *IEEE Transactions on Power Systems*, vol. 20, no. 4, pp. 1905–1913, 2005.

[16] "Grid code - high and extra high voltage," E.ON Netz GmbH, Bayreuth, Germany, Tech. Rep., Apr. 2006.

[17] "Technical requirements for the connection of generation facilities to the hydro-quebec transmission system: Suppl. requirements for wind generation," Hydro-Quebec, Tech. Rep., May 2003 Revised 2005.

[18] "Nordic grid code 2007 (nordic collection of rules)," Nordel, Tech. Rep., January 2004 Updated 2007.

[19] National Grid, "Grid code documents - connection conditions, Tech. Rep. Issue 4, 24 June 2009.

[20] K. Li and Z. Chen, "Overview of different wind generator systems and their comparisons," *IET Renewable Power Generations*, vol. 2, no. 2, pp. 123–138, 2008.

[21] A. Arulampalam, G. Ramtharan, N. Jenkins, V. K. Ramachandaramutrhy, J. Ekanayake, and G. Strbac, "Trends in wind power technology and grid code requirements," in *Second International Conference on Industrial and Information Systems, ICIIS 2007*, 2007, pp. 129–134.

[22] T. Burton, N. Jenkins, D. Sharpe, and E. Bossanyi, *Wind energy handbook*. Chichester (UK): John Wiley and Sons, 2001, ch. 8.3.2, pp. 481–482.

[23] L. Holdsworth, J. B. Ekanayake, and N. Jenkins, "Power system frequency response from fixed speed and doubly fed induction generator-based wind turbines," *Wind Energy*, vol. 7, no. 1, pp. 21–35, 2004.

[24] A. Mullane and M. O'Malley, "The inertial response of induction-machine-based wind turbines," *IEEE Transactions on Power Systems*, vol. 20, no. 3, pp. 1496–1503, 2005.

[25] R. de Almeyda and J. Peças Lopes, "Participation of doubly fed induction wind generators in system frequency regulation," *IEEE Transactions on Power Systems*, vol. 22, no. 3, pp. 944–950, 2007.

[26] L. Chang-Chien, W. Lin, and Y. Yin, "Enhancing frequency response control by DFIGs in the high wind penetrated power systems," *IEEE Transactions on Power Systems*, vol. 26, no. 2, pp. 710–718, 2011.

[27] J. Ekanayake and N. Jenkins, "Comparison of the response of doubly fed and fixed-speed induction generator wind turbines to changes in network frequency," *IEEE Transactions on Energy Conversion*, vol. 19, no. 4, pp. 800–802, 2004.

[28] J. Mauricio, A. Marano, A. Gómez-Exposito, and J. Martínez Ramos, "Frequency regulation contribution through variable-speed wind energy conversion systems," *IEEE Transactions on Power Systems*, vol. 24, no. 1, pp. 173–180, 2009.

[29] F. M. Hughes, O. Anaya-Lara, N. Jenkins, and G. Strbac, "Control of DFIG-based wind generation for power network support," *IEEE Transactions on Power System*, vol. 20, no. 4, pp. 1958–1966, 2005.

[30] P. Moutis, E. Loukarakis, S. Papathanasiou, and N. D. Hatziargyriou, "Primary load-frequency control from pitch-controlled wind turbines," *PowerTech, 2009 IEEE Bucharest*, pp. 1–7, 2009.

[31] N. van Deelen, A. Jokic, P. van den Bosch, and R. Hermans, "Exploiting inertia of wind turbines in power network frequency control: A model predictive control approach," *2011 IEEE International Conference on Control Applications (CCA)*, pp. 1309–1314, 2011.

[32] D. Angeli and P. Kountouriotus, "A stochastic approach to 'dynamic-demand' refrigerator control," *IEEE Transactions on Control Systems Technology*, vol. 20, no. 3, pp. 581–592, 2012.

[33] J. P. Hespanha, "Modelling and analysis of stochastic hybrid systems," *Control Theory and Applications, IEE Proceedings*, vol. 153, no. 5, pp. 520–535, 2006.

[34] S. Asmussen and P. W. Glynn, *Stochastic Simulation: Algorithms and Analysis.* New York: Springer, 2007.

[35] F. Hanson, *Applied Stochastic Processes and Control for Jump-Diffusions: Modeling, Analysis and Computation, pp. 4256-4261.* SIAM books, 2007.

[36] J. Ackermann, *Robust Control - The Parameter Space approach.* London (UK): Springer-Verlag, 2002, pp. 19–20.

[37] A. Papachristodoulou and S. Prajna, "On the construction of Lyapunov functions using the sum of squares decomposition," *Proceedings of the 41st IEEE Conference on Decision and Control, 2002*, vol. 3, pp. 3482–3487, 2002.

[38] S. Prajna, A. Papachristodoulou, and P. Parrilo, "Introducing SOSTOOLS: A general purpose sum of squares programming solver," *Proceedings of the 41st IEEE Conference on Decision and Control, 2002*, vol. 1, pp. 741–746, 2002.

[39] M. Farkas, *Periodic Motions (Applied Mathematical Sciences), Thm. 7.2.3, pp 417-418.* London, UK: Springer-Verlag, 1994.

[40] D. Shevitz and B. Paden, "Lyapunov stability theorem of nonsmooth systems," *IEEE Transactions on Automatic Control*, vol. 39, no. 9, pp. 1910–1914, 1994.

[41] J. Slootweg, H. Polinder, and W. Kling, "Dynamic modelling of a wind turbine with doubly fed induction generator," in *Power Engineering Society Summer Meeting, 2001*, vol. 1, pp. 644–649.

[42] G. C. Evans, "Volterra's integral equation of the second kind, with discontinuous kernel," *Transactions of the American Mathematical Society*, vol. 11, no. 4, pp. 393,413, 1910.

[43] S. Boyd and L. Vandenberghe, *Convex optimization.* Cambridge University Press, 2004, ch. 5, pp. 243–244.

[44] R. K. Sundaram, *A first course in optimization theory.* Cambridge University Press, 2014, ch. 9.2.2, pp. 237–238.

[45] G. Birkhoff and G. C. Rota, *Ordinary differential equations.* John Wiley and Sons, 1978, ch. 12, pp. 26–27.

[46] D. Angeli and E. Sontag, "Monotone control systems," *IEEE Transactions on Automatic Control*, vol. 48, no. 10, pp. 1684–1698, 2003.

[47] Department for Business Innovation & Skills. (2013) The smart city market: Opportunities for the UK. [Online]. Available: https://www.gov.uk/government/uploads/system/uploads/attachment_data/file/249423/bis-13-1217-smart-city-market-opportunties-uk.pdf

[48] M. Dijk and M. Yarime, "The emergence of hybrid-electric cars: Innovation path creation through coevolution of supply and demand," *Technological Forecasting & Social Change*, vol. 77, pp. 1371–1390, 2010.

[49] X. Luo, J. Wang, M. Dooner, and J. Clarke, "Overview of current development in electrical energy storage technologies and the application potential in power system operation," *Applied Energy*, vol. 137, pp. 511–536, 2015.

[50] K. Bhattacharya, M. Bollen, and J. Daalder, *Operation of Restructured Power System*. London: Kluwer Academic Publishers, 2001.

[51] S. Vazquez, S. M. Lukic, E. Galvan, L. G. Franquelo, and J. M. Carrasco, "Energy storage systems for transport and grid applications," *IEEE Transactions on Industrial Electronics*, vol. 57, no. 12, pp. 3881–3895, 2010.

[52] M. Black and G. Strbac, "Value of bulk energy storage for managing wind power fluctuations," *IEEE Transactions on Energy Conversion*, vol. 22, no. 1, pp. 197–205, 2007.

[53] S. D. Howell, P. W. Duck, P. V. Johnson, G. Strbac, A. Hazel, N. Proudlove, and M. Black, "A PDE system for modelling stochastic storage in physical and financial systems," *IMA Journal of Management Mathematics*, vol. 22, no. 3, pp. 231–252, 2011.

[54] R. J. Kerestes, G. F. Reed, and A. R. Sparacino, "Economic analysis of grid level energy storage for the application of load leveling," in *Power and Energy Society General Meeting, 2012 IEEE*, 2012, pp. 1–9.

[55] A. Oudalov, D. Chartouni, and C. Ohler, "Optimizing a battery energy storage system for primary frequency control," *IEEE Transactions on Power Systems*, vol. 22, no. 3, pp. 1259–1266, 2007.

[56] (2013) Lithium Energy Japan. [Online]. Available: http://lithiumenergy.jp/en/products/

[57] (2013) ELII Power Co. Ltd. [Online]. Available: http://eliiypower.co.jp/english/lithium-ion/

[58] G. Strbac, "Demand side management: Benefits and challenges," *Energy Policy*, vol. 36, no. 12, pp. 4419–4426, 2008.

[59] M. Albadi and E. El-Saadany, "A summary of demand response in electricity markets," *Electric Power Systems Research*, vol. 78, no. 11, pp. 1989–1996, 2008.

[60] "Benefits of demand response in electricity markets and reccomendations for achieving them," US Department of Energy, Washington, USA, Tech. Rep., Feb. 2006.

[61] P. Khajavi, H. Abniki, and A. B. Arani, "The role of incentive based demand response programs in smart grid," in *Environment and Electrical Engineering (EEEIC), 2011 10th International Conference on*, 2011, pp. 1–4.

[62] Z. Zhao, L. Wu, and G. Song, "Convergence of volatile power markets with price-based demand response," *IEEE Transactions on Power Systems*, vol. 29, no. 5, pp. 2107–2118, 2014.

[63] C. L. Su and D. Kirschen, "Quantifying the effect of demand response on electricity markets," *IEEE Transactions on Power System*, vol. 24, no. 3, pp. 1199–1207, 2009.

[64] P. Samadi, H. Mohsenian-Rad, R. Schober, and V. W. S. Wong, "Advanced demand side management for the future smart grid using mechanism design," *IEEE Transactions on Smart Grid*, vol. 3, no. 3, pp. 1170–1180, 2012.

[65] T. D. Voice, P. Vytelingum, S. D. R. A. Rogers, and N. R. Jennings, "Decentralised control of micro-storage in the smart grid," *AAAI-11: Twenty-Fifth Conference on Artificial Intelligence, 2011*, pp. 1421–1426.

[66] Z. Fan, "A distributed demand response algorithm and its application to PHEV charging in smart grids," *IEEE Transactions on Smart Grid*, vol. 3, no. 3, pp. 1280–1290, 2012.

[67] P. Vytelingum, T. D. Voice, S. D. Ramchurn, A. Rogers, and N. R. Jennings, "Theoretical and practical foundations of large-scale agent-based micro-storage in the smart grid," *Journal of Artificial Intelligence Research*, vol. 42, no. 1, pp. 765–813, 2011.

[68] Z. Ma, D. Callaway, and I. Hiskens, "Decentralized charging control of large populations of plug-in electric vehicles," *IEEE Transactions on Control Systems Technology*, vol. 21, no. 1, pp. 67–78, 2013.

[69] L. Gan, U. Topcu, and S. H. Low, "Optimal decentralized protocol for electric vehicle charging," *IEEE Transactions on Power Systems*, vol. 28, no. 2, pp. 940–951, 2013.

[70] D. Papadaskalopoulos and G. Strbac, "Decentralized participation of flexible demand in electricity markets," *IEEE Transactions on Power Systems*, vol. 28, no. 4, pp. 3658–3666, 2013.

[71] M. Huang, P. E. Caines, and R. P. Malhamé, "An invariance principle in large population stochastic dynamic games," *Journal of Systems Science and Complexity*, vol. 20, no. 2, pp. 162–172, 2007.

[72] M. Huang, P. E. Caines, and R. P. Malhamé, "Large population stochastic dynamic games: Closed-loop mckean-vlasov systems and the nash certainty equivalence principle," *Communications in Information and Systems*, vol. 6, no. 3, pp. 221–252, 2006.

[73] J. M. Lasry and P. L. Lions, "Mean field games," *Japanese Journal of Mathematics*, vol. 2, no. 1, pp. 229–260, 2007.

[74] O. Guéant, J. M. Lasry, and P. L. Lions, "Mean field games and applications," *Paris-Princeton Lectures on Mathematical Finance 2010*, vol. 2003, pp. 205–266, 2011.

[75] P. Cardaliaguet. Notes on mean field games. [Online]. Available: https://www.ceremade.dauphine.fr/~cardalia/MFG100629.pdf

[76] M. Nourian and P. E. Caines, "ϵ-nash mean field game theory for nonlinear stochastic dynamical systems with major and minor agents," *SIAM Journal on Control and Optimization*, [To Be Published].

[77] H. Tembine, "Nonasymptotic mean-field games," *IEEE Transactions on Cybernetics*, vol. 44, no. 12, pp. 2744–2756, 2014.

[78] Y. Achdou and I. Capuzzo-Dolcetta, "Mean field games: Numerical methods," *SIAM Journal on Numerical Analysis*, vol. 48, no. 3, pp. 1136–1162, 2010.

[79] Y. Achdou, F. Camilli, and I. Capuzzo-Dolcetta, "Mean field games: Numerical methods for the planning problem," *SIAM Journal on Control and Optimization*, vol. 50, no. 1, pp. 77–109, 2012.

[80] A. Lachapelle and M. T. Wolfram, "On a mean field game approach modeling congestion and aversion in pedestrian crowds," *Transportation Research Part B: Methodological*, vol. 45, no. 10, pp. 1572–1589, 2011.

[81] C. Dogbé, "Modeling crowd dynamics by the mean-field limit approach," *Mathematical and Computer Modelling*, vol. 52, no. 9-10, pp. 1506–1520, 2010.

[82] A. Lachapelle, J. Salomon, and G. Turinici, "Computation of mean field equilibria in economics," *Mathematical Models and Methods in Applied Science*, vol. 20, no. 4, pp. 567–588, 2010.

[83] G. Y. Weintraub, C. L. Benkard, and B. V. Roy, "Markov perfect industry dynamics with many firms," *Econometrica*, vol. 76, no. 6, pp. 1375–1411, 2008.

[84] M. Nourian and P. E. C. nd R. P. Malhamé, "Nash, social and centralized solutions to consensus problems via mean field control theory," *IEEE Transactions on Automatic Control*, vol. 58, no. 3, pp. 639–653, 2013.

[85] R. Couillet, S. M. Perlaza, H. Tembine, and M. Debbah, "Electric vehicles in the smart grid: a mean field game analysis," *IEEE Transactions on Control Systems Technology*, vol. 21, no. 1, pp. 67–78, 2013.

[86] A. C. Kizilkale, S. Mannor, and P. E. Caines, "Large scale real-time bidding in the smart grid: A mean field framework," *Proceedings of the 51st IEEE Conference on Decision and Control, 2012*, pp. 3680 – 3687, 2013.

[87] F. Bagagiolo and D. Bauso, "Mean-field games and dynamic demand management in power grids," *Dynamic Games and Applications*, vol. 4, no. 2, pp. 155–176, 2014.

[88] L. G. Esparza, G. M. Torres, and L. M. S. Torres, "Introduction to differential games," *International Journal of Physical and Mathematical Sciences*, vol. 4, no. 1, pp. 396–411, 2013.

[89] A. Seierstad and K. Sydsaeter, "Sufficient conditions in optimal control theory," *International Economic Review*, vol. 18, no. 2, pp. 367–391, 1977.

[90] R. P. Agarwal, D. O'Regan, and D. Sahu, *Fixed Point Theory for Lipschitzian-type Mappings with Applications*. London: Springer, 2009.

[91] D. A. Gomes and J. Saúde, "Mean field games models - a brief survey," *Dynamic Games and Applications*, vol. 4, no. 2, pp. 110–154, 2014.

[92] E. Carlini and F. Silva, "A fully discrete semi-lagrangian scheme for a first order mean field game problem," *SIAM Journal on Numerical Analysis*, vol. 52, no. 1, pp. 45–67, 2014.

[93] M. Bardi and I. Capuzzo-Dolcetta, *Optimal Control and Viscosity Solutions of Hamilton-Jacobi-Bellman Equations*. Basel: Birkhauser, 2008.

[94] S. Wang, F. Gao, and K. L. Teo, "An upwind finite-difference method for the approximation of viscosity solutions to hamilton-jacobi-bellman equations," *IMA Journal of Mathematical Control and Information*, vol. 17, no. 2, pp. 167–178, 2000.

[95] R. J. LeVeque, *Numerical Methods for Conservation Laws.* Basel: Birkhauser-Verlag, 1990.

[96] National Grid. Metered half-hourly electricity demands. [Online]. Available: http://www.nationalgrid.com/uk/Electricity/Data/Demand+Data/

[97] P. Vytelingum, T. D. Voice, S. D. Ramchurn, A. Rogers, and N. R. Jennings, "Agent-based micro-storage management for the smart grid," *The Ninth International Conference on Autonomous Agents and Multiagent Systems (AAMAS 2010)*, pp. 39–46.

[98] R. Doherty and M. O'Malley, "A new approach to quantify reserve demand in systems with significant installed wind capacity," *IEEE Transactions on Power Systems*, vol. 20, no. 2, pp. 587–595, 2005.

[99] D. S. Kirschen and G. Strbac, *Fundamentals of Power System Economics.* Chichester (UK): John Wiley and Sons, 2004, pp. 186–187.

[100] H. Federer, *Geometric Measure Theory.* Berlin, DE: Springer, 1996, pp. 90–91.

[101] N. L. Carothers, *Real Analysis.* Cambridge, UK: Cambridge University Press, 2000, pp. 287–288.

[102] X. Dai, "Continuous differentiability of solutions of ODEs with respect to initial conditions," *The American Mathematical Monthly*, vol. 113, no. 1, pp. 66–70, 2006.